The role of Cauliflower Mosaic Virus P6 in Modulating Plant Hormone Signalling

Yousef Jalil Mater

Submitted in fulfilment of the requirements of the Degree of Doctor of Philosophy

Institute of Molecular Cell & Systems Biology

College of Medical, Veterinary, and Life Sciences

University Of Glasgow

August 2021

Abstract

Pathogens have evolved mechanisms to manipulate host responses and physiology to facilitate their survival, spread, and promote invasion. The production of effector proteins by pathogens to manipulate and control host cellular mechanisms is a key feature of host-pathogen interactions and is employed by diverse types of pathogens, from fungi and bacteria to viruses. *Cauliflower mosaic virus* (CaMV) a plant pararetrovirus has been shown to modulate phytohormone synthesis and signalling pathways in infected plants. These include those involving salicylic acid (SA) signalling pathway, auxin (Aux) signalling pathway, jasmonic acid (JA) signalling pathway. The modulation of phytohormone signalling can be enacted directly or indirectly, impacting diverse aspects of plant physiology, including growth, development, reproduction, and responses to various biotic and abiotic stresses.

CaMV encodes a multifunctional 520 amino acid (aa) protein, P6, which was initially identified as playing an essential role in virus replication by facilitating the expression of multiple open reading frames from the virus-encoded 35S RNA transcript. More recently P6 has been shown to function as an effector protein, where Arabidopsis plants ectopically expressing P6 exhibit symptom-like phenotypes (stunting and yellowing) and alterations in plant defense signalling. In particular, P6 suppresses innate immunity by down regulating aspects of responses to salicylic acid (SA) and enhancing jasmonic acid/ethylene (JA/ET) responses. This result in increased susceptibility to biotrophic pathogens but increased resistance to herbivores and necrotrophic pathogens. The translational transactivation function and the suppression of innate immunity are both dependent on the ability of P6 to bind to the multifunctional receptor kinase TOR which plays a key role in multiple aspects of signalling and biochemical responses in eukaryotic organisms including plants. However, the role of P6-TOR interaction in the ability of P6 to modulate other aspects of hormone signalling in plants in particular those involving JA, ET, and Aux are unknown.

To dissect the role of the interaction of P6 with TOR, independent homozygous transgenic Arabidopsis plants were constructed that express either a wild-type P6 or a

mutant version of P6 with a deletion of the TOR binding domain (Δaa 136–182), P6(ΔTOR) were constructed and analyzed at the transcriptional and phenotypic level. Transgenic Arabidopsis lines in Arabidopsis Col-0 background expressing P6 wildtype sequence (P6WT) fused to a C-terminal GFP, and P6 (ΔTOR) fused to a C-terminal GFP were generated under the control of a constitutive promoter (35S), pEZR-P6WT-GFP and pEZR-P6(ΔTOR)-GFP lines, or under the control of a β-estradiol-inducible promoter; pER8-P6WT-GFP and pER8-P6(ΔTOR)-GFP lines and two lines of each newly constructed transgenic Arabidopsis line were selected for further analysis. Our western blot and confocal analysis indicated that all pER8 lines had a higher level of transgene expression than pEZR lines and had a controllable expression to avoid unwanted phenotypes.

Transgenic Arabidopsis lines expressing (P6WT) and P6(ΔTOR) were used to highlight the expression impact on the phytohormonal signalling pathways and responses. The work described here was performed to confirm that P6 modulates phytohormonal signalling pathways, particularly the P6 impact on the ethylene signalling pathway and auxin signalling pathway. Transgenic Arabidopsis lines expressing P6 and P6(ΔTOR) were phenotypically assessed using ethylene sensitivity assay and auxin transport inhibitor treatment. The transgenic Arabidopsis lines expressing P6 showed a decrease in ethylene sensitivity compared to Arabidopsis Col-0. Transgenic Arabidopsis lines expressing P6(ΔTOR) retained wild-type sensitivity to ethylene, i.e., P6 modulates the ethylene signalling pathway in a TOR binding domain manner. Both transgenic Arabidopsis lines expressing P6 and P6(ΔTOR) displayed an increase in the resistance to an auxin transport inhibitor compared to Arabidopsis Col-0, i.e., P6 does not require the presence of a functional TOR binding domain to modulate the auxin signalling pathway. Taken together, these data suggest that P6 modulates both auxin and ethylene signalling pathways during CaMV infection in nature. P6, via its TOR-binding domain, can modulate ethylene signalling pathways by interacting with the plant TOR kinase, but in the case of auxin signalling interactions, another domain of P6 may be important.

Here, the regulatory impact of P6 on plant gene expression profiles were investigated by executing RNA sequencing (RNA-seq). The transgenic line expressing P6 from an estradiol inducible promoter exhibited an expression profile distinct from the P6(ΔTOR) expressing line. They displayed a different impact on the global Arabidopsis gene expression profile, including genes known to participate in plant development and biotic and abiotic stress responses, i.e., genes contribute to defense response, stress response, signalling, metabolism, cell proliferation, and differentiation. Our results reveal P6 expression leads to extensive regulation of expression of genes frequently used as a marker for the plant defense and phytohormones signalling pathway, including SA, JA/ET, Aux, abscisic acid (ABA), brassinosteroids (BR), and gibberellins (GA) pathway. Moreover, P6 suppressed the expression of several genes associated with Plant responses more than P6(ΔTOR), i.e., the lack of TOR binding domain would attenuate the P6 ability to suppress the expression of several important genes, resulting in modification of the P6 impact on the plant phenotypes and responses. Interestingly, some genes are regulated by different P6 domains, i.e., in a non-TOR binding domain manner. Collectively, these findings highlight both the P6 impact and the TOR binding domain's robust role in modulating Arabidopsis responses.

“He who is not courageous enough to take risks will accomplish nothing in life.”

World Champion Mohammed Ali

Author's declaration

"I declare that, except where explicit reference is made to the contribution of others, that this dissertation is the result of my own work and has not been submitted for any other degree at the University of Glasgow or any other institution."

Printed Name: Yousef Mater

Signature:

Acknowledgments

First and foremost, praises and thanks to God for all his blessings throughout my journey to complete the research successfully.

Being a graduate student at University of Glasgow has been an incredible experience, and I would never have been able to reach to this accomplishment without the guidance, truly dedication, mentor and tremendous academic support of Prof. Joel Milner and I extend my deepest gratitude. It was a great privilege and honor to work and study under his guidance.

I am tremendously appreciative to Prof. John Christie for his academic support, time, willingness, being supportive, extreme patience, and guidance. He helped me to understand and how to solve problems from various angles.

Also, I am greatly indebted to my guidance committee members Prof. Gareth Jenkin and Prof. William Cushley, who helped deal efficiently with challenges, insights in discussing my research ideas and contributions to my development as a scientist.

Similarly, deep gratitude goes to Dr. Stuart Sullivan who has been supportive, patient and was there whenever needed. I am particularly indebted to Ms. Janet Laird for her constant help in lab work and doing research.

I would like to extend thanks to the Kuwait University faculty and Kuwait government, who believed in me and gave me the chance and the support to pursue my work.

I would also like to thank all friends, co-workers in the Joel Milner lab and Bower Building, especially Dr. William Rooney, Dr. Chantal Keijzer for providing such support, help when needed, humor and friendly laboratory environment.

Finally, but by no means least, thanks go my family. Special mention goes to my father, mother, four sisters, cousins, aunts, uncle, nephews, and brother-in-law. Also, I lovingly thank my beloved wife Dr. Sarah Rajab who was there whenever needed, always

supportive, and taking care of our family. They are the most important people in my world, and I dedicate this thesis to them.

Table of Contents

List of Tables

List of Figures

Table of abbreviations

CaMV	***Cauliflower mosaic virus***
TOR	**The target of rapamycin kinase**
SA	**Salicylic acid**
JA	**Jasmonic acid**
ET	**Ethylene**
P6 WT	**Wild type protein number 6 of *Cauliflower mosaic virus***
P6(ΔTOR)	**P6 mutant lacking the TOR-binding site (Δaa 136–182)**
TAV	**Translational activator**
ssDNA	**Single-stranded deoxyribonucleic acid**
dsDNA	**Double-stranded deoxyribonucleic acid**
ORF	**Open reading frame**
P	**Protein**
D	**Domain**
MP	**Movement protein**
NES	**Nuclear export signal**
NLS	**Nuclear localization signals**
PTGS	**Posttranscriptional gene silencing**
ETI	**Effector-triggered immunity**
PTI	**Pathogen-associated molecular pattern-triggered immunity**
VSR	**Virus-encoded suppressor of RNA silencing**
ETR	**Triple Response Assay**
NT	**Non-transgenic**
P8P6	**pER8-P6WT-GFP**
P8TOR	**pER8-P6(ΔTOR)-GFP**
PZP6	**pEZR-P6WT-GFP**
PZTOR	**pEZR-P6(ΔTOR)-GFP**
LR	**Lateral root**
PCA	**Principal Component Analysis**

DEGs	**Differentially expressed genes**

Chapter I: Introduction to Cauliflower mosaic virus (CaMV) and Phytohormone signalling

Chapter I: Introduction to Cauliflower mosaic virus (CaMV) and Phytohormone signalling

1.1. Viruses as pathogens and their impact on the agricultural industry

Viruses are infectious pathogens that are too small to be seen under a light microscope, submicroscopic with a size range of 5-300 nanometers (nm). In a host-specific manner, they infect all types of living organisms, including animals, plants, fungi, and bacteria (Jones, 2009). Plant viruses have significant economic impacts on agricultural production, worldwide (Haas et al., 2002, Geering and Randles, 2012, Maule, 2007, Geering, 2014, Martiniere et al., 2009). Plant viruses infect a broad range of hosts, including economically important perennial and annual crops, resulting in lowering the quantity or/and quality of yields. The worldwide losses annually are estimated to be at least $30 billion. *Cassava mosaic begomoviruses*, *Tomato yellow leaf curl virus*, *Potato leafroll polerovirus*, *Citrus Tristeza closterovirus*, *Cucumber mosaic virus,* and *Barley yellow dwarf luteovirus* are examples of viruses that cause up to hundreds of millions of dollars losses in crops such as tomato, orange, tobacco, cassava, beet, cucumber, and alfalfa (Leisner and Schoelz, 2018, Love et al., 2007a, Geering and Randles, 2012, Jones, 2009, Sasaya et al., 2014, Nicaise, 2014).

Plants produce proteins, molecules, induce physiological changes, and defense responses to neutralize the pathogen invasion and prevent disease development. At the same time, pathogen evolved mechanisms and weapons such as effectors, toxins, proteins, and small molecules to overcome host defense responses and cause diseases (Figure 1.1). The plants immune system lacks specialized immune cells found to circulate in humans and animals. However, they possess receptors that recognize and respond to pathogens located on the surface or intracellular. The pattern recognition receptors (PRRs) are known to recognize extracellular effector proteins,

conserved pathogen-associated molecular patterns (PAMPs), microbe-associated molecular patterns (MAMPs), and damage-associated molecular patterns (DAMPs). In contrast, the nucleotide-binding leucine-rich repeat (NLR) receptors identify pathogen effectors and pathogens inside the host cell. The PRRs and NLR receptors will activate defense responses, phosphorylation cascade, and modified plant gene expression profile (Lolle et al., 2020, Jones and Dangl, 2006). The Plants innate immune system is considered to be the first line of defense against pathogens (Jones and Dangl, 2006). The plants have a microbial/patterns-associated molecular-triggered immunity (M/PTI) and effector-triggered immunity (ETI). Both M/PTI and ETI lead to defense responses such as reactive oxygen species (ROS) generation, calcium influx, and expression of defense responsive genes, but in terms of timing, location, strength, and duration of defense responses, they differ (Lolle et al., 2020, Wang and Bouwmeester, 2017, Couto and Zipfel, 2016, Chow and McCourt, 2006, Jones and Dangl, 2006). The M/PTI is considered plant basal resistance, while ETI triggers a more robust resistance, such as a hypersensitive response and programmed cell death (PCD) at the infection site (Chiang and Coaker, 2015, Lolle et al., 2020). Phytohormones play a crucial role in the plant; they are responsible for several physiological responses and responses to abiotic and biotic stress. Salicylic acid (SA) is one of the phytohormones proven to participate in plant defense, including local and systemic defense responses. One of the robust defense responses against a broad range of pathogens and constrain secondary infection is the systemic acquired resistance (SAR) which is dependent on the SA signalling pathway (Gao et al., 2015, Islam et al., 2019b). Moreover, plants constrain pathogen infection by RNA interference (RNAi) and gene silencing; this defense mechanism is highly effective against viruses. The genetic material of viruses triggers gene silencing defense response, which occurs in the nucleus or cytoplasm, i.e., at transcriptional or posttranscriptional levels (Palukaitis et al., 2017, Campos et al., 2014b, Moissiard and Voinnet, 2004).

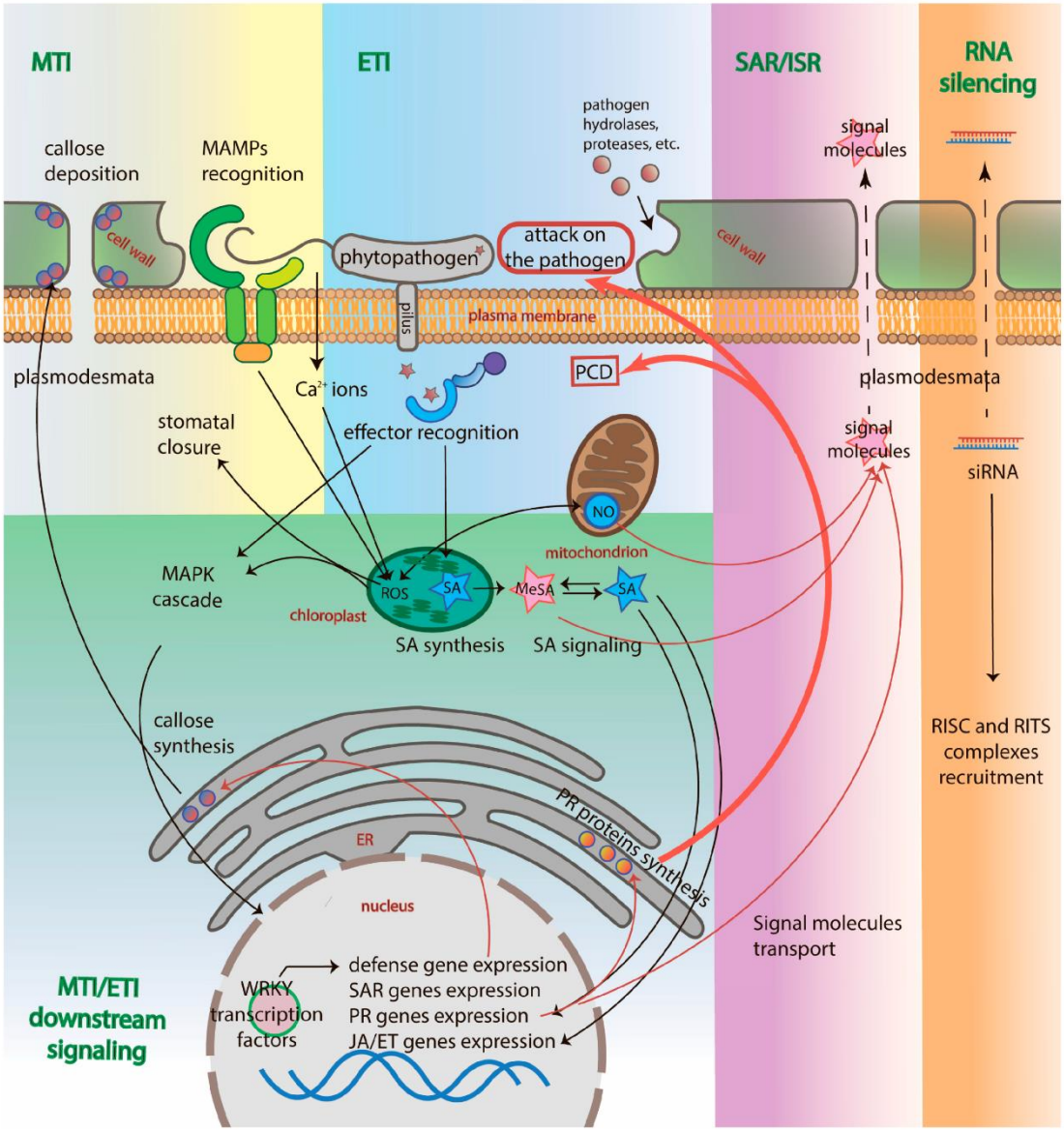

Figure 1.1. Scheme representation of plant defense mechanisms. The induction of MTI by MAMPs triggers the deposition of callose, closure of stomata, and increases the cytosolic calcium ions, ROS, and RNI generation. Effectors trigger ETI by binding to R proteins (NB-LRRs) that modulate the phytohormones signalling, such as SA, JA/ET, induction of PR proteins production, siRNA, JA/ET-dependent ISR-related genes, and SAR-related genes. These responses will constrain the pathogens by direct combat or trigger the PCD of the infected cell. Adapted from (Balakireva and Zamyatnin, 2018).

1.1.1. Correlation between viral defense responses and phytohormone signalling

Findings of (Hunter et al., 2013, Campos et al., 2014a, Love et al., 2012, Love et al., 2007b) indicate a robust association between viral defense responses and phytohormone signalling. Phytohormones are known to be associated with the modulation of RNA silencing defense mechanism (Leisner and Schoelz, 2018, Collum and Culver, 2016, Earley et al., 2010, Campos et al., 2014a). Salicylic acid (SA) is a fundamental phytohormone for plant virus defense response, in which it is involved R gene-mediated resistance, systemic acquired resistance (SAR), and basal defense responses. In contrast, the accumulation of reactive oxygen species, induction of pathogenesis-related (PR) protein expression, induction of the hypersensitive response, and callose deposition occur when the SA pathway is activated (Collum and Culver, 2016, Robert-Seilaniantz et al., 2011, Jones and Dangl, 2006). SA and JA/ET mediated defense pathways are commonly antagonistic, where if one is enhanced, the other one will be suppressed. Thus, synergism occurs between these pathways occasionally. The SA is mainly responsible for defenses against biotrophic pathogens such as viruses and bacteria, while JA/ET is mainly accountable for defenses against necrotrophic pathogens and insects (Jones and Dangl, 2006, Gimenez-Ibanez and Solano, 2013, Robert-Seilaniantz et al., 2011, Collum and Culver, 2016, Love et al., 2012). Studies showed that the SA signalling pathway's disruption would increase viral infections' susceptibility, where defense response would be constrained (Love et al., 2012, Love et al., 2007b, Leisner and Schoelz, 2018, Zvereva et al., 2016, Collum and Culver, 2016).

TMV infection shows that it directs the degradation of transcription factor ATAF2 by its replication protein, resulting in the suppression of SA-mediated defenses (Derksen et al., 2013, Wang et al., 2009, Padmanabhan et al., 2005, Oka et al., 2013). Additionally, TMV's coat protein also interferes with the crosstalk between the GA, SA, and JA signalling pathways, in which it will interfere with the growth of the plant, floral transition, and suppress SA defense responses (Depuydt and Hardtke, 2011, Robert-Seilaniantz et al., 2011, Derksen et al., 2013, Love et al., 2012). Moreover, in geminivirus infection,

C2 protein will interfere with the JA signalling pathway to modulate host resistance (Lozano-Duran et al., 2011). Similarly, CaMV P6 acts as a pathogenicity effector by mediating the host transcriptional regulator of the Nonexpressor of pathogenesis-related genes 1 (NPR1), which plays a central role in SA- and the jasmonic acid (JA)-dependent signalling (Love et al., 2012). The modification of NPR1 localization and expression by P6 results in SA signalling alteration. The P6 expression suppresses the SA-dependent defense responses while enhancing JA-signalling responses, i.e., increasing susceptibility to biotrophic pathogens (SA-sensitive pathogens) and the host resistance to necrotrophic pathogens and insects (JA-sensitive pathogens) (Haas et al., 2005, Love et al., 2012, Laird et al., 2013, Geri et al., 2004). However, a direct interaction between P6 and ET pathway components was not identified yet.

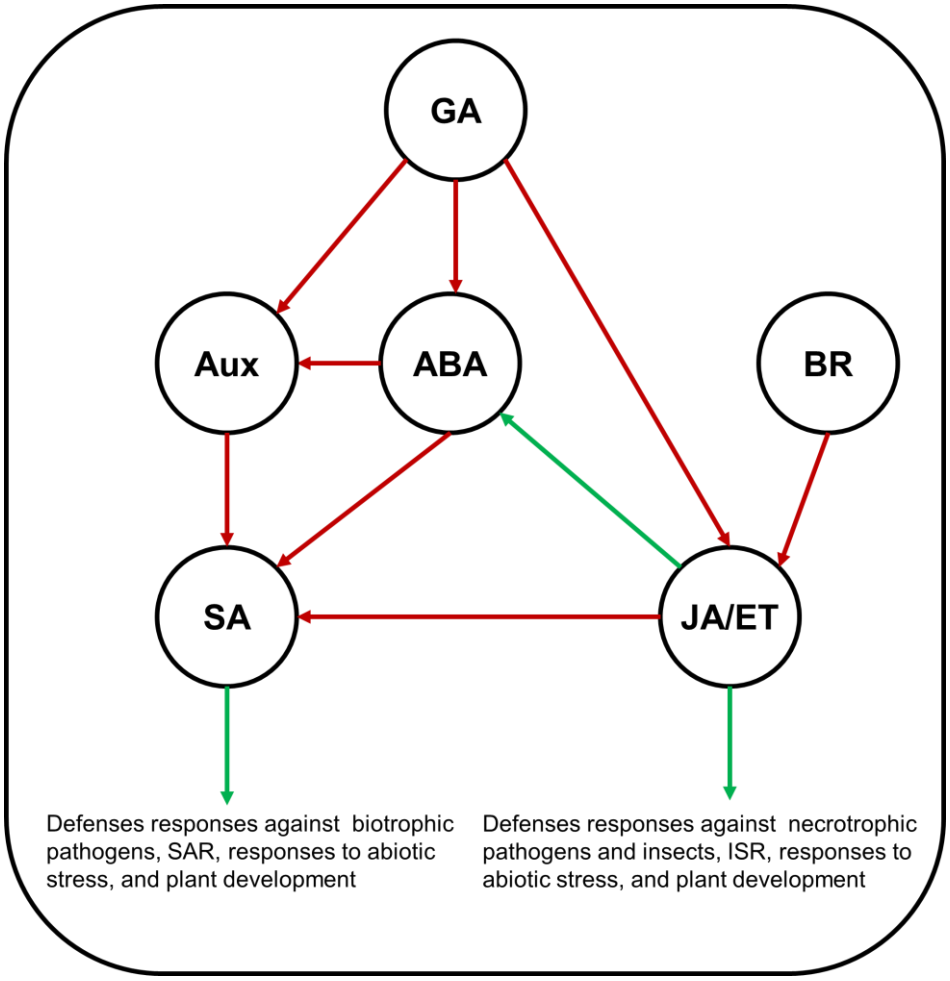

Figure 1. simplified diagram synergistic and antagonistic crosstalk between phytohormones signalling pathway. Commonly the JA is involved in modulating plant defense responses against necrotrophic pathogens, while SA modulates plant defense responses against biotrophic (Robert-Seilaniantz et al., 2011). The involvement of one phytohormone signalling pathway or more can modulate plant responses (Liu and Timko, 2021, Derksen et al., 2013). Red arrows indicate a reduction, down-regulation, and suppression, while green arrows indicate accumulation, up-regulation, and activation. Black arrows represent the downstream responses. The simplified diagram does not represent all phytohormones crosstalk in all plant responses status, or host variations in crosstalk might occur depending on plant status and responses. The abbreviations: SA is salicylic acid, JA/ET is jasmonic acid/ ethylene, Aux is auxin, ABA is abscisic acid, GA is gibberellins, BR is brassinosteroids, SAR is systemic acquired resistance, and ISR is induced systemic response.

1.1.2. Disruptions of phytohormonal pathways associated with symptom development

Plant viruses will induce different symptoms in their hosts, whereas some of them are associated with the disruptions in the phytohormonal pathway, such as leaf curling, chlorosis, and stunting (Collum and Culver, 2016, Derksen et al., 2013, Durbak et al., 2012). Although our knowledge is insufficient in this aspect, and we need to expand our understanding of the role of the interaction between the viral factors and phytohormone pathways in disease symptoms induction. Some explanations of how viruses-hosts components interactions regulate host phytohormone pathways and how those modulations resulted in symptoms induction were achieved. One example of a virus that directly interferes with the phytohormonal pathway is the *Tobacco mosaic virus* (TMV), where the 126 kDa replication protein (RP) of TMV interrupts the Aux signalling pathway through the interaction with members of the Aux/IAA proteins family by interfering with their nuclear localization. The Aux/IAA proteins are considered to be negative regulators for Aux responsive transcription factors (ARF) and modulate plant

metabolisms, which will lead to the induction of symptoms, including leaf curling and stunting. RP–Aux/IAA interaction is essential for disease development (Kazan and Manners, 2009, Derksen et al., 2013, Collum and Culver, 2016).

Furthermore, viral gene silencing suppressors showed involvement in the modification of Aux signalling and disease symptom development. Whereas transgenic Arabidopsis plants expressing HC-Pro, the silencing suppressor protein of the *Turnip mosaic virus* (TuMV), targets miRNA regulated pathways including the Aux responsive transcription factors and miRNA regulated pathways under the control of Aux, which will direct the development of abnormalities similar to virus disease symptoms including leaf abnormalities (Kasschau et al., 2003, Chapman and Estelle, 2009). The second example of viral protein that modulates the phytohormonal pathway and induces disease is the capsid protein P2 of *Rice dwarf virus* (RDV), where it interferes with the gibberellins (GA) biosynthesis pathway and induces stunting, lesions development, and leaf darkening (Zhu et al., 2005, Song et al., 2014). *Cauliflower mosaic virus* (CaMV) is an example of a plant virus that can directly or indirectly modify the host, in which the multifunctional viral protein P6 plays a role in virus replication, movement, phytohormones signalling, suppression of innate immunity and RNAi (Love et al., 2007a, Harries et al., 2009). P6 induces stunting, chlorosis, vein banding and ET-insensitive phenotype when expressed in host plants (Cecchini et al., 1997, Yu et al., 2003, Geri et al., 2004, Love et al., 2007b).

1.2. *Cauliflower mosaic virus* (CaMV)

Cauliflower mosaic virus (CaMV) is a member of Pararetroviruses, the *Caulimoviridae* family, one of the important plant virus groups. *Caulimoviridae* comprises eight genera with genome sizes between 7.5 and 9.3 kb that are subdivided into two groups based on the distinct virion morphologies, in which *Caulimovirus*, *Soymovirus*, *Solendovirus*, *Cavemovirus*, *Petuvirus*, and *Rosadnavirus* have isometric particles, whereas *Badnavirus* and *Tungrovirus* have bacilliform particles. (Geering, 2014, Geering ADW, 2012, Bhat et al., 2016). They possess a circular, double-stranded deoxyribonucleic

acid (dsDNA) and replicate by reverse transcription of an RNA intermediate, whereas their replication is independent of genome integration into the host chromosomes. The family *Caulimoviridae* was found to infect plants only, with no members infecting either animals or insects (Leisner and Schoelz, 2018, Bak et al., 2013, Diop et al., 2018). Infections by members of the *Caulimoviridae* are a major constraint on agriculture in tropical regions, causing significant diseases in crops including rice, cacao, banana, and yams (Sukal et al., 2018).

CaMV belongs to the genus Caulimovirus and is one of the most significant viruses in this group. It contains a genome of a relaxed, non-covalent double-stranded deoxyribonucleic acid (dsDNA) with one break in the minus DNA strand and two or more breaks in the positive DNA, encapsidated within a T = 7 icosahedral capsid of 50 nm diameter containing 420 protein subunits (Figure 1.3) (Geering, 2014, Lutz et al., 2012, Khelifa et al., 2007, Haas et al., 2002, Bousalem et al., 2008, Cheng et al., 1992, Shepherd et al., 1968). Most Caulimoviruses, including CaMV, form inclusion bodies within infected cells that can be visualized under a light microscope. The CaMV virus particles and inclusion bodies are very stable. Like animal retroviruses, CaMV has a high recombination rate and replicates by reverse transcription. However, CaMV will not integrate its genome into host cell chromosomes as part of the replication cycle (McFadden and Simon, 2011, Haas et al., 2002, Schoelz and Leisner, 2017, Hohn and Rothnie, 2013, Rothnie et al., 1994, Pfeiffer and Hohn, 1983). Unlike geminiviruses (ssDNA plant viruses), CaMV is independent of the host DNA replication machinery and will not integrate into the host genome (Schoelz and Leisner, 2017, Hohn and Rothnie, 2013). CaMV contains a 35S promoter extensively used in both research and commercial plant biotechnology applications due to its ability to induce a high level of transgene expression in different plant tissues and in both monocots and dicots. Also, the 35S promoter was functional in animals, particularly in the hamster ovary and the enterocyte-like human cell line Caco-2, where the reporter genes *gfp* and *luc* were expressed. (Myhre et al., 2005, Tepfer et al., 2004). CaMV is a well-studied plant virus model explaining the principle of virus replication, cell-to-cell movement, vector transmission and used as a molecular tool (Haas et al., 2002).

1.3. CaMV transmission and host range

CaMV is transmitted by aphids in a semi-persistent non-circulative manner, with low specificity for aphid species. CaMV infects members of *Brassicaceae,* including radish, turnip, canola, cauliflower, broccoli, and cabbage, and some members of the *Solanaceae* species including trumpets and tobacco (Saunders et al., 1990, Haas et al., 2002). CaMV might induce different symptoms and infection severity in different hosts. Common symptoms of CaMV infections are mottles, mosaics, and chlorotic vein clearing (Maule, 2007, Geering, 2014, Geering and Randles, 2012). Arabidopsis is a natural host for CaMV and is extensively used for molecular and genetic research as a model plant system (Fink, 1998, Koornneef and Meinke, 2010, Pagán et al., 2010, Bak and Emerson, 2020, Bergès et al., 2020). Therefore, the CaMV and Arabidopsis make an excellent model pathosystem to extend our understanding of virus-host interaction.

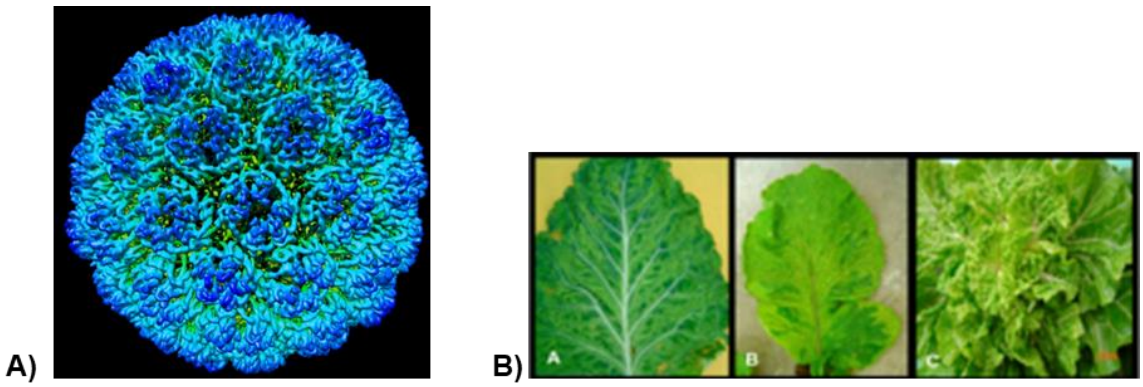

Figure 1.3 (A) The Cryo-electron microscopy (cryo-EM) structure of CaMV at 5.7Å. Photo: Ranson and Milner (2017), unpublished. **(B) CaMV symptoms in several cruciferous crops.** A) Mosaic and vein-clearing symptoms on cauliflower, B) mosaic on small radish, C) leaf deformation, stunting, and vein-clearing on Chinese cabbage. Photo: Farzadfar et al (2007).

1.4. CaMV genome

CaMV has a circular dsDNA genome with a size of ~ 8.0 kb. The genome size and sequence slightly vary between isolates. In 1980, the whole genome sequence was published, known to be one of the first plant viruses to be sequenced, and genome analysis revealed that CaMV encodes seven open reading frames (ORFs), as shown in the Figure1.2 (Bonneville et al., 1989). ORF I encodes for P1 has been shown to be a 37 kDa protein required for both cell-cell and long-distance virus movement. It is associated with plasmodesmata modification and has nucleic acid binding properties (Haas et al., 2002). ORF II encodes P2, an 18 kDa protein involved in aphid transmission (Uzest et al., 2007, Khelifa et al., 2007, Hoh et al., 2010, Lutz et al., 2012, Bak et al., 2013). ORF III encodes P3, a 15 kDa virion-associated protein that is essential for aphid transmission and cell-to-cell movement of the virus (Lutz et al., 2012, Hoh et al., 2010, Khelifa et al., 2007, Plisson et al., 2005, Tsuge et al., 1999). ORF IV encodes P4a 56 KDa protein, which is the virus capsid's major component and is required for cell-to-cell and long-distance movement (Plisson et al., 2005, Haas et al., 2002). ORF V encodes P5, 60 kDa protein with reverse transcriptase (RTase) activity, protease activity, and has ribonuclease H activity. ORF VI encodes P6, a 62 kDa multifunctional protein that is translated predominantly from CaMV 19S RNA and possibly from the 35S RNA (Geering, 2014, Haas et al., 2005, Haas et al., 2002), which will be discussed in detail later. ORF VII encodes P7, 11 kDa protein of unknown function found to be not essential for the infection and found to bind to P6 but not to P2 or P3 in yeast 2-hybrid analysis (Lutz et al., 2012, Tsuge et al., 1999).

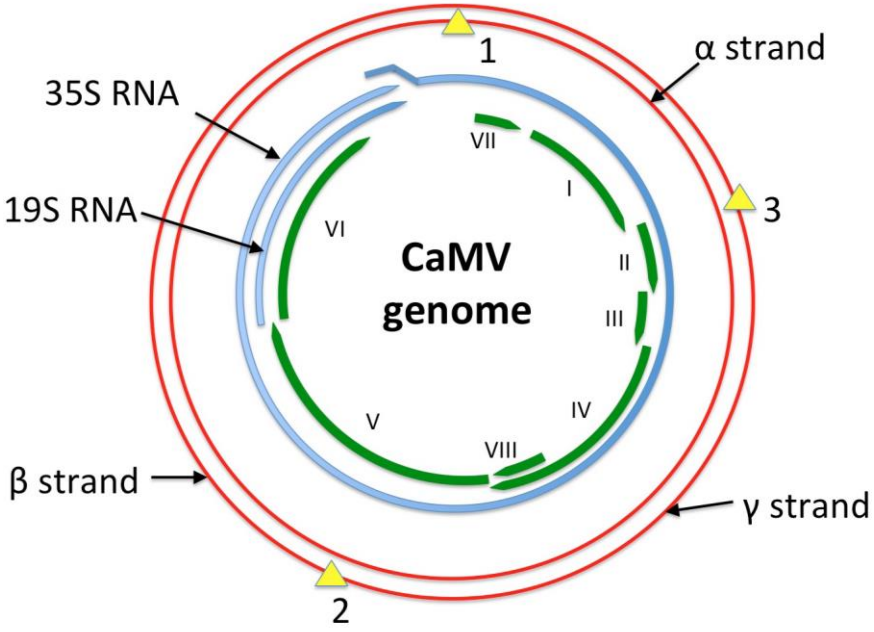

Figure 1.4. Genomic maps of CaMV. The CaMV genome is represented in red, with single-strand discontinuities presented as yellow triangles. mRNA transcripts, the 35S RNA, and the 19S RNA are shown in blue. ORFs are presented in green. The functions for each of the ORFs: ORF I movement protein, ORF II encodes P2, aphid transmission factor, ORF III virion-associated protein that is essential for aphid transmission and cell-to-cell movement of the virus, ORF IV encodes P4, the coat protein, ORF V encodes P5, which has reverse transcriptase (RTase), protease, and has ribonuclease H activities, ORF VI encode P6, multifunctional protein. ORF VII encodes P7, a protein of unknown function. Adapted from (Rybicki, 2015)

1.5. Proposed domains of P6

Although the three-dimensional structure of P6 has not been determined, it has been divided into four domains, D1 to D4, based on function. D1 comprises amino acids 1 to 112 and is involved in nuclear localization, virulence, and avirulence (Vi/Av) and stability. D1 is necessary for CaMV spread in different cruciferous and solanaceous hosts, in which deletions within D1 impacts P6 structure and reduce the virus intra- or

intercellular movement (Kobayashi and Hohn, 2004, Kobayashi and Hohn, 2003, Li and Leisner, 2002). Deletion of the N-terminal 20-30 amino acids of D1 results in P6 localization to the nucleus most likely because these amino acids comprise a nuclear export signal that acts in conjunction with proposed nuclear localization signals in domains (D2 and D3) to shuttle P6 between nucleus and cytoplasm (Haas et al., 2008). D1 also contains residues that are needed to establish P6-P6 intermolecular interactions and viroplasm development (Haas et al., 2005, Schoelz and Leisner, 2017). D1 deletion abolished genome replication in single cells (Kobayashi and Hohn, 2003) but did not abolish symptoms induction (Yu et al., 2003).

D2 comprises amino acids 112 to 242 and contains nuclear localization signals, a putative RNase H homologous domain that binds RNA-DNA hybrids, double-stranded RNA binding domain, and the interaction motif for ribosomal protein L18 (RL18)(Schoelz et al., 2016, Kobayashi and Hohn, 2004). Crucially it contains the mini-TAV domain identified by as the minimum domain required for translational transactivation. The mini-TAV domain encompasses a target of rapamycin (TOR) kinase binding motif, an ssRNA-binding motif that is associated with TOR binding and triggers TOR activation, which is essential to enable the translation transactivation (Schepetilnikov et al., 2011, Schepetilnikov et al., 2013, Angel et al., 2013). In addition, D2 has been reported to interact with CHUP1 (Angel et al., 2013), thereby facilitating the movement of virus particles along the cytoskeleton in infected cells.

D3 comprising amino acids 242 to 400 is crucial for stability, multimerization, RNA-binding, the interaction with multiple host proteins. These include eukaryotic translational initiation factors (eIF3, eIF4G, and eIF2B) and ribosomal protein L24 (RL24) (Ryabova et al., 2004, Podevin and du Jardin, 2012). These interactions point to an important role for D3 in translating the 35S and possibly 19S RNAs.

D4 comprising amino acids 400 to 520, includes a zinc-finger domain (Li and Leisner, 2002, Podevin and du Jardin, 2012, Kobayashi and Hohn, 2004, Thiebeauld et al.,

2009, De Tapia et al., 1993) and along with D2, plays a role in the interaction with CHUP1 (Angel et al., 2013).

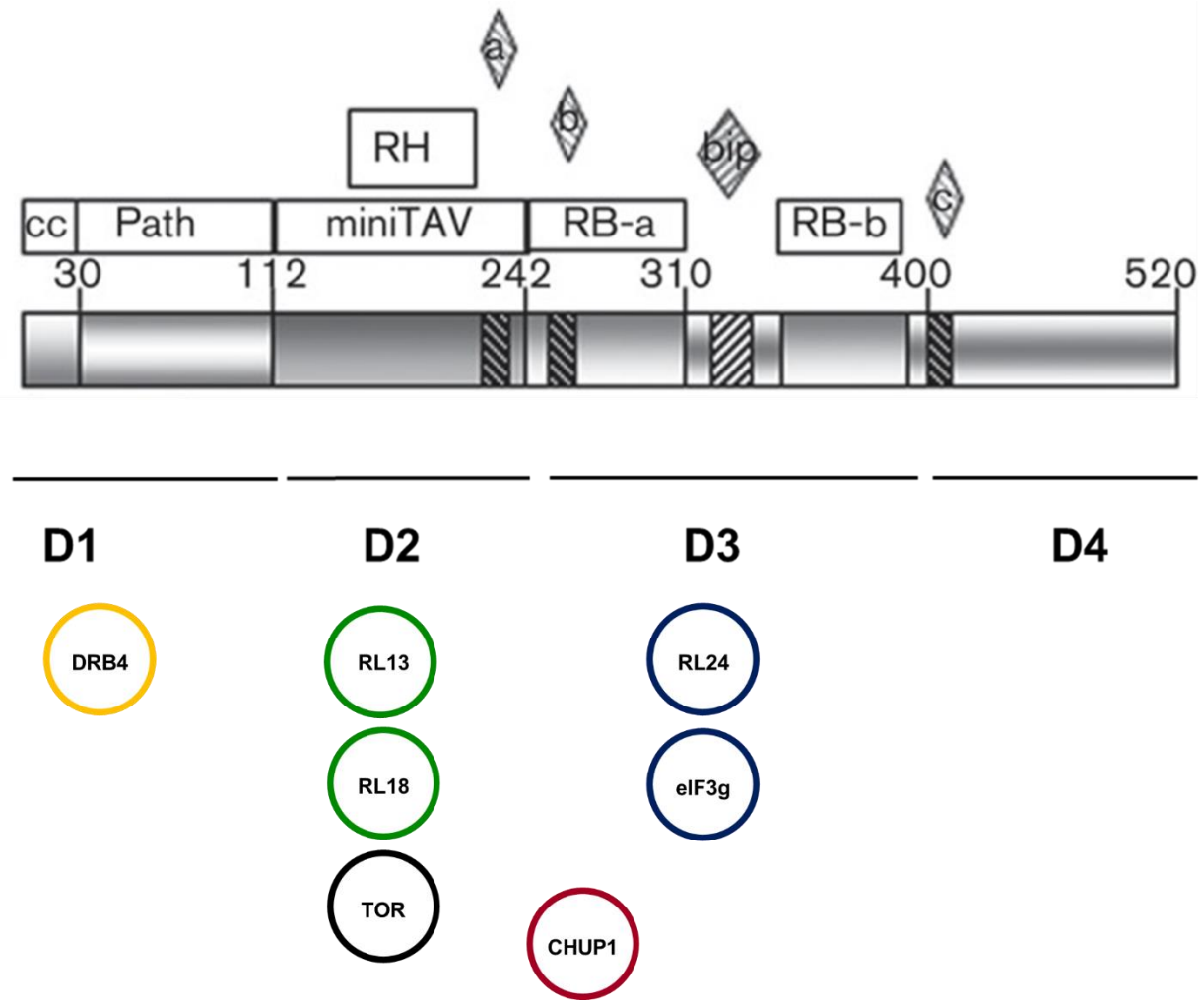

Figure 1.5. Schematic map of the P6 protein domains, which is divided into four domains (D1–D4). The solid lines indicate the four domains (D1–D4), the proposed domains labeled with the amino acid numbers at the boundaries. Above boxes display the coiled-coil (cc) α-helix, pathogenicity (Path), minimum transactivator domain (miniTAV), RNase H (RH) and RNA binding (RB-a and RB-b). Diamonds indicate the nuclear localization signals (NLS). **Circles represent the identified interactors of CaMV P6.** Adapted from Schepetilnikov **(**2011) and Laird et al., (2013).

1.6. The cauliflower mosaic virus P6 protein: a multifunctional virus encoded protein

1.6.1. P6 protein mediated control of viral replication and translation

P6 is translated predominantly from CaMV 19S RNA and possibly from the 35S RNA (Geering, 2014, Haas et al., 2005, Haas et al., 2002). P6 comprises a polypeptide of 520 amino acids, the 3D protein structure being as yet undetermined (Schoelz et al., 2016, Haas et al., 2002). The 62 kDa P6 is distinctive and unique; despite extensive analysis to try to identify homologs in other genomes, it appears to be a protein that is unique to two of the seven groups of Caulimoviruses, and it does not share significant homologies to any other gene products, viral or otherwise, identified in the genome databases. Hence its evolutionary origin remains unclear. Moreover, P6 is the translational activator (TAV), where P6 aggregates and transactivates the translation of all ORFs on 35S RNA in the cytoplasm. P6 mediates the translation of the other CaMV proteins through its TAV domain (Figure 1.4 and 1.3) (Khelifa et al., 2010, Zijlstra and Hohn, 1992, Hohn and Rothnie, 2013). The expression of the polycistronic mRNA 35S RNA is mediated by P6 interaction with several host proteins, including ribosomal proteins (L13, L18, and L24), the target of rapamycin (TOR), eIF3g, reinitiation supporting protein (RISP), and translation factors (Figure 1.5) (Park et al., 2001, Hohn and Rothnie, 2013, Hohn et al., 2001, Thiebeauld et al., 2009, Schepetilnikov et al., 2013, Schepetilnikov et al., 2011, Schoelz and Leisner, 2017). The research showed that P6 is the site where reverse transcription of the 35S RNA into DNA occurs, and virions encapsidation with CaMV DNA. Also, P5 found to participate in the CaMV DNA replication through an RNA intermediate (Schoelz and Leisner, 2017, Hohn and Rothnie, 2013, Schoelz et al., 2016, Harries et al., 2009). Furthermore, P6 is known to be the matrix protein of the CaMV inclusion body (viroplasm), the virus factories found in infected cells, which can be visualized under the light microscope (Schoelz et al., 2016, Schepetilnikov et al., 2011, Haas et al., 2005). Also, it is accountable for the virion’s aggregation (Harries et al., 2009, Schoelz and Leisner, 2017).

1.6.2. P6 protein suppresses plant defense responses and induces symptoms

To cause disease, pathogens must possess mechanisms to overcome host defense responses. Delivering effector proteins into host cells is one mechanism where pathogen modulate defense responses, metabolism, signalling, and modify host physiology (Toruno et al., 2016). Biotrophic plant pathogens, in particular, need to maintain living host cells for successful infection. Biotrophic plant pathogenic bacteria use the Type III secretion system (TTSS) to deliver their effectors into the host, and biotrophic fungi and oomycetes use haustoria or similar structures to transfer effectors to the host cell (Mudgett, 2005, Toruno et al., 2016). As obligate intracellular parasites, plant viruses are dependent on overcoming or suppressing host defenses for their lifecycle. Many plant viruses suppress host RNA silencing, a major component of plant antiviral defense responses. In particular, by encoding virus silencing suppressor proteins (VSSPs) (Leisner and Schoelz, 2018, Moissiard and Voinnet, 2004, Tungadi et al., 2017). It is now established that a virus infection activates plant basal defense responses in susceptible hosts. These include those involving phytohormones such as salicylic acid (SA), jasmonic acid (JA), and ethylene (ET) (Collum and Culver, 2016, Derksen et al., 2013, Robert-Seilaniantz et al., 2011). External application of SA to wild-type plants increased the resistance to several viruses such as the *Tobacco mosaic virus* (TMV), *Tomato yellow leaf curl virus* (TYLCV), *Cucumber mosaic virus* (CMV), and *Cauliflower mosaic virus* (CaMV) (Collum and Culver, 2016, Campos et al., 2014b, Campos et al., 2014a, Palukaitis et al., 2017, Li et al., 2019, Murphy et al., 2020). Similar findings were observed when SA mutant plants that constitutively activated the SA signalling pathway were exposed to TMV and CaMV (Palukaitis et al., 2017, Krasavina et al., 2002, Lee et al., 2016, Arena et al., 2020, Islam et al., 2019b, Love et al., 2012, Love et al., 2007b). This finding suggested that SA responses are involved in the resistance to viruses, particularly CaMV, and the viruses regulate the SA pathways to have a successful infection (Laird et al., 2013, Love et al., 2012, Love et al., 2007b). The Arabidopsis mutants defected in JA/ET signalling pathway increased virus susceptibility than the Arabidopsis wild type (Collum and Culver, 2016, Derksen et al., 2013, Robert-Seilaniantz et al., 2011, Liu and Timko, 2021). The crosstalk

between the JA–SA (antagonism relationship) modulates the virus defense responses, i.e., regulating the R gene (Liu and Timko, 2021, Islam et al., 2019b). The antagonism impact of crosstalk was identified when exogenously applied JA on N gene-resistant tobacco, and TMV resistance was decreased. Not only that, the silencing of the JA receptors, such as COI1, or enzymes involved in the JA biosynthesis, such as allene oxide synthase, of N gene tobacco increased SA accumulation and reduced the virus titer. Moreover, plants with a deficiency in SA accumulation gain resistance to CMV when they are mutated in COI (Islam et al., 2019b, Song et al., 2014, Derksen et al., 2013, Oka et al., 2013, Takahashi et al., 2004, Liu and Timko, 2021). However, the increase JA level does not always support the viral infectivity. In some cases, high endogenous levels of JA fount to alter host resistance to some viruses such as the geminivirus, in which high JA level altered C2 protein ability to modulate host defense responses. Moreover, external JA application interfered with the geminivirus infection. Also, elevated JA levels increased the incompatible level between plant and viruses in tobacco and potato plants (Dhondt et al., 2000, Liu and Timko, 2021, Kovač et al., 2009, Lozano-Duran et al., 2011)

During infections of Arabidopsis, CaMV infection has been reported to upregulate the expression of ET-responsive and SA-responsive genes and activate the production of reactive oxygen species (Chesnais et al., 2019, Zvereva et al., 2016, Love et al., 2012, Love et al., 2007a, Love et al., 2007b, Love et al., 2005, Roberts et al., 2007), whereas Arabidopsis mutants with constitutively activated SA mediated defense responses in Arabidopsis showed enhanced resistance to CaMV (Laird et al., 2013, Love et al., 2012, Love et al., 2007a, Love et al., 2007b, Roberts et al., 2007, Love et al., 2005). Although the role of P6 was originally identified as translational transactivation, studies have also shown that P6 plays a vital role in determining symptom severity and host range (Cecchini et al., 1998, Bak and Emerson, 2020). Indeed, expression via a transgene in Arabidopsis results in a phenotype that mimics many of the aspects of CaMV symptoms in infected plants (Geri et al., 2004, Laird et al., 2013, Love et al., 2012, Love et al., 2007a, Love et al., 2007b, Cecchini et al., 1997, Zijlstra and Hohn, 1992). Symptoms such as chlorosis and stunting will be induced in the host plants (Zvereva et al., 2016,

Love et al., 2012, Angel et al., 2013, Laird et al., 2013). These results suggest that P6 is the primary pathogenicity determinant for CaMV and participates in suppressing not only RNA silencing but also defense signalling pathways involving a variety of phytohormones such as SA, ET, and JA (Laird et al., 2013, Love et al., 2007a, Love et al., 2012, Love et al., 2007b, Love et al., 2005, Leisner and Schoelz, 2018).

Suppression of host gene silencing pathway and modification of host physiology are two general explanations of how viral diseases are developed. In addition to the role of virus-encoded proteins, there are many reports that implicate small RNAs (siRNAs) produced during infection in the development of symptoms, probably via downregulation of the accumulation of host mRNAs (Pesti et al., 2019, Palukaitis et al., 2017, Campos et al., 2014b, Islam et al., 2019b). *Tomato yellow leaf curl virus* (TYLCV) and Apple geminivirus (AGV) are two viruses that belong to the single-stranded DNA virus family Geminiviridae. They encode V2 protein in their genomes, which is found to be a vital virulence determinant that can suppress posttranscriptional gene silencing (PTGS), induce severe necrosis, and crumple (Fondong, 2013, Zhan et al., 2018).

Nevertheless, some viral proteins may also directly modify host physiology, resulting in symptom induction and disease, such as the C4 protein of *Beet curly top virus* (BCTV), which interacts with host kinase and induces hyperplasia (Leisner and Schoelz, 2018, Mills-Lujan and Deom, 2010, Maule, 2007, Piroux et al., 2007). Similarly, P6 protein, not the siRNAs, was responsible for inducing symptoms, in which the developed symptoms were impacted by point mutations that changed individual amino acids of P6 (Lutz et al., 2015, Yu et al., 2003). Also, P6 acts as an avirulence factor, where it triggered a hypersensitive response in *Nicotiana edwardsonii* and *Datura stramonium*, and non-necrotic resistance response in *Nicotiana bigelovii* (Love et al., 2012, Kobayashi and Hohn, 2004).

1.6.3. P6 acts as a suppressor of gene silencing defense mechanism

P6 comprises a nuclear export signal (NES) at the N-terminus, TAV domain, two nuclear localization signals (NLS), RNA binding domains, and a putative zinc finger at the C-terminus (Haas et al., 2008). P6 shuttles between the cytoplasm and the nucleus, a nucleocytoplasmic shuttle protein, whereas its nuclear localization and export properties are critical for infectivity (Schoelz and Leisner, 2017, Schoelz et al., 2016, Rodriguez et al., 2014, Bak et al., 2013, Haas et al., 2008). Mutations within the nuclear export signal (NES) found at the N terminus of P6 will prohibit infectivity. Similarly, mutations in the NLS at C-terminal will compromise P6's ability to infect and suppress RNA silencing, i.e., suppressing RNA silencing was carried in an NLS-dependent manner (Haas et al., 2008, Kobayashi and Hohn, 2004, Feng et al., 2018, Laird et al., 2013, Love et al., 2007a). Also, deletion in the P6 domain 1 (D1) at the distal end of the N-terminal NES constrained symptom development and silencing suppression ability. In contrast, a mutation in the TAV domain, located in domain 2 (D2), constrained the virus replication but kept silencing suppression ability, i.e., the P6 ability to suppress gene silencing is dependent on intact D1 (Feng et al., 2018, Laird et al., 2013, Love et al., 2007a). However, D1 is not sufficient to suppress gene silencing when expressed individually, i.e., other P6 regions are required to suppress gene silencing (Laird et al., 2013, Haas et al., 2008, Love et al., 2007a). Additionally, a study carried by (Lukhovitskaya and Ryabova, 2019) suggested that P6 interferes with mRNA degradation in plants by targeting the 5′-3′ mRNA de-capping mechanism. Here P6 interacts with one of the structural proteins of the de-capping complex VARICOSE (VCS). In the suppression of the RNA silencing defense mechanism, P6 was found to mediates the processing precursors of siRNAs (Laird et al., 2013, Love et al., 2007a). Haas et al. (2008) reported that P6 might direct the suppression by interfering with DCL4, yet further experiments need to be conducted to determine the P6-DCL4 association. The host range or pathogenicity of CaMV strains is not based on P6 suppression of RNA silencing (Haas et al., 2008, Love et al., 2007a, Lukhovitskaya and Ryabova, 2019, Shivaprasad et al., 2008).

1.6.4. The CaMV P6 protein suppresses effector-triggered immunity, pathogen-associated molecular pattern–triggered immunity, and interferes with host hormonal signalling pathways

The plant developed defense responses to counter pathogen attacks and prevent infection; this is accomplished by triggering the microbe-associated molecular patterns (MAMP)-triggered immunity (MTI), effector-triggered immunity (ETI), systemic acquired resistance (SAR), induced systemic resistance (ISR), and RNA silencing. The plant recognizes the pathogens through plant pattern-recognition receptors (PRRs) that detect pathogen/microbe-associated molecular patterns (P/M-AMPs), such as flagellin, chitin, lipopolysaccharides, and peptides. The receptors contain leucine-rich repeats (LRR), receptor-like kinases (RLKs), or receptor-like kinases proteins (RLPs) that would connect the RRs to MAMPs. The detection of MAMPs will induce the mitogen-activated protein kinase (MAPK) cascade that modulates the expression of responsive defense genes, trigger basal defense or MTI (Figure 1.). The induction of the cascade will result in cellular status modifications where the production of reactive oxygen species (ROS) and reactive nitrogen intermediates (RNI) will be induced, and the levels of Ca2+ concentration will be elevated and induce physiological changes such as stomata closure and callose deposition (Balakireva and Zamyatnin, 2018). P6 is a multifunctional effector, interacting with a broad range of host proteins that can trigger innate immunity reactions in non-hosts and modulate defenses in hosts (Leisner and Schoelz, 2018, Schoelz and Leisner, 2017, Laird et al., 2013). Transgenic plants expressing P6 were constructed to understand the mechanisms of P6-host interactions, i.e., modulating defenses, and determine how P6 will regulate the symptom development during natural CaMV infection.

Both CaMV infection in susceptible hosts and P6-transgenic Arabidopsis plants triggered the production of oxygen species and up-regulation of marker genes of the ET and SA defense pathways, thus it would not constrain the CaMV spread and replication (Love et al., 2005, Laird et al., 2013). The NPR1 was upregulated and localized in the nucleus as a result of P6 expression. The upregulation of NPR1 resulted

in interference with the SA/JA crosstalk where SA-responsive genes expression (such as BGL2 and PR1) was suppressed while JA-responsive genes expression was enhanced, increased the biotrophic susceptibility pathogen, and increased the resistance to necrotrophic pathogens (Love et al., 2012, Wu et al., 2012).

Similar to the P6 effect of expressing P6 transgenically in Arabidopsis, P6 transient expression in *Nicotiana benthamiana* suppresses expression of representative SA responsive expression and up-regulates expression of representative jasmonic acid (JA) responsive genes. Transgenics plants that express P6 show a significant reduction in the abundance of transcripts for several genes encoding pathogenesis-related proteins, e.g., PR-1. The expression of PR proteins is usually induced in response to infections by various pathogens and is routinely used as molecular markers for the SAR response. These findings support the role of P6 in modulating the host immune response (Leisner and Schoelz, 2018, Derksen et al., 2013, Love et al., 2007b, Geri et al., 2004, Laird et al., 2013, Love et al., 2012, Love et al., 2007a, Yu et al., 2003). In addition, it has been reported that transgenic Arabidopsis plants that express P6 suppressed SA-dependent responses and ET-dependent responses, and Arabidopsis ET insensitive mutants showed reduced susceptibility to CaMV infection (Love et al., 2007b, Geri et al., 2004).

Overall, the results of several different studies demonstrate that in addition to its role as a translational transactivator during virus replication, P6 also functions as a pathogenicity effector protein that suppresses SA-dependent defense responses and enhancing JA-signalling responses, i.e., increases the susceptibility to biotrophic pathogens but decreases susceptibility to necrotrophic pathogens (Haas et al., 2005, Love et al., 2012, Laird et al., 2013, Geri et al., 2004). A key study, (Love et al., 2012) showed that transgenic Arabidopsis that express P6 show significantly enhanced susceptibility to virulent and avirulent strains of the biotrophic bacterial pathogen *Pseudomonas syringae* pv. Tomato (Pst) but reduce the susceptibility to *Botrytis cinerea*, a necrotrophic fungus. Zvereva et al. (2016) demonstrated that P6-transgenic

Arabidopsis plants were deficient in enacting basal defense responses as evidenced by reduced ROS bursts following treatment with the bacterial PAMP flg22.

In other words, P6 suppressed ETI and PTI induced by *P. syringae*, whereas P6 modulates NPR1 expression and subcellular localization, which modulates the SA and JA signalling pathways, as well as the expression of critical proteins involved in plant defense responses, resulting in a delayed hypersensitive response and constraining SA-dependent defense responses, i.e., suppresses defense responses against biotrophic pathogens (Love et al., 2012, Zvereva et al., 2016).

One of the crucial defense mechanisms in plants is autophagy, a degradation pathway that the plant usually uses to reprocess cellular components using a vacuole or lysosome. Plants manage to use the lysosomes to neutralize and decompose pathogens, especially viruses, i.e., intercellular antiviral defense mechanisms. As part of the evolution, plant viruses developed mechanisms and produced effectors that will allow them to modulate the autophagy pathway and overcome defenses to induce disease within the host (Yang et al., 2020). P6 is one of the examples of virus protein that interact and phosphorylate TOR to modulate the translation of CaMV 35S RNA and suppresser defense responses, including autophagy (Dobrenel et al., 2016, Zvereva et al., 2016).

Interestingly, like many animal viruses (Liang et al., 2015), CaMV suppresses antiviral autophagy by modulating TOR activation. This suppression of autophagy occurs when P6 induces phosphorylation of TOR, elevate levels of active TOR. Mutant forms of P6 that have lost the ability to interact with TOR lose the ability to suppress autophagy and PTI-mediated defense in Arabidopsis. Arabidopsis lines with continuously reduced TOR expression by RNA interference (RNAi) had a less successful systemic infection or no infection of *watermelon mosaic virus* (WMV) and a delayed infection of *turnip mosaic virus* (TuMV) (Ouibrahim et al., 2015). These findings lead to two conclusions; one, viruses have varied TOR needs, and two, viruses encode proteins with a TOR binding domain, like P6, will take advantage of the high level of TOR to spread their

infection and modulate the host responses. Not only is the P6-TOR interaction essential for suppressing autophagy, but it also contributes to the suppression of PTI-mediated defense, gene silencing defense responses, and the CaMV 35S RNA genes translation by forming a complex with P6 and ribosomal proteins (Zvereva et al., 2016, Schepetilnikov et al., 2013). These papers show that P6 acts as a pathogenicity effector by suppressing plant defense responses and interferes with the hormonal signalling pathways.

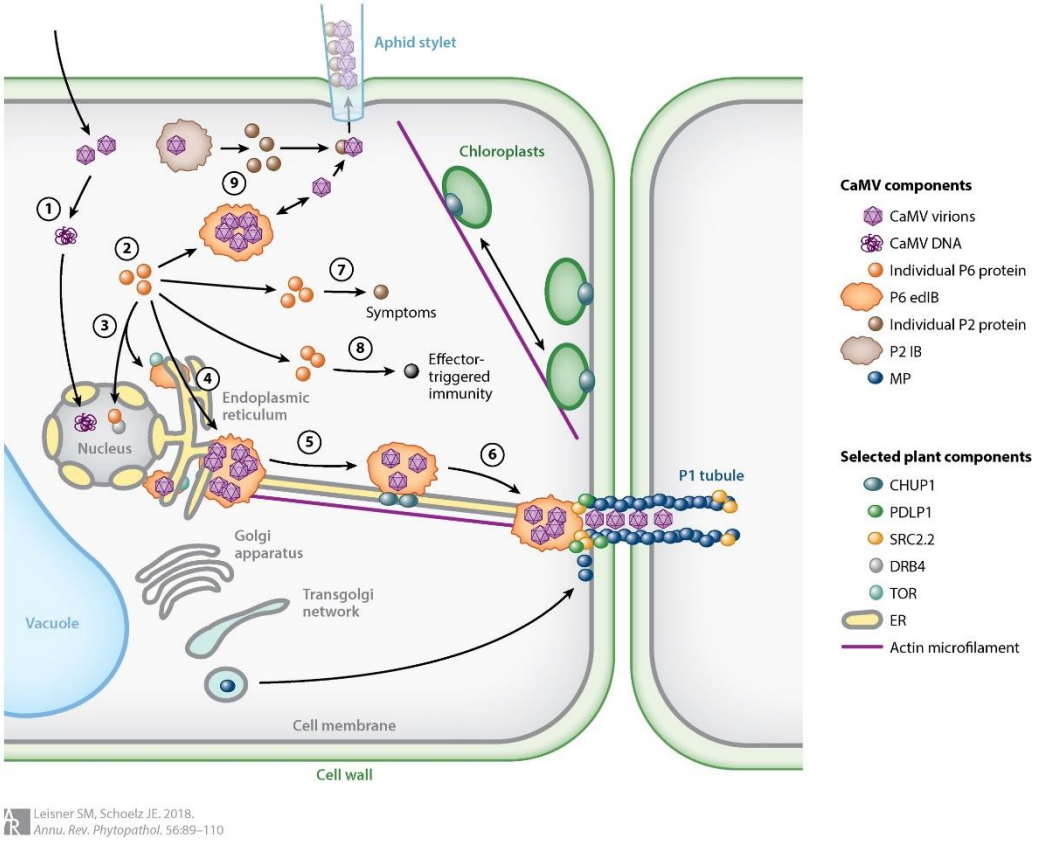

Figure 1.9 Proposed roles of P6 during CaMV infections. 1) CaMV virions enter the cell and release the viral DNA, which will be transported into the nucleus, where the 35S and 19S RNAs are transcribed. 2)Translation of 19S RNA happens in the cytoplasm, and P6 subsequently spreads to different locations within the cell. 3) P6-TOR interaction occurs in the cytoplasm to modulate host immune response and moves into the nucleus to suppress gene silencing and modulate plant genome

expression. 4) P6 adjusts and directs the ribosomes to translate the polycistronic 35S RNA, whereas viral inclusion body and P6 aggregation (P6 edIBs) follow. 5) P6 edIBs travel on microfilaments via CHUP1 and other unidentified proteins. 6) P6 edIBs transport virions to the modified plasmodesmata via P1 (MP) and host proteins and are transported to adjacent cells. 7) P6 interacts with unknown host proteins to induce chlorosis and mosaic symptoms in susceptible hosts. 8) P6 interacts with host receptors to trigger ETI in resistant hosts. 9) Aphid feeding triggers dissociation/uptake of virion complexes (P2-P6) into the aphid stylet. Adapted from Leisner and Schoelz (2018).

1.7. The impact of virus infection on phytohormones

1.7.1. Plant viruses manipulate host phytohormone pathways

Plant viruses manipulate the host's cellular system and modify host physiology by several strategies, in which they program it to one that is more favorable for viral replication, spread, and survival. In general, plants regulate their response to environmental factors or pathogens by extensive cross-talk between the different phytohormone pathways (Derksen et al., 2013, Song et al., 2014, Durbak et al., 2012, Depuydt and Hardtke, 2011). During infection, viruses can directly or indirectly impact the host hormone synthesis and signalling pathways. These modifications will make the host more susceptible to the virus infection, replication, spread, and uptake by the vector (Collum and Culver, 2016). As a result of the interference with phytohormone signalling, which is central to numerous aspects of plant biology, a variety of symptoms may develop, and plant behavior changes might also occur. Different viruses might have different levels of phytohormones signalling interference, resulting in a different impact on the growth, development, reproduction, metabolism, and pathogen defense responses (Santner and Estelle, 2009, Dong et al., 2015). Also, the virus replication and movement were proposed to be impacted by phytohormones signalling, in which phytohormones participate in modulating plasmodesmata, which is a means for establishing systemic infections (Collum and Culver, 2016, Durbak et al., 2012, Robert-

Seilaniantz et al., 2011, Lucas, 2006). Literature demonstrated that phytohormones are major plant components that interfere and associate with the virus infection process, where the virus accumulation and plant phenotypes changes have been associated with the modulation of phytohormones. Plant viruses manipulate host responses against their vectors and modify the plant physiology to be more favorable for their vector, i.e., enhance the attraction, feeding, and vector performance (Li et al., 2014a, Wu and Ye, 2020, Carr et al., 2020, Chesnais et al., 2019, Tungadi et al., 2017). Interestingly, they interfere with the jasmonate pathway, which plays a major role in plant defenses against biotic and abiotic factors (Wu and Ye, 2020, Carr et al., 2020).

Phytohormones are categorized into five main groups based on their chemical structure (Figure1.4) auxin, cytokinins, ethylene, abscisic acid, and gibberellins (Zhao, 2010, Wullschleger et al., 2006). Phytohormones, including salicylic acid (SA), jasmonic acid (JA), and ethylene (ET), are mainly involved in plant defense mechanisms (Derksen et al., 2013, Robert-Seilaniantz et al., 2011). Whereas auxin (Aux), abscisic acid (ABA), brassinosteroids (BR), cytokinins (CK), and gibberellins (GA) are mainly involved in plant developmental and physiological processes. Interestingly, extensive interaction (cross-talk) between the different phytohormone pathways occurs to regulate responses to abiotic and biotic factors, i.e., environmental factors and pathogen (Santner and Estelle, 2009, Chow and McCourt, 2006, Durbak et al., 2012, Depuydt and Hardtke, 2011, Robert-Seilaniantz et al., 2011, Song et al., 2014).

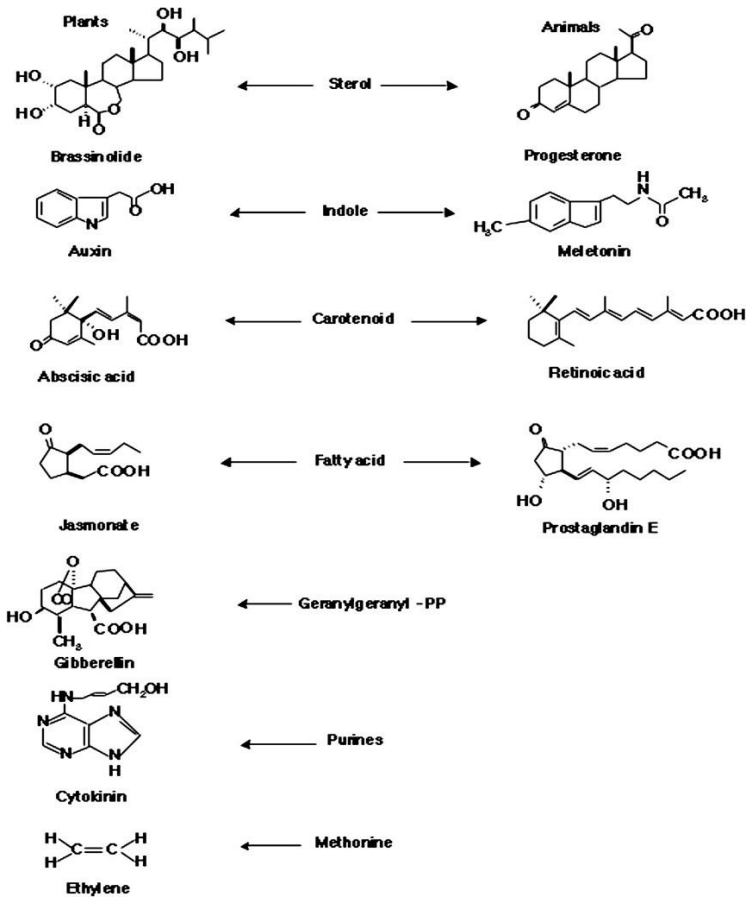

Figure 1.6. The chemical structure of phytohormones and animal hormones. The names in the middle represent the hormones precursors (Chow and McCourt, 2006). Adapted from Chow et al., (2006).

1.7.2. Auxin signalling

Auxins are compounds consisting of an aromatic ring and a carboxylic acid group. The complete pathway of de novo auxin biosynthesis in plants has not yet been established (Zhao, 2010). Recent studies uncovered several genes in tryptophan-dependent auxin biosynthesis pathways, and transportation of auxin to specific tissues would trigger a signalling cascade leading to developmental responses, such as polarity of the root-shoot axis during embryogenesis, cell elongation, cell differentiation, apical dominance, lateral root formation, and adventitious root formation and fruit formation (Benjamins and Scheres, 2008). Auxin transportation is unique as it displays directionality, which

is shown by the specific subcellular localization of auxin efflux and auxin influx machinery (Benjamins et al., 2005, Benjamins and Scheres, 2008). The subcellular targeting of these fundamental proteins is controlled by components involved in endosomal trafficking, the phosphorylation status of the proteins, and components that determine membrane composition. (Friml et al., 2004, Geldner et al., 2003, Michniewicz et al., 2007, Willemsen et al., 2003). One of the important members of the auxin family in the plant is the indole-3-acetic acid (IAA), which is the most predominant form of auxin in plants (Bonner and Bandurski, 1952, Zhao, 2010, Zhao, 2008, Stone et al., 2008). The IAA can be produced from tryptophan (Trp) via the Trp-dependent pathways or an indolic Trp precursor via Trp-independent pathways (Woodward and Bartel, 2005, Jiang et al., 2017). The IAA can be transported across the whole plant from the shoot to the root, necessary for normal development and tropic responses. A second endogenous auxin is an indole-3-butyric acid (IBA), which can also be oxidized to produce IAA. The IAA and IBA are known to impact the morphology of newly gown plants, particularly in root generation (Sevik and Guney, 2013). The IAA, 4-chloroindole-3-acetic acid (4-Cl-IAA), and phenylacetic acid (PAA) are active forms of auxin. The indole-3-pyruvic acid (IPA), indole acetamine (IAM), indole-3-acetaldoxime (IAOx), indole-3-acetonitrile (IAN), and indole-3-acetaldehyde (IAAld) are inactive auxin precursors. The IBA, methyl-IAA (MeIAA), and auxins conjugated to amino acids or sugars are storage forms of auxin. Together, these forms of auxin modulate the levels of active auxin in plants, i.e., IAA can be produced by biosynthesis or release from conjugates (Jiang et al., 2017, Sevik and Guney, 2013, Durbak et al., 2012, Vanneste and Friml, 2009). Auxin interacts with specific receptors, which are characterized to be a member of the TRANSPORT INHIBITOR RESPONSE 1 (TIR1) family, directing the proteolysis of AUXIN/INDOLE-3- ACETIC ACID (Aux/IAA) proteins and prompting inhibitory effect on transcription factors that regulate auxin gene expression, AUXIN RESPONSE FACTORS (ARFs) (Fukaki et al., 2002, Chapman and Estelle, 2009). Auxin is synthesized in aerial tissues (e.g., apical meristems) and locally and systemically transported throughout the plant. The polar auxin transport (PAT) is known to be the cell-to-cell active movement, while the direct and rapid transport of auxin is from shoots to roots through the phloem (Vanneste and Friml, 2009, Spalding, 2013).

The PAT contains two general types of transporters, the auxin influx carriers that pumps auxin into the cell, AUXIN RESISTANT 1 (AUX1) and LIKE AUXIN RESISTANT 1 (LAX1), and the auxin efflux carriers that pump auxin out of the cell: PIN-FORMED (PIN) and ATP- binding cassette type B (ABCB) families (Spalding, 2013). Another class of auxin carriers that have also been identified based on their structural similarity to the PIN family is the PIN-LIKES (PILS) (Figure 1.7 A).

The PIN proteins localization within the cell affects the auxin transport direction (Barbez et al., 2012). The relationship between hormones signalling and TOR regulation is not well defined, although studies have shown that TOR is activated by auxin and regulates expression of auxin-responsive genes by supporting translation (Schepetilnikov et al., 2013). TOR plays a vital role at the crossroad of the plasma membrane and nuclear auxin signalling pathways to link auxin with general nutrient signalling (Schepetilnikov et al., 2013, Bogre et al., 2013). Downregulation of both abscisic acid synthesis and response resulted in the long-term inhibition of the TORC1, TOR high-molecular-mass complex 1 (Kravchenko et al., 2015). The most convincing example that insight hormonal and TOR signalling association is the activation of TOR by auxin. Auxin at high concentration in the root meristem will activate TOR and regulate shoot development, suggesting that auxin is an upstream signal TOR pathway. Also, modulating TOR might lead auxin to indirectly modulate the brassinosteroids (BR) signalling, where TOR inhibits autophagy and controls the accumulation of the brassinosteroid signaling transcription factor BZR1(Dobrenel et al., 2016, Zhang et al., 2016). Additionally, the S6K2 is a TOR kinase substrate that phosphorylates Brassinosteroid Insensitive 2 (BIN2), a downstream effector of the TOR signaling pathway that regulates photoautotrophic growth in Arabidopsis (Xiong et al., 2017, Dobrenel et al., 2016, Jiang et al., 2017). However, TOR-AUX-BR interaction needs to be experimentally further verified. Auxin activates TOR, where activated TOR phosphorylates the inactive S6K resulting in its activation and dissociating from the polysomes (Schepetilnikov et al., 2013, Jiang et al., 2017). Consequently, the S6K will selectively regulate mRNAs' translation of genes involved in phytohormone responses, sugar signalling, and cellular metabolism. Moreover, the active S6K will phosphorylate

translation initiation factors (eIFs) such as eIF3h in TOR- dependent manner, which will regulate translation reinitiation in response to auxin (Figure1. 5 A & B)(Inaba and Nagy, 2018, Schepetilnikov et al., 2013, Bogre et al., 2013).

Moreover, the contribution of TOR activity to downstream auxin signalling mediated processes suggested that the TOR pathway overlays at least partially with some phytohormone responses (Schepetilnikov et al., 2013, Menand et al., 2004, Bogre et al., 2013). This was confirmed by transcriptomic analysis of seedlings treated with the TOR inhibitor AZD-8055, in which the expression of some genes involved in the abscisic acid, ET/JA, and SA pathways were upregulated. In contrast, some genes involved in the auxin, cytokinin, brassinosteroid, and gibberellin pathways were suppressed (Dong et al., 2015).

In summary, TOR interact with auxin signalling to regulate translation preinitiation, where protein translation selection of central transcriptional regulators could determine and regulate auxin-responsive transcription within the nucleus. The TOR and S6 kinase (S6K) signalling pathway regulators the balance between growth and proliferation through several mechanisms (Figure 1.7 and 1.7) and is important for the directional growth regulated by auxin.

Due to the multifunction role of P6 and what it has already published about P6 impact on plant responses, I am interested in taking the P6 study further to determine the P6-TOR interaction and their effect on phytohormones such as SA, ET, and auxin and how this might affect the host's susceptibility, growth, and development.

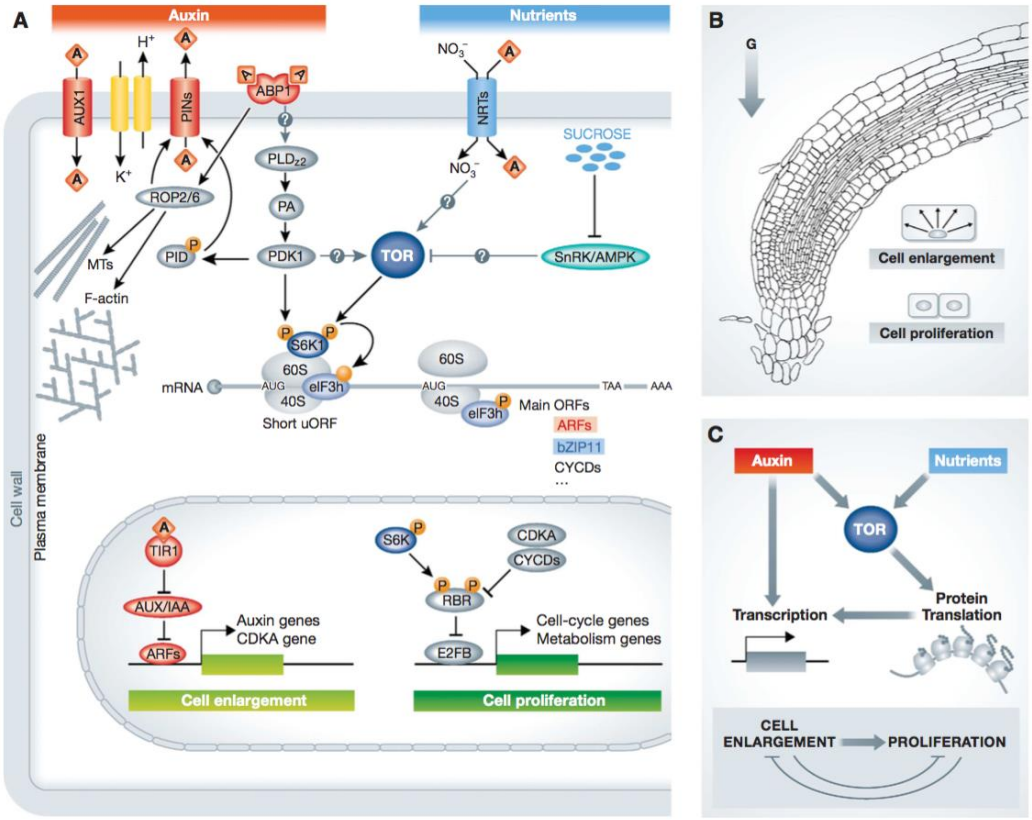

Figure 1.7. Cell growth and proliferation are regulated by growth hormones, auxin, and nutrients. (A) Auxin signalling modules are labeled in red. The signal transduction of auxin through the receptor system and TOR regulates the selective translation based on nutrient signalling. (B) Plant growth is dependent on environmental conditions. The auxin abundancy in epidermal layers controls the gravitropic growth of roots, where Aux-TOR interaction was involved in the selective cell enlargement and cell proliferation, demonstrated by Schepetilnikov et al. (2013). (C) TOR incorporates auxin and nutrient signalling mainly by regulation of protein translation, in which selective protein translation of vital transcriptional regulators will regulate the auxin-responsive transcription. Protein translation supports growth that direct cell proliferation (Bogre et al., 2013). Adapted from Bogre et al., (2013).

1.7.3. Ethylene signalling

Ethylene is a plant hormone involved in developmental processes and fitness responses such as germination, senescence, ripening, abscission, root nodulation, programmed cell death, biotic stresses (responses to the pathogen), and abiotic stresses (Bleecker and Kende, 2000, Johnson and Ecker, 1998). Ethylene drives the so-called 'triple response' of dicotyledonous seedlings described by the inhibition of hypocotyl and root cell elongation, swelling of the hypocotyl, and curving of the apical hook (Guo and Ecker, 2004). The results of Boutrot et al. (2010) show a direct role for ET signalling in the modulation of an innate immune receptor, particularly the pathogen-associated molecular pattern triggered immunity (PAMPs) in which mutation in the plant ET-signalling protein EIN2 compromised the plant leucine-rich repeat receptor kinase FLS2-mediated responses. These constrained responses were suggested to be associated with the reduction in the FLS2 expression and protein accumulation. Moreover, the FLS2 expression is also impacted by the EIN3, and EIN3-like transcription factors controls. These findings highlight that ET signalling has a direct impact on the innate immune and defense responses (Figure 1.8) (Song et al., 2014, Gimenez-Ibanez and Solano, 2013, Derksen et al., 2013, Robert-Seilaniantz et al., 2011, Boutrot et al., 2010). Also, pathogen proteins such as P6 of CaMV were shown to alter the plant responses, in which transgenic Arabidopsis plants expressing P6 demonstrated an ET-insensitive phenotype (Geri et al., 2004, Geri et al., 1999). Next, Zvereva et al (2016) revealed that P6 mediates the suppression of oxidative burst and SA-dependent autophagy, promotes bacterial infection to the plants, and TOR binding domain is required to suppress these plant defense responses (Zvereva et al., 2016). This might suggest that P6-TOR interaction is also required to develop these phenotypes by modulating and interacting with the ET pathway components.

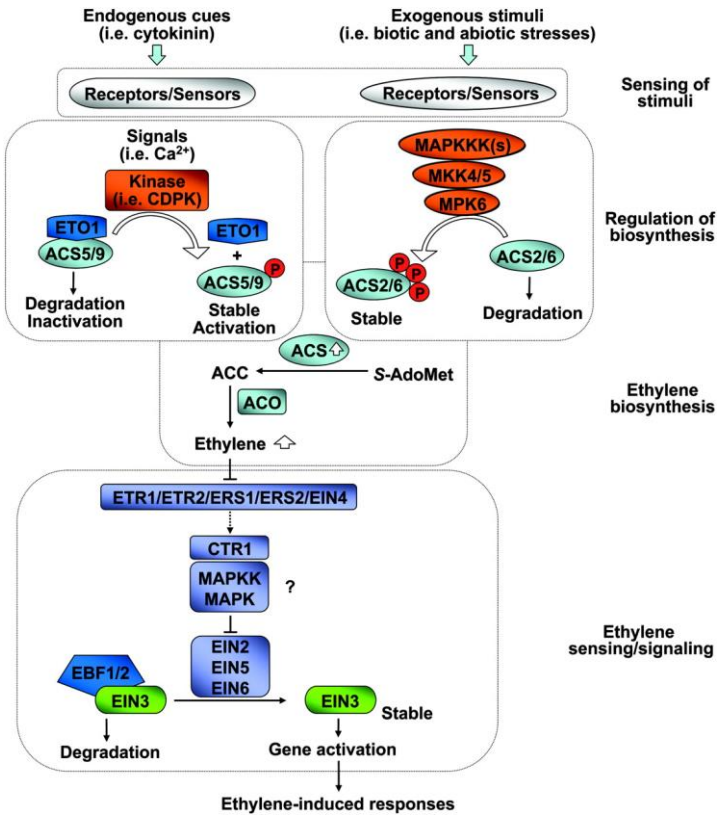

Figure 1.8. Model of ethylene biosynthesis and the downstream ethylene sensing / signalling pathway. Internal and external factors direct the induction or suppression of ethylene biosynthesis. An increase in the ACS activity induces ET biosynthesis. Phosphorylation of ACS5 and ACS6 will activate and induce the interaction with ET expression factors and pathway components. The stress will impact the ACS6 activity, hence modulating the ET responses. The ACC oxidase (ACO) activity will also modulate the ET biosynthesis. The EIN2, EIN5, EIN6, and EIN3 are positive regulators of ethylene pathways where they will trigger gene expression and modulate ethylene responses. The ER-associated receptors family: including ETR1, ETR2, ERS1, ERS2, and EIN4, will also modulate ET responses and biosynthesis. The CTR1 is considered to be a negative regulator of ET responses. Adapted from Ecker et al (2004).

1.8. The target of rapamycin (TOR)

The target of rapamycin (TOR) protein kinase is a vital regulatory protein that plays a central role in regulating transcription, translation, and metabolism to support cell proliferation, growth, metabolism, interconnected signalling, and stress responses in yeasts, plants, and animals, in which TOR is modulated by nutrient, cellular energy status, hormones, and stress inputs (Dobrenel et al., 2016, Shimobayashi and Hall, 2014, Xiong and Sheen, 2014, Aramburu et al., 2014, Robaglia et al., 2012, Loewith and Hall, 2011). TOR is an uncommon serine/threonine protein kinase (PK) that is closely related to the phosphatidylinositol 3-kinase-related protein kinase (PIKK) family, conserved among yeasts, plants, and humans, where PIKKs contain a lipid PI3K-like catalytic domain bordered on the N-terminal and FAT-FRB-kinase-FATC domains on the C-terminal region as shown in Figure 1.10. The N-terminal part of TOR contains several HEAT repeats, a tandem repeat protein structural motif consisting of two α-helices linked by a short loop, which participates in protein-protein interactions (Lieberthal and Levine, 2012, Dobrenel et al., 2016, Xiong and Sheen, 2014).

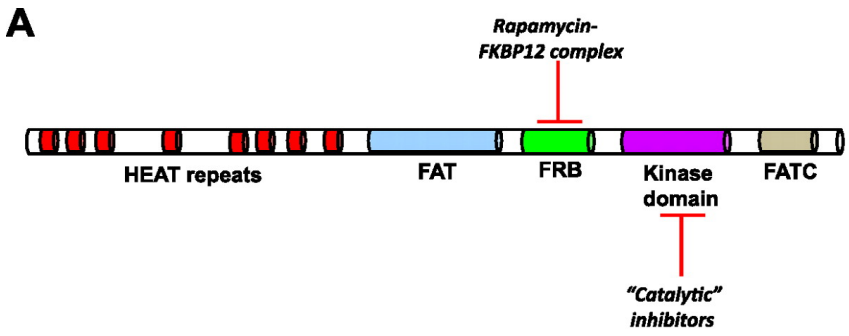

Figure 1.10. Domain structure of mammalian target of rapamycin (mTOR) kinase. Adapted from Lieberthal W et al (2012).

TOR substrates in animals and yeasts, such as ribosomal protein S6 kinase (S6K) and the type 2A phosphatase associated protein 42 (TAP42)/α4 subunit of protein phosphatase 2A (PP2A), are found in plants (Schmelzle et al., 2004, Wullschleger et al., 2006). In the Arabidopsis genome, there are two S6K-encoding genes (S6K1 and

S6K2) sharing similarity to S6K sequences from yeast and animal. The S6K activity is triggered by auxin, which appears to increase the amount of TOR protein in Arabidopsis (Dobrenel et al., 2016, Barrada et al., 2015, Menand et al., 2004). Figure 1.11 represents examples of the interactions that occur between TOR and effector kinases and substrates. In plant effectors, such as PI3K, αKG, glucose, and SnRK1, direct the TOR to phosphorylate substrates, S6K, Tap46, and E2F Atg13 Atg1, leading to the regulation of translation, N assimilation, cell division, and autophagy, respectively (Dobrenel et al., 2016). It was found from previous work (Zvereva et al., 2016) that TOR binds to the P6 protein of CaMV at the N-terminus, including the TOR-binding site, which might affect the phytohormone pathway regulation such as auxin signalling (hormones of interest in this study).

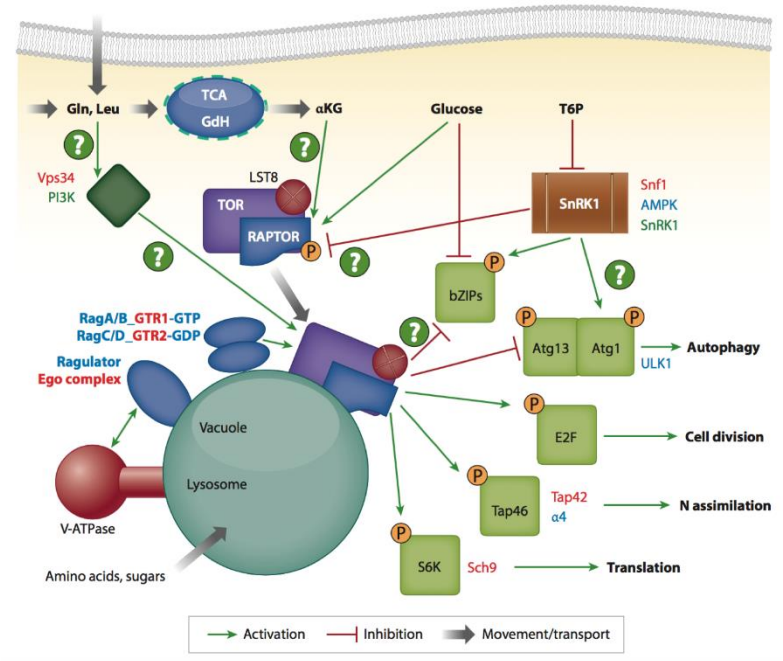

Figure 1.11. A representational model of TOR regulation by nutrients, presenting the several ways in which nutrients regulate the TOR kinase and the interactions between TOR and effector kinases and substrates in eukaryotes. The names of the regulatory or substrate proteins of animals, yeasts, and plants are indicated in blue,

red, and green, respectively (Dobrenel et al., 2016). Adapted from Dobrenel et al., (2016).

1.9. Project aims

To expand our understanding of the P6 role and impact on hosts, particularly for their role in modulating phytohormonal signalling pathways, more specifically the ET signalling pathway and the auxin signalling pathway, I proposed to pursue these objectives:

1) To determine if P6 expression impacts plant phenotype or genotype.

2) To characterize the role of P6 as a pathogenicity effector in regulating all aspects of phytohormone signalling and its regulation specificity, particularly its ability to modulate auxin and ethylene signaling

3) To study the impact of P6-TOR interaction in modulating phytohormones signalling, auxin and ethylene signalling.

4) To determine the P6 expression impact on host gene expression and responsive genes involved phytohormone signalling (auxin and ethylene signalling), and defense response.

5) To identify P6 host interactors which might be involved in phytohormones regulation, P6 mode of interaction, and the interaction role in the virus infection cycle.

1.10. Study design

We conducted a series of studies on wild-type Arabidopsis plants and transgenic Arabidopsis plants, either expressing P6 or mutant version of P6 (ΔTOR). The lines were grown on sterile soil and half-strength Murashige and Skoog (1⁄2 MS) salt media agar plates at 22 °C under 16 hrs day length. Two weeks old seedlings were harvested

and processed for PCR, Western blot, proteomics, and transcriptomics analysis. The P6 impact on Arabidopsis' ethylene sensitivity was determined by measuring the root and shoot length using Fiji analysis software after one week of incubation. Also, P6 impact on auxin inhibitor resistance was measured by counting the number of successfully germinated seeds and compared between the wild type and P6 transgenic Arabidopsis lines. Lastly, determining the P6 expression impact on host gene expression profile for responsive genes involved phytohormones signalling, such as auxin and ethylene signalling, and defense responses. Tissues from these lines were also collected and analyzed to identify the critical gene transcripts associated with phytohormone signalling pathways. However, a metabolic study needs to be carried out because the collected gene expression data would not highlight the downstream impact on translation, post-transcriptional regulation, and modifications. This study reveals the importance of the transcriptome in predicting viral protein impact on the host plant.

Furthermore, this study's results expand our understanding of the multifunctional role of CaMV P6 and support the concept that P6 modulates phytohormone synthesis, signalling pathways, and plant defense response, and TOR might play a role in this regulation. This study highlights the molecular role and multifunctional nature of CaMV P6 and demonstrates its similarities to other viral proteins. Moreover, investigating pathogen-plant interaction at the molecular level, such as studying the P6-host interaction, will help us acquire the knowledge that will help us improve crop production efficiency and sustainability.

Chapter II: Materials and Methods

2.1. Seeds surface sterilization

The desired number of seeds (50 µl) was kept in a 1.5ml Eppendorf tube. Next, 1ml of 100% ethanol was added, mixed by inverting tube, and incubated for 1 min, then discarded using a 1000 µl pipette. The sterilization buffer of 1 ml: 2.5% Sodium Hypochloride + 0.1% Tween 20 was added, mixed by inverting the tube for every 2 min and incubated for 5 min, then discarded using a 1000 µl pipette. The seeds were washed with 1ml of sterile water, then the water was discarded using a 1000 µl pipette. This step was repeated five times, except in the last repeat, where the sterile water was kept (Clough and Bent, 1998). The tube was warped with aluminum foil and kept in the fridge at 4°C for two days. All the work was carried under a laminar flow hood.

2.2. Plants and growth conditions

Sterilized seeds were sown on sterile soil or half-strength Murashige and Skoog (1⁄2 MS) salt media (Sigma-Aldrich Corporation, Westport Center Dr, St. Louis, MO, USA) with 0.8% phytoagar and grown at 22°C under 16 hrs day length continuous white light (120 µmol m-2 s1) and 8 hrs dark with 60% humidity. The lines used in this study were the previously constructed transgenic line A7 that express P6WT transgene under the control of 35s promoter in Ler gl1 background (Cecchini et al., 1997) and newly constructed transgenic lines in Table 4.1.

2.3. DNA isolation

2.3.1. Genomic DNA isolation from Arabidopsis lines

Leaves from wild-type and transgenic lines were collected. Total genomic DNA was extracted from leaves with a modified Dellaporta method (Dellaporta SL, 1983, Chen et al., 2009). The leaves were ground in 500 µl of grinding buffer (100 mM Tris pH8, 50

mM EDTA, 500 mM NaCl, 10 mM 2-mercaptoethanol) with sterile pestles, then 33 µl of 20% SDS was added, vortex for 2 minutes, and incubated for 10 minutes at 65°C. Next, 160 µl 5M KoAc was added, vortex for 2 minutes, kept on ice for 10 minutes and spin for 10 minutes at 13000 rpm. 450 µl of supernatant was removed to new sterile tube. Then add 0.5 volume of isopropenal, 225 µl, vortex for up to 30 seconds kept on ice for 10 minutes and spin for 10 minutes at 13000 rpm. Remove the supernatant and wash the pellet with 500 µl 70% ethanol, spin for 10 minutes at 13000 rpm. Carefully remove the supernatant as much of as possible. The resultant DNA pellet was dried, resuspended in 50-100 µl of sterile distilled water, and 1-5 µl of the DNA solution was used in the PCR.

2.3.2. Plasmid extraction

The transformed *Escherichia coli* (E. coli) with the plasmid of interest were grown in 5ml of Luria Broth (LB) containing the corresponding selective antibiotic for 24hrs at 37°C and 180 rpm. Pellet the cells by centrifugation at 13,000 rpm for 5min under room temperature and discard the supernatant. The pelleted cells were treated according to the QIAprep Spin Miniprep Kit (Qiagen, # 27106) manufacturer's instructions. The plasmids were extracted following the manufacture protocol, except the plasmids were eluted with 20-50 µl of warm 50°C sterile distilled water instead of the elution solution.

2.3.3. Polymerase chain reaction (PCR)

Transgene DNA detection was carried out using GoTaq G2 Hot Start Green Master Mix (Promega Corporation, Delta House, Southampton Science Park, Southampton SO16 7NS, UK) using specific primer pair sets for each of the transgene and PCR reactions conditions. Following manufacturer's protocol, single PCR reaction (25µl) contain: 12.5µl of GoTaq® G2 Hot Start Green,1.0µl of forward primer (10µM), 1.0µl of reverse primer (10µM), extracted DNA 5µl (<250ng), and 5.5µl Nuclease-Free Water. The PCR conditions used to detect P6 and P6 (ΔTOR) transgenes were as follows; initially denatured for 2 min at 95ºC; followed by 30 cycles of 30 s denaturation at 95ºC, 1 min

annealing at 55ºC, and 1.40 min extension at 72ºC, finally kept at 4ºC for further analysis. The primer pair sets are described in Table 2.1. The expected size of PCR-amplified DNA fragments is ~1.6-kb. The PCR conditions used to amplify P6WT-GFP and P6(ΔTOR)-GFP transgenes were as follows; initially denatured for 2 min at 95ºC; then 30cycles of 30 s denaturation at 95ºC, 1 min annealing at 63ºC, 3 min extension at 72ºC, and finally incubated at 4ºC for further analysis. Table 2.1The primer pair sets are described in Table 2.2. The expected size of PCR-amplified DNA fragments is ~2.4-kb. Independent biological triplicate was carried out for each sample.

P6 PCR primer pairs sequences
P6 608 forward: CACCATGGAGAACATAGAAAAACTCCTC
P6 608 reverse: ATCCACTTGCTT TGAAGACG

Table 2.1. Primer set used for the polymerase chain reaction. The expected size of PCR-amplified DNA fragments is ~1.6 kb.

2.3.4. DNA gel electrophoresis

The PCR products were loaded in SYBR Safe stained 0.8 % agarose gel (w/v) (Thermo Fisher Scientific 3 Fountain Dr, Inchinnan, Renfrew PA4 9RF, UK, # S33102) with 0.5x Tris Borate EDTA (TBE) buffer (90 mM Tris-HCL, 90 mM Boric acid, 2 mM EDTA). The plant genomic DNA or plasmid samples were mixed with a 6x loading buffer (New England Biolabs, County Road Ipswich, MA, USA, #B7025) before loading them into the gel. The samples were resolved with by applying ~90 volts for 35min.The gels were visualized using the ChemiDoc™ MP Imaging System (Bio-Rad Laboratories Ltd., Hertfordshire, UK), and the DNA bands were detected.

2.3.5. Gel extraction

The digested vector and PCR were resolved following the previous conditions. Then gel was visualized under a blue LED light visualizer, and using sterile razors, the bands

of interest were sliced and kept into 2mL Eppendorf. The DNA from the sliced gel was extracted using a Qiagen Gel extraction kit, following the manufacture's protocol.

2.3.6. Construction of transgenic Arabidopsis lines

To identify the mechanisms involved, we have constructed transgenic Arabidopsis lines that express two different P6 variants fused to a C-terminal GFP tag; P6WT, containing the wild-type P6 sequence, and P6(ΔTOR), mutant with a deletion in the TOR-binding domain (comprising a deletion in amino acids 136–182). Proteins are either expressed constitutively from a 35S promoter or an β-estradiol-inducible promoter.

2.3.6.1. Construction of Ti plasmids

Gibson assembly PCR primer pair sets designed using NEB Builder web. The full-length clone of P6WT-GFP and P6(∆TOR)-GFP was released from pGWB5 plasmids by PCR amplification with the use of Phusion DNA Polymerase (New England Biolabs, County Road Ipswich, MA, USA) and the Gibson assembly PCR primer pair sets (Table 2.2). The PCR product was subsequently cloned into SpeI and digested pER8 (Zuo et al., 2000), and HindIII digested pEZR (Christie et al., 2002) plasmids using Gibson cloning kit (New England Biolabs, County Road Ipswich, MA, USA) (Gibson et al., 2009, Gibson et al., 2010) following the manufacture protocol to generate pER8-P6WT-GFP, pER8-P6(∆TOR)-GFP, pEZR-P6WT-GFP and pEZR-P6(∆TOR)-GFP.

Gibson assembly PCR primer pairs sequences	
pER8	pER8 forward: GGCCCAGGCCTACGCGTTTAATTAACACCATGGAGAACATAGAAAAAC pER8 reverse: ACGAAAGCTGGGAGGCCTGGATCGATTACTTGTACAGCTCGTCCATG
pEZR	pEZR forward: AGAGGACACGCTCGAGCTCACACCATGGAGAACATAGAAAAAC pEZR reverse: CCGTCGACTGCAGAATTCGATTACTTGTACAGCTCGTCCATG

Table 2.2. List of Gibson assembly PCR primer pairs sequences.

2.3.6.2. Transformation of *E. coli*

The generated constructs were chemically transformed into NEB 5-alpha Competent *E. coli* (High Efficiency, NEB #C2987) provided with the Gibson kit. Transformants were identified based on growth on media supplemented with spectinomycin (100 µg/mL) for pER8 and kanamycin (50 µg/mL) for pEZR, coupled with PCR analysis with the Gibson assembly PCR primer pairs for the detection of P6WT-GFP and P6(∆TOR)–GFP, restriction enzyme digestion analysis, and sequencing. Reaction tube insertion fragments and cloning vectors (empty vector) were used as the negative controls (Gibson et al., 2009, Gibson et al., 2010).

2.3.6.3. Development of Agrobacterium inoculation systems

The binary vectors, pER8-P6WT-GFP, pER8-P6(∆TOR)-GFP, pEZR-P6WT-GFP, and pEZR-P6(∆TOR)-GFP were validated and transformed into chemically competent *Agrobacterium tumefaciens* (GV3101). Transformants were identified based on growth at 28ºC after 2-3 days on media supplemented with spectinomycin (100 µg/mL) for pER8 and kanamycin (50 µg/mL) for pEZR, followed by PCR analysis for the isolated plasmid with the Gibson assembly PCR primer pair sets for the detection of P6WT-GFP

and P6(ΔTOR)-GFP. Reaction tube insertion fragments and cloning vectors (empty vector) were used as the negative controls (Kon and Gilbertson, 2012, Chen et al., 2009, Martiniere et al., 2009).

2.3.6.4. Transient expression in *Nicotiana benthamiana*

The developed *A. tumefaciens* strain GV3101 transformed with pER8-P6WT-GFP, pER8-P6(ΔTOR)-GFP, pEZR-P6WT-GFP, and pEZR-P6(ΔTOR)-GFP plasmids were used for agroinfiltration assays. The Transformants were grown overnight in LB media supplemented with spectinomycin (100 µg/mL) for pER8 and kanamycin (50 µg/mL) for pEZR with shaking at 180 rpm and 28ºC. The cells were centrifuged at 4000 rpm for 8-10 minutes, and the supernatant was removed carefully. The pelleted cells were resuspended in agroinfiltration buffer (10 mM MgCl2, 100 µM Acetosyringone). Leaves of *N. benthamiana* seedlings (~ 3 weeks old) were infiltrated with the agrobacterial suspension at OD600 = 0.4 using a 1ml syringe on the backside of leaves. The leaves were collected 2-3 dpi and processed for confocal microscope examination and western blot analysis. Note that one day post-infiltration, infiltrated leaves with pER8-P6WT-GFP and pER8-P6(ΔTOR)-GFP were painted with 50 0r 100 µM β-estradiol; 5% ethanol was the β-estradiol solvent (Leuzinger et al., 2013).

2.3.6.5. Floral dipping

Transformations of *Arabidopsis thaliana* Col-0 were performed by following the modified floral dip protocol (Clough and Bent, 1998, Davis et al., 2009), using *Agrobacterium tumefaciens* strain GV3101 transformed with either pER8-P6WT-GFP, pER8-P6(ΔTOR)-GFP, pEZR-P6WT-GFP, or pEZR-P6(ΔTOR)-GFP plasmids. The following binary plasmids pER8-P6WT-GFP and pER8-P6(ΔTOR)-GFP plasmids will add resistance phenotype to seedlings grown in the presence of Hygromycin B resistance, and pEZR-P6WT-GFP and pEZR-P6(ΔTOR)-GFP plasmids will add kanamycin resistance. The following non-transformed Arabidopsis seeds were used for transformations, and as negative controls, Col-0 and previously characterized

transgenic line A7 were used as positive controls for Hygromycin resistance. The selection of transgenic seeds was on 1⁄2 MS agar plates containing 50 µg/ml Hygromycin B for pER8-P6WT-GFP and pER8-P6(∆TOR)-GFP and on 1⁄2 MS agar plates containing kanamycin (50 µg/mL) for pEZR-P6WT-GFP and pEZR-P6(∆TOR)-GFP, incubated ~2 weeks (Harrison et al., 2006, Davis et al., 2009, Cecchini et al., 1997). The 2 weeks old resistance seedlings were transferred to soil and grown in long day growth chamber or green house for seed collection after 2-3 months.

2.3.6.6. Selection of transgenic plants

Seeds of transformed Arabidopsis were collected and sterilized, as mentioned earlier. Seeds were then stratified for 2 d in the dark at 4°C. Sterilized seeds were sown onto 0.8% agar containing ½ MS medium (Harrison et al., 2006) and Kanamycin at a concentration of 50 µg/mL (Sigma-Aldrich Corporation, Westport Center Dr, St. Louis, MO, USA. # 10106801001 Roche) or Hygromycin B at a concentration of 50 µg/mL (Thermo Fisher Scientific 3 Fountain Dr, Inchinnan, Renfrew PA4 9RF, UK. # 10687010) grown for two weeks at 22 °C under 16 hrs day length continuous white light (120 µmol m-2 s1) and 8 hrs dark with 60% humidity. The potential transgenic seedlings were rescued on soil and grown on long day growth chamber or green house for seed collection after 2-3 months. Note that the germination ratio for T2 seeds should be 3:1 or ~ 75%, and for T3 seeds should be ~ 100% of the homozygous line.

2.3.7. Reporter gene detection

2.3.7.1. Confocal microscopy

The presence of GFP in 2cm leaf disc samples from 2-week-old kanamycin-resistant seedlings: pEZR-P6WT-GFP and pEZR-P6(∆TOR)-GFP, and Hygromycin B-resistant seedlings: pER8-P6WT-GFP and pER8-P6(∆TOR)-GFP after induction by growing them on 1⁄2 MS plant containing 30µM β-estradiol or spray them with 50µM β-estradiol on the 9 day, was detected using Zeus or Leica confocal microscope coupled with

western blot analysis and transgene PCR detection. The Confocal Microscope settings were used to detect the GFP expression was 488 nm excitation wavelength, 10% power, green channel (wavelengths 495 - 552 nm) were for GFP detection, and red channel (wavelengths 620 - 690 nm) were offset GFP spectrum.

2.3.7.2. Transgene detection

Leaves of construed lines were collected after two weeks of incubation. Total genomic DNA was extracted as previously described using the modified Dellaporta method (Dellaporta SL, 1983, Chen et al., 2009) described above in section 2.3.1. Gibson Assembly primer pairs (Table 2.2) were used for transgenes DNA detection. The expected size of PCR-amplified DNA fragments was ~2.4-kb.

2.4. protein electrophoresis and western blot analysis

2.4.1. Protein extraction from plant tissue

Plant leaves were collected in Eppendorf tubes and homogenized using a sterile pistol and SDS loading buffer (62.5 mM Tris-HCl, pH 6.8, 2% SDS, 10% glycerol, 5% β-mercaptoethanol, 0.004% bromophenol blue), boiled at 100°C for 5 min and centrifuged for 10min at 13,000 g. The supernatant was transformed into new Eppendorf tubes and kept on ice or in the fridge at 4°C.

2.4.2. SDS-Polyacrylamide Gel Electrophoresis (SDS-PAGE) and protein transformation

The extracted proteins were separated on a 10% SDS-PAGE, then transferred onto nitrocellulose membrane by electroblotting following the Invitrogen mini-tank manual protocol (A25977). The protein ladder was SeeBlue Plus2 Pre-Stained Standard, and the buffers were NUPAGE MES SDS running buffer and transfer buffer (Invitrogen, NP0002, and NP00061).

2.4.3. Immunodetection

After transformation, the membrane was washed with 1xTBS and stained with Ponceau S for ~1 min to visualize and confirm protein transformation. The membrane was distained by multiple washes with 1x TBS with 0.1%Tween20 (TBST), then washed by distilled water. The membrane was blocked with 8% non-fat dried milk in 1xTBS for 1 hour at room temperature with gentle shaking. Then the membrane was washed with 1x TBS for 5 min at room temperature with gentle shaking; this step was repeated three times. The membrane was kept with 1:1000 dilution of Primary Antibody in 2% milk 1X TBS overnight at 4Co with gentle shaking. The membrane was washed with 1xTBST for 10 min with gentle shaking; this step was repeated three times. The membrane was incubated with 1:10000 dilution of horseradish peroxidase (HRP)-linked secondary antibody (anti-rabbit IgG- HRP, # W4011 Promega) in 1X TBS for an hour at room temperature with gentle shaking. The membrane was washed with 1x TBS with 0.1%Tween20 and 0.05% Titron (TBSTT) for 10 min at room temperature with gentle shaking; this step was repeated three times. The membrane was washed with sterile water and developed with Pierce ECL Plus Western Blotting Substrate (Thermo Fisher Scientific) to visualize protein bands. Note that the primer antibody used to detect the protein expression was an anti-P6 polyclonal antibody, HRP or anti-GFP Polyclonal Antibody, HRP (# A10260, Thermo Fisher Scientific).

2.4.4. Coomassie blue staining

The SDS- page was stained using ~ 10ml of SimplyBlue Safe Stain (Thermo Fisher Scientific 3 Fountain Dr, Inchinnan, Renfrew PA4 9RF, UK) and microwaved for 3-5 min then kept on a shaker for 2hrs to overnight. Then the gel was washed with sterile water and photographed.

2.5. Physiological measurements

To identify the P6 impact on the phytohormones signalling pathway and plant responses by measuring the sensitivity of transgenic lines expressing P6 and mutant version of P6 to ethylene precursor or auxin transport inhibitor.

2.5.1. Determination of plant sensitivity to ethylene

To identify the modifications in plant responses to ethylene; 12 sterilized seeds of tested Arabidopsis lines (Ler-gl1, A7, Col-0, pER8-P6WT-GFP, pER8-P6(ΔTOR)-GFP, pEZR-P6WT-GFP, and pEZR-P6(ΔTOR)-GFP) were sown and cultured on 1⁄2 MS plates containing different 1-Aminocyclopropane-1-carboxylic acid (ACC) (Sigma-Aldrich Corporation, Westport Center Dr, St. Louis, MO, USA) concentrations (0 µM,1µM, 3 µM, and 5 µM). The plates were kept vertically in the darkroom for five days at room temperature. The estradiol inducible lines were grown on plates containing the different TIBA concentrations with or without 30µM β-estradiol. The treatments were carried in 3 independent biological replicates for each tested line. ACC is an ethylene precursor used in place of ethylene gas (Merchante and Stepanova, 2017). The plates were scanned using an Epson Scanner, and the root and shoot measurements were taken using Fiji analysis software after five days of incubation.

2.5.2. Determination of plant sensitivity to an auxin transport inhibitor

To identify the P6 impact on the auxin signalling pathways; 12 sterilized seeds of tested Arabidopsis lines were sown and cultured on 1⁄2 MS plates containing different TIBA (2,3,5-triiodobenzoic acid) (Sigma-Aldrich Corporation, Westport Center Dr, St. Louis, MO, USA) concentrations (10 µM, 20 µM, 30 µM, 40 µM, 50 µM, 60 µM, 70 µM, and 100 µM). Plates were kept in a growth chamber at 22 °C under 16 hours of continuous white light (120 µmol m-2 s1) and 8 hours dark with 60% humidity for two weeks. The estradiol inducible lines were grown on plates containing the different TIBA concentrations with or without 30µM β-estradiol. Germination rate measurements of the

different tested Arabidopsis lines were taken based on successfully germinated seeds after two weeks. Three independent biological replicates for each tested line were carried out. TIBA is an auxin transport inhibitor (ATIs), which interferes with directional auxin transport by inhibiting vesicle motility, auxin transport, and plant development (involving auxin transport-dependent developments). It also has a lethal effect on plants at a certain concentration (Dhonukshe et al., 2008, Merchante and Stepanova, 2017).

2.5.3. Statistical analysis

Statistical differences in the seedlings' total length between the different tested Arabidopsis lines under different ACC concentration (0 µM,1 µM, 3 µM, and 5 µM) or differences in the germination rate under different TIBA concentration (10 µM, 20 µM, 30 µM, 40 µM, 50 µM, 60 µM, 70 µM, and 100 µM) were assessed by a two-way analysis of variance (ANOVA) using Statistical Analysis System – JMP (SAS JMP®, 14.0.0; SAS Institute Inc., Cary, NC). If the ANOVA implied significance ($p \leq 0.05$), then the means were tested with Tukey-Kramer Honestly Significant Difference *post hoc* test to determine the differences.

2.6. RNA-Seq analysis

2.6.1. Plant material and growth conditions

Sterilized seeds of pER8-P6WT-GFP line, pER8-P6(ΔTOR)-GFP line (Table 2.3), and Arabidopsis Col-0 were sown on ½ MS medium with 0.8% agar and grown at 22 °C under 16 hrs day length continuous white light (120 µmol m-2 s1) and 8 hrs dark with 60% humidity. One week old seedlings were transplanted to 1⁄2 MS with 0.8% agar containing 30µM β-estradiol and grown for five days under the same growth conditions. Plant tissue, ~100 mg tissue, was collected from three independent biological replicates for each line, 20 plants per biological replicate, and directly were flash-frozen in liquid nitrogen and stored at -80°C. Stored seedlings samples were sent to Qiagen in a box full of dry ice for total RNA extraction and library preparation for RNA-Seq using the

Illumina platform (Figure 2.1). The libraries were sequenced using 75 bp single read chemistry on the Illumina NexSeq 500 and ~35.8 million reads per sample (further details are described in chapter 6).

Sample Name	Sample Groups	QIAGEN ID
Arabidopsis thaliana Col 0	WT	30097-001
Arabidopsis thaliana Col 0	WT	30097-002
Arabidopsis thaliana Col 0	WT	30097-003
pER8-P6WT-GFP number 10-121	P6WT-GFP	30097-004
pER8-P6WT-GFP number 10-121	P6WT-GFP	30097-005
pER8-P6WT-GFP number 10-121	P6WT-GFP	30097-006
pER8-P6(ΔTOR)-GFP number 2-11	P6 (TOR-GFP)	30097-007
pER8-P6(ΔTOR)-GFP number 2-11	P6 (TOR-GFP)	30097-008
pER8-P6(ΔTOR)-GFP number 2-11	P6 (TOR-GFP)	30097-009

Table 2.3. Lists all the samples in the RNA-Seq project and their specifications.

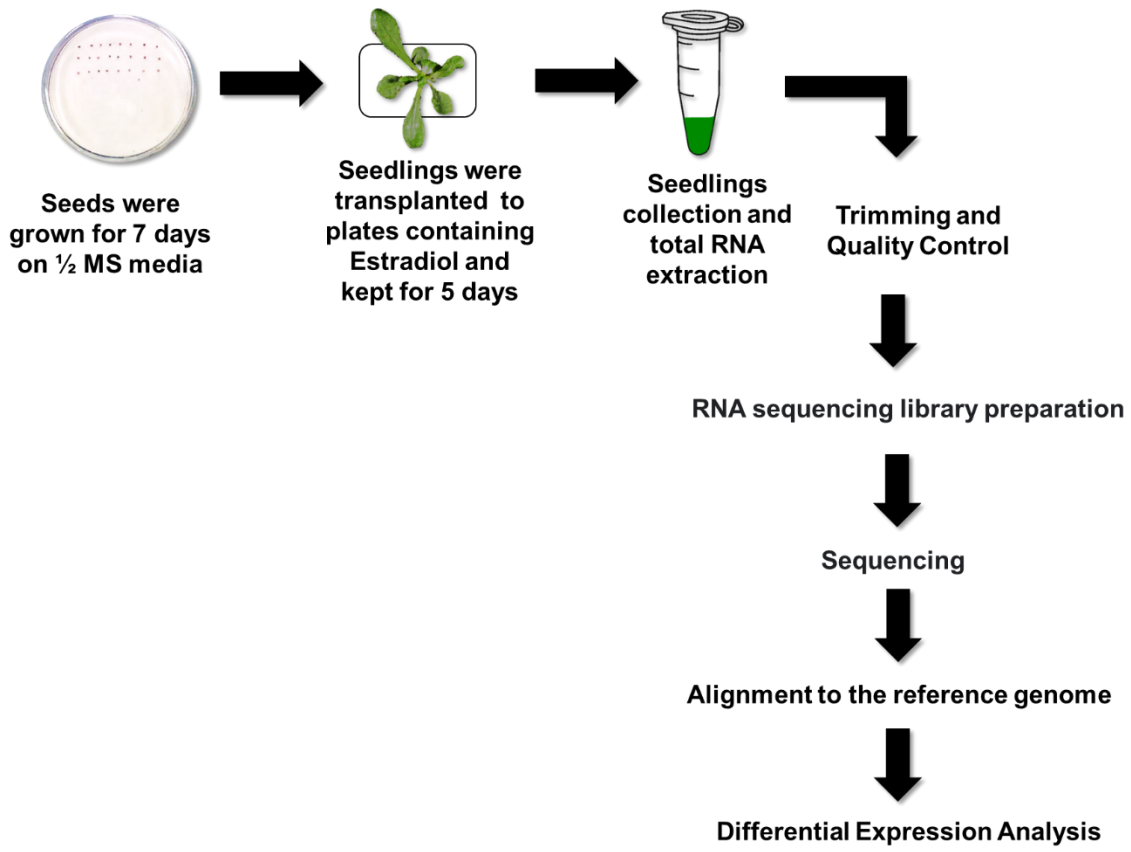

Figure 2.1. Flowchart of the RNA-seq settings and transcriptome analysis steps. The transcriptome analysis, annotations are based on Arabidopsis. The ratio of sequenced reads mapped on Arabidopsis genome sequence and P6-GFP sequence (see chapter 6 for detailed information).

Chapter III. Impact of CaMV P6 on the auxin and ethylene signalling pathways

3.1. Introduction

3.1.1. An overview of Cauliflower mosaic virus (CaMV) ORF VI, P6

CaMV encodes P6, a multifunctional protein that was found to act as a pathogenicity effector where it exhibited multiple roles in the suppression of plant defense. P6 was found to participate in suppressing both gene silencing and innate immunity defense responses (Schoelz et al., 2016, Zvereva et al., 2016, Schepetilnikov et al., 2011). P6 modulates the expression of plant genes such as the Nonexpressor of pathogenesis-related genes 1 (*npr1*), known to interfere with the cross-talk between SA and JA/ET signalling pathways (Love et al., 2012, Schoelz et al., 2016). Moreover, P6 expression induced the suppression of the SA defense response while enhanced JA defense responses, i.e., increase susceptibility to biotrophic pathogens and interferes with the SA and JA/ET pathway (Love et al., 2012, Laird et al., 2013, Geri et al., 2004).

3.1.2. The Ethylene triple response assay

Ethylene is a plant hormone that contributes to plant development and responses such as germination, plant morphology (cell proliferation and differentiation), and plant responses to biotic stresses and abiotic stresses (Bleecker and Kende, 2000, Johnson and Ecker, 1998, Guo and Ecker, 2004). The plants' morphology will change because of ethylene exposure (Merchante and Stepanova, 2017). Plant seedlings germinated in the presence of ethylene concentrations in the dark display a distinct phenotype defined as the triple response, in which seedlings will have shortens and thickens of both hypocotyls and roots with increased apical hooks' curving. In Arabidopsis, the triple response phenotype was evaluated by measuring the seedlings' length (shoot and root) after being grown on media supplemented with ethylene precursor 1-Aminocyclopropane-1-carboxylic acid (ACC) under dark conditions (Merchante and

Stepanova, 2017). The triple response is used to assess plants' responses and, i.e., the assay will display the impact of P6 on JA/ET biosynthesis, signalling pathway and plant sensitivity to ethylene.

3.1.3. Plant Polar Auxin Transport Inhibitors

The auxin signalling pathway plays a critical role in regulating plant physiology and development. Remarkably, it is transported directionally across plant tissues, i.e., polar transport via auxin efflux carriers such as members of the Long PINs (PIN1-8), the PIN-LIKES (PILS) family, and the ATP-dependent ABCB transporters (ABCB 1 and 19) unlike other phytohormones (Zhao, 2010, Spalding, 2013, Durbak et al., 2012, Jiang et al., 2017). Polar auxin transport inhibitors such as 1-naphthylphthalamic acid (NPA), 2,3,5-triiodobenzoic acid (TIBA), and 2-(1-pyrenoyl) benzoic acid (PBA) are known to have several effects on plant physiology and development, such as constraining the elongation and tropism of roots and stems. They inhibit the polar movement of auxin between cells. Also, TIBA was found to have a lethal effect on the plant at high concentration (Spalding, 2013, Dhonukshe et al., 2008).

3.2. Study Design

To assess the impact of P6, P6 transgenic plants were compared to non-transgenic controls with respect to their responses in the Ethylene triple response and TIBA germination assays. P6 transgenic plants have previously been shown to exhibit altered responses in the Ethylene triple response assay (Geri et al., 2004) and to differ from non-transgenic (NT) controls in their susceptibility to the auxin transport inhibitor TIBA (Smith, 2007). The results presented in this chapter confirm and extend these earlier studies.

3.3. Results

The P6 transgenic line A7, which expresses P6 from the CaMV 35S promoter in a Ler-gl1 background, was previously shown to exhibit partial non-responsiveness to the ET precursor ACC in the ethylene triple response assay (Geri et al 2004). However, these experiments were carried out at only a single ACC concentration. To better characterize the effect of P6 expression on ET responses, the assays were carried out at a series of different ACC concentrations.

3.3.1. Validation of transgenic line expressing P6

Before carrying out the assays, the A7 line was checked to confirm the expression of P6. Polymerase chain reaction (PCR) was used to detect the transgene's presence in plant DNA and western blot (WB) to detect the protein expression of the transgene.

3.3.1.1. Transgene detection

The P6 transgene was successfully detected from the leaf extracts of the A7 transgenic lines using P6 primer pairs (Table 2.1), in which the expected full-length fragments of P6 1.6-kb were amplified (Figure 3.1A). The P6 was amplified from the plasmid used as a positive control. No transgene amplification occurred for the Ler-gl1 wild-type background, which was used as a negative control (Figure 3.1A). Our results confirmed that the seeds of Ler-gl1 and A7 lines were not contaminated, and A7 contains the gene of interest for further analysis and experiments.

3.3.1.2. Western blot detection of P6 protein in transgenic plants

The western blot results (Figure 3.1B) confirmed that the tested transgenic lines expressed the proteins and were not silenced. Consistent with transgenes DNA detection results, the P6 protein expression was detected (62KDa) using a P6 antibody. The P6 transgenic lines A7 showed a high protein expression level, similar to previously western blot results (Love et al., 2012, Love et al., 2007a). Expectedly, the negative

control Ler-gl1 line did not have any protein expression detection. The anti-P6 antibody was also found to cross interact with Arabidopsis proteins and P6 breakdown products.

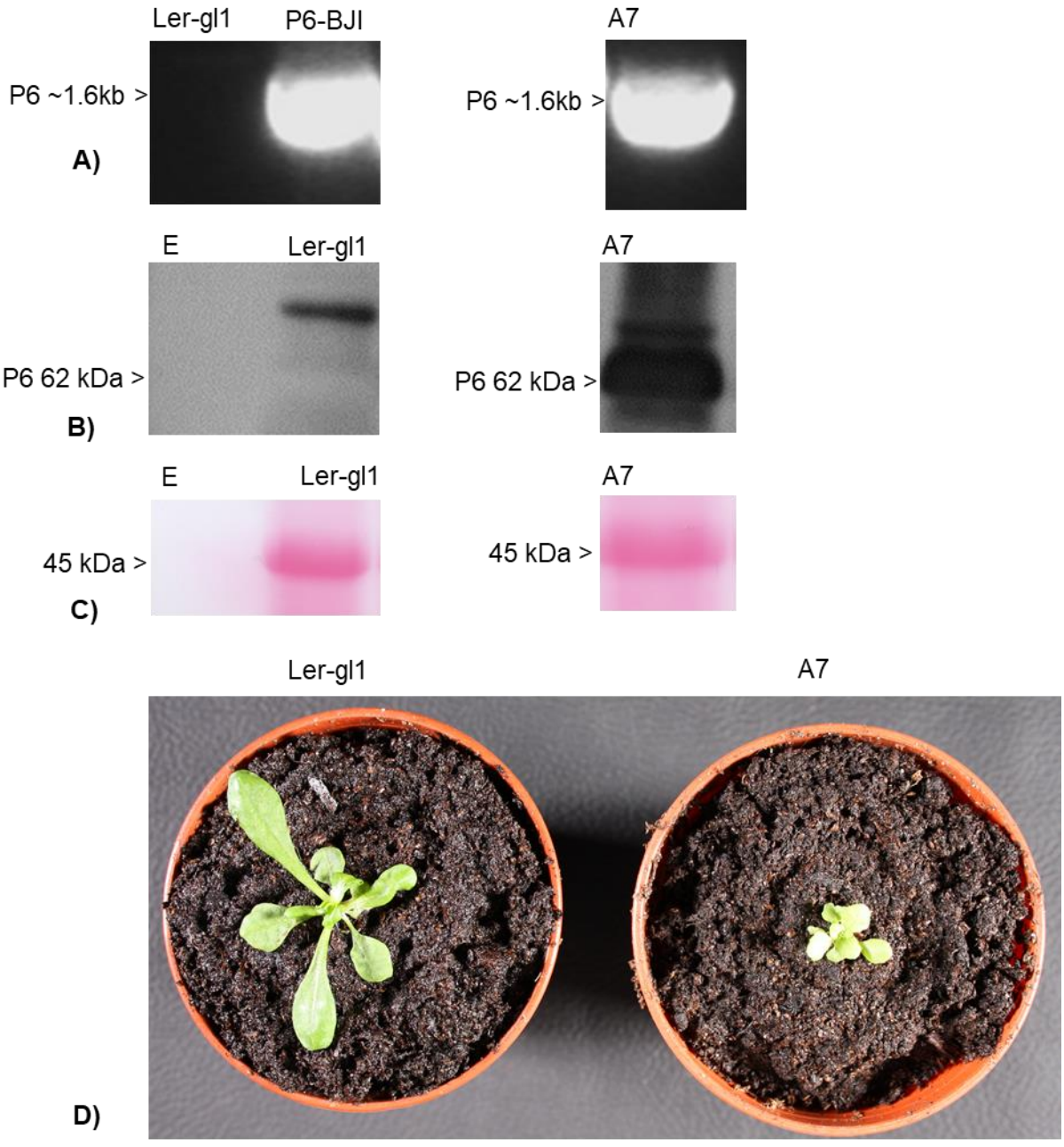

Figure 3.1. Validation of transgenic Arabidopsis line expressing P6. A) PCR analysis of P6 transgenic Arabidopsis line. P6 transgene was detected from the

transgenic line using P6 primer pairs in Table 2.1 and resolved using 0.8% agarose TBE gel**.** Ler-gl1 is a negative control, P6-BJI plasmid (Cecchini et al. 1997) used as positive controls, transgenic line A7 described in Table 2.1. **B)** Western blot analysis of P6 transgenic Arabidopsis line. The protein expression of P6 was detected from the transgenic line using the anti-P6 antibody**.** (Lane 1) empty (lane 2) Ler-gl1 as negative control (lane 3) P6 transgenic Arabidopsis line, A7. Arrows indicate the expected P6 band (62KDa), in which the blots were probed with the anti-P6 antibody. **C)** Shows Ponceau stained loading control, Rubisco. Arrows indicate the expected Rubisco band (45KDa). **D)** Photograph of 3 weeks old non-transgenic (Ler) and P6 transgenic Arabidopsis seedlings (A7).

3.3.2. Determination of sensitivity to ethylene and auxin transport inhibitor

The transgenic line expressing P6WT (A7) was compared to the control line (Ler-gl1) to assess the modification in the plant physiology and responses after exposure to ethylene precursor or auxin transport inhibitor, i.e., identify if P6 has an impact on the phytohormones signalling pathway. The A7 and the Ler-gl1 control line were grown in the dark on 1⁄2 MS media containing different concentrations of ACC (0 µM, 1 µM, 2 µM, 3 µM, 5 µM, and 10 µM) to assess the sensitivity to ethylene. Plants were assessed at day 5 by taking measurements of the total seedlings' length, the sum of the shoot, and root length. Then, the same lines were grown on 1⁄2 MS media containing different TIBA concentrations (10 µM, 20 µM, 30 µM, 40µM, 50 µM, 60 µM, 70 µM, and 100µM) for 14 days under the light to assess the sensitivity to the auxin transport inhibitor. The plant sensitivity was determined by counting the number of successfully germinated seeds. All treatments were carried in 3 independent biological replicates, 12 sterilized seeds of each line per biological replicate. The results below showed that A7 is more resistant to auxin transport inhibitor and less sensitive to the ethylene precursor than the Ler-gl1.

3.3.2.1. CaMV-P6 interferes with the ethylene signalling pathway

To analyze the effect of P6 on responses to ethylene, the ethylene triple response assay results for Ler-gl1 and A7 were compared. The ethylene sensitivity was analyzed by measuring the total seedling length (root plus shoot) after five days of incubation on ½ MS media containing different concentrations of ACC (0 µM, 1 µM, 3 µM, 5 µM) using Fiji analysis software on digital images of the plants on plates (details shown in Figure 3.2A).

The results are shown in Figure 3.2B and Table 3.1. The trend here shows a gradual decline or shorting in the total length as the ACC concentration increases. However, the total length of A7 was significantly shorter than the total length of Ler-gl1 at 0 µM of ACC because of the stunting symptoms induced by P6 expression (Cecchini et al., 1997, Yu et al., 2003).

To determine whether there was a difference in the effect of exposure to increasing concentrations of ACC between A7 and the Ler-gl1 control, the data were analyzed statistically using JMP software for two-way ANOVA statistical analysis, in which If the ANOVA implied significance ($p \leq 0.05$), then the means were tested with Tukey-Kramer Honestly Significant Difference post hoc test to determine the differences. The ANOVA revealed a statistically significant interaction between the effects of different lines and different ACC concentrations on plant total length ($p=0.0462$). The initial effect analysis demonstrated that different lines had a statistically significant effect on plant total length ($p = <.0001$). Similarly, the initial effect analysis demonstrated that different ACC concentrations had a statistically significant effect on plant total length ($p = <.0001$). In other words, different lines showed a different level of sensitivity to ethylene. Both lines showed a statistically significant reduction in total length at 1µM ACC (ANOVA p-value = <.0001). The results are shown in Tables 3.1 and 3.2.

The two-way a nova analysis demonstrated that the Ler-gl1 had a statistically significant difference on plant total length ($p = <.0001$) at all ACC concentrations (1 µM, 2 µM, 3

μM, 5 μM, and 10 μM), i.e., showed high sensitivity to ethylene where the plant total length was reduced at all ACC concentrations. Statistical analysis showed that the ***relative*** length reduction for Ler-gl1 with increasing ACC concentration was statistically significantly different. The total length of Ler-gl1 at 1 μM was higher than 2 μM and had a p-value of = <.0001, similarly the p-value was <.0001 when the total length at 2 μM was compared to 3 μM, 3 μM to 5 μM and 5 μM to 10 μM of ACC, i.e., the total length decreases as the concertation of ACC increases. The Ler-gl1 displayed significantly higher sensitivity to ACC with respect to total length than A7.

Statistical analysis showed that the ***relative*** length reduction for A7 with increasing ACC concentration was not statistically significantly different except at 1 μM of ACC. The reduction in total length of A7 at 1 μM was statistically significantly different than the length at 0 μM of ACC (p-value of = <.0001), shorter. Interestingly, there was no statistically significant difference detected between the total length of A7 as the concertation of ACC increases. The A7 displayed significantly less sensitivity to ACC with respect to total length reduction than Ler-gl1, i.e., P6 modified the plant sensitivity to ethylene.

Statistical analysis showed that the ***relative*** length reduction for A7 with increasing ACC concentration was much less than for Ler-gl1 at 1 μM, 2 μM, 3 μM, 5 μM, and 10 μM, i.e., the A7 line displayed significantly less sensitivity to ACC with respect to total length than did Ler-gl1 plants over this range of ACC concentrations: 2 μM, 3 μM, 5 μM, and 10 μM. At concentrations 2 μM, 3 μM, 5 μM, and 10 μM of ACC, A7 was less sensitive to ACC in which the reduction in seedlings total length was statistically insignificant. In contrast, Ler-gl1 showed a statistically significant reduction in the total length as the ACC concentration increased (1 μM, 2 μM, 3 μM, 5 μM, and 10 μM). These findings implied that P6 modified the plant responses to ethylene, i.e., modulated the ethylene signalling pathway.

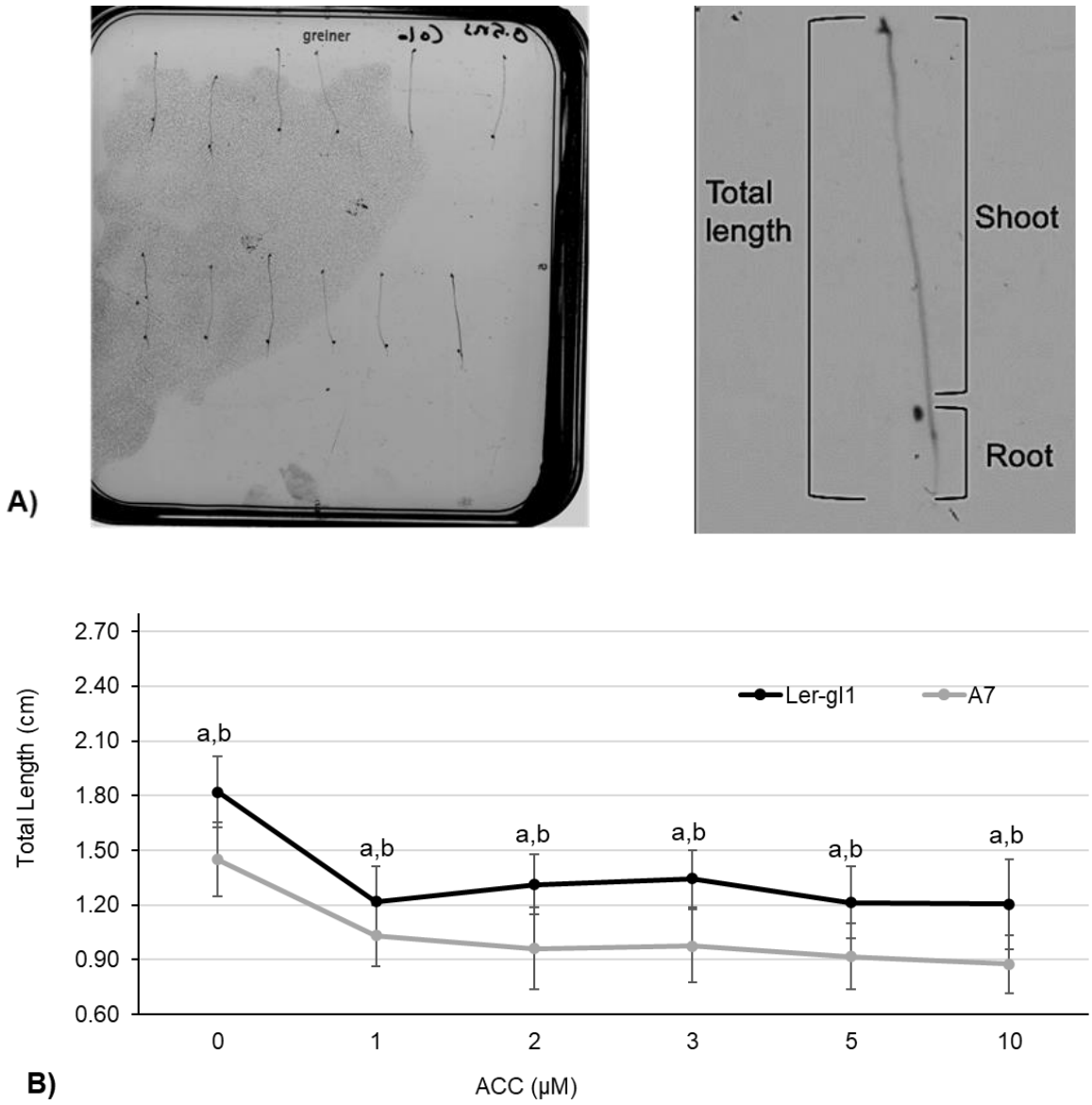

Figure 3.2. Ethylene sensitivity of transgenic Arabidopsis lines expressing P6WT under the control of a 35S promoter. (A) A representative image of the morphometric measurements of the root and shoot (total length) of five days old seedlings germinated under dark conditions using Fiji image analysis software. **(B)** Line chart showing the germination assay, i.e., total length (cm), of tested lines; Ler-gl1 (black bar) and A7 (light gray) on ½ MS plates containing different concentrations of ACC, i.e., 0 µM, 1 µM, 2 µM, 3 µM, 5 µM, and 10 µM. Each point in the line represents an average of seedlings' total length values for 36 replicates per experimental line. Points with the

same letters indicate mean values that are not significantly different using the Tukey-Kramer HSD test. The A7 total length was significantly different from Ler-gl1 at all ACC concentrations; hence there were different letters (a & b) at each point. The response pattern is a gradual decline or shorting in the total length as the ACC concentration increases.

	Total length (cm)					
ACC (µM)	**0**	**1**	**2**	**3**	**5**	**10**
Ler-gl1	1.820 ± 0.196	1.220 ± 0.193	1.312 ± 0.164	1.344 ± 0.156	1.214 ± 0.199	1.206 ±0.247
A7	1.449 ± 0.203	1.031 ± 0.170	0.963 ± 0.224	0.976 ± 0.200	0.918 ± 0.182	0.876 ±0.160

Table 3.1. Plant responses to different concentration of ACC. The total length average of A7 and Ler-gl1 seedlings grown for five days on different concentrations of ACC; 0 µM, 1 µM, 2 µM, 3 µM, 5 µM, and 10 µM. Each number represents average values for 36 replicates per experimental line at specific ACC concentration. Values are average seedlings total length ± standard deviations (average N = 36 seedlings per line).

	ACC (µM)					
	0	**1**	**2**	**3**	**5**	**10**
Ler-gl1 vs. A7						
p-value (ANOVA, α=0.05)	<.0001	<.0001	<.0001	<.0001	<.0001	<.0001
Tukey HSD test	a, b	a, b	a, b	a, b	a, b	a, b

Table 3.2. Plant responses to ethylene. Comparison between the average total length average of A7 and Ler-gl1 seedlings at different ACC concentration (0 µM, 1 µM, 2 µM, 3 µM, 5 µM, and 10 µM) after five days of incubation. The significant statistical differences between lines were determined based on a two-way analysis of variance

(ANOVA) and Tukey-Kramer Honestly Significant Difference post hoc test ($P \leq 0.05$). P-value with different letter superscripts indicates values that are statistically significantly different.

3.3.2.2. CaMV-P6 interferes with the auxin signalling pathway

To determine if P6 interferes with auxin signalling, we used the same lines used in the ethylene triple response assay; A7 and Ler-gl1 (NT). The successful seed germination rate of each line was measured after 14 days of exposure to TIBA on plates. The results are shown in Figure 3.3. The data shown here are from three independent experiments. Both lines showed germination rates of near 100% in the absence of TIBA, but for the NT plants, this was reduced to 17% in the presence of as little as 10 μM TIBA and at 20 μM no plants were able to germinate. In contrast, germination rates for A7 were in excess of 80% at TIBA concentrations of up to 30 μM and still germinated at 11% at 60 μM. Germination was only completely inhibited at 70 μM. Thus, P6 transgenic plants retained the ability to germinate in much higher TIBA concentrations than did the NT controls, pointing to a role for P6 in modulating auxin responses (Figure 3.3). Furthermore, all tested lines showed a reduction in seedlings' size when grown in the presence of 10 μM of TIBA.

To confirm that there was a difference in response to increasing concentrations of TIBA between A7 and the Ler-gl1 control, the data were analyzed statistically using JMP software for two-way ANOVA statistical analysis, in which If the ANOVA implied significance ($p \leq 0.05$), then the means were tested with Tukey-Kramer Honestly Significant Difference post hoc test to determine the differences. The ANOVA revealed a statistically significant interaction between the effects of different lines and different TIBA concentrations on seed germination ($p = <.0001$). The initial effect analysis demonstrated that different lines had a statistically significant effect on seed germination ($p = <.0001$). Likewise, the initial effect analysis demonstrated that different TIBA concentrations had a statistically significant effect on seed germination ($p =$

<.0001). In other words, different lines showed a different germination rate to auxin transport inhibitor.

The two-way a nova analysis demonstrated that the Ler-gl1 had a statistically significant difference in seed germination in the presence of TIBA (p = <.0001), i.e., showed high sensitivity to auxin inhibitor where seed germination was inhibited at 20 μM of TIBA or more. Statistical analysis showed that the relative seed germination rate for Ler-gl1 decreased as increasing TIBA concentration was statistically significantly different. The seed germination of Ler-gl1 at 10 μM was less than seed germination in the absence of TIBA (P = <.0001). Similarly, the p-value was <.0001 when the seed germination at 10 μM was compared to 20 μM of TIBA, i.e., the seed germination rate decreases as the concertation of TIBA increases. The Ler-gl1 displayed significantly higher sensitivity to TIBA with respect to the seed germination rate of A7.

Statistical analysis showed that the relative seed germination of A7 with increasing TIBA concentration was not statistically significantly different, except at two concentrations 30 μM and 50 μM of TIBA. The seed germination of A7 at 50 μM of TIBA was statistically significantly different than the germination at 30 μM of TIBA (p-value of = <.0.0228), which had a lower number of germinated seeds. Likewise, seed germination at 50 μM was statistically significantly different from germination at 60 μM of TIBA (P = <.0001). Interestingly, there was no statistically significant difference detected between the seed germination at 10 μM, 20 μM and 30 μM, and between 40 μM and 50 μM. The A7 displayed significantly increased resistance to TIBA with respect to seed germination than Ler-gl1, i.e., P6 modified the plant responses to the auxin transport inhibitor.

Statistical analysis showed that the germination rates for A7 were consistently statistically significantly greater than for NT Ler-gl1 were (ANOVA p-value = <.0001) at all of the TIBA concentrations (10 μM, 20 μM, 30 μM, 40μM, 50 μM, 60 μM, 70 μM, and 100μM). There was also a significant difference between the lines when they were grown without the addition of TIBA (ANOVA p-value = 0.0278). However, this was

attributable to 2 out of 36 Ler-gl1 seeds not germinating in the experiment shown. These findings suggested that P6 modulates the auxin signalling pathway, i.e., increased plant resistance to TIBA.

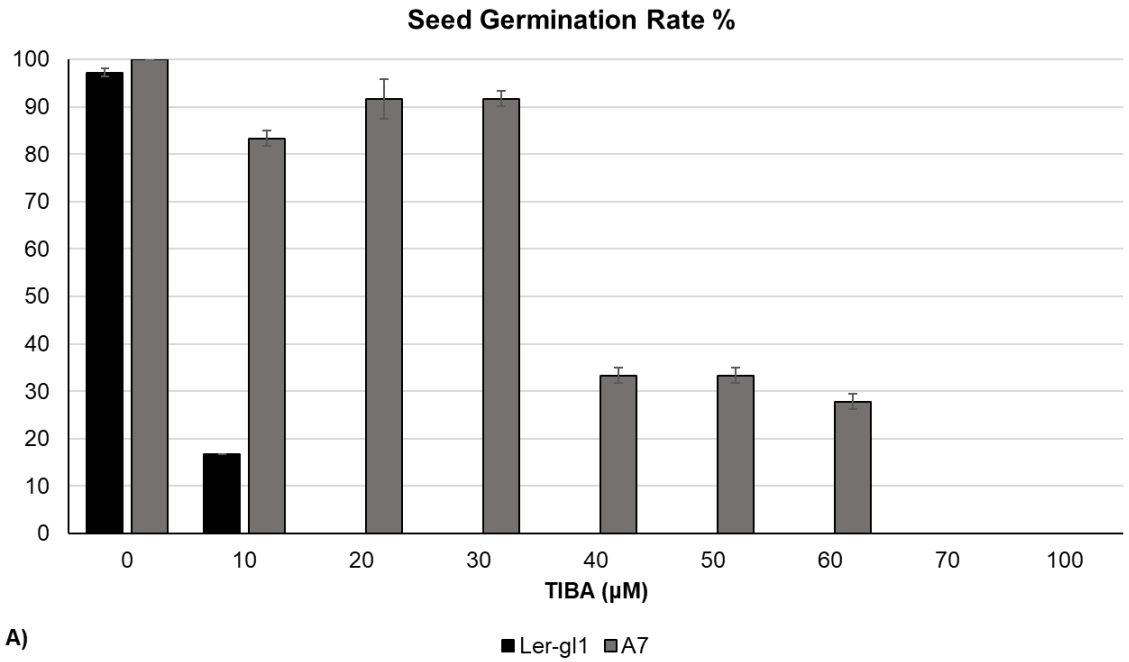

A)

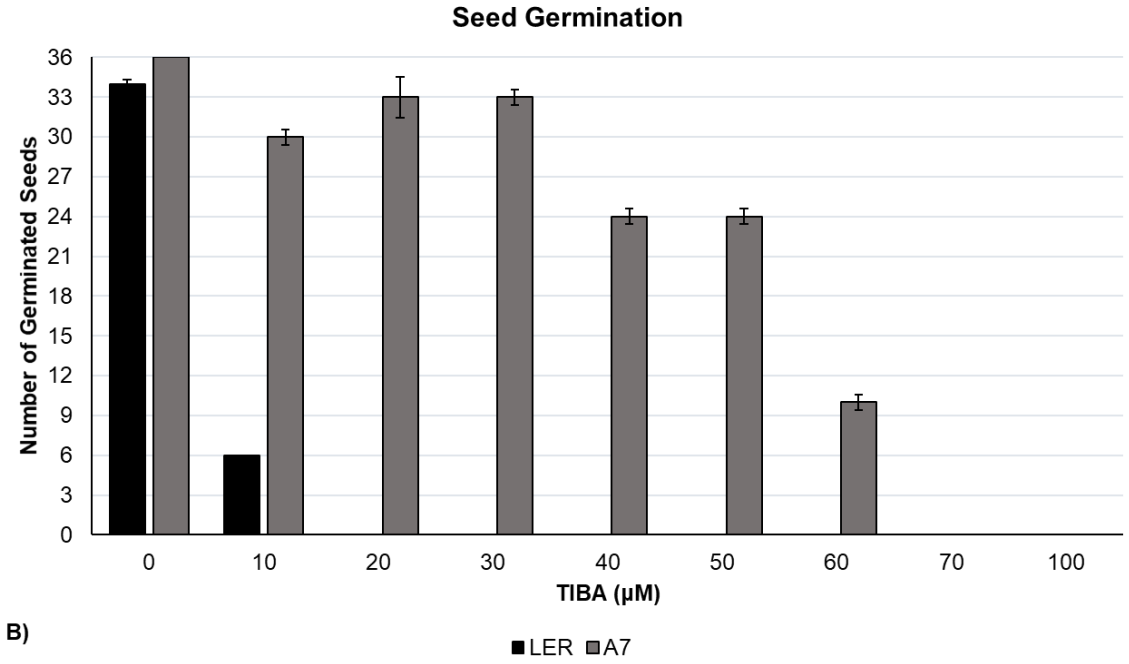

B)

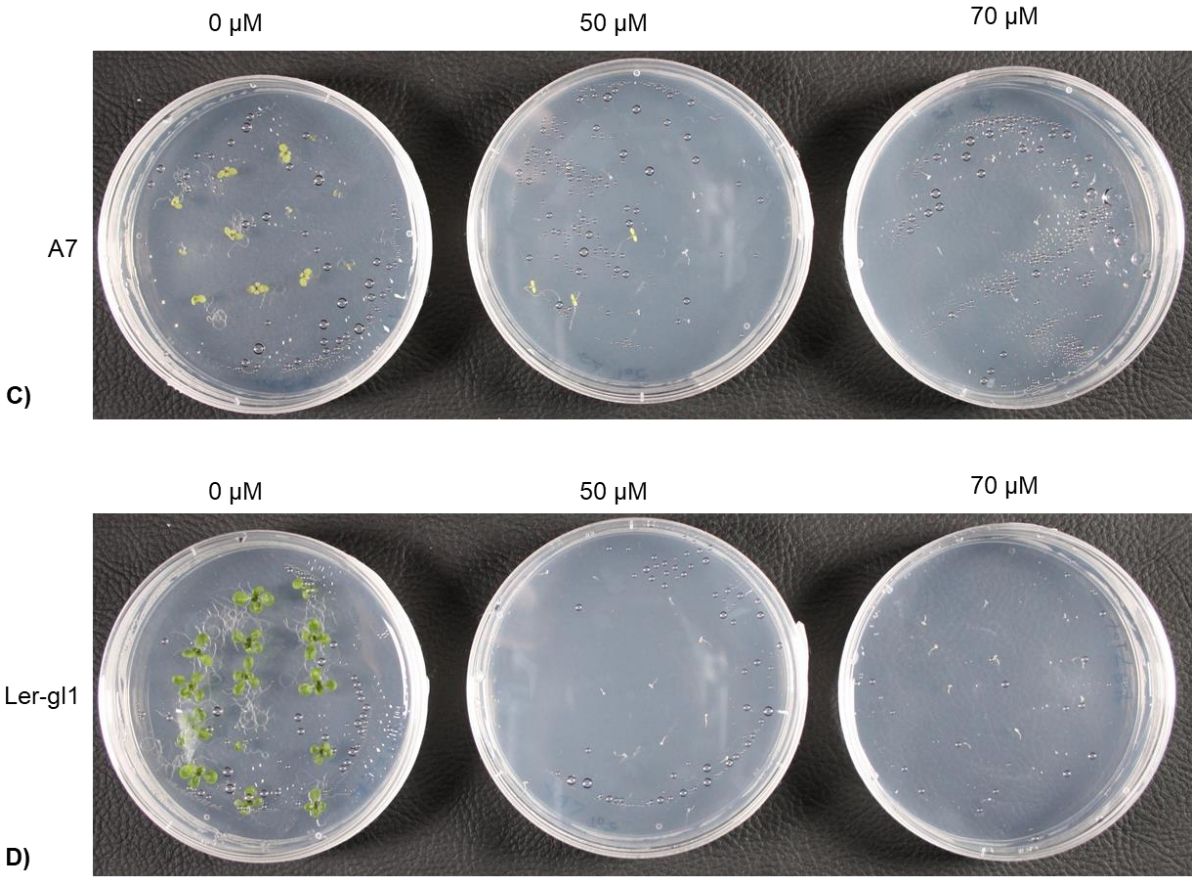

Figure 3.3. Effects of TIBA on seed germination. **A)** Bar chart of seed germination rate assay; Ler-gl1 (black bar) and A7 (light gray) on 1⁄2 MS plates containing different TIBA concentrations. For each line, 12 seeds sowed and grown on 1⁄2 MS plates containing different concentrations of TIBA: 10 µM, 20 µM, 30 µM, 40µM, 50 µM, 60 µM, 70 µM, and 100µM. Results were taken after two weeks of incubation. Each bar represents the percentage values of germinated seeds of 36 replicates per experimental line. **B)** Bar chart of seed germination assay; Ler-gl1 (black bar) and A7 (light gray) on 1⁄2 MS plates containing different TIBA concentrations. For each line, 12 seeds sowed and grown on 1⁄2 MS plates containing different concentrations of TIBA: 10 µM, 20 µM, 30 µM, 40µM, 50 µM, 60 µM, 70 µM, and 100µM. Results were taken after two weeks of incubation. Each bar represents the values of germinated seeds of 36 replicates per experimental line. **C)** Representative plates containing different germination levels of A7 respond to 0, 50, and 70µM TIBA concentrations after two

weeks **D)** Representative plates containing different germination levels of Ler-gl1 respond to 0, 50, and 70µM TIBA concentrations after two weeks.

3.4. Discussion

Cauliflower mosaic virus (CaMV) ORF VI encodes a multifunctional protein P6 comprising 520 amino acids and plays a vital role in virus infection. P6 was initially found to be required for the translation of the downstream open reading frames on the 35S RNA, induce disease symptoms, suppress SA-dependent defense responses, and enhance ET-defense responses (Laird et al., 2013, Love et al., 2012, Love et al., 2007a, Love et al., 2007b, Geri et al., 2004). The work described in this chapter was performed to extend our understanding of how P6 modulates phytohormonal signalling pathways, particularly the ethylene and auxin signalling pathways. Here, transgenic Arabidopsis plants of line A7 that expresses P6 from a 35S promoter (Cecchini et al., 1997) were compared to plants of the same wild-type background (Ler-gl1) to assess the impact of P6 expression on sensitivity to ethylene and auxin transport inhibitor. The results presented here represent an initial attempt to repeat and extend the earlier results that reported altered responses to ET and Aux inhibitor in P6 transgenic plants (Geri et al., 2004, Smith, 2007). The data confirm the earlier findings that expression of P6 from a transgene affects both ethylene and auxin signalling. Taken together, these data support the hypothesis that one of the multifactional roles of P6 is to modulate phytohormones signalling pathways.

3.4.1. Validation of transgenic lines expressing P6

The A7 line was validated for the transcription of P6 transgene, where they showed strong bands in the PCR and WB analysis, and the severe symptoms developed on the plant, such as stunting. The transcription of the P6 transgene was remarkably high, which might relate to the fact they were constructed in a vector, pJO530, in which expression is driven by an enhanced 35S promoter to maximize transcription of the transgene. Moreover, western blot analysis showed that the anti-P6 antibody cross

interacted with other Arabidopsis proteins and some of the P6 breakdown products; this emphasis on using a fresh batch or a better approach would be to construct a new anti-P6 antibody.

3.4.2. CaMV-P6 interferes with the ethylene signalling pathway

Previously (Geri et al., 2004), ETR assay results showed that transgenic line A7 showed less sensitivity than wild-type plants at high concentration of ACC, 50µM. This experiment expands our understanding of the P6 impact against several concentrations of ACC. This allowed us to investigate whether P6 will sustain the ACC insensitivity phenotype observed at different ACC concentrations and determine the ACC's threshold concentration required to lose the insensitivity phenotypic changes to occur. Our results indicated that P6 expressing lines were less sensitive to the ACC than Ler-gl1, in which the reduction of the seedlings' total length was much less. All tested plant lines showed a statistically significant difference in the seedlings' total length reduction when exposed to ACC, 1 µM of ACC. In other words, plants will be sensitive to ET as soon as it is added to the growth media; thus, P6 expression will make the plant less sensitive to higher ET concentrations.

Our findings implied that P6 modified plant responses to ethylene, i.e., modulated the JA/ET signalling pathway, which might interfere with the plant growth and responses to abiotic and biotic stress during CaMV infection. This modulation might be achieved through P6 interacting directly with one or more of the ET signalling components. These outcomes support the previous proposal that P6 enhances the host defense responses against JA-sensitive pathogens and increases the host vulnerability to SA-sensitive pathogens supporting the previous findings (Laird et al., 2013, Love et al., 2012, Love et al., 2007b).

However, A7 is a transgenic line with a high P6 protein expression level under the control of 35S promoter, i.e., continuously expressed, in which P6 will constrain the plant growth and induce severe stunting symptoms at all times. This P6 phenotype

might influence our measurements of the total length. The assessments would be more conclusive and resolute the P6 impact on the plant using a moderate P6 expressing line. In the future, carrying a combination of measurements such as volatile components profiling analog with the ethylene triple response assay will aid in further explaining and determining the P6 impact on plant performance.

3.4.3. CaMV-P6 interferes with the auxin signalling pathway

Unlike our previous ethylene sensitivity assay where the total length of germinated seedlings was measured to determine the responses, the auxin inhibitory treatment was assessed by measuring the number of successfully germinated seeds because the inhibitors such as TIBA will have a lethal effect at a certain concentration. Previously (Smith, 2007) transgenic lines expressing P6 were assessed for responses to auxin transport inhibitor at a single concentration TIBA concentration. Here, it was demonstrated that P6 would increase the resistance to different concentrations of auxin transport inhibitors.

Moreover, TIBA impacted the growth of all tested lines, in which the seedlings' sizes were reduced in the presence of TIBA compared to seedlings grown without TIBA in the media. Interestingly, the germination of the wild-type plant (Ler-gl1) seeds was remarkably inhibited at higher TIBA concentrations (≥ 20 μM) in contrast to the transgenic line expressing P6 (A7) seeds where they germinated and resisted the lethal effect of TIBA at higher concentrations, up to 50 μM. In other words, P6 is making plants less sensitive to TIBA lethal effect by altering the lethal threshold concentration. Our findings suggested that P6 modulated the plant responses to abiotic stress, i.e., P6 interfered with the auxin signalling pathway and enhanced the plant resistance to the TIBA lethal inhibitor. This interference might be through direct or indirect interaction with a component of the Aux signalling pathway.

The transgenic line A7 used in these studies, although expressing P6 at high levels, had a number of limitations. For example, the absence of an affinity tag required the

use of an anti-P6 antibody with only modest affinity for P6 and that cross interacted with other Arabidopsis proteins and some of the P6 breakdown products. More importantly, with identifying the TOR binding domain as playing an important role in P6 function (Yu et al., 2003, Lukhovitskaya and Ryabova, 2019, Schepetilnikov et al., 2011), it was decided to construct a new series of transgenic lines with P6 fused at the C-terminal to GFP as an affinity tag and to aid localization studies. These would be constructed using both the wild-type (native) P6 coding sequence from CaMV Cabb B-JI and a mutant form in which the TOR binding domain (aa 136–182) had been deleted, P6(ΔTOR) (Schepetilnikov et al., 2013).

3.5. Conclusion

Our findings indicated that P6 modulates phytohormone signalling pathways, particularly the auxin and ethylene signalling pathways. P6 might directly or indirectly impact the other phytohormones pathway's regulation because of the established cross-talk between the phytohormones pathway and results in modifying plant phenotypes and responses. This study will expand our understanding of the role of P6 as a pathogenicity effector regulating all aspects of phytohormones signalling pathways.

Chapter IV: Construction of new P6 transgenic lines

4.1. Introduction

4.1.1. Constitutive and inducible transgene expression

For the constitutive expression of transgenes, we used pEZR, a vector in which the CaMV 35S promoter drives the expression of the transgene (Christie et al., 2002). The CaMV 35S promoter is widely used in transgenic plants and a well-known tool in genetic engineering research. In plant biotechnology, the CaMV 35S promoter is the number one choice for the construction of genetically modified plants. It is compatible with a wide variety of different plants, is one of the strongest promoters in terms of expression, and continuously expresses the transgene at high levels. The 35S prompter has been used to transform plants for many purposes, such as increasing disease resistance and tolerance, increasing tolerance to abiotic stress, producing the desired phenotype, enhancing yield production and vaccine production (Chen et al., 2013, Myhre et al., 2005). However, constitutive transgene expression can lead the plant to regulate the transgene at the transcriptional and translational level via silencing and other feedback mechanisms. Also, the transgene product might be toxic to the plant or induce undesired phenotypes. The undesired effects and limitations of constitutive overexpression of protein can be overcome using chemically inducible expression systems. One system successfully applied in a broad range of research applications is the β-estradiol mediated protein expression system. The pER8 vector system (Schlucking et al., 2013, Zuo et al., 2000), which is strongly regulated, has high leak-tightness, and shows strong expression at low β-estradiol concentrations, was chosen for these experiments. This vector provides a high level of protein expression when induced. Additionally, it contains several restriction sites that facilitate transgenes cloning, and the leading promoter can be changed to meet the research requirement. Moreover, one of the advantages is that transgene expression is triggered by simple inducer application, painting, spraying, and adding to the growth media (Schlucking et al., 2013, Zuo et al., 2000).

4.2. Study design

To assess the impact of P6 on plant performance during CaMV infection and the role of the P6 TOR binding domain, we studied the modification of plant phenotypes and responses using newly constructed transgenic plants that express P6 and P6(ΔTOR) under constitutive or inducible promoters. This study aims to provide the tools to study and confirm the P6 impact on phytohormones signalling pathways and evaluate the TOR binding domain's role.

4.3. Results

4.3.1. Characterisation of newly constructed P6 and P6(ΔTOR) expressing lines.

4.3.1.1. Construction of Ti plasmids expressing P6WT and P6(ΔTOR)

Gibson Assembly was used to create the Ti plasmids expressing P6WT-GFP and P6(ΔTOR)-GFP. First, the P6WT-GFP and P6(ΔTOR)-GFP fragments were amplified using Phusion DNA Polymerase and pER8 GA primer pairs and pEZR GA primer pairs, separately. The P6WT-GFP and P6(ΔTOR)-GFP (~ 2.5kb) were subsequently cloned into linearized pER8 and pEZR using Gibson Assembly master mix. The results of PCR analyses confirmed that pER8-P6WT-GFP, pER8-P6(ΔTOR)-GFP, pEZR-P6WT-GFP, and pEZR-P6(ΔTOR)-GFP were generated, where the P6WT-GFP and P6(ΔTOR)-GFP insertions were detected using Phusion DNA Polymerase and their allocated GA primer pairs. Consistent with this result, digestion with restriction enzymes and partial sequencing results confirmed the correct assembly of each of the plasmids (Figure 4.1).

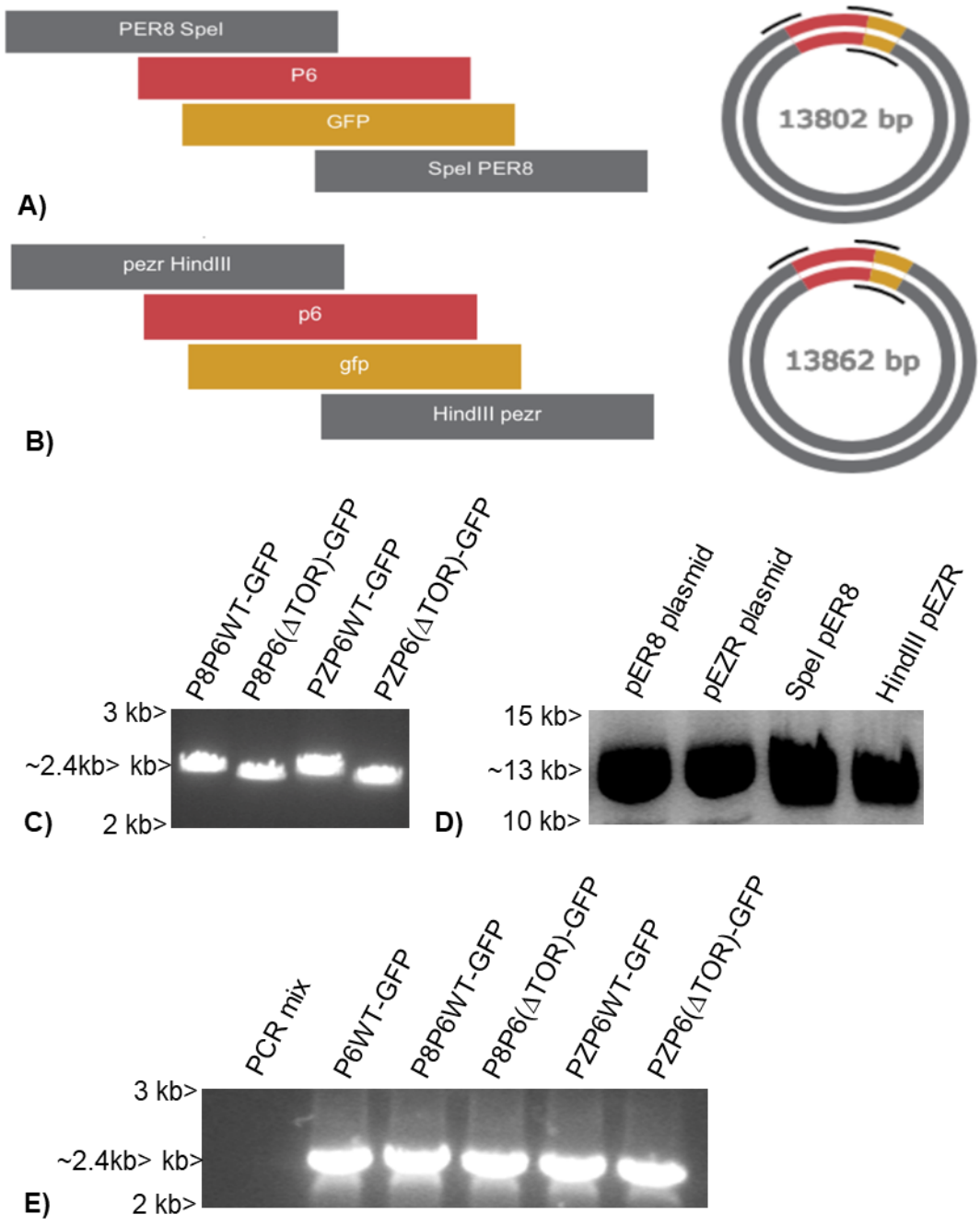

Figure 4.1. Construction of Ti plasmids expressing P6WT and P6(ΔTOR). Gibson assembly diagram: genes and vector backbones are used in a one-step assembly reaction to produce DNA constructs of interest. (A) Representative schematic of arrangements of genes P6WT-GFP or P6(ΔTOR) flanked by the pER8 vector sites. **(B)** Representative schematic of arrangements of genes P6WT-GFP or P6(ΔTOR)-GFP

flanked by the pEZR vector sites. **(C)** Insert amplification and purification. The cloning insert: (lane 1 & 2) P6WT-GFP and P6(ΔTOR)-GFP were PCR amplified using Phusion DNA Polymerase and pER8 GA primer pairs and gel purified with 0.65% agarose TBE gel and (lane 3 & 4) P6WT-GFP and P6(ΔTOR)-GFP were PCR amplified using Phusion DNA Polymerase and pEZR GA primer pairs and gel purified with 0.65% agarose TBE gel**. (D)** Ti plasmid construction: pER8-P6WT-GFP, pER8-P6(ΔTOR)-GFP, pEZR-P6WT-GFP, and pEZR-P6(ΔTOR)-GFP were constructed. P8P6WT-GFP and P8P6(ΔTOR)-GFP were the insert in linearized plasmid vector pER8 and: P8P6WT-GFP and P8P6(ΔTOR)-GFP was the insert in linearized plasmid vector pEZR. (Lane 1) undigested pER8 vector, (Lane 2) undigested pEZR vector, (lane 3) SpeI linearized pER8, and (lane4) HindIII linearized pEZR. **(E)** Ti plasmid construction conformation: P6WT-GFP and P6(ΔTOR)-GFP were detected from the four different constructs using Gibson assembly primer pairs, Phusion DNA Polymerase, and 0.65% agarose TBE gel. (lane1) negative control: PCR reaction mixture with tested primers plasmid, (lane2) positive control: P6WT-GFP was PCR amplified from P6BJI-P6WT-GFP using Phusion DNA Polymerase and P6BJI-GFP primer pairs, respectively, (lane 4 & 5) P6WT-GFP and P6(ΔTOR)-GFP were PCR amplified from pER8-P6WT-GFP and pER8-P6(ΔTOR)-GFP plasmids, respectively, using Phusion DNA Polymerase and pER8 GA primer pair set, and (lane 6 & 7) P6WT-GFP and P6(ΔTOR)-GFP were PCR amplified from the pEZR-P6WT-GFP and pEZR-P6(ΔTOR)-GFP plasmids, respectively, using Phusion DNA Polymerase and pEZR GA primer pair set.

4.3.1.2. Preliminary analysis of the plasmid constructs by transient expression of P6 in *N. benthamiana*

To confirm that the plasmids above were suitable for the construction of transgenic Arabidopsis lines, they were first checked for their ability to induce the expression of P6WT and P6(ΔTOR) by transient transformation assays. *N. benthamiana* plants were agroinfiltrated with Agrobacterium containing the appropriate P6 construct under the control of the 35S or the estradiol inducible promoter in pER8. Leaves infiltrated with

Agrobacterium containing pER8 plasmids were painted with 50 μM β-estradiol one day post-infiltration and visualized by confocal microscopy two days post-induction.

For the pEZR lines, extracts three days post infiltration were analyzed for expressing the P6-GFP fusion protein by western blots using an anti-GFP antibody. The results are shown in figure 4.2. Control plants were infiltrated with a plasmid expressing GFP from a 35S promoter and an empty vector. The western blots confirmed that the plants infiltrated with Agrobacterium containing plasmids, pEZR-P6WT-GFP, and pEZR-P6(ΔTOR)-GFP contained proteins of the expected size for the fusion protein (89 KDa). In addition, antibody-reacting bands were observed at 55 KDa and 27 KDa. In the plants infiltrated with the 35S GFP control, only the 27 KDa band was present. No bands were observed in the infiltrated controls, indicating that all of the observed bands were derived from transient expression from the Ti plasmids (Figure 4.2). Presumably, the bands at 27 KDa observed in plants infiltrated with the P6-GFP constructs derive from the cleavage of the GFP tag *in planta,* and the 55 KDa band probably represents a breakdown intermediate. These results suggest that the plasmids are capable of driving the expression of both P6 constructs at high levels but that there is considerable turnover/breakdown of the protein. P6 transgenic lines produced previously by other groups (Cecchini et al., 1997, Schepetilnikov et al., 2013) did not include an affinity tag on their constructs and used an antibody against P6 for immune detection. It is possible that the turnover or breakdown of P6 in these lines may have escaped detection.

Ordinarily inducible promoters are not used in transient assays, so it was necessary to establish the optimum conditions for transgene expression of the PER8 constructs. All pER8 constructs demonstrated generally similar expression levels and patterns of GFP fluorescence when induced by spraying or painting with 50 μM or 100 μM of β-estradiol. To further analyze expression, GFP fluorescence was visualized by confocal microscopic examination of *N. benthamiana* leaves that were Agroinfiltrated with plasmids pER8-P6WT-GFP, pER8-P6(ΔTOR)-GFP, pEZR-P6WT-GFP, and pEZR-P6(ΔTOR)-GFP (Figure 4.3). All pER8 and pEZR constructs demonstrated broadly similar expression levels and patterns of GFP fluorescence to those reported by Laird

et al. (2013). The GFP signal and expression patterns were also broadly similar between the 35S and estradiol inducible constructs (pEZR and pER8, respectively). Fluorescent aggregations were also detected within the cells, which is known to be a P6 phenotype (Rodriguez et al., 2014). Large and small inclusion bodies were detected in all pER8 and pEZR constructs. No apparent differences were detected in the localization, aggregation, and patterns between the P6WT and P6(ΔTOR) constructs. The leaves infiltrated with pER8-P6WT-GFP and pER8-P6(ΔTOR)-GFP also showed no protein expression (as evidenced by a complete lack of fluorescent signal) without the β-estradiol induction. Because of the high sensitivity of detection by confocal microscopy, this provides a good confirmation that the promoter is not leaky in the absence of β-estradiol.

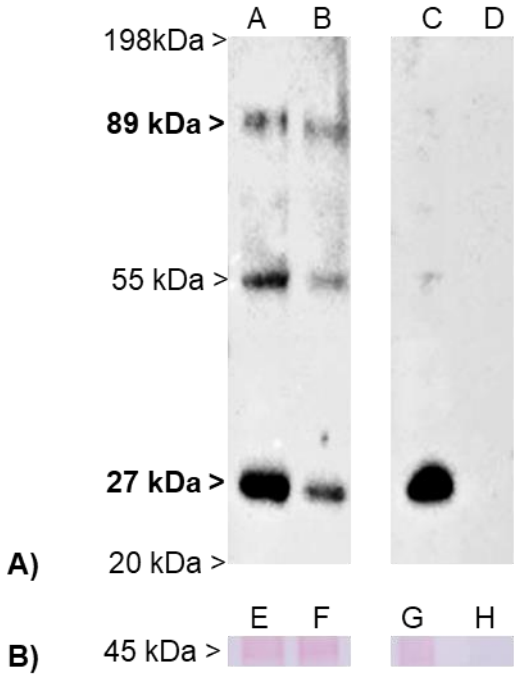

Figure 4.2 Transient expression of P6WT-GFP and P6(ΔTOR)-GFP. (A) Immunoblot analysis of total protein extracts from leaves of *N. benthamiana* transiently transformed with wild-type Col-0, pEZR-P6WT-GFP, and pEZR-P6(ΔTOR)-GFP probed with anti-GFP antibody. Lane A) pEZR-P6WT-GFP, Lane B) pEZR-P6(ΔTOR)-GFP, Lane C) 35s: GFP as the positive control, and lane D) Empty Col-0 as the negative control were

probed with anti-GFP antibody. Arrow indicates the molecular weight of P6WT-GFP and P6(ΔTOR)-GFP (~89 kDa) and GFP (27 kDa). **(B**) shows Ponceau stained loading control, Lane E-H) Rubisco. Arrows indicate the expected Rubisco band (45KDa).

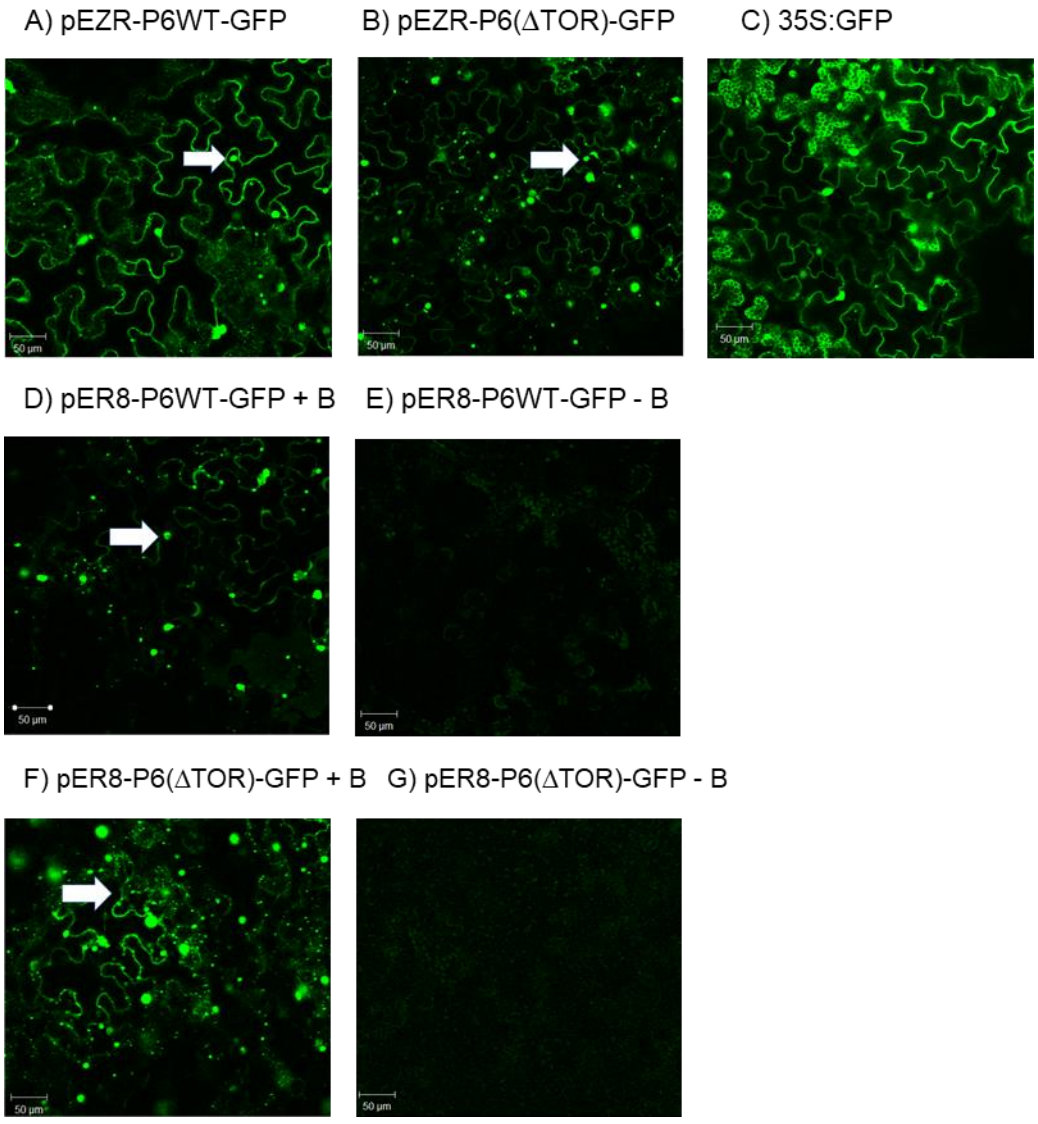

Figure 4.3 Transient expression of P6WT-GFP and P6(ΔTOR)-GFP in *N. benthamiana*. **(A&B)** Leaves of *N. benthamiana* transiently transformed with pEZR-P6WT-GFP and pEZR-P6(ΔTOR)-GFP. **(C)** Leaves of *N. benthamiana* transiently transformed with 35S: GFP, positive control. **(D&E)** Leaves of *N. benthamiana* transiently transformed with pER8-P6WT-GFP painted with 50μM β-estradiol (+B) to

induce GFP expression and pER8-P6WT-GFP without 50 μM β-estradiol (-B). **(F&G)** Leaves of *N. benthamiana* transiently transformed with pER8-P6(ΔTOR)-GFP painted with 50μM β-estradiol to induce GFP expression and pER8-P6(ΔTOR)-GFP without 50μM β-estradiol. Arrows indicate P6 aggregations.

4.3.1.3. Generation and selection of transgenic plants expressing P6

Having confirmed that the plasmid constructs gave a good expression of P6 when used for transient express in *N. benthamiana*, they were used to construct a series of transgenic Arabidopsis lines by floral dip.

For selection, seeds harvested from dipped plants (T1) of pER8-P6WT-GFP, pER8-P6(ΔTOR)-GFP, pEZR-P6WT-GFP, and pEZR-P6(ΔTOR)-GFP were germinated on ½ MS agar plates containing 50 μg/ml Hygromycin B (pER8 lines) or 50 μg/ml Kanamycin (pEZR lines). All had a germination rate of ~3%, suggesting that the transformation had been successful. Twenty seedlings of each transformed Arabidopsis line were transplanted for seed collection (T2 seeds). The T2 seeds of pER8-P6WT-GFP, pER8-P6(ΔTOR)-GFP, pEZR-P6WT-GFP, and pEZR-P6(ΔTOR)-GFP were screened on ½ MS agar plates containing selective antibiotic and five lines with a germination rate of ~75% (3:1) were chosen of each line for seeds collection (T3 seeds). The collected T3 seeds of pER8-P6WT-GFP, pER8-P6(ΔTOR)-GFP, pEZR-P6WT-GFP, and pEZR-P6(ΔTOR)-GFP were germinated on ½ MS agar plates containing selective antibiotic and two lines of each construct with a germination rate of ~ 100% (homozygous line) were chosen of each line for seed collection (T4 seeds).

4.3.1.4. P6 and P6 mutant expression level in the constructed transgenic lines.

Homozygous T4 progeny lines from each transgene construct, pER8-P6WT-GFP, pER8-P6(ΔTOR)-GFP, pEZR-P6WT-GFP, and pEZR-P6(ΔTOR)-GFP, were chosen for further study. The transgenic lines continuously expressing P6WT-GFP; pEZR-P6WT-GFP number 3-31 and number 2-91 (referred as PZP6-3-31 and PZP6-2-91,

respectively), continuously expressing P6(ΔTOR)-GFP; pEZR-P6(ΔTOR)-GFP number 4-10 and number 2-81 (referred as PZTOR-4-10 and PZTOR-2-81, respectively), inducible expressing P6WT-GFP; pER8-P6WT-GFP number 10-121 and 7-78 (referred as P8P6-10-121 and P8P6-7-78 respectively), and inducible expressing P6(ΔTOR)-GFP; pER8-P6(ΔTOR)-GFP number 2-11 and 2-10 (referred as P8TOR-2-11 and P8TOR-2-10) were selected for further analysis. To determine protein expression, Western blots were carried out using an anti-GFP antibody, and both sets of lines were examined by confocal microscopy (Figure 4.4-6).

The western blot results confirmed newly constructed transgenic lines: PZP6-3-31, PZP6-2-91, PZTOR-4-10, PZTOR-2-81, P8P6-10-121 P8P6-7-78, P8TOR-2-11, and P8TOR-2-10 showed protein expression (Figure 4.5). The immunoreacting bands of the appropriate size (~89 KDa) were present in lines PZP6-3-31, PZP6-2-91, PZTOR-4-10, PZTOR-2-81 (Figure 4.5 B). Thus, they were faint bands. In addition, the other bands: ~62 KDa, 49 KDa, and 27 KDa, were stronger than the 89KD band. These lower molecular weight bands were similar to those seen in western blots of protein extracted from *N. benthamiana* plants following transient transformation (Figure 4.2). They presumably represent similar breakdown products derived from the full-length fusion protein and suggest that P6-GFP may not be very stable and appears to be cleaved in *planta*.

For the lines with the estradiol-inducible promoter, plants were treated with 30 μM β-estradiol to induce expression according to (Schlucking et al., 2013, Zuo et al., 2000). Controls were untreated plants. Consistent with the pEZR lines, immunoreacting bands of the appropriate size (~89 KDa) and a band of 27 KDa, corresponding to the correct size for GFP, was detected in protein extracted from the seedlings of the newly constructed transgenic lines: P8P6-10-121 P8P6-7-78, P8TOR-2-11, and P8TOR-2-10 (Figure 4.5 D). Thus, the 89 KDa bands were much stronger than the faint bands detected in the pEZR lines. None of the estradiol inducible lines P8P6-10-121 P8P6-7-78, P8TOR-2-11, and P8TOR-2-10 containing a pER8-P6WT-GFP or pER8-P6(ΔTOR)-GFP construct showed any detectable protein expression in immunoblots

without β-estradiol induction (Figure 4.4 and 4.5 D). These results show that the pER8 lines show a robust induction by estradiol.

To determine the optimum conditions for inducing expression in the pER8 lines. The results are shown in Figure 4.4. The western blots confirmed that the same level of protein expression was achieved by induction with 30 µM, 50 µM, and 100 µM of β-estradiol five days post-induction. Consistent with the previous findings that pER8 expression can be induced by different β-estradiol concentrations ranging between 5-100 µM (Schlucking et al., 2013, Zuo et al., 2000) and the optimum level of protein expression reached after 3-5 days post-induction. For inducing P6 protein expression in the pER8 lines, it was found that when painting or spraying the leaves, it is better to use 50 µM of β-estradiol, and 30 µM when they are germinated on ½ MS agar plates. The examination of protein expression should be performed at least two days post-induction to have a strong expression. The strongest signal of inclusion bodies and P6 aggregation phenotype was detected 3-5 days post-induction by confocal microscopy (Figure 4.3 and 4.7).

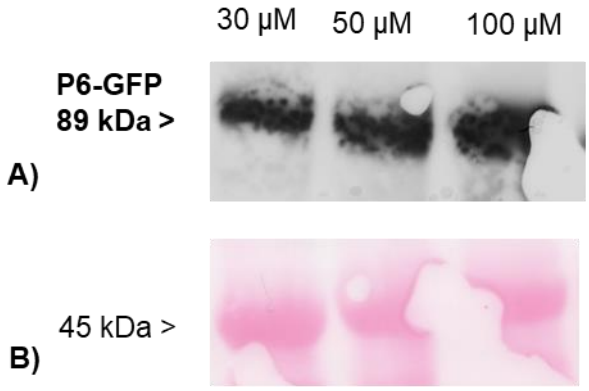

Figure 4.4. Optimum β-estradiol concentration for inducing expression in transgenic lines expressing P6WT-GFP under the control of a β-estradiol inducible promoter. (A) Immunoblot analysis of total protein extracts from 5-days old P8P6-10-121 Seedlings were germinated on ½ MS agar plates containing either 30 µM, 50 µM, and 100 µM of β-estradiol to induce GFP expression. Blots were detected

with a GFP antibody. **(B)** shows Ponceau stained loading control, Rubisco. Arrow indicates the expected Rubisco band (45KDa).

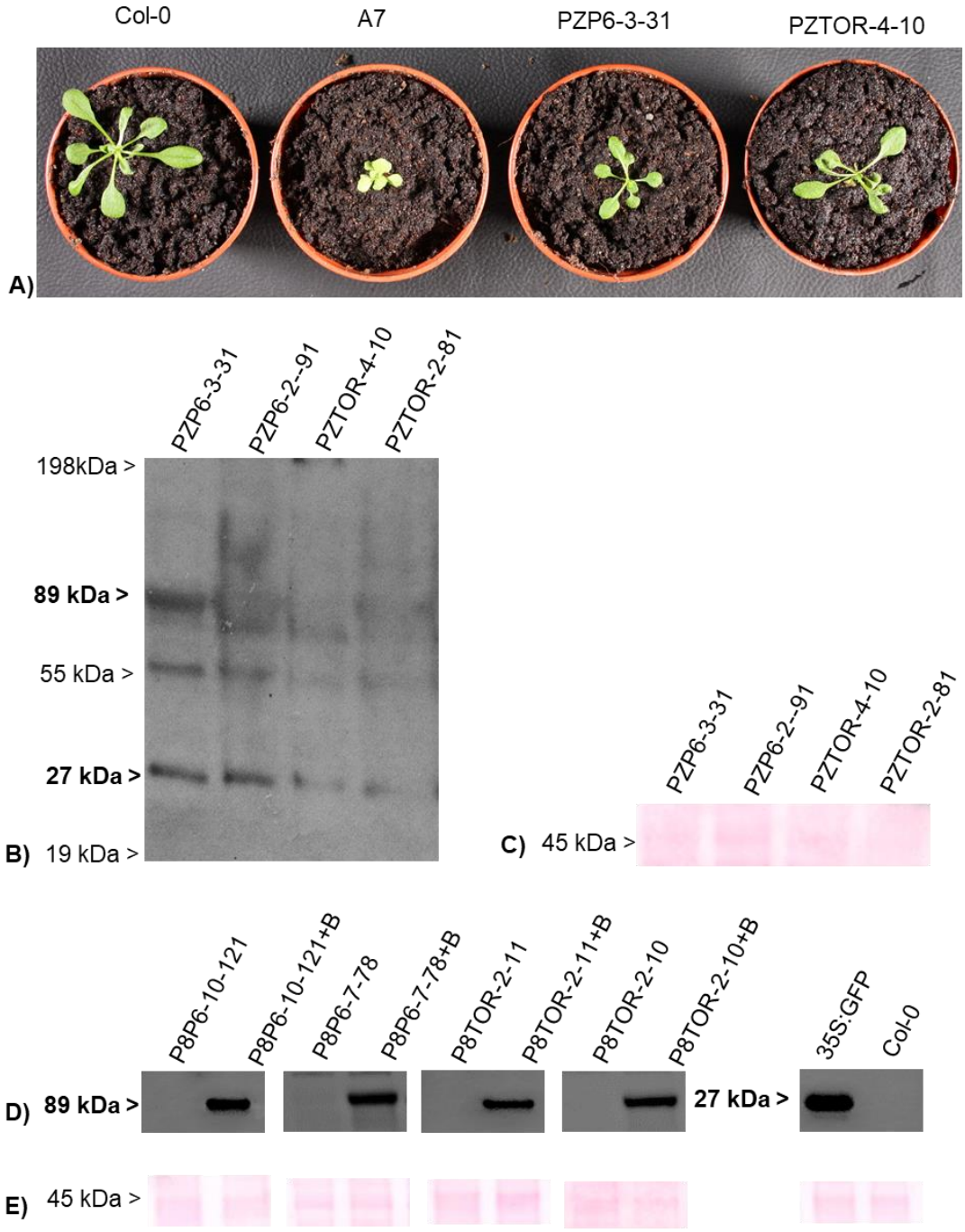

Figure 4.5. Expression of P6WT-GFP or P6(ΔTOR)-GFP in selected homozygous T4 transformant lines. Transgenic lines express P6WT-GFP or P6(ΔTOR)-GFP

under the control of a 35S promoter. (A) Photographs of 3 weeks old non-transgenic (Col-0) and P6 transgenic Arabidopsis seedlings; A7, PZP6-3-31, and PZTOR-4-10. **(B)** Immunoblot analysis of total protein extracts from 5-days old Arabidopsis seedlings: PZP6-3-31, PZP6-2-91, PZTOR-2-81, and PZTOR-4-10 were germinated on ½ MS agar plates. Blots were probed with a GFP antibody. **(C)** shows Ponceau stained loading control, Rubisco. Arrow indicates the expected Rubisco band (45KDa). **Transgenic lines express P6WT-GFP or P6(ΔTOR)-GFP under the control of β-estradiol inducible promoters. (D)** Immunoblot analysis of total protein extracts from 5-days old Arabidopsis seedlings: P8P6-10-121, P8P6-7-78, P8TOR-2-11, and P8TOR-2-10 were germinated on ½ MS agar plates with 30 μM β-estradiol (+B) or without β-estradiol. Col-0 was used as the negative control, and a line constitutively expressing 35S:GFP was used as the positive control (Cloix and Jenkins, 2008). Blots were probed with an anti-GFP antibody. **(E)** shows Ponceau stained loading control, Rubisco. Arrow indicates the expected Rubisco band (45KDa).

Line	Vector Plasmid	Promoter	Transgenic gene	Background
PZP6-3-31	pEZR	35S	P6WT-GFP	Col-0
PZP6-2-91	pEZR	35S	P6WT-GFP	Col-0
PZTOR-4-10	pEZR	35S	P6(ΔTOR)-GFP	Col-0
PZTOR-2-81	pEZR	35S	P6(ΔTOR)-GFP	Col-0
P8P6-10-121	pER8	estradiol-inducible	P6WT-GFP	Col-0
P8P6-7-78	pER8	estradiol-inducible	P6WT-GFP	Col-0
P8TOR-2-11	pER8	estradiol-inducible	P6(ΔTOR)-GFP	Col-0
P8TOR-2-10	pER8	estradiol-inducible	P6(ΔTOR)-GFP	Col-0

Table 4.1. Description of T4 transgenic lines used in the experiments. Transgenic lines expressing wild type P6 under the control of 35S promoter, pEZR-P6WT-GFP: PZP6-3-31 and PZP6-2-91, transgenic lines expressing P6 with TOR binding domain deletion under the control of 35S promoter, pEZR-P6(ΔTOR)-GFP: PZTOR-4-10 and PZTOR-2-81, transgenic lines expressing wild type P6 under the control of the β-

estradiol inducible promoter, pER8-P6WT-GFP: P8P6-10-121 and P8P6-7-78, and transgenic lines expressing P6 with TOR binding domain deletion under the control of the β-estradiol inducible promoter, pER8-P6(ΔTOR)-GFP: P8TOR-2-11 and P8TOR-2-10.

4.3.2. The localization, aggregation, and stunting impact of P6WT-GFP and P6(ΔTOR)-GFP

The GFP fusion protein expression was further characterized in selected newly constructed transgenic lines: PZP6-3-31, PZP6-2-91, PZTOR-4-10, PZTOR-2-81, P8P6-10-121 P8P6-7-78, P8TOR-2-11, and P8TOR-2-10 (Table 4.1). These lines were selected based on their seeds yield, western blot results, and consistency in their growth rate. The pEZR lines were selected based on their mild symptom and the modest protein expression, consistent with the next generation, T5. The pER8 lines were selected for their strong protein expression after estradiol induction, hence not leaky. To further analyze expression, GFP fluorescence was visualized by confocal microscopic examination. Each of the newly constructed transgenic lines: PZP6-3-31, PZP6-2-91, PZTOR-4-10, PZTOR-2-81, P8P6-10-121 P8P6-7-78, P8TOR-2-11, and P8TOR-2-10 demonstrated broadly similar expression levels and patterns of GFP fluorescence consistent with the earlier findings of plasmids transient expression in *N. benthamiana* (Figure 4.3, 4.6, and 4.7). Moreover, the P6 aggregation phenotype was observed in all lines(Figure 4.3, 4.6 and 4.7), consistent with previous findings (Rodriguez et al., 2014)

Leaves from the transgenic lines were examined by confocal microscopy. In all lines, both P6WT-GFP and P6(ΔTOR)-GFP were observed to localize in both epidermal and mesophyll cells on the actin microfilaments, associated with the nucleus, and in the cytoplasm, consistent with previous findings (Harries et al., 2009, Haas et al., 2005, Laird et al., 2013). Interestingly, high expression levels of both P6WT-GFP and P6(ΔTOR)-GFP were found in stomatal guard cells.

For the lines with the estradiol-inducible promoter, plants were treated with 30 μM β-estradiol to induce expression according to (Schlucking et al., 2013, Zuo et al., 2000). Controls were untreated plants. None of the estradiol inducible lines P8P6-10-121 P8P6-7-78, P8TOR-2-11, and P8TOR-2-10 showed any GFP signal without 30 μM β-estradiol induction, which provides further confirmation that the promoter is not leaky (Figure 4.7). There were no apparent differences detected among the pER8 lines (containing P6WT-GFP or P6(ΔTOR)-GFP) after β-estradiol induction; they shared similar expression levels, patterns of GFP fluorescence, localization, and aggregation.

A) PZP6-3-31

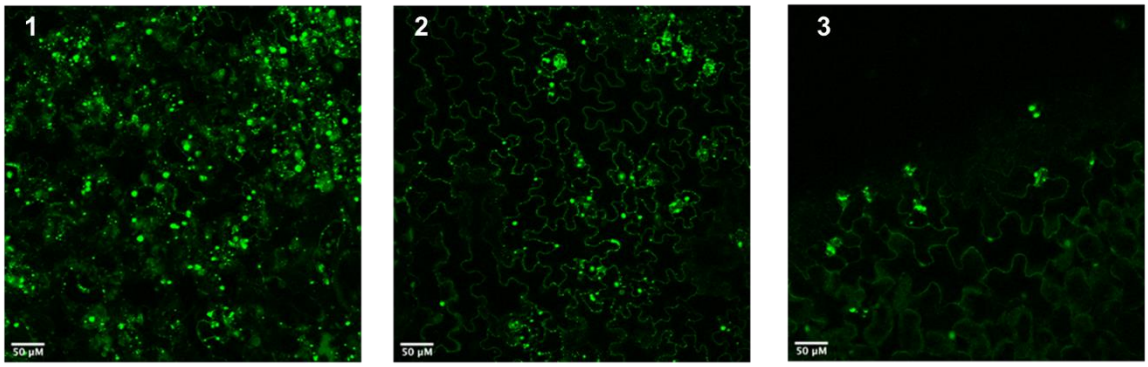

B) PZP6-2-91

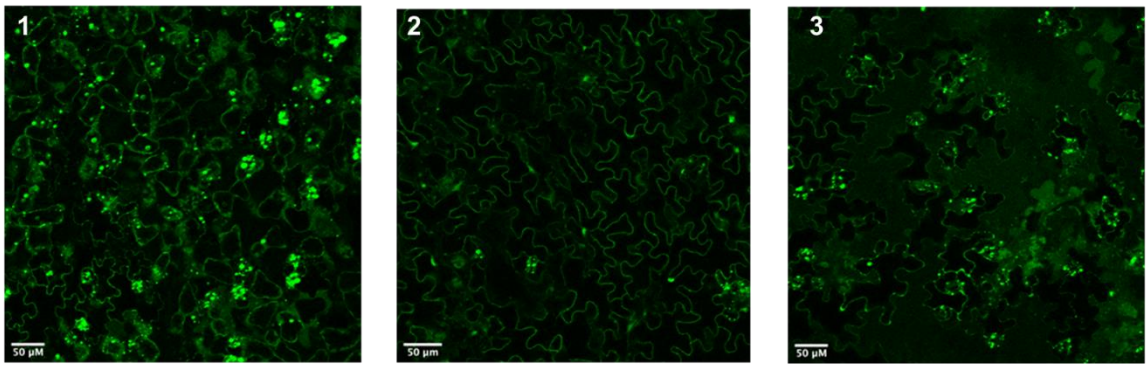

C) PZTOR-4-10

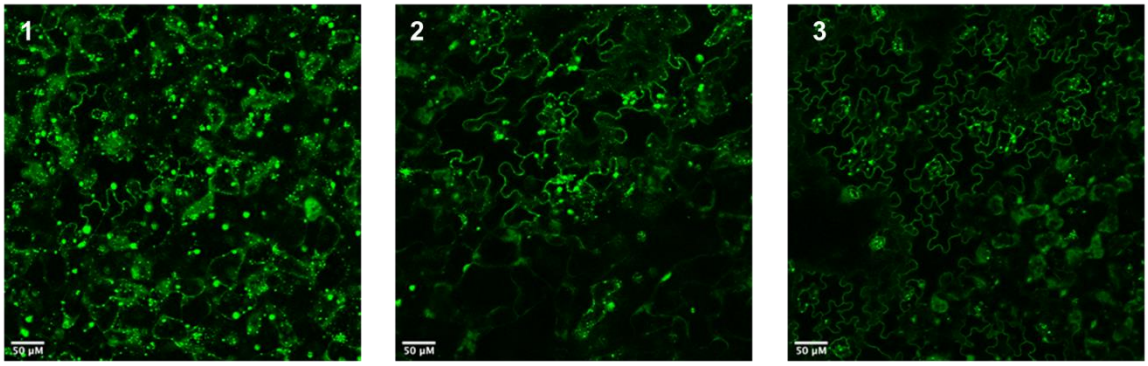

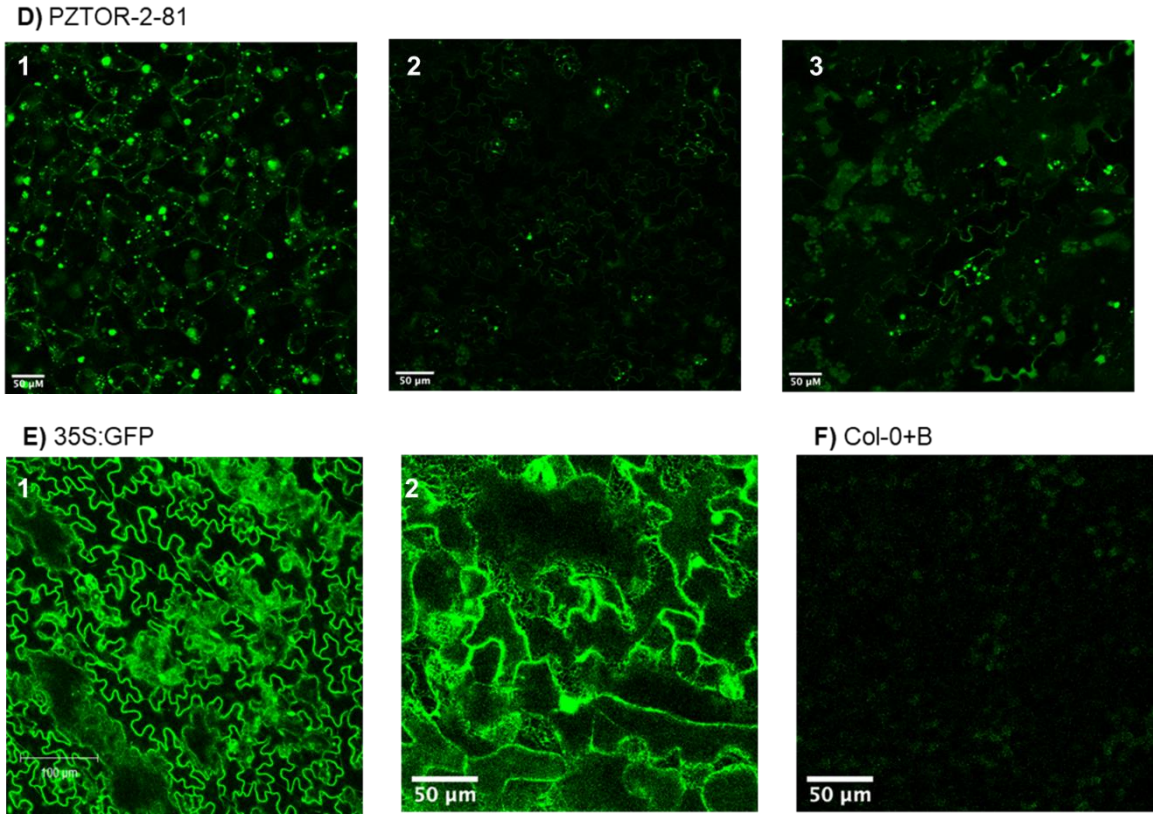

Figure 4.6. Confocal microscopy analysis of transgenic Arabidopsis lines expressing P6WT-GFP and P6(ΔTOR)-GFP under the control of a 35S promoter. Leaves of transgenic Arabidopsis line**: (A1-3)** PZP6-2-91**, (B1-3)** PZP6-3-31, **(C)** PZTOR-2-81, **(D)** PZTOR-4-10, **(E1&2) 35S: GFP** as the positive control, and **(F)** Col-0 as the negative control.

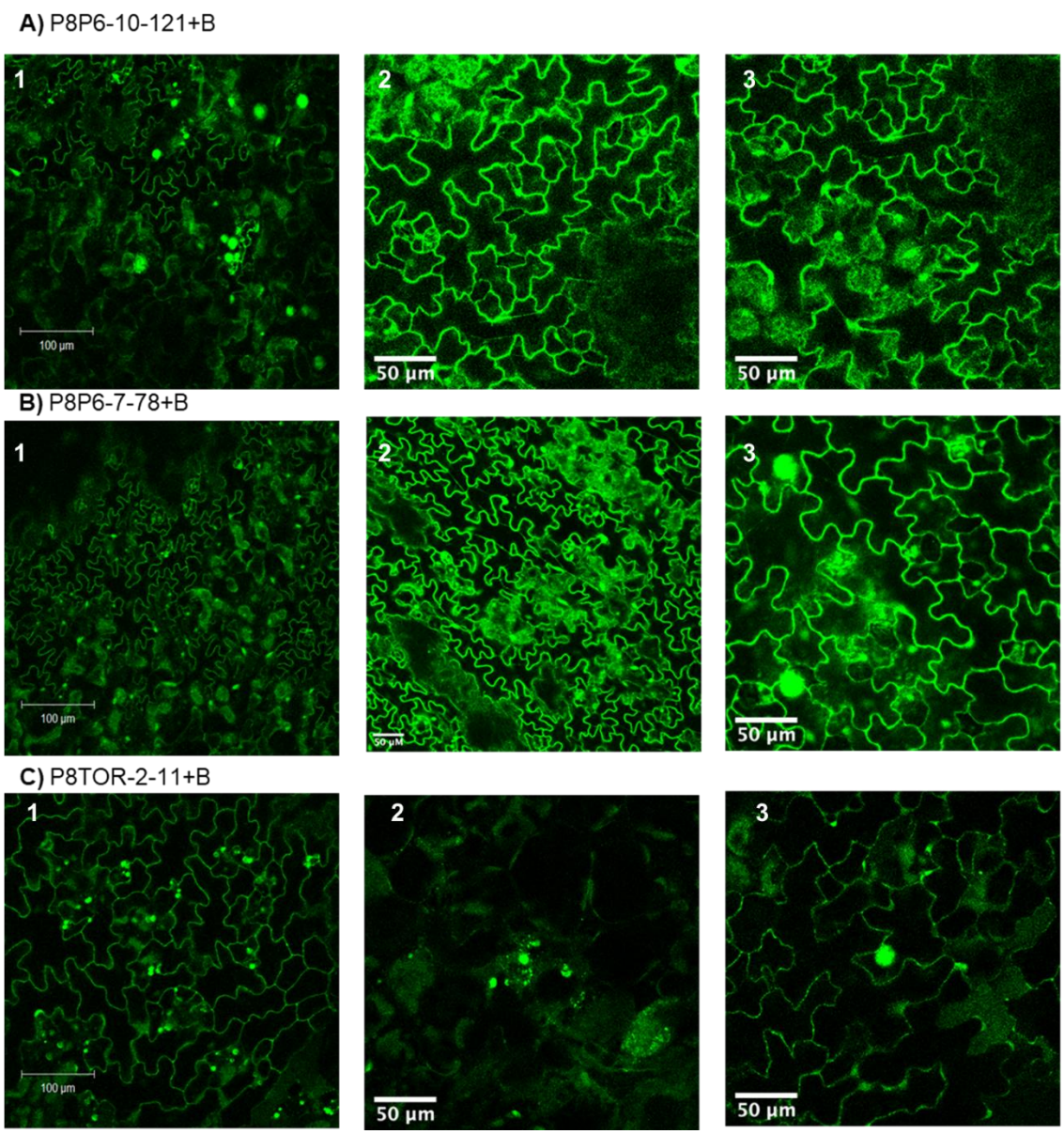
A) P8P6-10-121+B
1
100 µm
2
50 µm
3
50 µm
B) P8P6-7-78+B
1
100 µm
2
50 µM
3
50 µm
C) P8TOR-2-11+B
1
100 µm
2
50 µm
3
50 µm

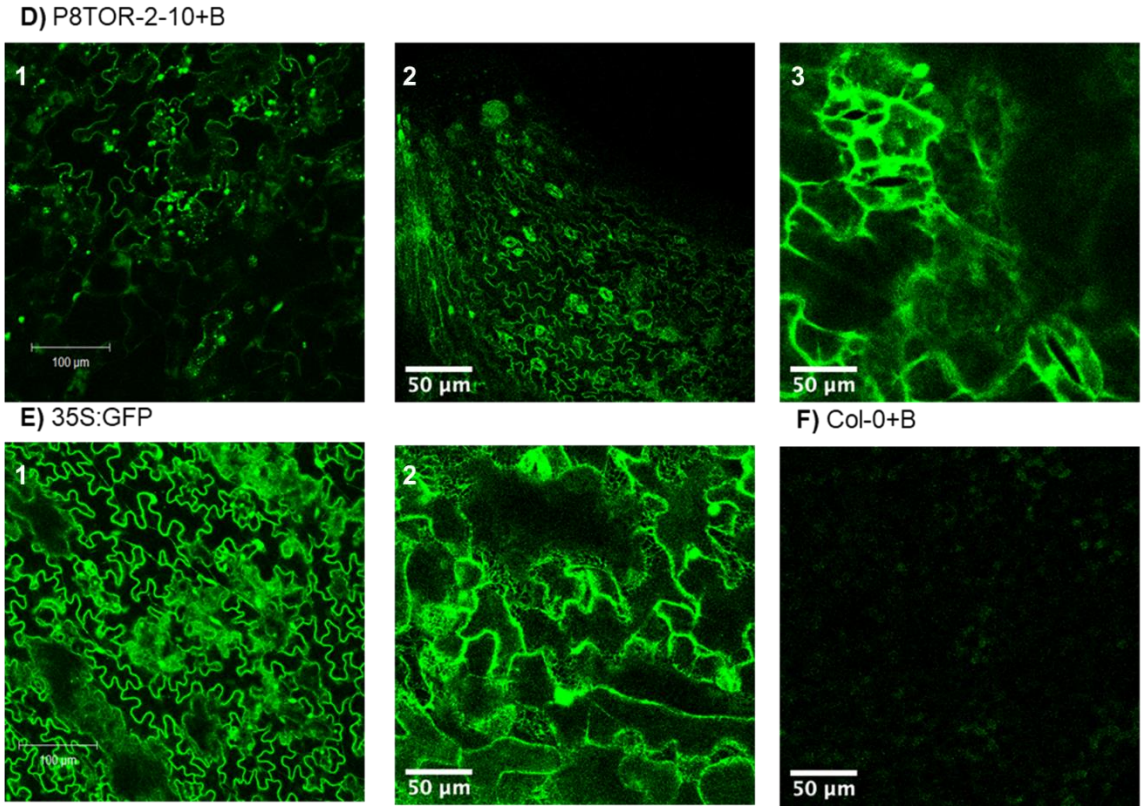

Figure 4.7. Confocal microscopy analysis of transgenic Arabidopsis lines expressing P6WT-GFP and P6(ΔTOR)-GFP under the control of a β-estradiol inducible promoter**.** Leaves of transgenic Arabidopsis line: **(A1-3)** P8P6-10-121, **(B1-3)** P8P6-7-78, **(C1-3)** P8TOR-2-11, **(D1-3)** P8TOR-2-10, **(E1&2)** 35S:GFP as the positive control, and **(F)** Col-0 as the negative control. All Seedlings were painted with 30 µM β-estradiol to induce GFP expression (+B).

4.4. Discussion

The results presented in chapter 3 confirm the role of P6 in modulating responses to ET and Auxin. A new series of transgenic lines were constructed to identify whether the interaction between P6 and TOR plays a part in these responses. These comprise CaMV P6 wild-type sequence (P6WT) fused to a C-terminal GFP, and CaMV P6 mutants containing short deletions of TOR binding domain (deletion from amino acids 136–182 of P6 protein (P6 (ΔTOR)) also fused to a C-terminal GFP. Two different sets

of transgenic lines were constructed with protein being expressed either under the control of a constitutive promoter CaMV 35S (pEZR lines) or under the control of a β-estradiol-inducible promoter (pER8 lines).

The confocal microscopy examination revealed that the TOR binding domain deletion did not affect the P6 aggregation phenotype, i.e., the TOR binding domain is not required for the P6 to aggregate. In contrast, the P6-dependent stunting phenotype was observed to depend on P6-TOR interaction because deleting the TOR binding domain reduced but did not entirely abolish the stunting severity. This observation implies induction of plant stunting by P6 is not completely independent of the interaction with TOR.

Generally, P6WT-GFP and P6(ΔTOR)-GFP were observed to share similar localization patterns, such as they localized on the stomatal guard cells, actin microfilaments, nucleus, and cytoplasm in Arabidopsis. This confirms the previous localization studies made only in *N. benthamiana* by transient expression. Further detailed localization assessment needs to be carried out to identify if deleting the TOR binding domain will impact the localization, movement from cell to cell, and protein-protein interaction (interactors).

Although the western blot results and confocal analysis showed that the pER8 lines were not leaky and had a robust protein expression after estradiol induction, the protein expression level, maximum GFP detected signal, reached about three or more days post-induction. This time required to build up P6 expression might interfere with some experiments and have a delayed impact on plant responses.

The pEZR plasmid containing constitutive promoter CaMV 35S was used because it was proven to express the protein in a moderate amount. Thus, the earlier results showed that the constructed pEZR lines showed modest protein expression, and it would be preferred to construct lines in the Col-0 background with the pJO530 plasmid (unpublished) that was used in the A7 line, a plasmid with enhanced constitutive

promoter CaMV 35S. The advantage of constructing the different lines in the Col-0 background is that different experiments can be carried and compared to well-characterized mutants in the Col-0 background, with easy access to stocks from the seed stock center. Moreover, producing new lines with pEZR, and pER8 plasmids in the Ler-gl1 background provide the tool to determine the differences of P6 impact on Col-0 and Ler-gl1. The next chapter demonstrated that the Col-0 plant behaved differently than Ler-gl1; this might also support that P6 might have a different impact on different host backgrounds (Col-0 and Ler-gl1). Hence, plant repones to abiotic and biotic stress might vary, phenotypes including stunting severity might decrease, and resistance to the P6 impact might increase. Additionally, robust expression of P6 in the A7 line (chapter 3) resulted in severe symptoms such as severe stunting, crumpling, and yellowing, while the modest expression of P6 in the pEZR failed to reproduce the same severe symptoms, i.e., more P6 expression results in severer symptoms.

The construct also can be modified by substituting the GFP tag with iLOV (Chapman et al., 2008). The iLOV is shown to be a better option than GFP for tagging viral proteins or cytosolic protein, especially to overcome the steric constraints or genome size constraints, and also proven to work in both mammalian cells and plant cells without interfering the protein function (Gawthorne et al., 2012, Christie et al., 2012, Chapman et al., 2008). The iLOV has a smaller molecular weight (10 kDa) than GFP (27 kDa) and is stable across different pH (Gawthorne et al., 2012, Christie et al., 2012, Chapman et al., 2008, Swartz et al., 2001). This substitution might help to overcome the P6-GFP cleavage and eliminate the potential interference with the P6 functionally. Finally, whole-genome sequencing of the newly constructed lines and probing with newly produced polyclonal anti-P6 antibody need to be carried out for further assessment.

4.5. Conclusion

Our findings indicated that P6-TOR interaction is not an absolute requirement for P6 to affect the plant but will increase some phenotypes. This study will expand our understanding of the P6 localization and P6-TOR interaction impact on the host.

Chapter V: The role of P6-TOR interaction in modulating ethylene and auxin signalling pathways

5.1. Introduction

5.1.1. Target of rapamycin (TOR) protein

The target of rapamycin (TOR) protein kinase is an essential plant regulatory protein that is involved in transcription, translation, metabolism, and signalling (Dobrenel et al., 2016). *Tomato bushy stunt virus* (TBSV) replication was found to be associated with the TOR activity. It was found that stimulation of the TOR pathway with glucose will enhance the replication of TBSV while inhibition of TOR activity reduces the TBSV accumulation (Inaba and Nagy, 2018). The TOR association with viral replication was also found with CaMV (Schepetilnikov et al., 2011). The mini-TAV domain of P6, one of the four domains, has been shown to carry out translational transactivation via the binding and activation TOR (Hohn and Rothnie, 2013, Schepetilnikov et al., 2013, Schepetilnikov et al., 2011). It was suggested that TAV-TOR interaction is highly specific, and deletion of a few amino acids of the TOR binding domain will abolish both binding and CaMV replication in plant protoplasts (Schepetilnikov et al., 2011, Schepetilnikov et al., 2013). The exact TAV contribution is yet to be uncovered. In addition to its role in virus replication, the P6-TOR interaction has also been shown to play a role in suppressing basal- and SA-mediated defense responses (Lukhovitskaya and Ryabova, 2019, Schepetilnikov et al., 2011). However, it has not been determined whether the P6-TOR interaction is involved in modulating ET signalling.

5.2. Study design

The results presented in this chapter confirm and extend these earlier studies in chapter 3. To assess the involvement of the P6 TOR binding domain, the newly constructed transgenic plants that express P6 and P6(ΔTOR) under constitutive or inducible

promoter were assessed using the Ethylene Triple Response Assay (ETR) and TIBA germination assays.

5.3. Results

5.3.1 Determination of the sensitivity of the P6 transgenics to ethylene and auxin transport inhibitors

The newly constructed transgenic Arabidopsis lines expressing P6WT and P6(ΔTOR) were evaluated for responses change relative to each other and to the NT control (Col-0) in the Ethylene Triple Response assay and the TIBA seed germination assay. The objective was to determine whether the TOR binding domain plays a role in promoting the ET-insensitive and TIBA-insensitive phenotypes reported earlier in chapter 3, by Geri et al (2004), and (Smith, 2007).

To avoid the possibility of effects due to the position of insertion of the transgene, two individual T4 progeny lines were tested for each construct, starting with the Arabidopsis lines under the control of the 35S promoter. These were for pEZR-P6WT-GFP; PZP6-3-31 and PZP6-2-91, and for pEZR-P6(ΔTOR)-GFP; PZTOR-4-10 and PZTOR-2-81. For lines under the control of the β-estradiol inducible promoter, the T4 lines were for pER8-P6WT-GFP; P8P6-10-121, and P8P6-7-78, and for pER8-P6(ΔTOR)-GFP; P8TOR-2-11 and P8TOR-2-10 (Table 4.1).

5.3.1.1. P6 and P6(ΔTOR) interference with the ethylene signalling pathway

To determine P6 impact on ethylene signalling, the two transgenic Arabidopsis lines expressing P6WT-GFP: PZP6-3-31 and PZP6-2-91, and two transgenic Arabidopsis lines expressing P6(ΔTOR)-GFP: PZTOR-4-10 and PZTOR-2-81 under the control of the 35S promoter and Col-0 as a reference control plant were used in the Ethylene Triple Response assay. Sensitivity to ethylene was evaluated as in chapter 3 by measuring the total length (combined the root length and the shoot length) of individual

seedlings using Fiji analysis software after five days of incubation in the dark on ½ MS plates containing different concentrations of ACC (1 µM, 2 µM, 3 µM, 5 µM, and 10 µM) (Table 5.2). As previously described in chapter 3 and by Geri et al. (2004), with the earlier generation of P6 transgenic plants, the experimental trend shows a gradual reduction in seedling total length as the ACC concentration increases. The data shown here are from three independent experiments.

5.3.1.1.1. Lines continuously expressing P6-GFP and P6(ΔTOR)-GFP

The results, based on the average total length of seedlings of Col-0, PZP6-3-3, PZP6-2-91, PZTOR-4-10, and PZTOR-2-8 are shown for the new transgenic lines in Table 5.2 and Figure 5.1 A-M. Generally, the ***relative*** reduction in the total length of the PZP6-3-31, PZP6-2-91 lines was less than for Col-0, PZTOR-4-10, and PZTOR-2-81.

The two-way ANOVA revealed a statistically significant interaction between the effects of different lines and different ACC concentrations on plant total length (p = <.0001). The initial effect analysis demonstrated that different lines had a statistically significant effect on plant total length (p = <.0001), and different ACC concentrations had a statistically significant effect on plant total length (p = <.0001). In other words, different lines showed a different level of sensitivity to ethylene. Similar to the findings in chapter 3, all lines showed a statistically significant reduction in total length at 1µM ACC (ANOVA p-value = <.0001). The results are shown in Table 5.1 and Figure 5.1 A-M.

The Col-0 had a statistically significant difference in the relative length reduction as ACC concentration increased where the Col-0 had a statistically significant difference between plant total length at 1 µM and all of the other ACC concentrations (p = <.0001), was longer, and between 2 µM and 10 µM (p = 0.0420). No statistically significant difference was detected between plant total lengths at 2, 3, and 5 µM or between lengths at 3, 5, and 10 µM.

The analysis revealed that PZP6 3-31 had a statistically significant difference in relative length reduction between 1 μM and all of the other ACC concentrations (p = <.0001). Similarly, a statistically significant difference was detected between 2 μM and 10 μM concentrations (p = <.0001), 2 and 3 μM (p = 0.0392) or 2 and 5 μM (p = 0.0392). Also, a statistically significant difference was detected in plant total lengths at 3 μM and all of the other ACC concentrations (p = <.0001) except between 3 and 5 μM; no statistically significant difference was detected. The PZP6 2-91 exhibited a statistically significant difference in relative length reduction where they were length at 1 μM was longer than length at 2 μM with a p = 0.0500, and longer than the lengths at all of the other ACC concentrations (p = <.0001). Similarly, a statistically significant difference was detected between 2 μM and 5 μM concentrations (p = <.0.0056), and longer than the lengths at all of the other ACC concentrations (p = <.0001). Also, a statistically significant difference was detected in plant total lengths at 3 μM and all of the other ACC concentrations (p = <.0001) except between 3 and 5 μM; no statistically significant difference was detected.

The two lines expressing native P6, PZP6 3-31 and PZP6 2-91, displayed statistically similar response patterns to different ACC concentrations (Table 5.2, Figure 5.6 A-E). Compared to the Col-0 control, both transgenic lines expressing native P6 showed a modest but statistically significant modest shortening at several ACC concentrations (2 and 5 μM of ACC) (Table 5.2 and Figure 5.6 C-E). These observations are consistent with the results presented in chapter 3 on the earlier P6 transgenic line A7 and the Geri et al (2004) report, which show that P6 transgenic plants show reduced sensitivity to ET in the ETR assay.

The analysis revealed that PZTOR 2-81 had a statistically significant difference in relative length reduction between 1 μM and lengths at all of the other ACC concentrations (p = <.0001), which was longer. The total length at 2 μM, 3 μM, and 5 μM were statistically significantly different when compared to length at 10 μM (p = <.0001). No statistically significant difference was detected between 2 and 3 μM, 2 and 5 μM, or 3 and 5 μM. Also, PZTOR 4-10 had a statistically significant difference in

relative length reduction between 1 μM and lengths at all of the other ACC concentrations (p = <.0001), which was longer. The total length at 2 μM, 3 μM, and 5 μM were statistically significantly different when compared to length at 10 μM (p = <.0001). No statistically significant difference was detected between 2 and 3 μM, 3 and 5 μM, 3 and 10 μM or 5 and 10 μM.

In contrast to the two lines expressing native P6, the two lines expressing P6(ΔTOR) showed behaved differently to each other with increasing ACC concentration. Seedling lengths for PZTOR 4-10 were similar to those for Col-0 at all ACC concentrations (Figure 5.6 F-I). This suggests that deleting the TOR binding domain abolishes the effect of P6 expression on the response of the plants in the ETR assay. However, for the second line tested, PZTOR2-81, comparison of seedling lengths to the NT control suggested that this line showed some reduced sensitivity to ET at least at intermediate ACC concentrations: 3 μM and 5 μM (ANOVA p-value =0.0002 and 0.0010, respectively) than Col-0 but responded similarly to the two lines expressing the native form of P6. In addition, the PZTOR2-81 generally had a longer seedling total length average than PZTOR-4-10, at 1 μM, 3 μM, and 5 μM had ANOVA p-value = 0.0003, 0.0027, and 0.0171, respectively (Table 5.2, 5.3, and Figure 5.6 F-M). No statistically significant difference was detected between all lines at 10 μM of ACC.

Overall, these results confirm the earlier findings that expression of P6 from a transgene leads to a reduced sensitivity to ET in the Triple Response assay, but the difference between the responses of the two lines expressing P6(ΔTOR) make it challenging to identify whether TOR binding is involved. It is possible differences in the relative levels of accumulation of P6 protein (Figure 4.5) may be an important factor responsible (at least in part) for variation between P6 transgenic lines. In addition, any effect of the P6WT-GFP and P6(ΔTOR)-GFP proteins might be affected by the breakdown of the P6-GFP fusion protein as shown in the western blot (Figure 4.5).

Total length (cm)						
ACC (μM)	**0**	**1**	**2**	**3**	**5**	**10**
Col-0	2.444 ± 0.161	1.541 ± 0.206	1.187 ± 0.179	1.131 ± 0.207	1.100 ± 0.198	1.054 ± 0.197
PZP6-2-91	2.364 ± 0.212	1.590 ± 0.181	1.470 ± 0.141	1.264 ± 0.197	1.321 ± 0.164	1.105 ± 0.152
PZP6-3-31	2.304 ± 0.121	1.571 ± 0.139	1.357 ± 0.208	1.220 ± 0.227	1.229 ± 0.183	1.081 ± 0.198
PZTOR-2-81	2.351 ± 0.230	1.603 ± 0.199	1.381 ± 0.181	1.342 ± 0.188	1.263 ± 0.165	1.084 ± 0.150
PZTOR-4-10	2.339 ± 0.156	1.426 ± 0.152	1.267 ± 0.235	1.164 ± 0.203	1.135 ± 0.151	1.076 ± 0.168

Table 5.1. Plant responses to different concentration of ACC. The total length average of Col-0, PZP6-2-91, PZP6-3-31, PZTOR-2-81, and PZTOR-4-10 seedlings grown for five days on different concentrations of ACC; 0 μM, 1 μM, 2 μM, 3 μM, 5 μM, and 10 μM. Each number represents average values for 36 replicates per experimental line at specific ACC concentration. Values are average seedlings total length ± standard deviations (average N = 36 seedlings per line).

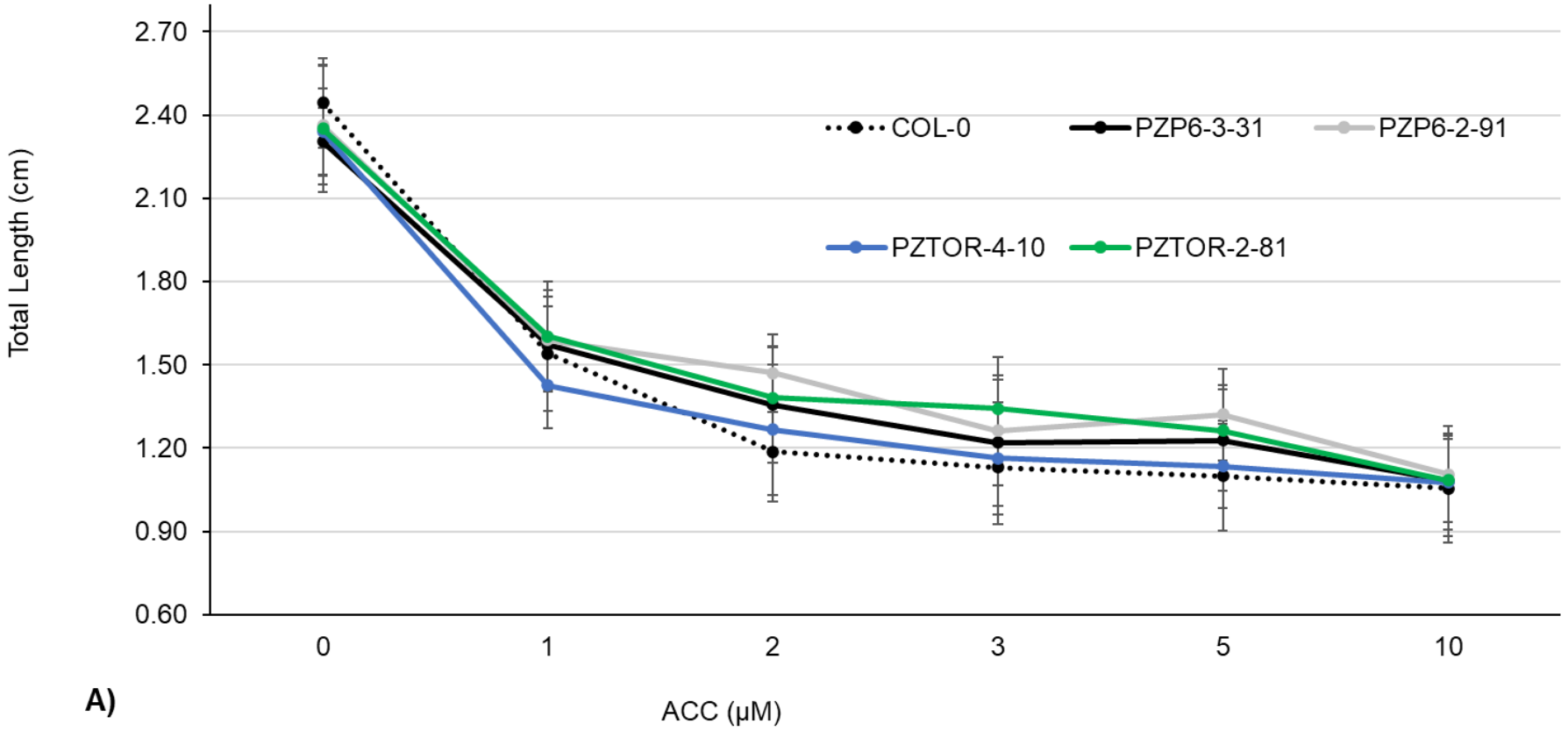
Total Length (cm)
2.70
2.40
2.10
1.80
1.50
1.20
0.90
0.60
COL-0
PZP6-3-31
PZP6-2-91
PZTOR-4-10
PZTOR-2-81
0
1
2
3
5
10
ACC (µM)

A)

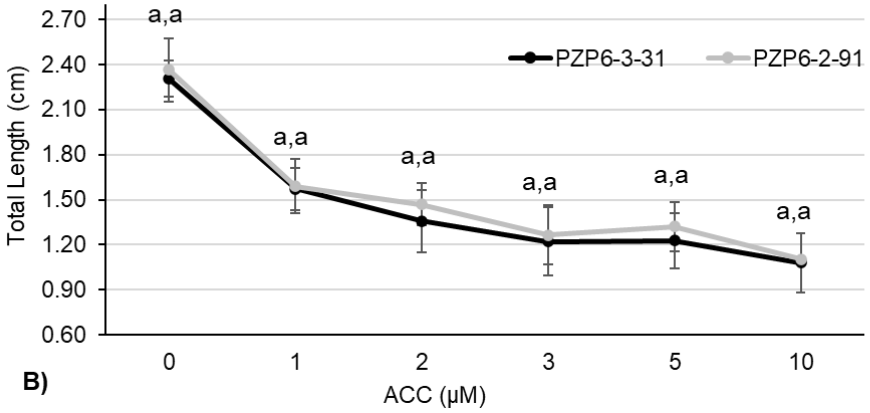
Total Length (cm)
2.70
2.40
2.10
1.80
1.50
1.20
0.90
0.60
a,a
a,a
a,a
a,a
a,a
a,a
PZP6-3-31
PZP6-2-91
0
1
2
3
5
10
ACC (µM)
B)

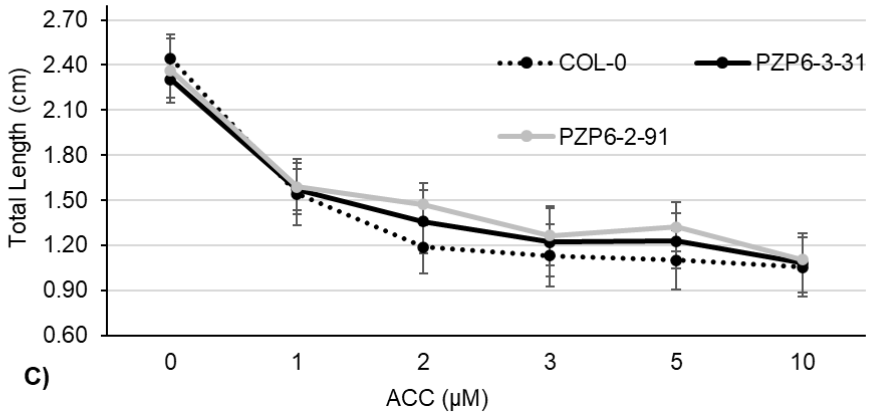
Total Length (cm)
2.70
2.40
2.10
1.80
1.50
1.20
0.90
0.60
COL-0
PZP6-3-31
PZP6-2-91
0
1
2
3
5
10
ACC (µM)
C)

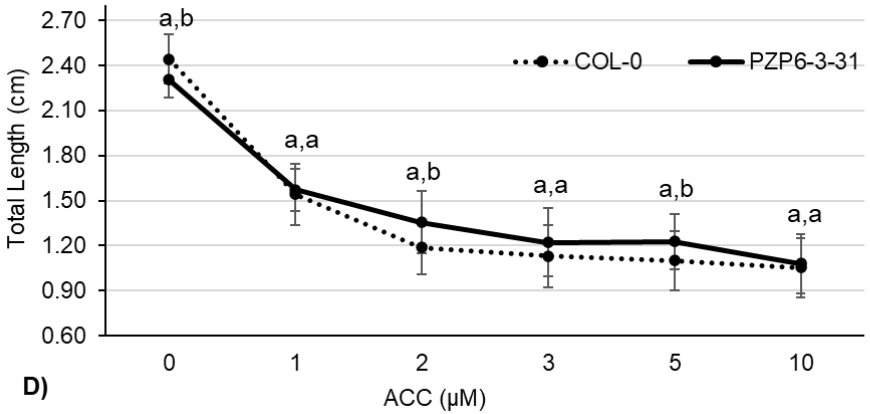
Total Length (cm)
2.70
2.40
2.10
1.80
1.50
1.20
0.90
0.60
a,b
a,a
a,b
a,a
a,b
a,a
COL-0
PZP6-3-31
0
1
2
3
5
10
ACC (µM)
D)

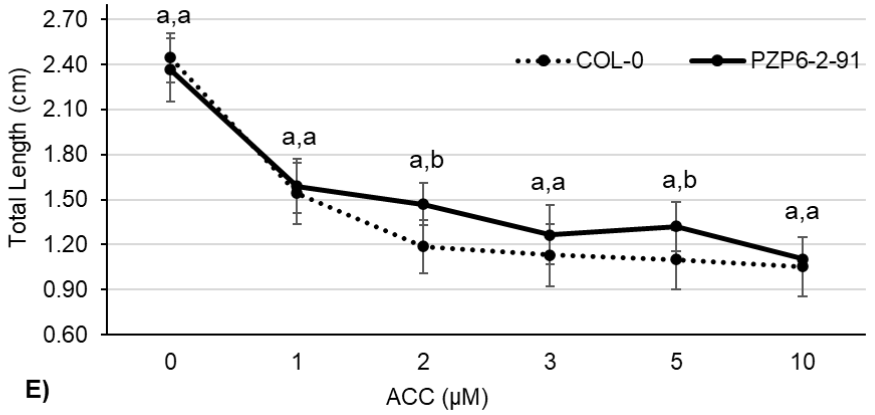
Total Length (cm)
2.70
2.40
2.10
1.80
1.50
1.20
0.90
0.60
a,a
a,a
a,b
a,a
a,b
a,a
COL-0
PZP6-2-91
0
1
2
3
5
10
ACC (µM)
E)

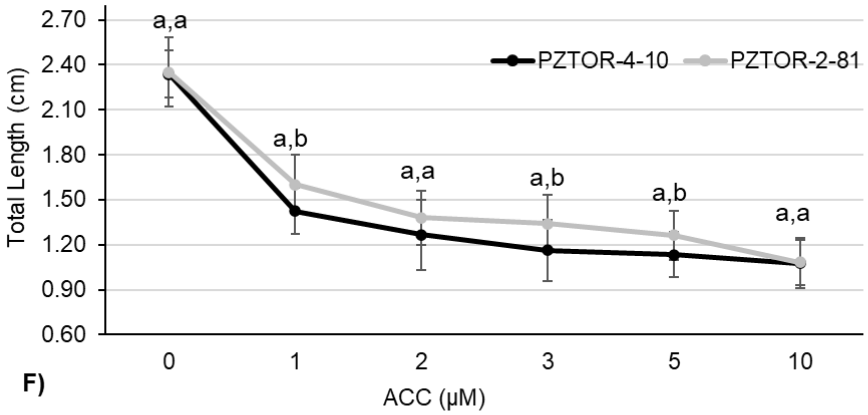
Total Length (cm)
2.70
2.40
2.10
1.80
1.50
1.20
0.90
0.60
a,a
a,b
a,a
a,b
a,b
a,a
PZTOR-4-10
PZTOR-2-81
0
1
2
3
5
10
ACC (µM)

F)

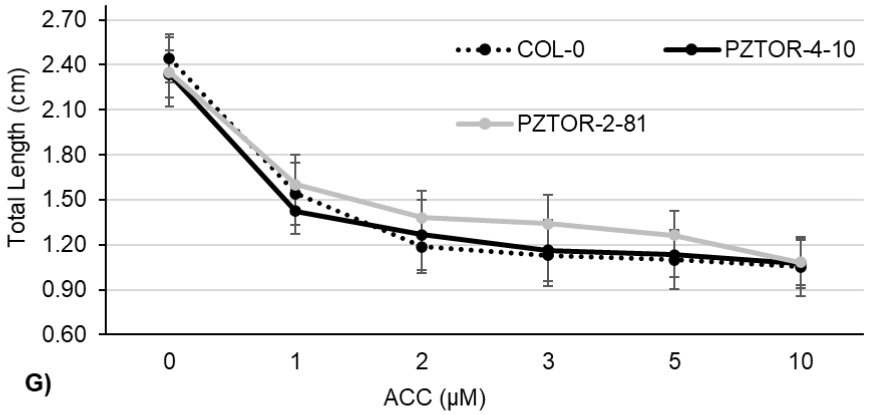
Total Length (cm)
2.70
2.40
2.10
1.80
1.50
1.20
0.90
0.60
COL-0
PZTOR-4-10
PZTOR-2-81
0
1
2
3
5
10
ACC (µM)

G)

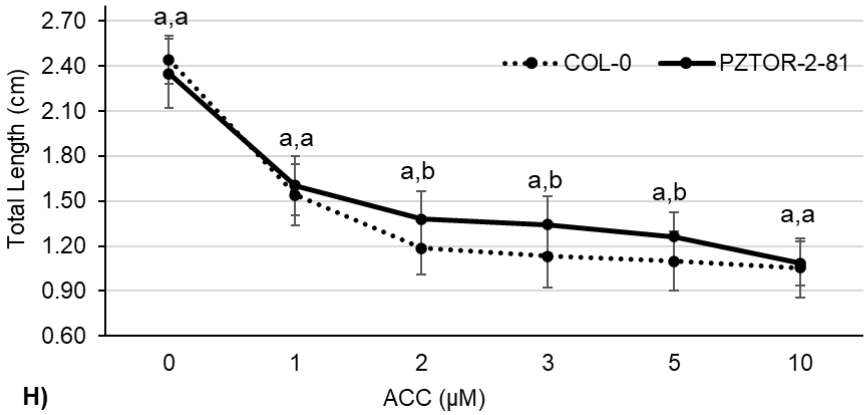
Total Length (cm)
2.70
2.40
2.10
1.80
1.50
1.20
0.90
0.60
a,a
a,a
a,b
a,b
a,b
a,a
COL-0
PZTOR-2-81
0
1
2
3
5
10
ACC (µM)

H)

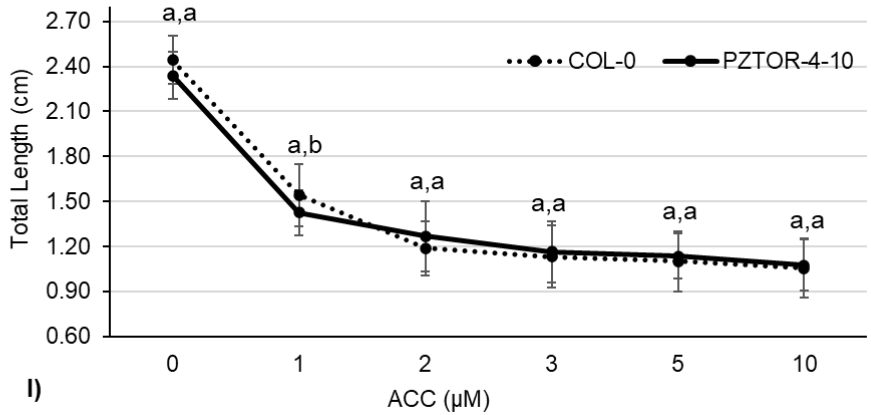
Total Length (cm)
2.70
2.40
2.10
1.80
1.50
1.20
0.90
0.60
a,a
a,b
a,a
a,a
a,a
a,a
COL-0
PZTOR-4-10
0
1
2
3
5
10
ACC (µM)

I)

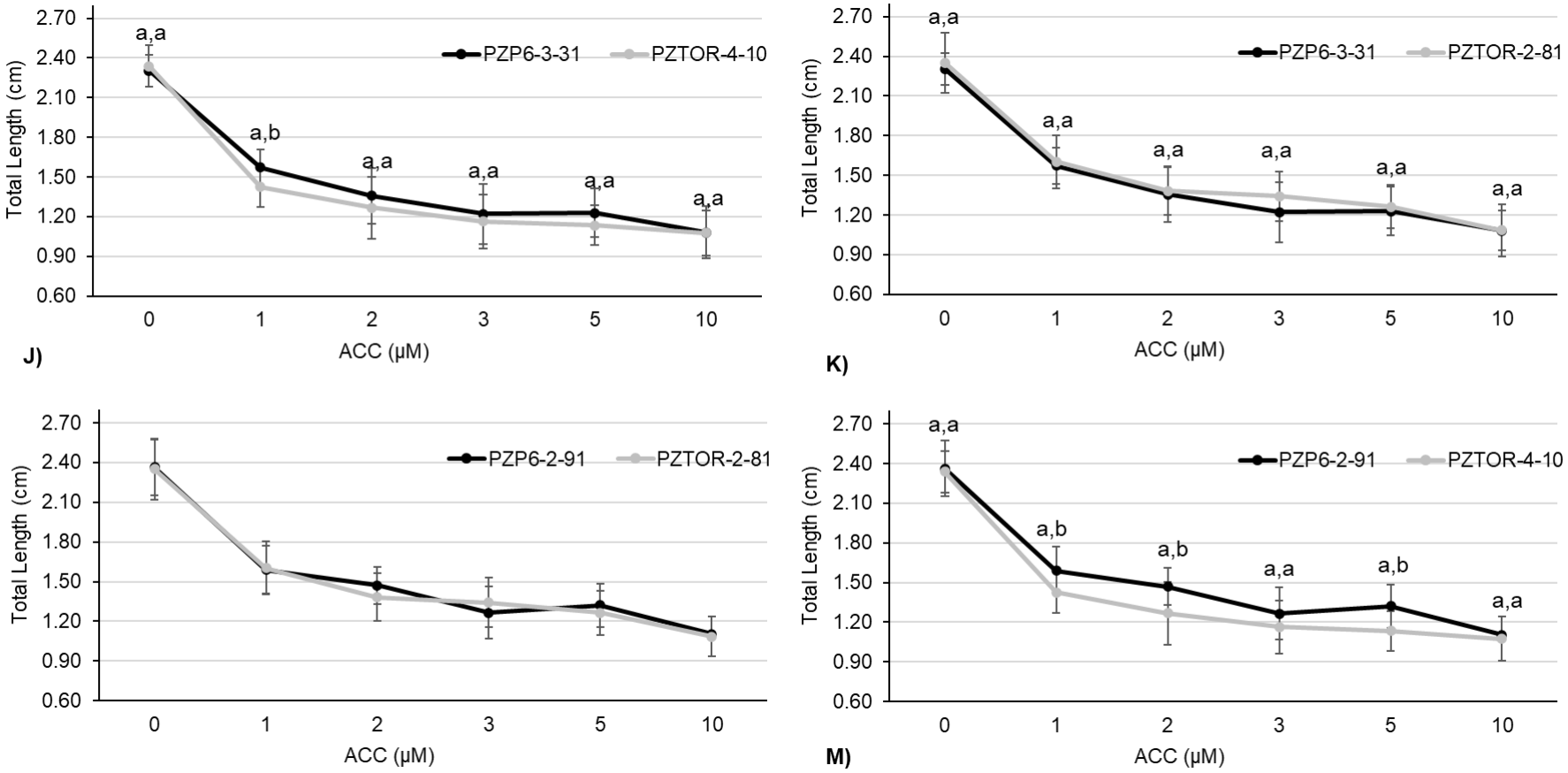

Figure 5.1. Ethylene sensitivity of transgenic Arabidopsis lines expressing P6WT-GFP and P6(ΔTOR)-GFP under the control of 35S promoter. (A) Line chart displays the ethylene triple response assay, i.e., total length (cm) comparisons. The transgenic lines under the control of the 35S promoter pEZR-P6WT-GFP: PZP6-3-31 and PZP6-2-91, pEZR-P6(ΔTOR)-GFP:

PZTOR-4-10 and PZTOR-2-8, and Col-0 on ½ MS plates containing different concentrations of ACC, i.e., 0 µM, 1 µM, 2 µM, 3 µM, 5 µM, and 10 µM **(B-M)** Pairwise comparisons of ethylene sensitivity of transgenic Arabidopsis lines expressing P6WT-GFP and P6(ΔTOR)-GFP under the control of 35S promoter**.** Line chart displays the ethylene triple response assay, i.e., total length (cm) comparisons of PZP6-3-31 and PZP6-2-91, PZTOR-4-10, PZTOR-2-8, and Col-0 on ½ MS plates containing different concentrations of ACC, i.e., 0 µM, 1 µM, 2 µM, 3 µM, 5 µM, and 10 µM. The morphometric measurements of the total length were taken after five days using Fiji image analysis software. Each point in the line represents an average of seedlings' total length values for 36 replicates per experimental line. Points with the same letters indicate mean values that are not significantly different at $p \leq 0.05$ (ANOVA and post hoc Tukey-Kramer HSD test). The response pattern is a gradual decline or shorting in the total length as the ACC concentration increases. P-value with different letter superscripts indicates statistically significantly different values, hence different in the total length and sensitivity to ethylene.

	ACC (µM)					
	0	**1**	**2**	**3**	**5**	**10**
Col-0 vs. PZP6-3-31						
p-value (ANOVA, α=0.05)	**0.0109**	0.9521	**0.0021**	0.3485	**0.0164**	1.0000
Tukey HSD test	a, b	a, a	a, b	a, a	a, b	a, a
Col-0 vs. PZP6-2-91						
p-value (ANOVA, α=0.05)	0.3282	0.7753	**<.0001**	0.0516	**<.0001**	1.0000
Tukey HSD test	a, a	a, a	a, b	a, a	a, b	a, a
PZP6-3-31 vs. PZP6-2-91						

p-value (ANOVA, α=0.05)	0.6337	0.9922	0.0943	0.8987	0.9753	1.0000
Tukey HSD test	a, a	a, a	a, a	a, a	a, a	a, a
Col-0 vs. PZTOR-4-10						
p-value (ANOVA, α=0.05)	0.1025	**0.0490**	0.3976	0.9616	0.9167	1.0000
Tukey HSD test	a, a	a, b	a,a	a, a	a, a	a, a
Col-0 vs. PZTOR-2-81						
p-value (ANOVA, α=0.05)	0.1926	0.5812	**0.0003**	**0.0002**	**0.0010**	1.0000
Tukey HSD test	a, a	a, a	a, b	a, b	a, b	a, a
PZTOR-4-10 vs. PZTOR-2-81						
p-value (ANOVA, α=0.05)	0.9984	**0.0003**	0.0899	**0.0027**	**0.0171**	1.0000
Tukey HSD test	a, a	a, b	a, a	a, b	a, b	a, a
PZP6-3-31 vs. PZTOR-4-10						
p-value (ANOVA, α=0.05)	0.9273	**0.0056**	0.2734	0.7656	0.1487	1.0000
Tukey HSD test	a, a	a, b	a, a	a, a	a, a	a, a
PZP6-3-31 vs. PZTOR-2-81						
p-value (ANOVA, α=0.05)	0.8064	0.9429	0.9841	0.0921	0.9212	1.0000
Tukey HSD test	a, a	a, a	a, a	a, a	a, a	a, a
PZP6-2-91 vs. PZTOR-4-10						
p-value (ANOVA, α=0.05)	0.9776	**0.0012**	**0.0001**	0.2382	**<.0001**	1.0000

Tukey HSD test	a, a	a, b	a, b	a, a	a, b	a, a
PZP6-2-91 vs. PZTOR-2-81						
p-value (ANOVA, α=0.05)	0.9984	0.9978	0.2831	0.4868	0.6059	1.0000
Tukey HSD test	a, a	a, a	a, a	a, a	a, a	a, a

Table 5.2. Statistical comparison of Plant responses to ethylene data. Comparison between the average total length average of Col-0, PZP6-2-91, PZP6-3-31, PZTOR-2-81, and PZTOR-4-10 seedlings at different ACC concentration (0 µM, 1 µM, 2 µM, 3 µM, 5 µM, and 10 µM) after five days of incubation. The significant statistical differences between lines were determined based on a two-way analysis of variance (ANOVA) and Tukey-Kramer Honestly Significant Difference post hoc test ($P \leq 0.05$). P-value with different letter superscripts indicates values that are statistically significantly different, hence different in the total length and sensitivity to ethylene

5.3.1.1.2. Estradiol-inducible lines expressing P6-GFP and P6(ΔTOR)-GFP

To better determine the impact of P6 expression and the role of the TOR binding domain on the Ethylene Triple Response, the experiments were repeated using the lines in which expression is driven by the estradiol-inducible promoter. In contrast to the pEZR lines, which constitutively express P6, plants from the pER8 lines contain much greater levels of P6 following estradiol induction (P6WT-GFP and P6(ΔTOR)-GFP) and less breakdown *in planta* of the fusion protein as it was shown in chapter 4. This should make it easier to identify differences in ET sensitivity.

The transgenic Arabidopsis lines expressing P6WT-GFP and P6(ΔTOR)-GFP under the control of the β-estradiol inducible promoter pER8-P6WT-GFP; P8P6-10-121, and P8P6-7-78, and pER8-P6(ΔTOR)-GFP; P8TOR-2-11 and P8TOR-2-10 (see Table 5.1) were tested in the Ethylene Triple Response assay. P6 expression was induced by including 30 μM of β-estradiol (+B) in the agar plate medium. All tested lines, including the NT control plants Col-0, were grown the seeds on ½ MS plates containing different concentrations of ACC, i.e., 0 μM, 1 μM, 3 μM, and 5 μM with 30 μM of β-estradiol (+B) and as additional controls were grown without 30 μM of β-estradiol. The sensitivity to ethylene was evaluated by measuring the total length of individual seedlings using Fiji analysis software after five days of incubation in the dark. As previously described, the experimental trend shows a gradual reduction in seedling total length as the ACC concentration increases. As an additional control, all the lines were also tested in the Ethylene Triple Response assay but in the absence of β-estradiol, with the expectation that in the absence of expression of the transgene, they should respond similarly to the NT controls. The results (figure 5.6) show that this was in fact the case. In the absence of ACC, NT Col-0 seedlings showed no statistically significant difference in length between estradiol treated or untreated controls demonstrating that estradiol treatment itself does not impact seedling length. The data shown here are from three independent biological replicas. The average total length of Col-0, P8P6-10-121, P8P6-7-78, P8TOR-2-11, and P8TOR-2-10 seedlings before and after β-estradiol induction and in the

presence and absence of increasing concentrations of ACC are shown in Table 5.3, and Figure 5.2-5.5.

Overall, in the presence of β-estradiol, seedlings from the P8P6-10-121 and P8P6-7-78 lines showed less reduction in the overall length than did the NT control. They also showed less reduction in the overall length than did the lines expressing P6(ΔTOR), P8TOR-2-11, and P8TOR-2-10 (Table 5.3 and Figure 5.2). Like the previous findings with A7 and the pEZR lines, all tested lines (transgenic and WT) showed a statistically significant reduction in seedling total length at > 1 μM of ACC with the most significant reduction at 5 μM of ACC (Figure 5.3, 5.4 and 5.5).

The two-way ANOVA revealed a statistically significant interaction between the effects of different lines and different ACC concentrations on plant total length (p = <.0001). The initial effect analysis demonstrated that different lines had a statistically significant effect on plant total length (p = <.0001), and different ACC concentrations had a statistically significant effect on plant total length (p = <.0001), i.e., different lines had a different level of sensitivity to ethylene. Similar to the findings in chapter 3 and pEZR lines sensitivity response to ET, all lines showed a statistically significant reduction in total length at 1μM ACC (ANOVA p-value = <.0001). The results are shown in Table 5.2 and 5.3, and Figure 5.3-5.5. The analysis revealed that Col-0 had a statistically significant difference in relative length reduction between 1 μM and lengths at all of the other ACC concentrations (p = <.0001) in the presence of β-estradiol, which was longer. The total length was decreased as ACC concertation increased.

The two-way ANOVA analysis revealed that in the presence of β-estradiol, the P8P6 10-121 had a statistically significant difference in relative length reduction between 1 μM and lengths at all of the other ACC concentrations (p = <.0001), which was longer. Likewise, a statistically significant difference was detected between 3 and 5 μM (p = 0.0019). The analysis also revealed that P8P6 7-78 had a statistically significant difference in relative length reduction between 1 μM and lengths at all of

the other ACC concentrations (p = <.0001), which was longer. Likewise, a statistically significant difference was detected between 3 and 5 μM (p = 0.0034).

Comparing the two lines expressing native P6, P8P6-10-121, and P8P6-7-78 with each other, there were no statistically significant differences in the response patterns to different ACC concentrations after β-estradiol induction (Table 5.2 and Figure 5.2 and 5.3 A-F). Compared to the Col-0 control, both transgenic lines expressing native P6 showed a statistically significant reduced shortening at ACC concentrations of 0 μM,3 μM, and 5 μM of ACC) (Table 5.2 and Figure 5.3 D-F). Although the estradiol induced transgenic lines were shorter than the Col-0 controls in the absence of ACC (ANOVA p-value = <.0001), the P8P6-10-121 and P8P6-7-78 displayed statistically significantly less reduction in seedling total length compared to Col-0 at 3 μM, and 5 μM of ACC (ANOVA p-value = <.0001, respectively). As an additional control, ethylene sensitivity was compared for lines P8P6-10-121 and P8P6-7-78 in the absence of β-estradiol, in which they behaved like Col-0 (Table 5.2 and Figure 5.5). Comparing seedling length in the absence of ACC for the two lines expressing P6WT, estradiol-induced P8P6-10-121 and P8P6-7-78 were shorter than non-induced seedlings of the same lines (ANOVA p-value = <.0001) but similar in length to Col-0 (Table 5.2, Figures 5.5). These results show that transgenic Arabidopsis lines expressing P6WT-GFP have a reduced response/sensitivity to ethylene compared to the wildtype plants in the Ethylene Triple Response assay. Again, these results are entirely consistent with the results presented in chapter 3 on the earlier P6 transgenic line A7, the findings on the pEZR lines (presented above), and the report of Geri et al (2004) that P6 transgenic plants show ET insensitivity.

In the presence of β-estradiol, the P8TOR 2-11 had a statistically significant difference in relative length reduction between 1 μM and lengths at all of the other ACC concentrations (p = <.0001), which was longer. Likewise, a statistically significant difference was detected between 3 and 5 μM (p = 0.0007). The P8TOR 2-10 had a statistically significant difference in relative length reduction between 1 μM and lengths at all of the other ACC concentrations (p = <.0001), which was

longer. Likewise, a statistically significant difference was detected between 3 and 5 μM ($p = 0.0002$).

In the presence of β-estradiol, the two lines expressing P6(ΔTOR) showed a similar degree of shortening with increasing ACC concentration when compared to each other. Seedling lengths for P8TOR-2-11 and P8TOR-2-10 were similar to those for Col-0 at 0 and 1μM ACC concentrations suggesting that deletion of the TOR binding domain does impact on the effect of P6 expression on ET sensitivity. However, at 3μM and 5 μM of ACC, they exhibited a statistically significant reduced shortening compared to the Col-0 (Table 5.3 and Figure 5.3 G-J), suggesting that these lines were less sensitive to ET. Comparing the two inducible lines expressing P6(ΔTOR), P8TOR-2-11 and P8TOR-2-10 shared the same sensitivity degree and response pattern to increasing ACC concentration (Table 5.2 and Figure 5.2 and 5.3 G-J). The P8TOR-2-10 displayed similar results to P6TOR-2-11 at 1 μM, 3 μM, and 5 μM of ACC, except at 0 μM of ACC where statistically significant difference was detected (ANOVA p-value = 0.0014), in which P8TOR-2-10 was shorter on seedling total length (Table 5.2 and Figure 5.2-5.5). There was no statistically significant difference in the total seedling length detected between Col-0 and P8TOR-2-11 in the absence of ACC or at 1 μM. However, at 3 μM and 5 μM ACC, P8TOR-2-11 showed less shortening than Col-0 (ANOVA p-value = <.0001 for both concentrations). The second P6(ΔTOR) expressing line, P8TOR-2-10 displayed similar results to P6TOR-2-11 except at 0 μM of ACC they had a shorter seedling total length compared to Col-0 (ANOVA p-value = 0.0006) (Table 5.2 and Figure 5.2-5.5). As an additional control, ETR is compared for lines P8TOR-2-11 and P8TOR-2-10 in the absence of β-estradiol. Similar to the lines expressing P6WT, both lines were found to behave like Col-0 (Table 5.2 and Figure 5.5). These results suggest that deleting the TOR binding domain may weaken the ability of P6 to reduce ethylene's sensitivity, displaying a more wild-type phenotype, but the major effect of P6 on the ETR is at least partially independent of TOR binding domain.

Additionally, transgenic Arabidopsis lines expressing P6WT-GFP and P6(ΔTOR)-GFP displayed different stunting severity. Comparisons between the two lines

expressing P6WT and two lines expressing P6(ΔTOR) indicated that all lines shared a similar sensitivity degree and response pattern to increasing ACC concentration. Similar to the two lines expressing P6WT, seedling lengths were significantly shorter in estradiol-induced P8TOR-2-11 and P8TOR-2-10 when compared to non-induced P8TOR-2-11 and P8TOR-2-10 (ANOVA p-value = <.0001) (Table 5.2 and Figure 5.5). However, the relative reduction in length in the induced seedlings for the P6(ΔTOR) lines was less than the induced lines expressing P6WT, P8P6-10-121 and P8P6-7-78 (Table 5.2 and Figure 5.3, 5.4 and 5.5). Also, lines expressing P6WT were shorter than lines expressing P6(ΔTOR) in the absence of ACC (Table 5.2 and Figure 5.10 and 5.11). Although the P6(ΔTOR) lines have a different phenotype from the P6WT lines in the absence of ACC, but when they were exposed to ACC in the triple response assay, they all come together and have similar responses, i.e., statistically significant indifference. Therefore, one suggestion is that the ethylene might compensate or trigger some pathways that will make the lines expressing P6(ΔTOR) behave the same as lines expressing P6WT in response to ethylene. These results suggest that transgene-mediated expression of P6 in Arabidopsis causes stunting in a partially-TOR binding domain-dependent manner.

Taking together, these findings suggested that the TOR domain is required for the stunting phenotype but may be dispensable for the reduced ET sensitivity phenotype.

	Total length (cm)			
ACC (μM)	**0**	**1**	**3**	**5**
Col-0	2.159 ± 0.141	1.205 ± 0.191	0.896 ± 0.163	0.852 ± 0.166
COL-0+B	2.134 ± 0.105	1.233 ± 0.116	0.930 ± 0.110	0.801 ± 0.107
P8P6-7-78	2.107 ± 0.164	1.128 ± 0.155	0.853 ± 0.136	0.904 ± 0.087
P8P6-7-78+B	1.917 ± 0.092	1.396 ± 0.123	1.133 ± 0.112	1.029 ± 0.101
P8P6-10-121	2.012 ± 0.110	1.290 ± 0.161	0.973 ± 0.116	0.892 ± 0.113
P8P6-10-121+B	1.808 ± 0.157	1.315 ± 0.162	1.099 ± 0.161	0.971 ± 0.104
P8TOR-2-10	2.190 ± 0.092	1.325 ± 0.143	1.089 ± 0.103	0.943 ± 0.130
P8TOR-2-10+B	2.000 ± 0.097	1.252 ± 0.151	1.081 ± 0.112	0.958 ± 0.114
P8TOR-2-11	2.335 ± 0.110	1.249 ± 0.108	1.221 ± 0.168	1.172 ± 0.140
P8TOR-2-11+B	2.127 ± 0.110	1.285 ± 0.143	1.110 ± 0.115	1.003 ± 0.082

Table 5.3. Plant responses to different concentration of ACC. The total length average of Col-0, P8P6-10-121, P8P6-7-78, P8TOR-2-11 and P8TOR-2-10 seedlings grown for five days on different concentrations of ACC; 0 μM, 1 μM, 3 μM, and 5 μM with or without β-estradiol induction. Each number represents average values for 36 replicates per experimental line at specific ACC concentration. Values are average seedlings total length ± standard deviations (average N = 36 seedlings per line).

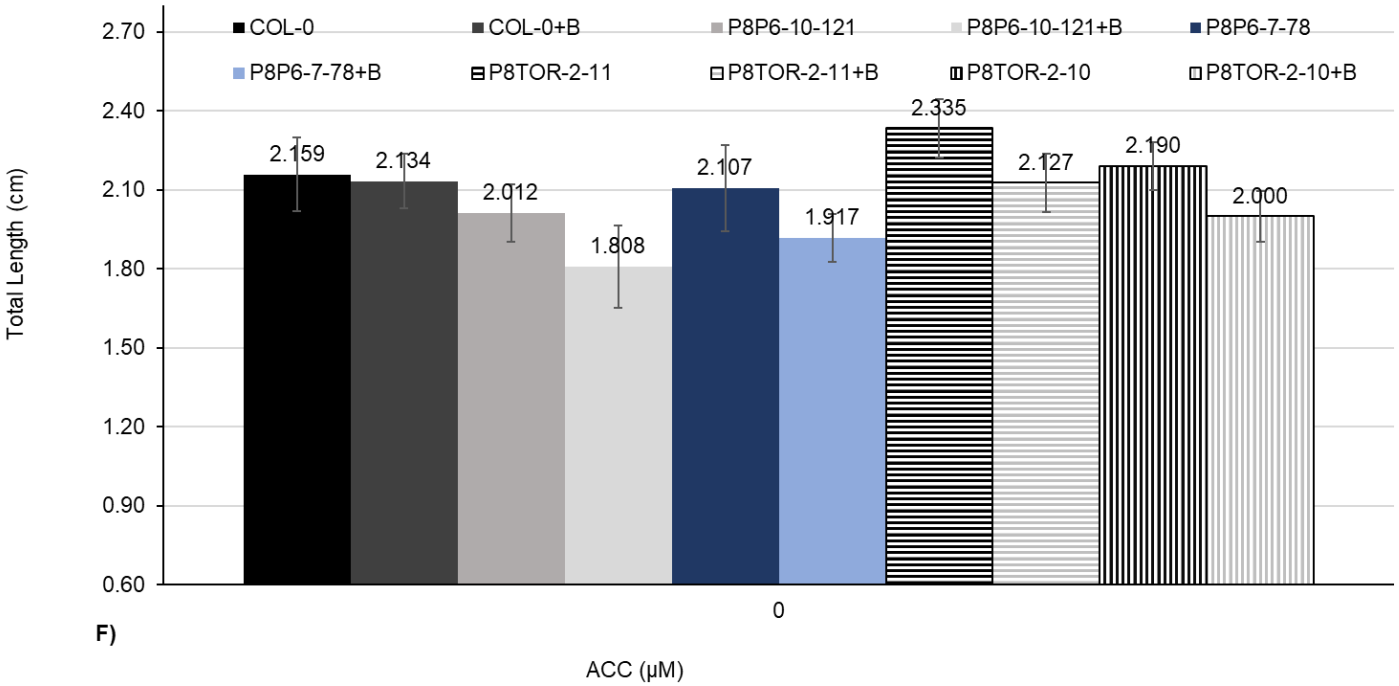

Figure 5.2. Impact of P6WT-GFP and P6(ΔTOR)-GFP expression on plant total length. The bar chart displays the ethylene triple response assay, i.e., total length (cm) comparisons of each line with 30 µM of β-estradiol (+B) and without β-estradiol. A) Col-0+B and Col-0 (black and dark gray, respectively), B) P8P6-10-121+B and P8P6-10-121 (gray and light gray, respectively), C) P8P6-7-78+B and P8P6-7-78 (blue and light blue, respectively), D) P8TOR-2-11+B and P8TOR-2-11 (black cross and gray cross, respectively), and E) P8TOR-2-10B and P8TOR-2-10 (black stripes and gray stripes, respectively) on ½ MS plates. The morphometric measurements

of the total length were taken after five days using Fiji image analysis software. Each bar represents an average of seedlings' total length values for 36 replicates per experimental line.

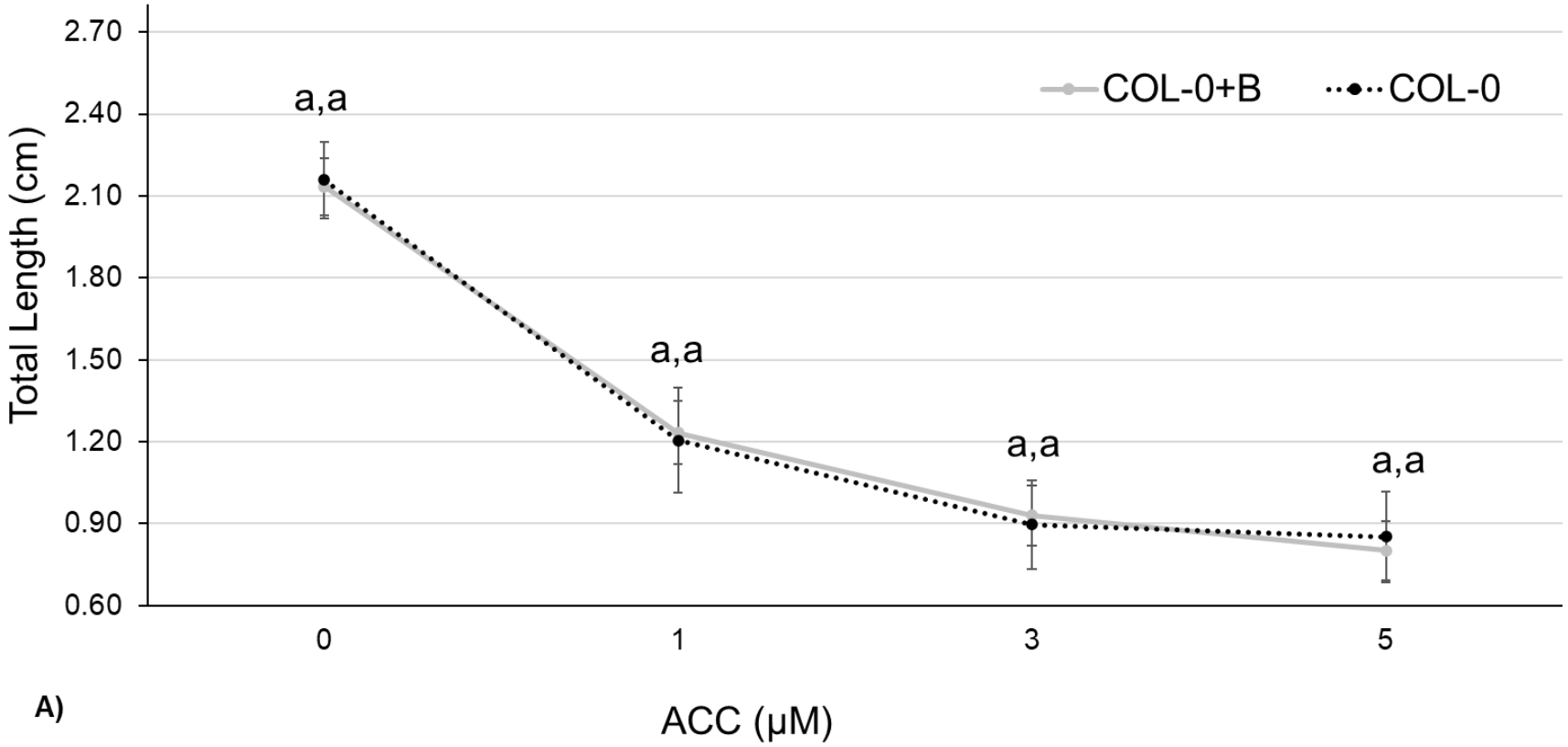

A)

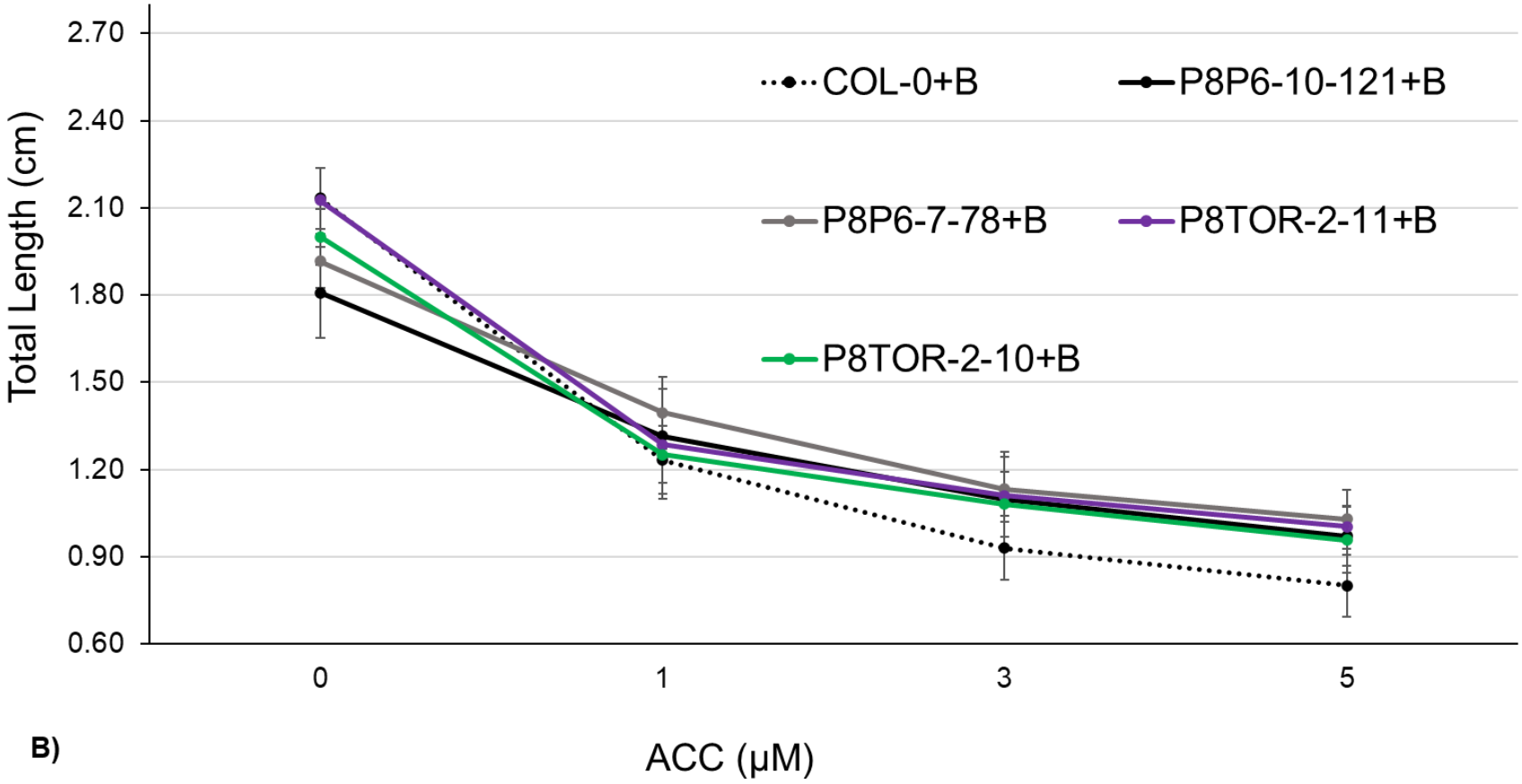
2.70
2.40
2.10
1.80
1.50
1.20
0.90
0.60
Total Length (cm)
COL-0+B
P8P6-10-121+B
P8P6-7-78+B
P8TOR-2-11+B
P8TOR-2-10+B
0
1
3
5
ACC (µM)

B)

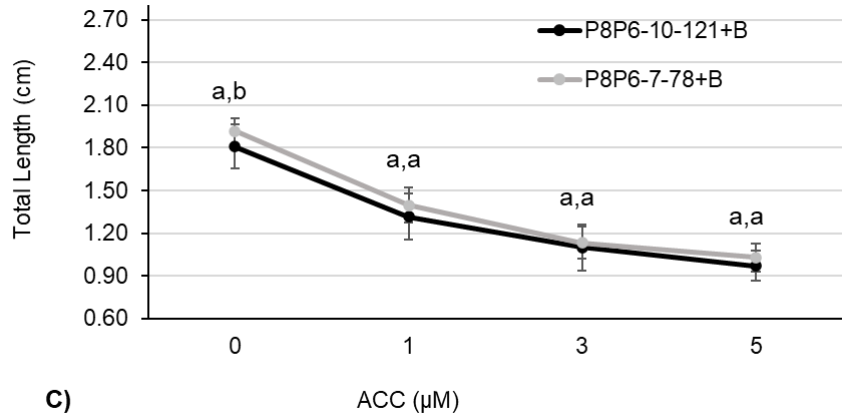
2.70
2.40
2.10
1.80
1.50
1.20
0.90
0.60
Total Length (cm)
P8P6-10-121+B
P8P6-7-78+B
a,b
a,a
a,a
a,a
0
1
3
5
ACC (µM)

C)

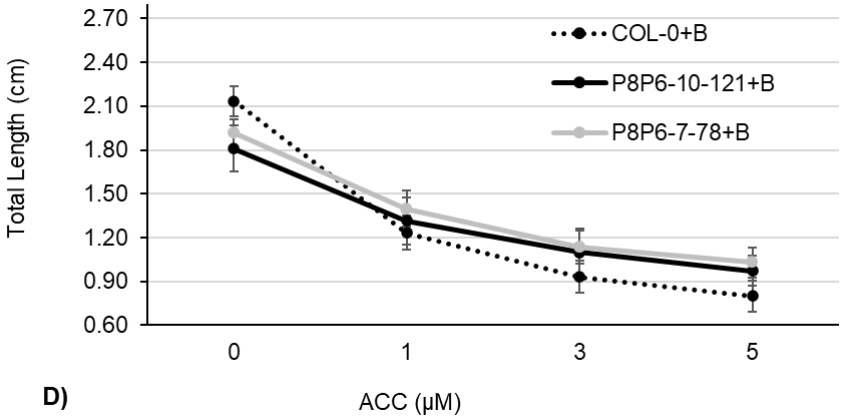
2.70
2.40
2.10
1.80
1.50
1.20
0.90
0.60
Total Length (cm)
COL-0+B
P8P6-10-121+B
P8P6-7-78+B
0
1
3
5
ACC (µM)

D)

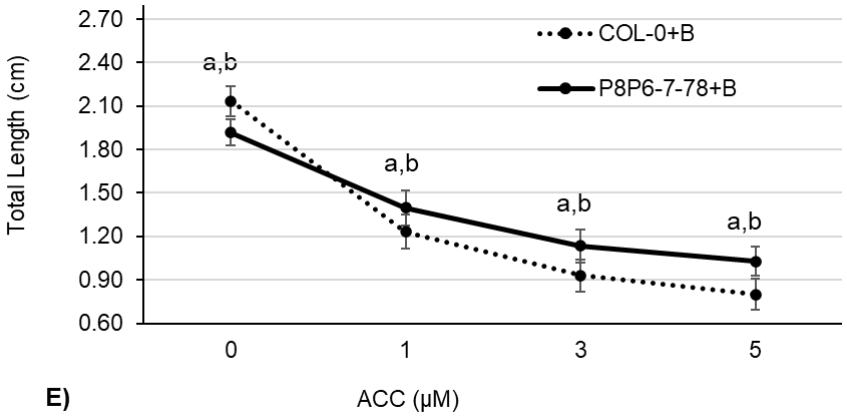
2.70
2.40
2.10
1.80
1.50
1.20
0.90
0.60
Total Length (cm)
COL-0+B
P8P6-7-78+B
a,b
a,b
a,b
a,b
0
1
3
5
ACC (µM)

E)

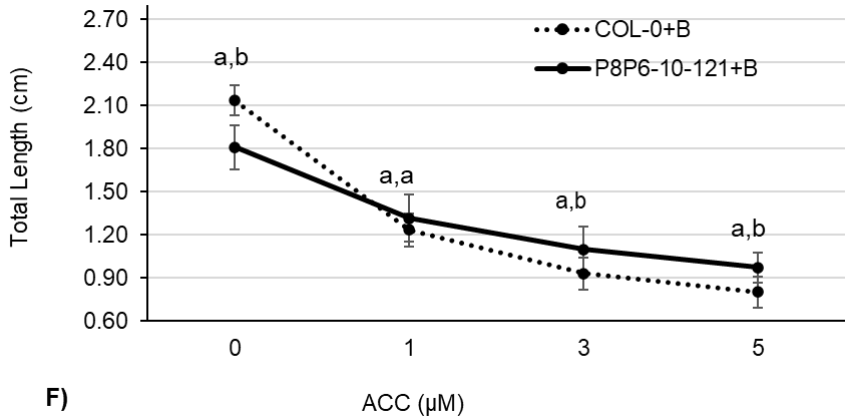
2.70
2.40
2.10
1.80
1.50
1.20
0.90
0.60
Total Length (cm)
COL-0+B
P8P6-10-121+B
a,b
a,a
a,b
a,b
0
1
3
5
ACC (µM)

F)

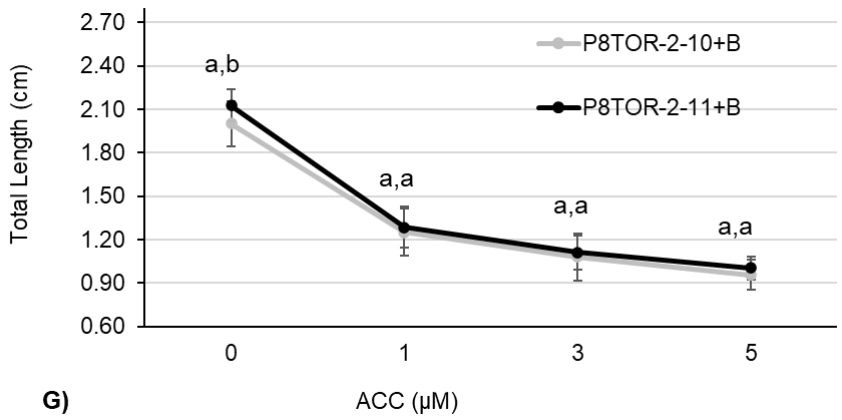
Total Length (cm)
2.70
2.40
2.10
1.80
1.50
1.20
0.90
0.60
P8TOR-2-10+B
P8TOR-2-11+B
a,b
a,a
a,a
a,a
0
1
3
5
ACC (µM)

G)

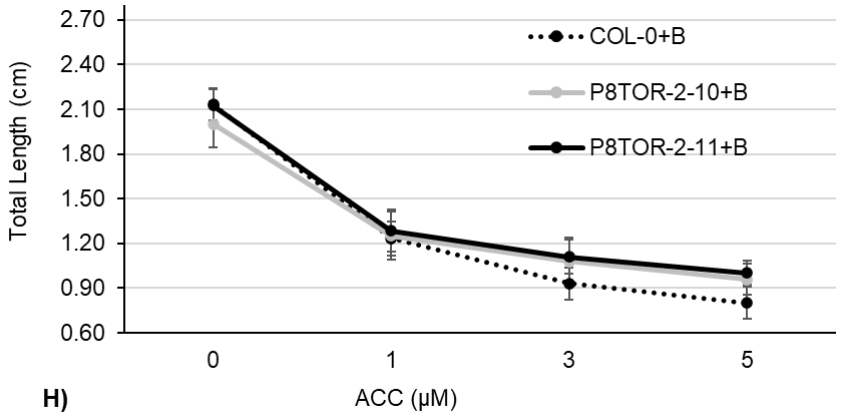
Total Length (cm)
2.70
2.40
2.10
1.80
1.50
1.20
0.90
0.60
COL-0+B
P8TOR-2-10+B
P8TOR-2-11+B
0
1
3
5
ACC (µM)

H)

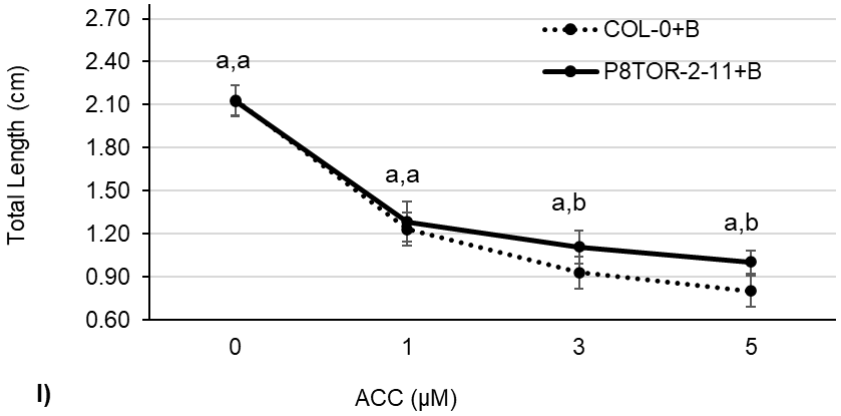
Total Length (cm)
2.70
2.40
2.10
1.80
1.50
1.20
0.90
0.60
COL-0+B
P8TOR-2-11+B
a,a
a,a
a,b
a,b
0
1
3
5
ACC (µM)

I)

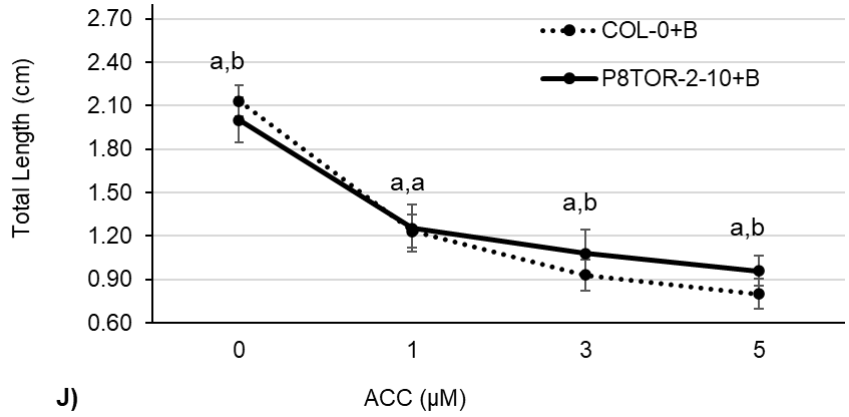
Total Length (cm)
2.70
2.40
2.10
1.80
1.50
1.20
0.90
0.60
COL-0+B
P8TOR-2-10+B
a,b
a,a
a,b
a,b
0
1
3
5
ACC (µM)

J)

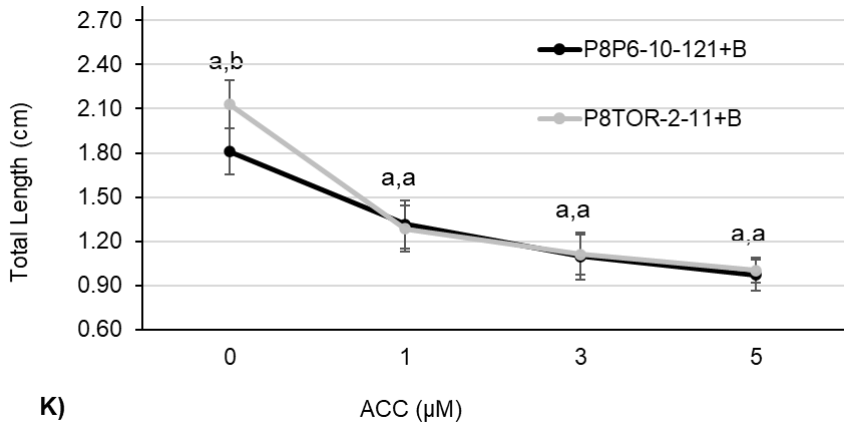
2.70
2.40
2.10
1.80
1.50
1.20
0.90
0.60
Total Length (cm)
P8P6-10-121+B
P8TOR-2-11+B
a,b
a,a
a,a
a,a
0
1
3
5
ACC (µM)

K)

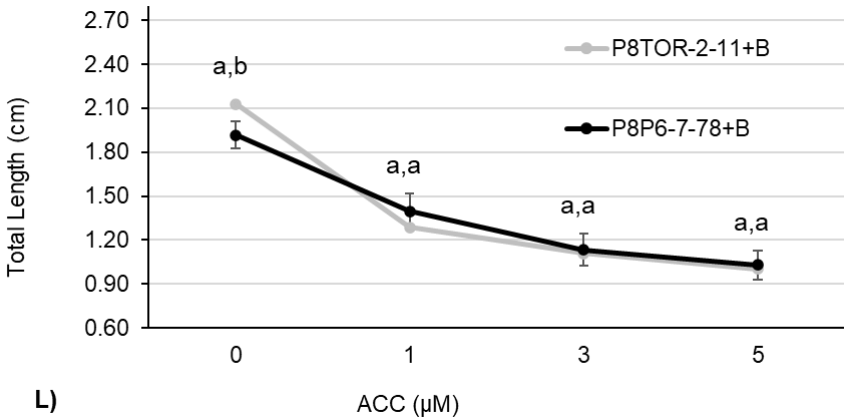
2.70
2.40
2.10
1.80
1.50
1.20
0.90
0.60
Total Length (cm)
P8TOR-2-11+B
P8P6-7-78+B
a,b
a,a
a,a
a,a
0
1
3
5
ACC (µM)

L)

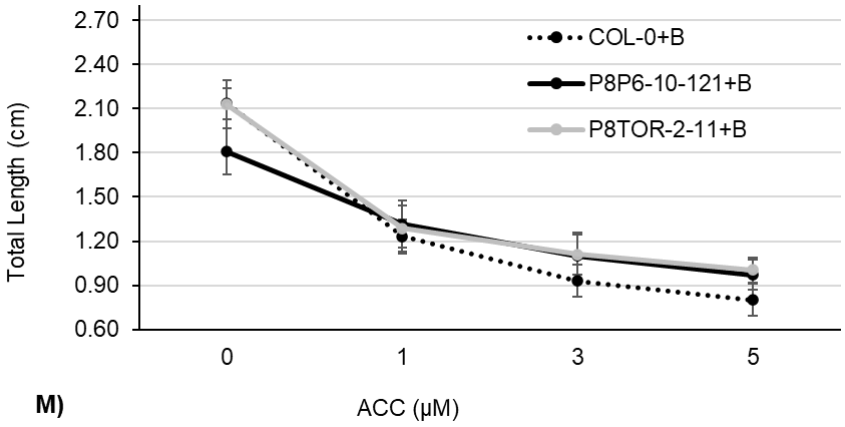
2.70
2.40
2.10
1.80
1.50
1.20
0.90
0.60
Total Length (cm)
COL-0+B
P8P6-10-121+B
P8TOR-2-11+B
0
1
3
5
ACC (µM)

M)

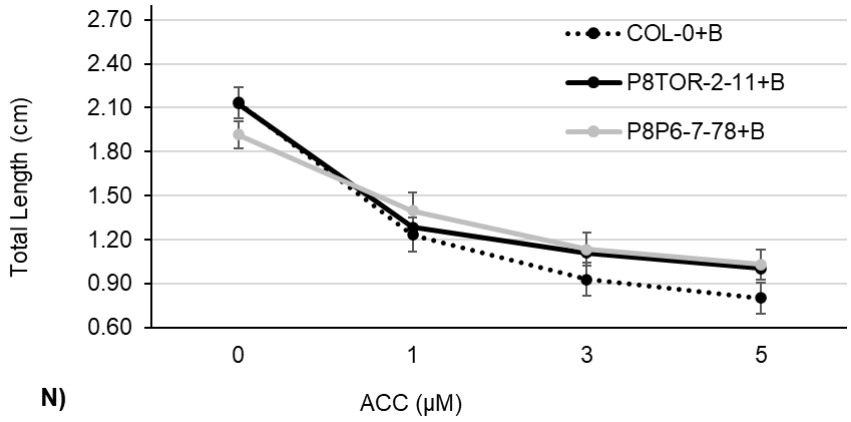
2.70
2.40
2.10
1.80
1.50
1.20
0.90
0.60
Total Length (cm)
COL-0+B
P8TOR-2-11+B
P8P6-7-78+B
0
1
3
5
ACC (µM)

N)

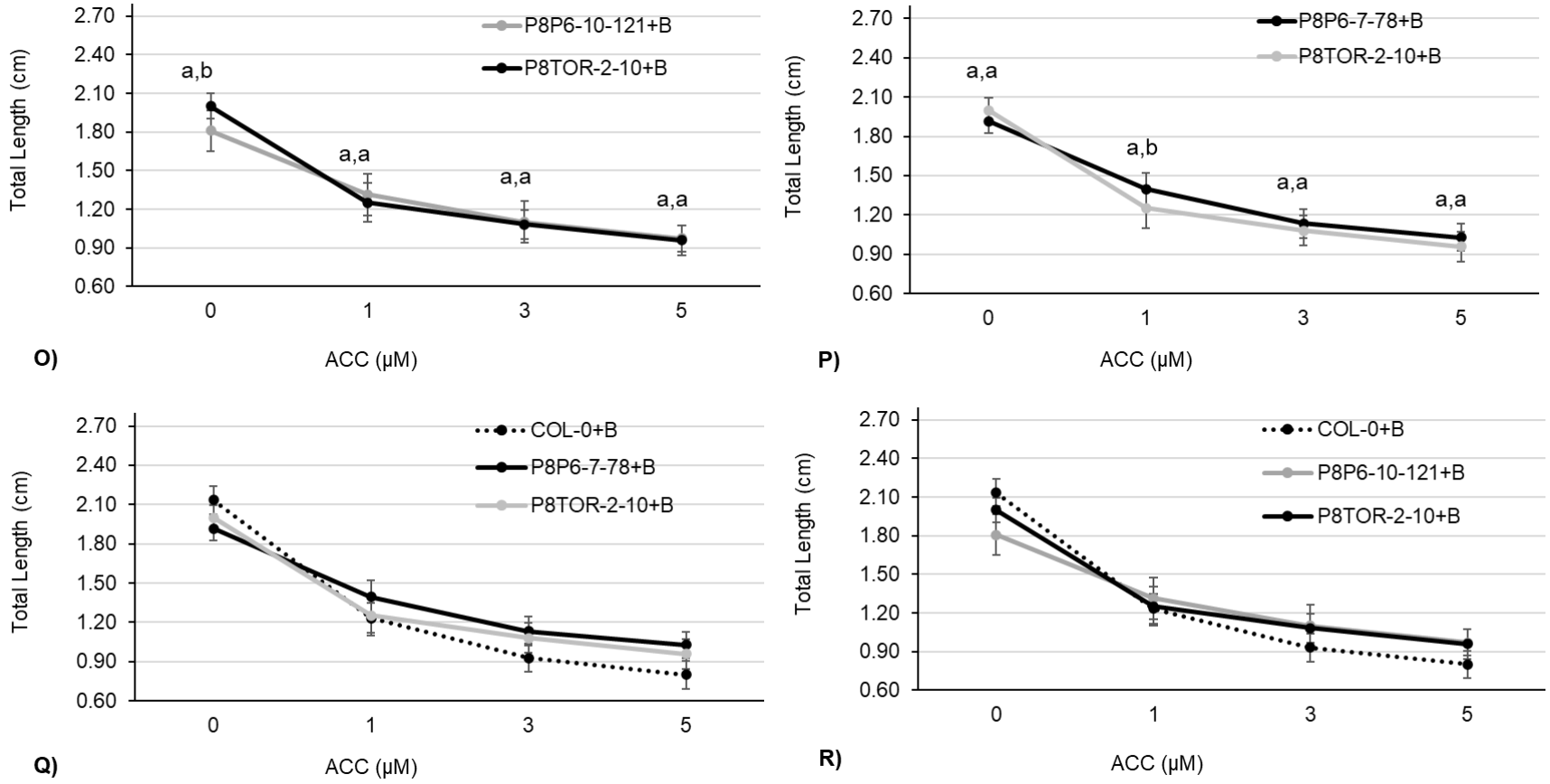

Figure 5.3. Ethylene sensitivity of transgenic Arabidopsis lines expressing P6WT-GFP and P6(ΔTOR)-GFP under the control of a β-estradiol inducible promoter. (A) Line chart displays the ethylene triple response assay, i.e., total length (cm) comparisons of Col-0 in the presence and absence of 30 µM of β-estradiol**. (B)** Line chart displays the ethylene triple response

assay, i.e., total length (cm) comparisons the transgenic lines under the control of β-estradiol inducible promoter pER8-P6WT-GFP: P8P6-10-121 and P8P6-7-78, pER8-P6(ΔTOR)-GFP: P8TOR-2-11 and P8TOR-2-10, and Col-0 grown on 1⁄2 MS plates containing different concentrations of ACC, i.e., 0 μM, 1 μM, 3 μM, and 5 μM with 30 μM of β-estradiol (+B). **(C-R)** Pairwise comparisons of ethylene sensitivity of transgenic Arabidopsis lines expressing P6WT-GFP and P6(ΔTOR)-GFP under the control of β-estradiol inducible promoters. Line chart displays the ethylene triple response assay, i.e., total length (cm) comparisons of P8P6-10-121, P8P6-7-78, P8TOR-2-11, P8TOR-2-10, and Col-0 grown on 1⁄2 MS plates containing different concentrations of ACC, i.e., 0 μM, 1 μM, 3 μM, and 5 μM with 30 μM of β-estradiol (+B). The morphometric measurements of the total length were taken after five days using Fiji image analysis software. Each point in the line represents an average of seedlings' total length values for 36 replicates per experimental line. Points with the same letters indicate mean values that are not significantly different at $p \leq 0.05$ (ANOVA and post hoc Tukey-Kramer HSD test). The response pattern is a gradual decline or shorting in the total length as the ACC concentration increases. Note +B= induced with 30 μM of β-estradiol. P-value with different letter superscripts indicates statistically significantly different values, hence different in the total length and sensitivity to ethylene.

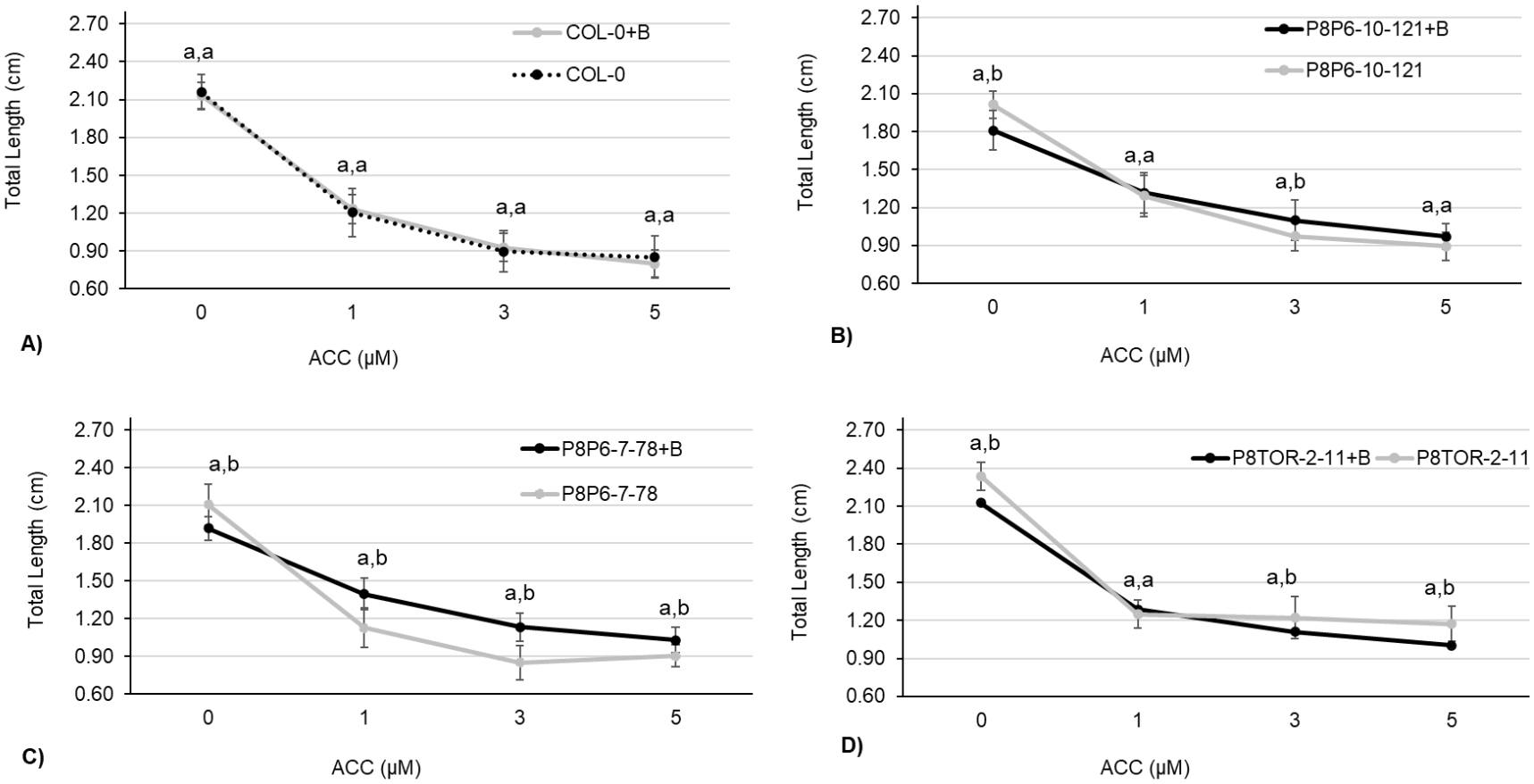
A)
Total Length (cm)
2.70
2.40
2.10
1.80
1.50
1.20
0.90
0.60
COL-0+B
COL-0
a,a
a,a
a,a
a,a
0
1
3
5
ACC (µM)
B)
Total Length (cm)
P8P6-10-121+B
P8P6-10-121
a,b
a,a
a,b
a,a
ACC (µM)
C)
Total Length (cm)
P8P6-7-78+B
P8P6-7-78
a,b
a,b
a,b
a,b
ACC (µM)
D)
Total Length (cm)
P8TOR-2-11+B
P8TOR-2-11
a,b
a,a
a,b
a,b
ACC (µM)

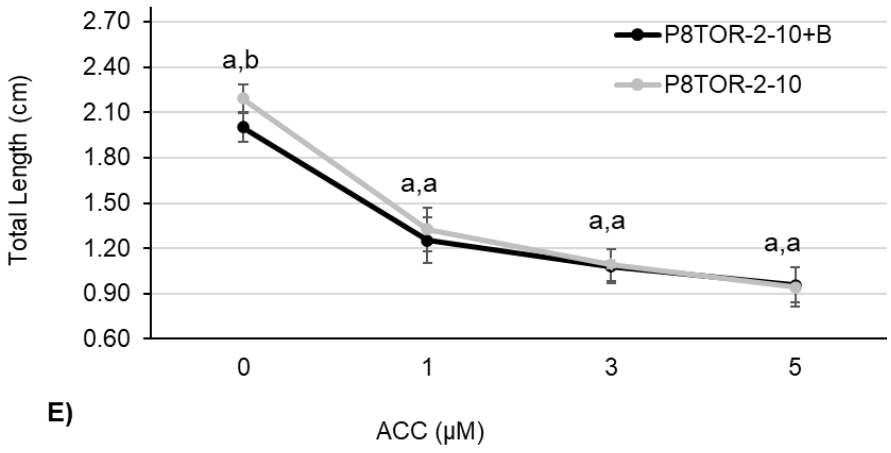

Figure 5.4. Ethylene sensitivity of transgenic Arabidopsis lines expressing P6WT-GFP and P6(∆TOR)-GFP under the control of a β-estradiol inducible promoter**.** Line chart displays the ethylene triple response assay, i.e., total length (cm) comparisons of each line with 30 µM of β-estradiol (+B) and without β-estradiol. A) Col-0+B and Col-0, B) P8P6-10-121+B and P8P6-10-121, C) P8P6-7-78+B and P8P6-7-78, D) P8TOR-2-11+B and P8TOR-2-11, and E) P8TOR-2-10B and P8TOR-2-10. on *½* MS plates containing different concentrations of ACC, i.e., 0 µM, 1 µM, 3 µM, and 5 µM. The morphometric measurements of the total length were taken after five days using Fiji image analysis software. Each point in the line represents an average of seedlings' total length values for 36 replicates per experimental line. Points with the same letters indicate mean values that are not significantly different at $p \leq 0.05$ (ANOVA and post hoc Tukey-Kramer HSD test). The response pattern is a gradual decline or shorting in the total length as the ACC concentration increases. Different letters a and b are shown at each point when there was a significantly different value.

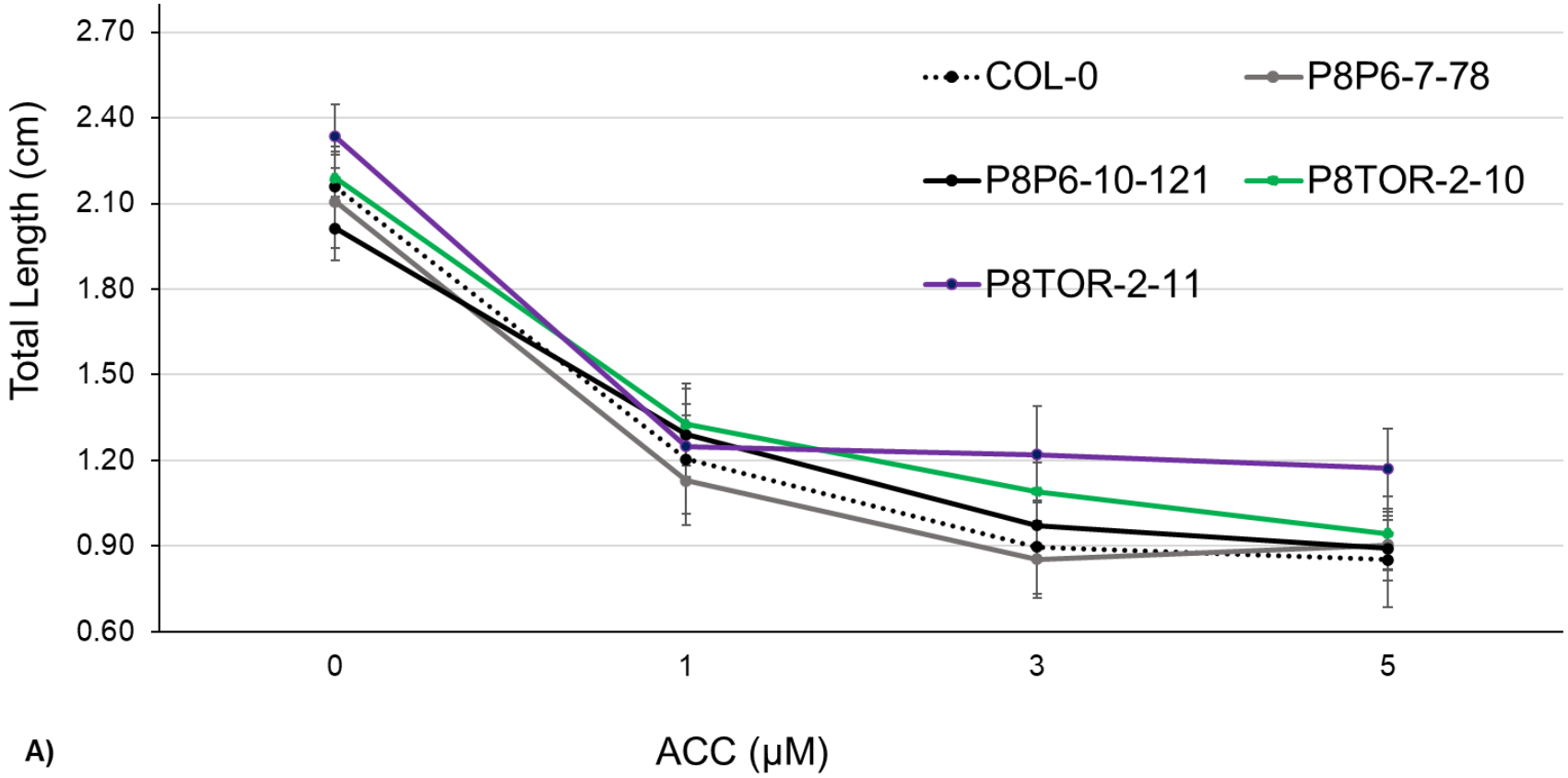
Total Length (cm)
2.70
2.40
2.10
1.80
1.50
1.20
0.90
0.60
0
1
3
5
ACC (µM)
COL-0
P8P6-7-78
P8P6-10-121
P8TOR-2-10
P8TOR-2-11

A)

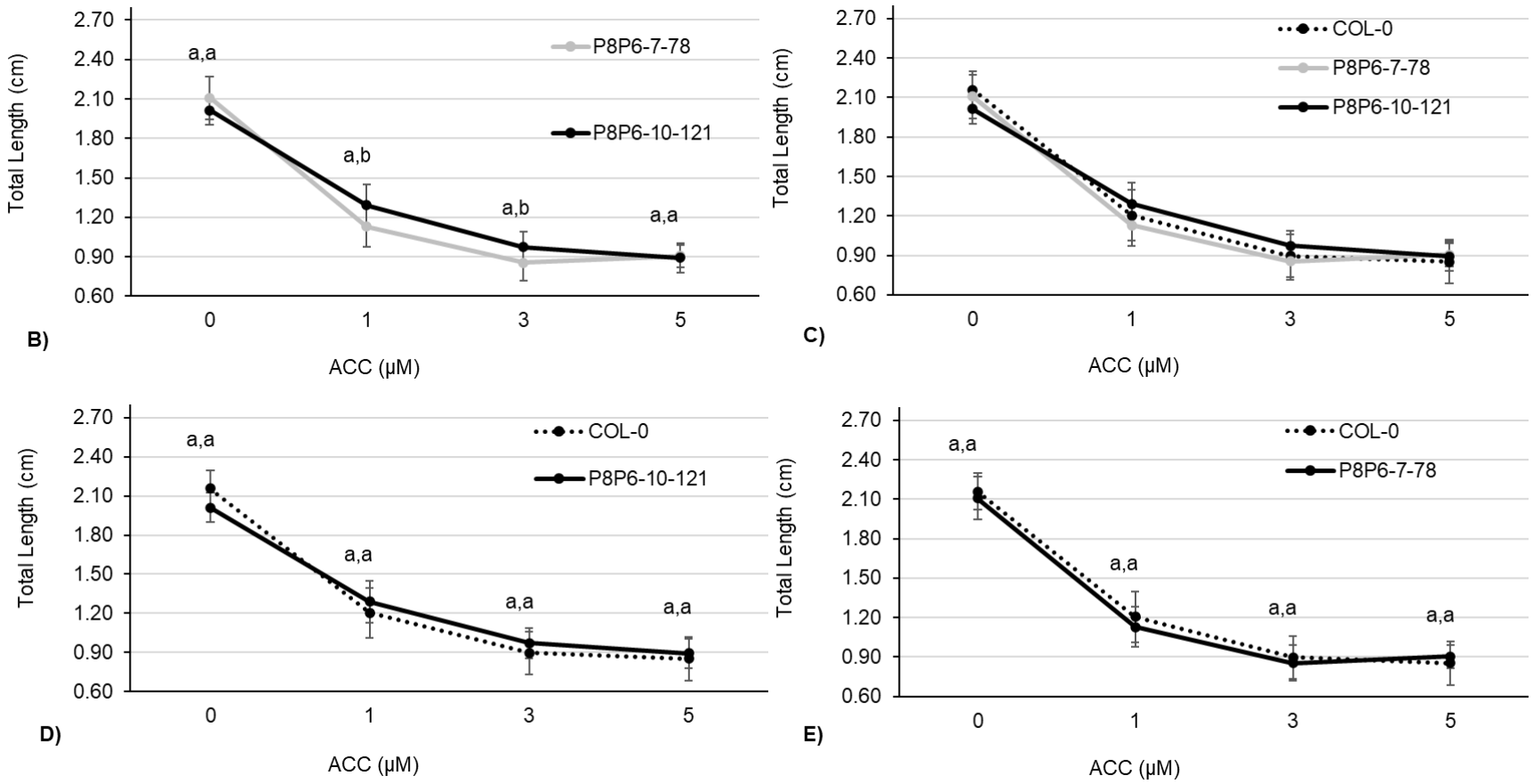
B)
Total Length (cm)
2.70
2.40
2.10
1.80
1.50
1.20
0.90
0.60
a,a
a,b
a,b
a,a
P8P6-7-78
P8P6-10-121
0
1
3
5
ACC (μM)
C)
COL-0
P8P6-7-78
P8P6-10-121
D)
a,a
a,a
a,a
a,a
COL-0
P8P6-10-121
E)
a,a
a,a
a,a
a,a
COL-0
P8P6-7-78

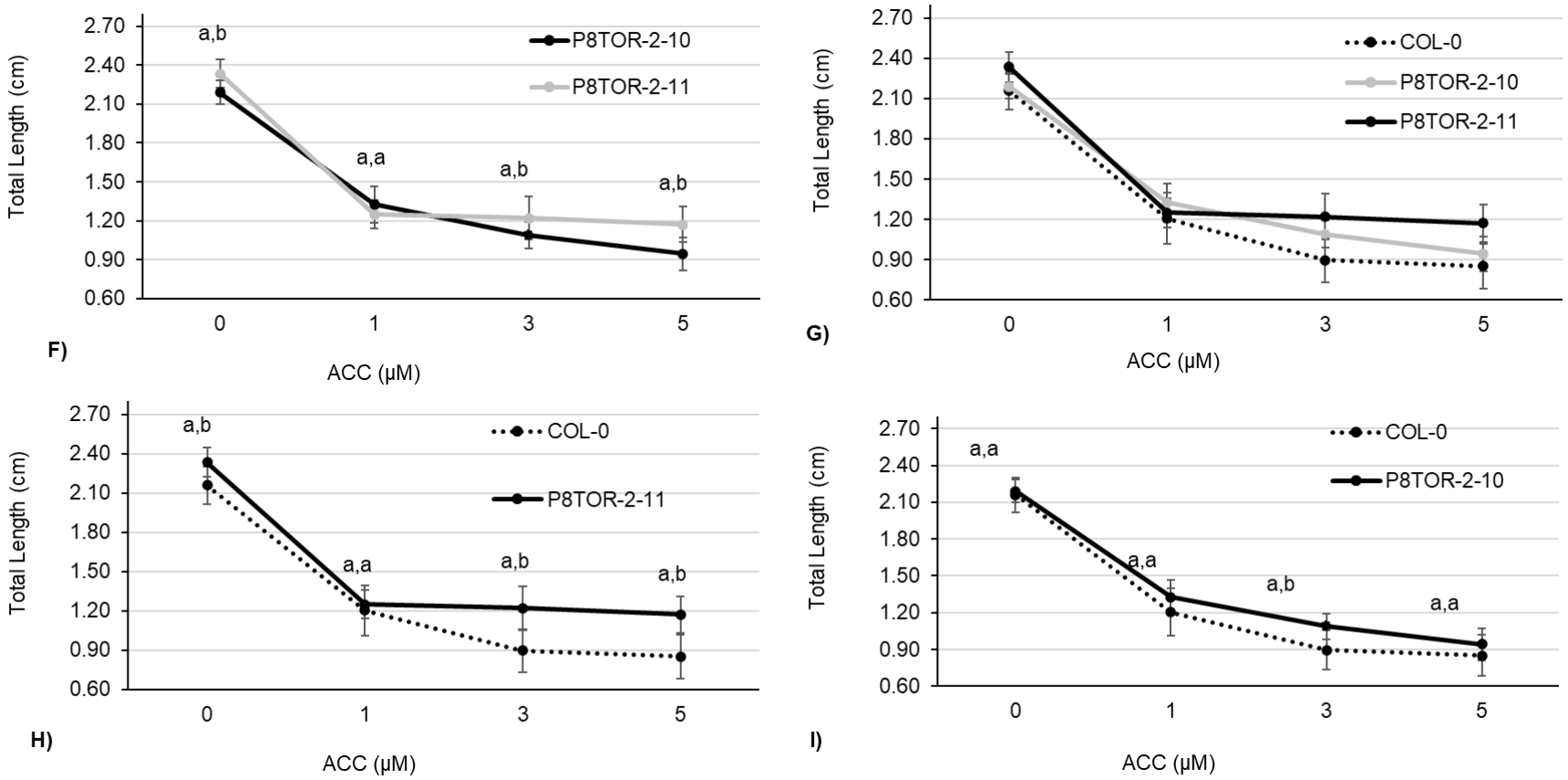

Figure 5.5. Pairwise comparisons of ethylene sensitivity of transgenic Arabidopsis lines expressing P6WT-GFP and P6(ΔTOR)-GFP under the control of a β-estradiol inducible promoter**.** Line chart displays the ethylene triple response assay, i.e., total length (cm) comparisons the transgenic lines under the control of β-estradiol inducible promoter pER8-P6WT-GFP: P8P6-10-

121 and P8P6-7-78, pER8-P6(ΔTOR)-GFP: P8TOR-2-11 and P8TOR-2-10, and Col-0 grown on ½ MS plates containing different concentrations of ACC, i.e., 0 µM, 1 µM, 3 µM, and 5 µM 30 µM without induction. The morphometric measurements of the total length were taken after five days using Fiji image analysis software. Each point in the line represents an average of seedlings' total length values for 36 replicates per experimental line. Points with the same letters indicate mean values that are not significantly different at p ≤ 0.05 (ANOVA and post hoc Tukey-Kramer HSD test). The response pattern is a gradual decline or shorting in the total length as the ACC concentration increases. P-value with different letter superscripts indicates statistically significantly different values, hence different in the total length and sensitivity to ethylene.

ACC (µM)				
	0	**1**	**3**	**5**
Col-0 vs. COL-0+B				
p-value (ANOVA, α=0.05)	0.9982	0.9986	0.9856	0.6833
Tukey HSD test	a, a	**a, a**	**a, a**	a, a
COL-0+B vs. P8P6-10-121+B				
p-value (ANOVA, α=0.05)	<.0001	0.3634	<.0001	**<.0001**
Tukey HSD test	**a, b**	**a, a**	**a, b**	a, b
COL-0+B vs. P8P6-7-78+B				
p-value (ANOVA, α=0.05)	<.0001	0.0002	<.0001	<.0001
Tukey HSD test	**a, b**	**a, b**	**a, b**	**a, b**
COL-0+B vs. P8TOR-2-11+B				
p-value (ANOVA, α=0.05)	1.0000	0.8952	<.0001	<.0001

Tukey HSD test	**a, a**	a, a	**a, b**	**a, b**
COL-0+B vs. P8TOR-2-10+B				
p-value (ANOVA, α=0.05)	0.0006	0.9999	<.0001	<.0001
Tukey HSD test	**a, b**	**a, a**	a, b	a, b
P8P6-10-121+B vs. P8P6-7-78+B				
p-value (ANOVA, α=0.05)	0.0138	0.3852	0.9811	0.5227
Tukey HSD test	**a, b**	a, a	a, a	a, a
P8TOR-2-11+B vs. P8TOR-2-10+B				
p-value (ANOVA, α=0.05)	0.0014	0.9947	0.9936	0.8167
Tukey HSD test	**a, b**	a, a	**a, a**	**a, a**
P8P6-10-121+B vs. P8TOR-2-11+B				
p-value (ANOVA, α=0.05)	<.0001	0.9976	1.0000	0.9765
Tukey HSD test	**a, b**	**a, a**	**a, a**	**a, a**
P8P6-10-121+B vs. P8TOR-2-10+B				
p-value (ANOVA, α=0.05)	<.0001	0.7336	0.9999	1.0000
Tukey HSD test	**a, b**	a, a	**a, a**	a, a
P8P6-7-78+B vs. P8TOR-2-11+B				
p-value (ANOVA, α=0.05)	<.0001	0.2215	0.9990	0.9950
Tukey HSD test	**a, b**	**a, a**	**a, a**	**a, a**
P8P6-7-78+B vs. P8TOR-2-10+B				
p-value (ANOVA, α=0.05)	0.1602	0.0020	0.7744	**<.0001**

Tukey HSD test	**a, a**	**a, b**	**a, a**	a, b
P8P6-10-121 vs. P8P6-10-121+B				
p-value (ANOVA, α=0.05)	<.0001	0.9995	0.0017	0.1131
Tukey HSD test	**a, b**	**a, a**	**a, b**	a, a
P8P6-7-78 vs. P8P6-7-78+B				
p-value (ANOVA, α=0.05)	<.0001	<.0001	<.0001	0.0003
Tukey HSD test	**a, b**	**a, b**	**a, b**	a, b
P8TOR-2-11 vs. P8TOR-2-11+B				
p-value (ANOVA, α=0.05)	<.0001	0.9898	0.0123	<.0001
Tukey HSD test	**a, a**	**a, a**	**a, b**	a, b
P8TOR-2-10 vs. P8TOR-2-10+B				
p-value (ANOVA, α=0.05)	<.0001	0.5310	1.0000	1.0000
Tukey HSD test	**a, b**	**a, a**	**a, a**	a, a

Table 5.4. Statistical comparison of Plant responses to ethylene data. Comparison between the average total length average of Col-0, P8P6-10-121, P8P6-7-78, P8TOR-2-11, and P8TOR-2-10 seedlings at different ACC concentration (0 μM, 1 μM, 3 μM, and 5 μM) after five days of incubation. The significant statistical differences between lines were determined based on a two-way analysis of variance (ANOVA) and Tukey-Kramer Honestly Significant Difference post hoc test ($P \leq 0.05$). P-value with different letter superscripts indicates values that are statistically significantly different. Note +B= with 30 μM of β-estradiol hence different in the total length and sensitivity to ethylene.

5.3.1.2. P6 and P6(ΔTOR) interaction with the auxin signalling pathway

A role for P6 in modulating auxin signalling has previously been suggested. In particular P6 transgenic plants have been reported to show reduced sensitivity to the polar auxin transport inhibitor TIBA in seedling germination assays (Smith, 2007), and this has been confirmed in the results presented in chapter 3. To extend these studies and determine whether the interaction of P6 with auxin signalling depends on its ability to interact with TOR, the P6 transgenic lines described above were assayed to determine the effect of increasing concentrations of TIBA on germination in plate assays.

5.3.1.2.1. Germination rate of lines continuously expressing P6-GFP and P6(ΔTOR)-GFP

In the initial experiments, seeds from the transgenic lines under the control of the 35S promoter lines, pEZR-P6WT-GFP (PZP6-3-31 and PZP6-2-91), pEZR-P6(ΔTOR)-GFP (PZTOR-4-10 and PZTOR-2-81) plus control plants Col-0 were germinated on plates containing TIBA concentrations; 10 μM, 20 μM, 30 μM, 40 μM, 50 μM, 60 μM, and 70 μM, and 100 μM, and the proportion of seeds germinating for each line was measured after 14 days. The data shown here are from three independent experiments. For all lines, transgenic and non-transgenic at 0 μM of TIBA germination rates were close to 100%. However, the proportion of seedlings that germinated was reduced with increasing TIBA concentrations (Figure 5.6), and seedlings of all tested lines showed a stunting phenotype at all TIBA concentrations. Also, the germination of all lines was inhibited at 100 μM of TIBA or more (Figure 5.6).

Interestingly, the NT Col-0 plants were more resistant to TIBA than the NT Ler-gl1 plants. In particular, Col-0 seeds germinated at higher TIBA concentrations, with some seeds germinating at up to 60 μM (Figure 5.10), whereas with Ler-gl1 seeds, germination was inhibited at a concentration ≥ of 20 μM of TIBA (Figure 3.3).

All pEZR transgenic lines, two lines expressing P6WT-GFP and two expressing P6(ΔTOR)-GFP, were considerably less sensitive to TIBA than the NT Col-0. The

reduction in the inhibition of germination was particularly apparent at 50-70 μM of TIBA (Figure 5.6). The transgenic lines PZP6-3-31, PZP6-2-91, PZTOR-4-10, and PZTOR-2-81 were less sensitive than Col-0 to TIBA at concentrations 0 μM, 60 μM, and 70 μM although for all lines germination was completely inhibited at 100 μM of TIBA.

At 50 μM TIBA, approximately half the seeds germinated successfully for all of the lines: PZP6-3-31, PZP6-2-91, PZTOR-4-10, and PZTOR-2-81, while for the NT Col-0 only about 14% of seedlings germinated on the plate. At 60 μM of TIBA, all of the tested pEZR lines and the NT Col-o were able to germinate. Even at 70 μM of TIBA, for all of the transgenic lines: PZP6-3-31, PZP6-2-91, PZTOR-4-10, and PZTOR-2-81 a small percentage of seeds were still able to germinate, whereas for Col-0 seed germination was completely inhibited.

Remarkably, although there were minor variations between the four transgenic lines in the proportion of seeds germinated at TIBA concentrations between 50 and 70 μM, there were no apparent differences between the lines expressing P6WT and lines expressing P6(ΔTOR). These results suggest that in these lines at least, the presence of the TOR binding domain is not required for the ability of P6 to confer resistance to TIBA.

5.3.1.2.2. Statistical analysis of lines continuously expressing P6-GFP and P6(ΔTOR)-GFP responses to TIBA

As in chapter 3, as a further confirmation step to detect if there was a difference in response to increasing concentrations of TIBA between the lines, the data were analyzed statistically using JMP software for two-way ANOVA statistical analysis, in which If the ANOVA implied significance ($p \leq 0.05$), then the means were tested with Tukey-Kramer Honestly Significant Difference post hoc test to determine the differences. The results are shown in Figure 5.6. The analysis revealed a statistically significant interaction between the effects of different lines and different TIBA concentrations on seed germination ($p = <.0001$). The initial effect analysis demonstrated that different lines had a statistically significant effect on seed germination ($p = <.0001$). Likewise, the initial effect analysis demonstrated that different

TIBA concentrations had a statistically significant effect on seed germination ($p = <.0001$).

Statistical analysis showed that NT Col-0 had a statistically significant difference (ANOVA p-value = <.0001) compared to NT Ler-gl1 at all of the TIBA concentrations. However as noted above, Col-0 is more resistant to TIBA, and seeds germinated more successfully than Ler-gl1 at similar TIBA concentrations. The Col-0 had a statistically significant difference in relative seed germination rate where the germination in the absence of TIBA was significantly higher than the germination at 50 μM of TIBA μM of TIBA ($p = <.0001$). There was no statistically significant difference detected between germination rate at 50 and 60 μM, and seed germination was inhibited at 70 μM of TIBA or more.

The PZP6 3-31 had a statistically significant difference in relative seed germination rate where the germination in the absence of TIBA was significantly higher than the germination at any of TIBA concentrations; 50, 60, 70, and 100 μM ($p = <.0001$). Likewise, a statistically significant difference was detected between the germination rate at 50 and 60 μM ($p = <.0001$), and 50 μM and 70 μM of TIBA ($p = <.0001$) in which germination was higher. There was no statistically significant difference detected between germination rates at 60, 70, and 100 μM. The seed germination was inhibited at 100 μM of TIBA or more.

The PZP6 2-91 showed a statistically significant difference in relative seed germination rate where the germination in the absence of TIBA was significantly higher than the germination at 50 μM of TIBA μM of TIBA ($p = <.0001$). likewise, statistically significant difference detected between germination rate at 50 and 60 μM ($p = <.0001$), and 50 μM and 70 μM of TIBA ($p = <.0001$). There was no statistically significant difference detected between germination rates at 60, 70, and 100 μM. The seed germination was inhibited at 100 μM of TIBA or more.

The PZTOR 2-81 had a statistically significant difference in relative seed germination rate where the germination in the absence of TIBA was significantly higher than the germination at any of TIBA concentrations; 50, 60, 70, and 100 μM ($p = <.0001$).

Likewise, a statistically significant difference was detected between the germination rate at 50 and 60 μM (p = <.0001), and 50 μM and 70 μM of TIBA (p = <.0001) in which germination was higher. There was no statistically significant difference detected between germination rates at 60, 70, and 100 μM. The seed germination was inhibited at 100 μM of TIBA or more.

The PZTOR 4-10 had a statistically significant difference in relative seed germination rate where the germination in the absence of TIBA was significantly higher than the germination at any of TIBA concentrations; 50, 60, 70, and 100 μM (p = <.0001). Likewise, a statistically significant difference was detected between the germination rate at 50 and 60 μM (p = <.0001), and 50 μM and 70 μM of TIBA (p = <.0001) in which germination was higher. There was statistically significant difference detected between germination rates at 60 and 70 μM, and 60 and 100 μM of TIBA (p = <.0001). There was no statistically significant difference detected between germination rates at 70 and 100 μM. The seed germination was inhibited at 100 μM of TIBA or more.

At 0 μM of TIBA, no statistically significant difference was detected between all pEZR transgenic lines expressing P6, P6(ΔTOR), and the NT Col-0 control.

At 50 μM of TIBA, all the transgenic lines showed statistically significant differences compared to the NT Col-0 (ANOVA p-value = < 0.0157), with a higher percentage of seeds germinating. However, there was no statistically significant difference between the germination rates for transgenic lines expressing P6 and P6(ΔTOR).

At 60 μM of TIBA, only PZTOR-4-10 showed a statistically significant difference when compared to all lines, including the Col-0 control (ANOVA p-value = < 0.0342). In contrast, no statistically significant difference was detected between all pEZR transgenic lines expressing P6WT, PZTOR-2-81, and the NT Col-0 control.

At 70 μM, the two transgenic lines expressing P6: PZP6 3-31 and PZP6 2-91 had statistically significant differences compared to NT Col-0 control (ANOVA p-value = < 0.0019 and 0.0286, respectively). In contrast, there was no statistically significant difference between all the pEZR transgenic lines expressing P6(ΔTOR) and the NT

Col-0 control. The pEZR transgenic lines expressing P6: PZP6 3-31 had statistically significant differences compared to the two lines expressing P6(ΔTOR); PZTOR 4-10 and PZTOR 2-81 (ANOVA p-value = 0.0286 for both lines). In contrast to PZP6 2-91, no statistically significant difference was detected compared to the two lines expressing P6(ΔTOR).

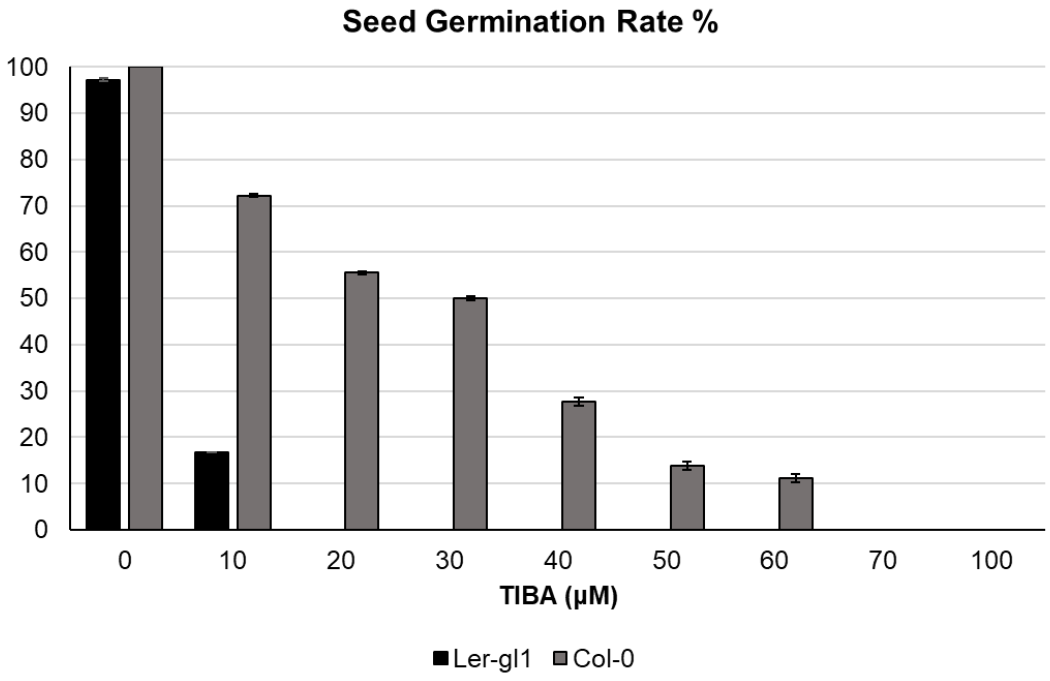

A)

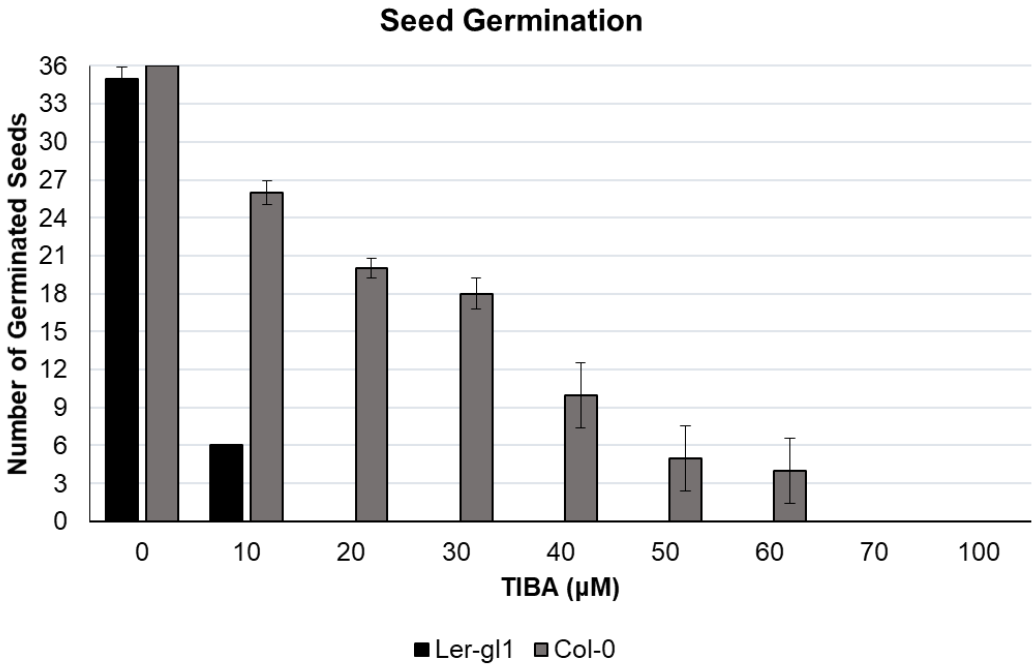

B)

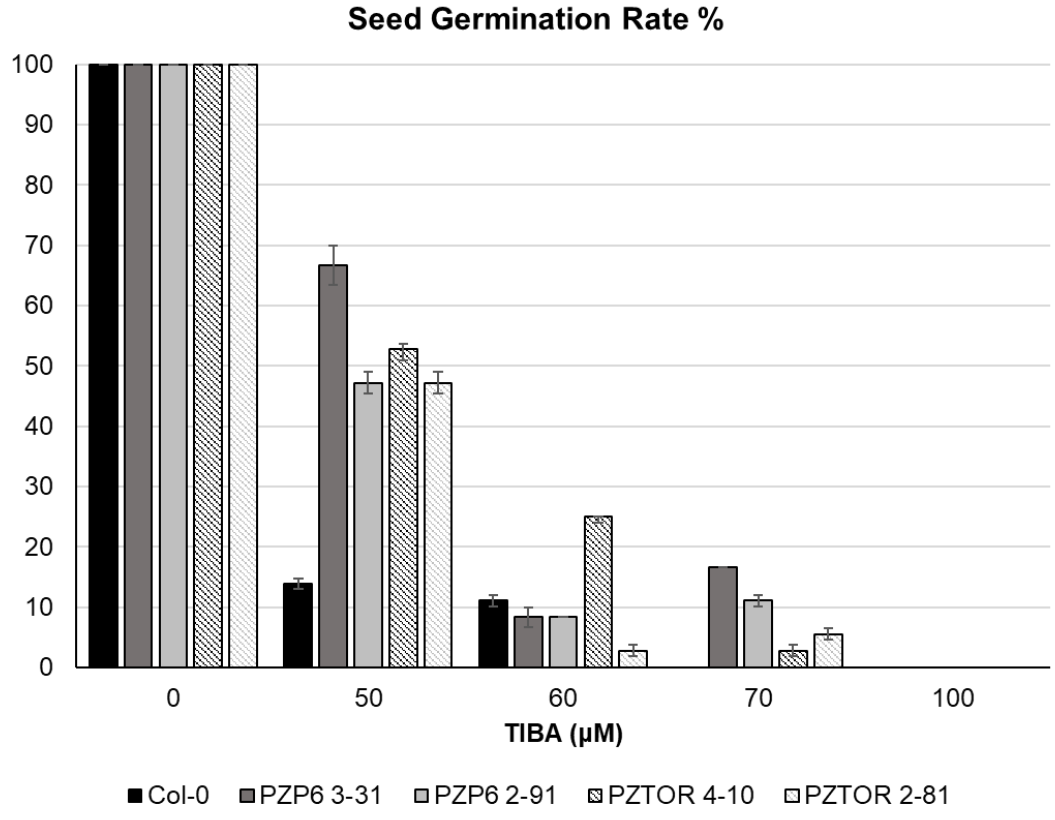

C)

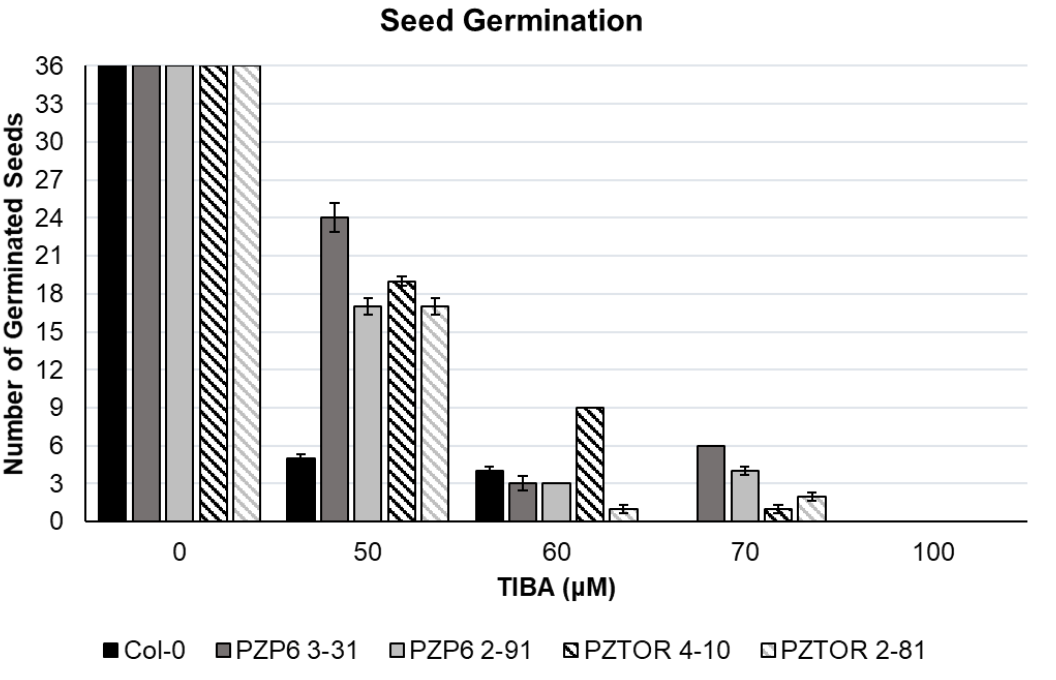

D)

Figure 5.6. Effects of TIBA on seed germination. (A and B) Bar charts of seed germination rate assay; Col-0 (black bar) and Ler-gl1 (light gray bar) on ½ MS plates containing different TIBA concentrations. For each line, 12 seeds sowed and grown on

½ MS plates containing different concentrations of TIBA: 0 µM, 10 µM, 20 µM, 30 µM, 40 µM, 50 µM, 60 µM, 70 µM, and 100 µM. Results were taken after two weeks of incubation. Each bar represents the values of germinated seeds of 36 replicates per experimental line. (C and D) Bar charts of seed germination rate assay; Col-0 (black bar), pEZR-P6WT-GFP 3-31 line (dark gray bar), pEZR-P6WT-GFP 2-91 line (light gray bar), pEZR-P6(ΔTOR)-GFP 4-10 line (black cross pattern bar), and pEZR-P6(ΔTOR)-GFP 2-81 line (gray cross pattern bar) on ½ MS plates containing different TIBA concentrations. For each line, 12 seeds sowed and grown on ½ MS plates containing different concentrations of TIBA: 0 µM, 50 µM, 60 µM, 70 µM, and 100 µM. Results were taken after two weeks of incubation. Each bar represents the percentage values of germinated seeds of 36 replicates per experimental line.

5.3.1.2.3. Germination rate of estradiol-inducible lines expressing P6-GFP and P6(ΔTOR)-GFP

Next, the experiments were repeated using the four inducible lines expressing P6WT and P6(ΔTOR), P8P6-10-121, P8P6-7-78, P8TOR-2-11, and P8TOR-2-10 plus control plants Col-0. They were germinated on plates containing TIBA concentrations; 10 µM, 20 µM, 30 µM, 40 µM, 50 µM, 60 µM, 70 µM, and 100 µM in the presence and absence of 30 µM β-estradiol (+B) in the growth media. The proportion of seeds germinating for each line was measured after 14 days. The results are shown in figure 5.7. The P8P6-10-121, P8P6-7-78, P8TOR-2-11, and P8TOR-2-10 lines were noticeably less sensitive to TIBA than the NT Col-0 after β-estradiol induction. They successfully germinated at up to 70 µM of TIBA but were inhibited at concentration 100 µM of TIBA. The increased success in germination was particularly apparent at 50-70 µM of TIBA. At 0 µM of TIBA, germination rates were close to 100% for all lines (the transgenic and non-transgenic). However, the proportion of seedlings that germinated was reduced with increasing TIBA concentrations (Figure 5.7), and seedlings of all tested lines showed a stunting phenotype at all TIBA concentrations. Also, seeds germination of all lines was inhibited at 100 µM of TIBA or more (Figure 5.7).

The seed germination rates of the Col-0 line were 100%, 8%, and 3% at 0 µM, 50 µM and 60 µM of TIBA, respectively, without β-estradiol induction and were 100%, 14%,

and 25% at 0 μM, 50 μM and 60 μM of TIBA when β-estradiol was added in the agar plates. The Col-0 with β-estradiol showed a germination rate of 2% at 70 μM; this seed might be a natural resistant mutant Col-0 to TIBA, an outlier (Figure 5.7A&B).

The seeds germination rates of induced P8P6-10-121 were 100% at 0 μM of TIBA, 28 % at 50 μM of TIBA, 33% at 60 μM of TIBA and 8% at 70 μM of TIBA. The seeds germination rates of P8P6-10-121 without β-estradiol induction 100% at 0 μM of TIBA, 22 % at 50 μM of TIBA, 3% at 60 μM of TIBA, and inhibited at 70 μM of TIBA. The seeds germination rates of P8P6-7-78 were 100% at 0 μM of TIBA, 19% at 50 μM of TIBA, 31% at 60μM of TIBA, and 11% at 70 μM of TIBA. The seeds germination rates of P8P6-7-78 without β-estradiol induction 100% at 0 μM of TIBA, 53% at 50 μM of TIBA, 6% at 60 μM of TIBA, and inhibited at 70 μM of TIBA (Figure 5.7 C-F).

The P8TOR-2-11 displayed seeds germination rate of 100% at 0 μM of TIBA, 8% at 50 μM of TIBA, 22% at 60μM of TIBA, and 6% at 70 μM of TIBA, whereas seeds germination rates without β-estradiol induction were 100% at 0 μM of TIBA, 30 % at 50 μM of TIBA, and inhibited at 60 μM of TIBA. The P8TOR-2-10 displayed seeds germination rate of 100% at 0 μM of TIBA, 14% at 50 μM of TIBA, 19% at 60μM of TIBA, and 6% at 70 μM of TIBA, whereas seeds germination rates without β-estradiol induction were 100% at 0 μM of TIBA, 11 % at 50 μM of TIBA, and inhibited at 60 μM of TIBA (Figure 5.7 C-F).

5.3.1.2.4. Statistical analysis of estradiol-inducible lines expressing P6-GFP and P6(ΔTOR)-GFP responses to TIBA

Next, the estradiol inducible pER8 lines and NT Col-0 germination data were statistically analyzed to confirm the increase in TIBA resistance phenotype. Like the previous findings of the pEZR lines, the two-way ANOVA analysis revealed a statistically significant interaction between the effects of different lines and different TIBA concentrations on seed germination ($p = <.0001$). The initial effect analysis demonstrated that different lines had a statistically significant effect on seed germination ($p = <.0001$). Likewise, the initial effect analysis demonstrated that different

TIBA concentrations had a statistically significant effect on seed germination ($p = <.0001$).

The Col-0+B had a statistically significant difference in relative seed germination rate where the germination in the absence of TIBA was significantly higher than the germination at any of TIBA concentrations; 50, 60, 70, and 100 μM ($p = <.0001$). Likewise, a statistically significant difference was detected between the germination rate at 50 and 70 μM ($p = <.0001$), and 60 μM and 70 μM of TIBA ($p = <.0001$) in which germination was higher. There was no statistically significant difference detected between germination rates at 50 and 60 μM 50 and 70 μM. The seed germination was inhibited at 100 μM of TIBA or more.

The P8P6 10-121+B revealed a statistically significant difference in relative seed germination rate where the germination in the absence of TIBA was significantly higher than the germination at any of TIBA concentrations; 50, 60, 70, and 100 μM ($p = <.0001$). There was a statistically significant difference between the germination rate at 50 μM and 70 μM ($p = <.0126$) or 60 μM and 70 μM ($p = <.0022$). No statistically significant difference was detected between germination rates at 50 μM and 60 μM or 70 μM and 100 μM. The seed germination was inhibited at 100 μM of TIBA or more. The P8P6 7-78+B revealed a statistically significant difference in relative seed germination rate where the germination in the absence of TIBA was significantly higher than the germination at any of TIBA concentrations; 50, 60, 70, and 100 μM ($p = <.0001$). There was a statistically significant difference between the germination rate at 60 μM and 70 μM ($p = <.0001$). No statistically significant difference was detected between germination rates at 50 μM and 60 μM or 70 μM and 100 μM. The seed germination was inhibited at 100 μM of TIBA or more.

The P8TOR 2-11+B showed a statistically significant difference in relative seed germination rate where the germination in the absence of TIBA was significantly higher than the germination at any of TIBA concentrations; 50, 60, 70, and 100 μM ($p = <.0001$). There was a statistically significant difference between the germination rate at 50 μM and 60 μM ($p = 0.0342$) or 60 μM and 70 μM ($p = 0.0116$). No statistically significant difference was detected between germination rates at 50 μM and 70 μM or

70 μM and 100 μM. The seed germination was inhibited at 100 μM of TIBA or more. P8TOR 2-10+B had a statistically significant difference in relative seed germination rate where the germination in the absence of TIBA was significantly higher than the germination at any of TIBA concentrations; 50, 60, 70, and 100 μM (p = <.0001). There was a statistically significant difference between the germination rate at 60 μM and 70 μM (p = <.0071). No statistically significant difference was detected between germination rates at 50 μM and 60 μM or 70 μM and 100 μM. The seed germination was inhibited at 100 μM of TIBA or more.

At 0 μM of TIBA, no statistically significant difference was detected between the two pER8 transgenic lines expressing P6, the two lines P6(ΔTOR), and the NT Col-0 control. At 50uM of TIBA, there was no statistically significant difference between any of the pER8 transgenic lines (expressing either P6WT or P6(ΔTOR) and the NT Col-0 control, although ANOVA did identify a difference between two of the transgenic lines P8P6-10-121+B, and P8TOR-2-11+B (ANOVA p-value = 0.0126). Furthermore, at 60 μM and 70 μM of TIBA no statistically significant differences were detected between any of the pER8 transgenic lines (expressing P6WT and P6(ΔTOR)) and the NT Col-0 control. Therefore, the statistical analysis suggests that unlike any of the lines expressing P6 from a 35S promoter, none of the estradiol inducible P6WT lines showed any statistically significant resistance to TIBA in this assay.

Finally, the estradiol inducible lines were tested in the presence or absence of estradiol. At 0 μM of TIBA, no statistically significant difference was detected between all estradiol-induced and non-induced pER8 transgenic lines expressing P6WT and P6(ΔTOR). Similarly, in the presence and absence of estradiol, the NT Col-0 control did not show any statistically significant difference. At 50 μM of TIBA, there was no statistically significant difference detected between all pER8 transgenic lines (P6WT and P6(ΔTOR)) and the NT Col-0 control, except between the induced and non-induced P8P6 7-78 (ANOVA p-value = < 0.0001), and between induced and non-induced P8TOR 2-11 showed statistically significant differences (ANOVA p-value = 0.0324). At 60 μM of TIBA, statistically significant differences were detected between all induced and non-induced pER8 transgenic lines (expressing P6WT and P6(ΔTOR). Interestingly, the NT Col-0 control showed a statistically significant difference for

germination between Col-0 grown in the presence and absence of estradiol, although this was because one seed successfully germinated. This outcome might be a side effect of estradiol, or the seed was a natural outlier (ANOVA p-value = < 0.0113). At 70 µM of TIBA, the only statistically significant difference detected was between induced and non-induced P8P6 7-78 (ANOVA p-value = < 0.0353).

Comparisons between the tested lines in the absence of estradiol showed that at 60 and 70 µM of TIBA, no statistically significant difference was apparent between all non-induced pER8 transgenic lines and NT Col-0 (expressing P6WT and P6(ΔTOR)). Similar results were found at 50 µM of except for P8P6 7-78 when compared the other pER8 transgenic lines (ANOVA p-value = < 0.0181) or Col-0 (ANOVA p-value = 0.0003).

One plausible explanation for the contrasting TIBA-sensitivity results between the estradiol-inducible lines and those expressing the transgene from a constitutive promoter might be the timing of P6 expression/accumulation in the assay. It takes several days of β-estradiol treatment to induce maximal expression of P6 (see Chapter 4), and it might be that the inhibitory effect of TIBA on germination occurs before sufficient P6 expression has occurred to promote TIBA resistance. As shown in chapter 3 and the earlier results of the pEZR lines, producing P6WT or P6(ΔTOR) continuously enhanced the resistance degree to TIBA and promoted higher seed germination than the NT controls. The confocal microscopy data (Chapter 4) showed that a strong GFP signal was only detected 2-3 days post-induction, at which point GFP fluorescence and the presence of P6 inclusion bodies became easily detectable. If the estradiol inducible lines are to be used to assess TIBA-sensitivity, modifications of the experiment design will be needed.

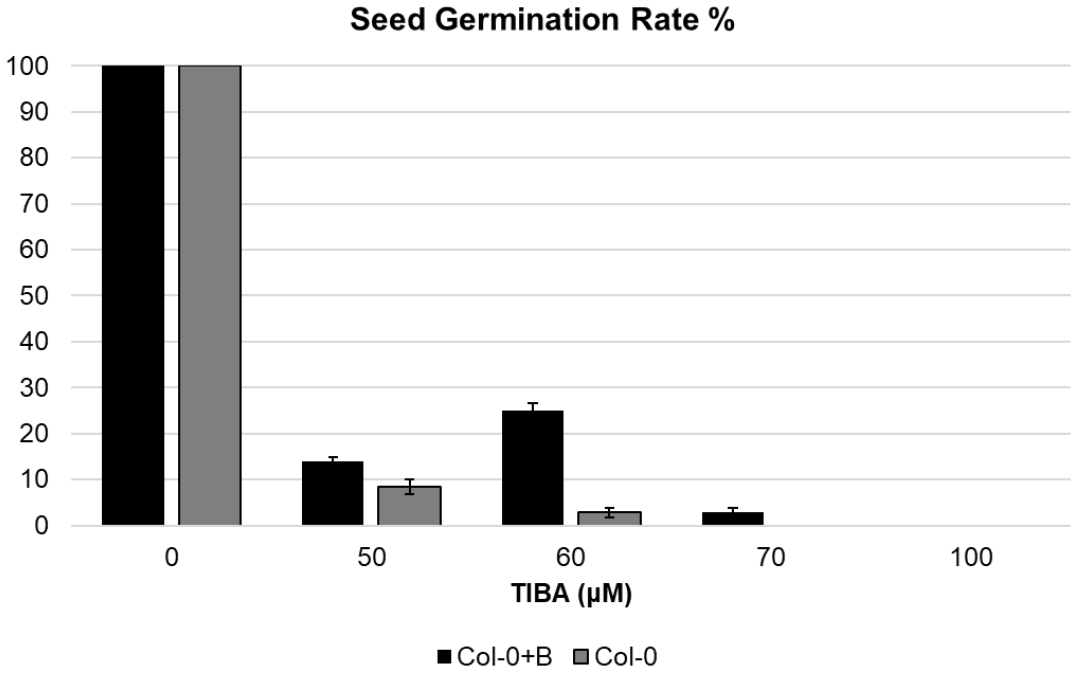
Seed Germination Rate %
100
90
80
70
60
50
40
30
20
10
0
0
50
60
70
100
TIBA (µM)
Col-0+B
Col-0

A)

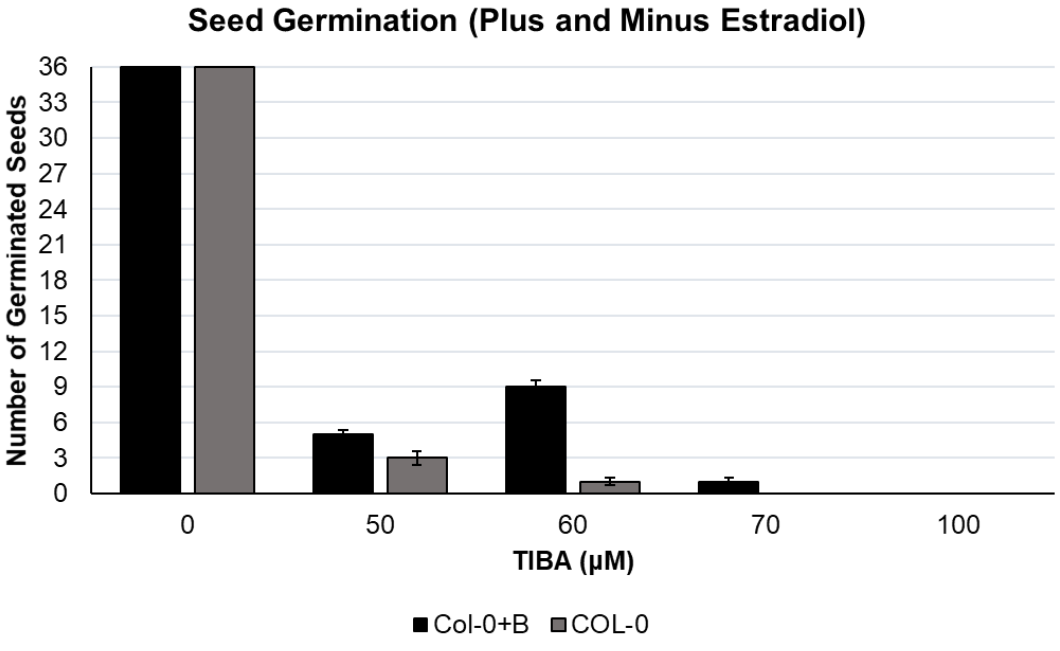
Seed Germination (Plus and Minus Estradiol)
Number of Germinated Seeds
36
33
30
27
24
21
18
15
12
9
6
3
0
0
50
60
70
100
TIBA (µM)
Col-0+B
COL-0

B)

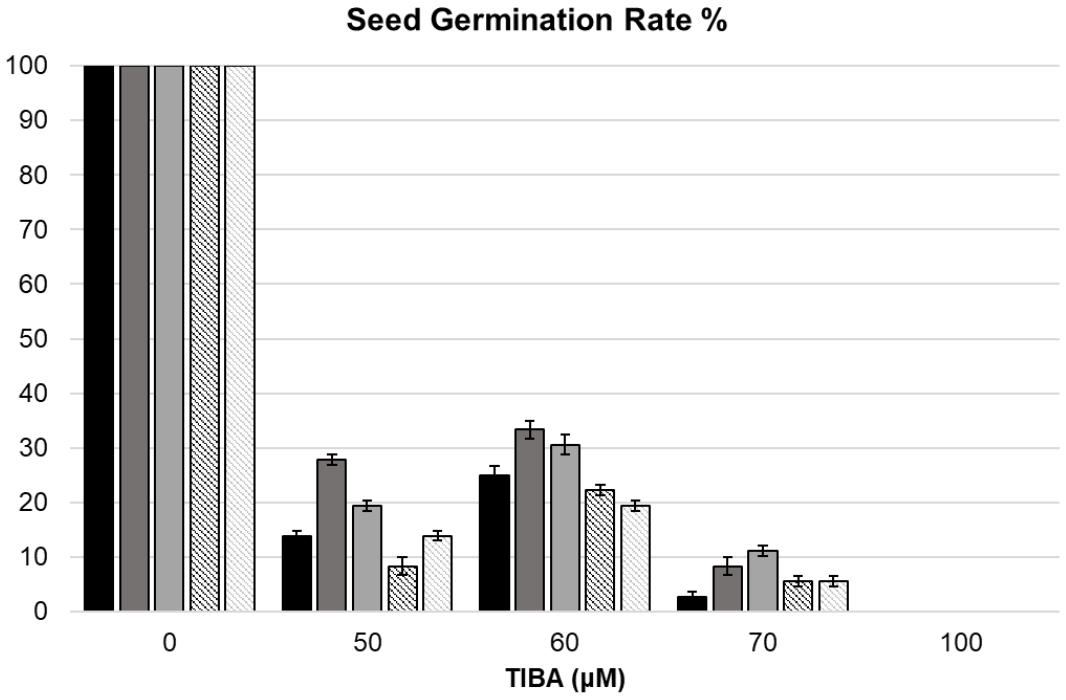

C) ■Col-0+B ■P8P6 10-121+B ■P8P6 7-78+B ■P8TOR 2-11+B ■P8TOR 2-10+B

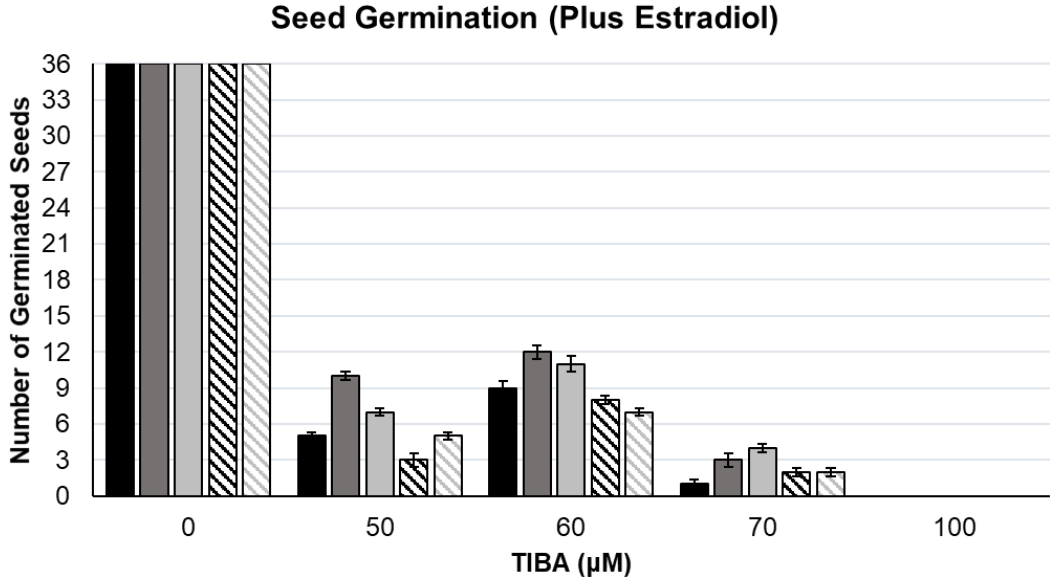

D) ■Col-0+B ■P8P6 10-121+B ■P8P6 7-78+B ■P8TOR 2-11+B ■P8TOR 2-10+B

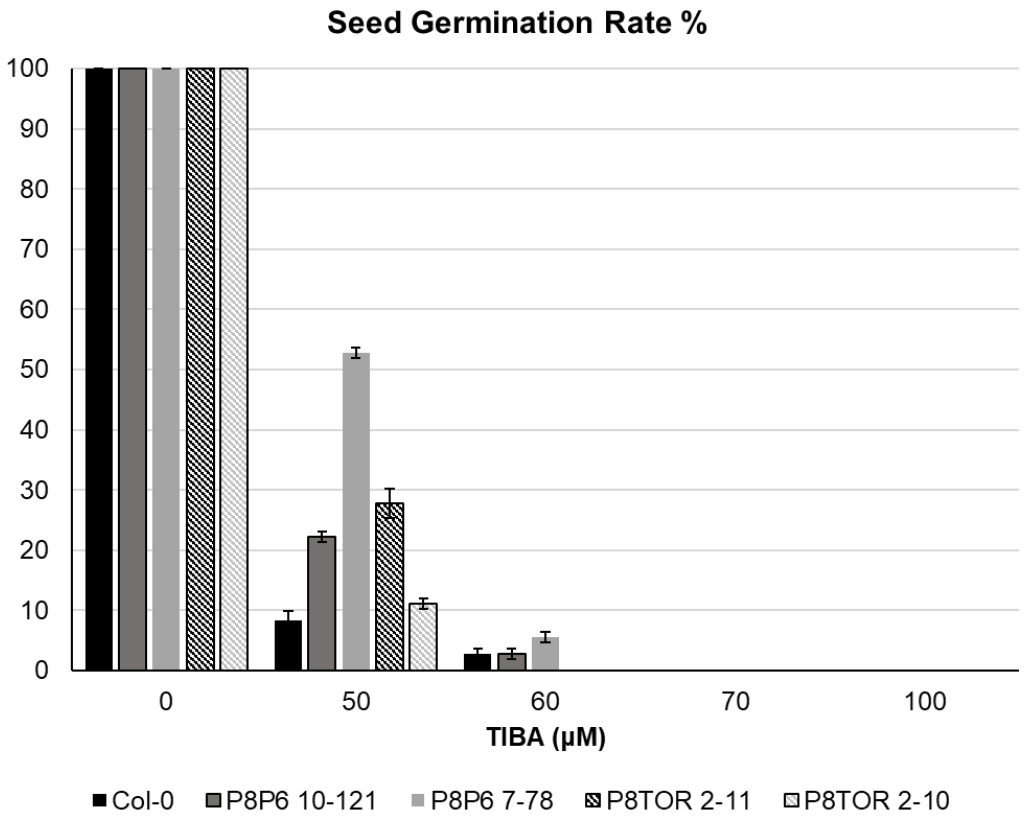
Seed Germination Rate %
100
90
80
70
60
50
40
30
20
10
0
0
50
60
70
100
TIBA (µM)
Col-0
P8P6 10-121
P8P6 7-78
P8TOR 2-11
P8TOR 2-10

E)

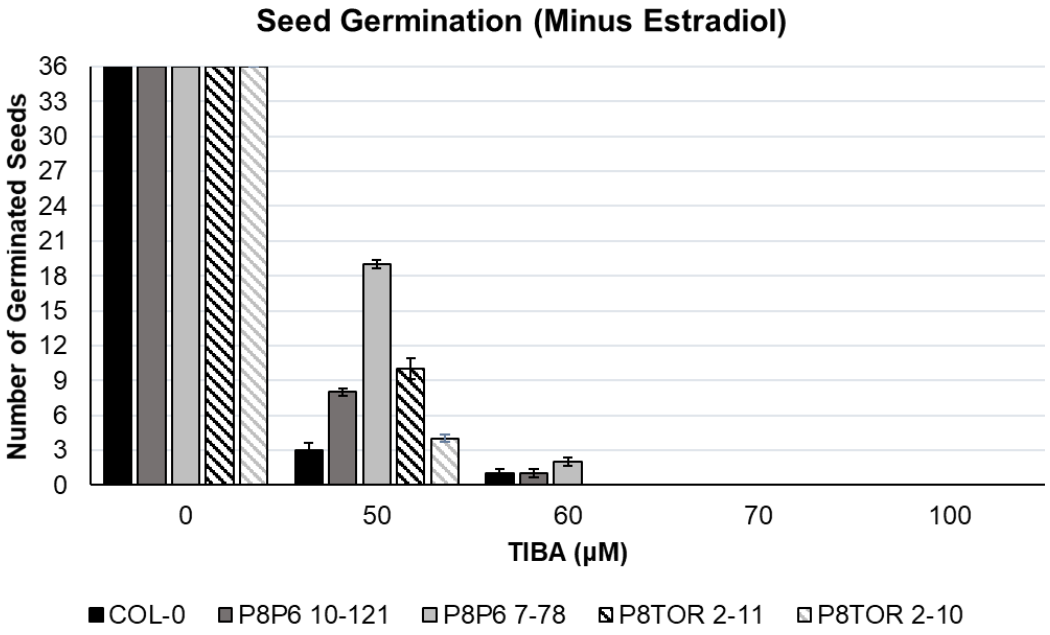
Seed Germination (Minus Estradiol)
Number of Germinated Seeds
36
33
30
27
24
21
18
15
12
9
6
3
0
0
50
60
70
100
TIBA (µM)
COL-0
P8P6 10-121
P8P6 7-78
P8TOR 2-11
P8TOR 2-10

F)

Figure 5.7. Effects of TIBA on seed germination. A and B) Bar chart of seed germination rate assay; Col-0 wild type plan) on ½ MS plates containing different TIBA concentrations (0 µM, 50 µM, 60 µM, 70 µM and 100 µM) in absence and presence of 30 µM of β-estradiol (+B). **C and D)** Bar chart of seed germination rate assay; Col-0 wild type plant, negative control, (black bar), pER8-P6WT-GFP 10-121 line (dark gray bar), pER8-P6WT-GFP 7-78 line (light gray bar), pER8-P6(ΔTOR)-GFP 2-11 (black cross pattern bar), and pER8-P6(ΔTOR)-GFP 2-10 line (light gray cross pattern bar) on ½ MS plates containing different TIBA concentrations (0 µM, 50 µM, 60 µM, 70 µM and 100 µM) with 30 µM of β-estradiol (+B). **E and F)** Bar chart of seed germination rate assay; Col-0 wild type plant, negative control, (black bar), pER8-P6WT-GFP 10-121line (dark gray bar), pER8-P6WT-GFP 7-78 line (light gray bar), pER8-P6(ΔTOR)-GFP 2-11 (black cross pattern bar), and pER8-P6(ΔTOR)-GFP 2-10 line (light gray cross pattern bar) on ½ MS plates containing different TIBA concentrations (0 µM, 50 µM, 60 µM, 70 µM and 100 µM) without 30 µM of β-estradiol. For figures A, C, and E, each bar represents the percentage values of germinated seeds of 36 replicates per experimental line, and for figures B, D, and F, each bar represents the values of germinated seeds of 36 replicates per experimental line.

5.4. Discussion

P6 acts as a pathogenicity effector by modulating the SA-dependent defense responses and JA/ET-dependent defense, in which P6 was found to suppresses the SA-dependent defense responses while enhancing JA/ET-dependent defense (Laird et al., 2013, Love et al., 2012). P6 might be directly or indirectly direct these modulations. Here, we have conducted a study using different newly constructed transgenic Arabidopsis lines expressing P6WT-GFP and P6(ΔTOR)-GFP to address the impact of P6 on the phytohormonal signalling pathway, outline the importance of the P6 TOR binding, and expand our understanding of P6 function.

In this chapter, the newly constructed transgenic Arabidopsis lines expressing P6WT-GFP were less sensitive to the ethylene precursor than Col-0 and transgenics lines expressing P6(ΔTOR)-GFP, i.e., P6 modulates the JA/ET signalling pathway in partial TOR binding domain manner. All constructed transgenic Arabidopsis lines expressing

P6WT-GFP and P6(ΔTOR)-GFP were more resistant to auxin transport inhibitor than Col-0, i.e., P6 modulates auxin signalling in a non-TOR binding-domain manner. It may be relevant that the stunting phenotype exhibited by P6 transgenic plants was also not entirely dependent on the TOR binding domain.

Interestingly, plants expressing P6(ΔTOR) showed some Ethylene resistance in the triple response assay suggesting that reliance on the TOR binding domain may be incomplete. Correspondingly, consistent with the results from the previous P6 transgenic lines (chapter 3), the auxin transport inhibitor results indicated that P6 interferes with the auxin signalling pathway, and the resistance to the inhibitor effect was enhanced. This enhancement occurred in both P6WT and P6(ΔTOR) expressing lines, i.e., the TOR-binding domain does not appear to be involved in modulating auxin-dependent responses.

5.4.1. P6 and P6(ΔTOR) interference with the ethylene signalling pathway

Previously (Laird et al., 2013, Love et al., 2012) showed that P6 could manipulate multiple plant defense signalling responses, including those dependent on SA and JA/ET pathways. Expression of P6 modulated the levels of expression of marker genes involved in the SA and JA/ET defense responses. Here, the transgenic Arabidopsis expressing P6WT-GFP under the control of constitutive promoter 35S promoter or β-estradiol inducible promoter demonstrated reduction in stunting effect of exposure to ethylene precursor (ACC), the reduction in the seedlings total length was less than the NT Col-0, i.e., increased in the insensitivity to ethylene similar to the previous findings for transgenic Arabidopsis expressing P6WT in chapter 3 and Geri et al. 2004. This is a piece of further evidence suggesting that P6 modulates and interferes with the JA/ET signalling pathway, resulting in modulating the plant responses to biotic or abiotic stress.

Previously the TOR-binding domain of P6 was found to be important in suppressing autophagy and PTI-mediated defense (Zvereva et al., 2016). The results presented in this thesis also show the TOR-binding domain participates in the P6 impact on reducing the Arabidopsis sensitivity to ethylene. However, it is dispensable for increasing the

Arabidopsis resistance to a polar auxin transport inhibitor. Assessing more transgenic lines expressing P6(ΔTOR) would further confirm and clarify any variation in responses between the tested lines.

5.4.2. P6 and P6(ΔTOR) interference with the auxin signalling pathway.

The previous auxin transport inhibitor treatments in chapter 3 showed that Arabidopsis expressing P6WT increased the resistance to the auxin transport inhibitor TIBA, where P6WT reduced plant sensitivity to the TIBA lethal effect by modulating the auxin signalling pathway. Consistent with this finding, transgenic Arabidopsis plants expressing P6WT-GFP under the control of constitutive promoter 35S promoter or β-estradiol inducible promoter increased resistance TIBA, in which seeds were germinated at higher TIBA concentration than the wildtype plant Col-0. Additional to P6WT-GFP impact in elevating TIBA resistance, it also aids TIBA tolerance in which the number of germinated seeds was increased at a TIBA concentration compared to wildtype plant Col-0. CaMV infection is also shown to impact the auxin signalling pathway of the host plant, and here the data suggested that P6 interferes with the auxin signalling pathway and plant auxin-dependent responses, i.e., P6 might play a role in modulating the auxin signalling pathway of the plant during CaMV infection. The modulation might occur through direct interaction between P6 and one or more components of the auxin signalling pathway components or indirectly, such as modulating the phosphorylation cellar states. Additionally, modulation might be achieved by interfering with the transcription initiation regulation, post-transcriptional gene regulation, and post-translation regulation of a particular protein. Like transgenic Arabidopsis plants expressing P6WT-GFP, transgenic Arabidopsis plants expressing P6(ΔTOR)-GFP under the control of either 35S promoter or β-estradiol inducible promoter displayed similar resistance level and tolerance to TIBA. Both Arabidopsis transgenic lines expressing P6WT-GFP or P6(ΔTOR)-GFP showed a significant difference in resistance to TIBA, where resistance level and seed germination rate were increased compared to the wild-type plant. These outcomes suggested P6 has a modulation role in the auxin signalling pathway, which occurs in a non-TOR binding domain manner. Further studies need to be carried out to determine which of the P6 domains involves in the auxin signalling pathway modulation and regulation mode.

Taken together, the data suggest that P6 would modulate both auxin and ethylene signalling pathways, which might modify the host to be more favorable for CaMV survival and spread. Some of these modulations might require a functional TOR-binding domain.

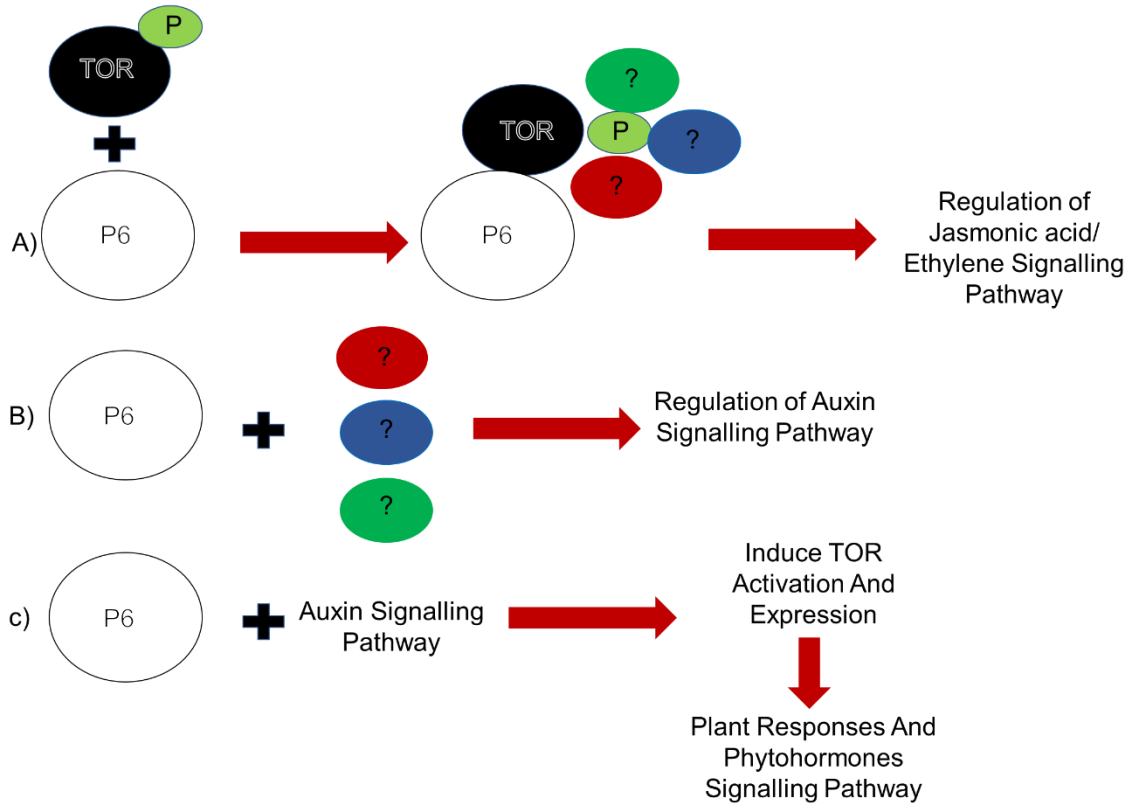

Figure 5.8. Representing P6 modulation of jasmonic acid/ethylene signalling and auxin signalling pathways. **(A)** P6-TOR interaction was found to be involved in the modulation of the JA/ET pathway. **(B)** P6 modulates the auxin signalling pathway and does not require P6-TOR interaction. **(C)** P6 modulates auxin signalling that modulates TOR levels, hence indirect modulation of TOR activation and expression.

5.5. Conclusion

In conclusion, this study expands our understanding of the etiology of CaMV and supports the vital multifunctional role of P6. Our findings support the role of P6 as a vital multifunctional protein involved in modulating different phytohormone responses, including the ethylene signalling pathway and auxin signalling pathway. Also, it

demonstrates that these effects are at least partially dependent on the P6-TOR interaction. The P6 transgenic lines developed and characterized in this study allowed for the validation of the earlier P6 observations, revealed differences in P6-host interactions, and will be useful for a more detailed analysis of P6 localization.

Chapter VI: The impact of transgene-mediated P6 expression on Arabidopsis gene expression.

6.1. Introduction

6.1.1. An overview of transcriptomics

Transcriptomics is a technique used to analyze the abundance of transcripts (i.e., the transcriptome) from a single cell or tissue and then in order to determine a gene expression profile, i.e., total RNA (Srivastava et al., 2019). Transcriptome analysis has now become extensively used to study and identify a wide variety of plant responses and signalling pathways through assessing changes in gene expression profiles (Depledge et al., 2019, Le Berre et al., 2017, Ascencio-Ibáñez et al., 2008, Rich-Griffin et al., 2020, Giolai et al., 2019, Yuan et al., 2019). For Arabidopsis, many studies have been performed to annotate genes, determine genes expression, and dissect cellular pathways at different growth conditions. In particular, studies on the gene expression and modification of plant responses grown under various abiotic and biotic stresses have been carried out. In these studies, expression of genes involved in cellular signalling, plant defense responses, stress responses, cell proliferation and differentiation, and metabolism were found to be modulated (Nutzmann and Osbourn, 2015, Sato et al., 2019, Dong et al., 2015, Herranz et al., 2019).

6.1.2. Impact of viral proteins on phytohormone pathways

Phytohormones play a key role in growth, metabolism, and responses to abiotic and biotic stress, including pathogens such as viruses. Plant viruses can manipulate plant growth and stress responses through rapid modification in phytohormone signalling pathways, for example, via the expression of viral effector proteins such as P6. Viruses can induce modulation of several phytohormone signalling pathways, resulting in symptom development, weakening plant defenses, enhancing their replication, and spread, i.e., making the host more favorable for their survival (Collum and Culver, 2016). In general, an extensive cross-talk between the different phytohormone pathways occurs to regulate the plant responses. In particular, viruses have been

shown to interfere with the plant SA and JA/ET pathways (Leisner and Schoelz, 2018, Laird et al., 2013, Love et al., 2012, Wu and Ye, 2020, Islam et al., 2019b, Collum and Culver, 2016, Derksen et al., 2013, Carr et al., 2020, Zhou et al., 2014). These pathways play a significant role in plant defenses against biotic and abiotic factors (Wu and Ye, 2020, Carr et al., 2020). The viral modulation of different phytohormone pathways may also direct antagonism and cross-talk to modulate small RNA (sRNA)-dependent defense mechanisms, which can be particularly effective, and show a high degree of specificity against viruses in particular (Islam et al., 2019b).

6.1.3. Virus infection changes the gene expression profile of hosts

Viruses were found to manipulate the host at a transcriptional and physiological level. This manipulation might result in symptom development and modification of plant responses (Pesti et al., 2019). The recent development of transcriptomics allows a quantitative assessment of the overall molecular landscape associated with a biological or physiological phenotype, i.e., at gene and metabolic levels. An RNA experiment was carried by (Agudelo-Romero et al., 2008) displayed that the gene expression profile of Arabidopsis was modified by infection *Tobacco etch potyvirus* (TEV), a well-studied positive-sense RNA plant viruses. The expression of 1727 Arabidopsis genes was modified, including plant defense responsive genes, abiotic stress responsive genes, and transcription factors such as the R2R3-MYB family and ABA-inducible TFs. Another example of a plant virus that infects and modify the gene expression profile of Arabidopsis is the *Turnip mosaic virus* (TuMV) (Yang et al., 2007).

Expression of some viral proteins induced infection-like symptoms, triggered plant responses, and had a global impact on the host gene expression profile plant responses (Geri et al., 2004, Leisner and Schoelz, 2018, Collum and Culver, 2016, Fondong, 2013). Assessment of the AC2 protein expression impact of *Mungbean yellow mosaic virus* (MYMV) and *African cassava mosaic virus* (ACMV), two Geminiviruses, displayed modification of expression of genes associated with systemic acquired resistance and WRKY transcription factor (Trinks et al., 2005). The transient expression of *Citrus leprosis virus C* (CiLV-C) P61 protein in *N. benthamiana* and Arabidopsis demonstrated that the CiLV-C P61 modulates the plant responses,

upregulates genes associated with SA and HR, and increases the SA levels while reduces the JA/ET levels plant responses(Arena et al., 2020). P6 is considered the primary pathogenicity determinant for CaMV, acting as a pathogenicity effector that suppresses plant defense responses, including RNA silencing. It has also been shown to interfere with various hormone signalling responses, e.g., those involving SA, JA, and ET (Laird et al., 2013, Love et al., 2007a, Leisner and Schoelz, 2018, Love et al., 2012, Love et al., 2007b, Love et al., 2005, Geri et al., 2004). However, much more information is needed to understand the overall regulatory impact of P6 on plant responses, particularly phytohormone signalling. The analysis may reveal unknown and unexpected biomarkers related to plant phytohormone signalling responses. This study chapter aimed to provide an in-depth view of the transcriptome of Arabidopsis Col-0 with the specific objective of providing an informative list of the most important genetic indicators involved in the phytohormonal signalling during P6 expression. Here, RNA-seq analysis of transgenic Arabidopsis expressing P6 (P6WT), transgenic Arabidopsis expressing mutant P6 (P6(ΔTOR)), and Arabidopsis wild type was conducted using Illumina next-generation sequencing to assess viral protein expression impact on the plant gene expression profile and highlight the genes expression differences between the tested lines including biomarkers, genes involved in plant responses and genes associated with phytohormones pathway. Here, it was identified that the expression of several differentially regulated genes was modulated during the P6 expression. The Arabidopsis transcription data demonstrate a robust response to expression of P6 from a transgene, which may reflect responses to CaMV infection in nature. Many of the genes identified have functions relating to plant growth, defense responses, and metabolism. Some genes were of which were found in responses associated with biotrophic or necrotrophic pathogens. This finding suggests that the P6 contributes to restricting pathogens sensitive to JA defense response and increases the host susceptibility to pathogens sensitive to SA defense response, consistent with the previous findings (Laird et al., 2013, Love et al., 2012, Love et al., 2007b). Some of these genes also participate in the crosstalk between abiotic and biotic stress responses.

6.2. Study Design

To assess the P6 expression impact on plant gene expression profile, three lines were used; two transgenic lines, which were under the control of an estradiol inducible promoter, and one wild type. Expression of P6 from a transgene induces symptom-like phenotype and modulates the Arabidopsis antimicrobial responses (Laird et al., 2013, Love et al., 2007b, Roberts et al., 2007, Geri et al., 2004, Love et al., 2012, Love et al., 2007a, Love et al., 2005, Leisner and Schoelz, 2018, Zvereva et al., 2016, Cecchini et al., 1997) and the results presented in chapters 3 and 5 demonstrate an effect on Auxin and ET signalling responses. However, the global impact of P6 on gene expression in plants is not established. The results presented in this chapter extended the earlier studies and provide an informative list of the most significant differentially expressed genes and biomarkers and assessed the P6-TOR interaction impact on plant gene expression profile.

6.3. RNA-Seq analysis

6.3.1. Gene expression analysis

Seedlings were grown for one week, then were transplanted and kept on media with 30μM β-estradiol for five days under the same conditions. Seedlings were harvested after 12 days, flash-frozen, and stored at -80°C before analysis. RNA extraction and library preparation for RNA-Seq using the Illumina platform was carried out by Qiagen (Manchester, M15 6SH, UK. # 74904). The libraries were sequenced using 75 bp single read chemistry on the Illumina NexSeq 500 and ~35.8 million reads per sample. Total RNA was extracted using the RNeasy Plant Mini kit (QIAGEN Manchester, M15 6SH, UK. # 74904). All experiments were conducted at QIAGEN Genomic Services. The library preparation was done using a TruSeq® stranded total RNA sample preparation kit with rRNA depletion (Illumina inc). The starting material (100 ng) of total RNA was rRNA depleted using biotinylated, target-specific oligos combined with Ribo-Zero rRNA removal beads. The isolated RNA was subsequently fragmented using enzymatic fragmentation. Next, first- and second-strand synthesis were performed, and the double-stranded cDNA was purified using an AMPure kit (XP, Beckman Coulter). The

cDNA was end-repaired, 3’ adenylated, Illumina sequencing adaptors were ligated onto the fragments ends, and the library was purified (AMPure XP). The RNA stranded libraries were pre-amplified with PCR and purified (AMPure XP) to identify the coding DNA strand that the transcript and sequences originated from. The library size distributions were validated, and quality inspected on a Bioanalyzer 2100 or BioAnalyzer 4200 TapeStation (Agilent Technologies). High-quality libraries were pooled in equimolar concentrations based on the Bioanalyzer Smear Analysis tool (Agilent Technologies). The library pool(s) were quantified using qPCR, and optimal concentrations of the library pool were used to generate the clusters on the surface of a flowcell before sequencing on a HiSeq500) instrument (76 cycles) according to the manufacturer instructions (Illumina Inc.). The experiments were performed using NextSeq500, Illumina platform, TruSeq Stranded Total RNA Library Kit, 75 bp single read, and ~35.8 million reads per sample. Annotation of the obtained sequences was performed using the reference annotation from The Arabidopsis Information Resource, TAIR,Arabidopsis_thaliana.TAIR10.46
https://www.Arabidopsis.org/servlets/TairObject?type=species_variant&id=90.

Sample Name	**Sample Groups**	**QIAGEN ID**
Arabidopsis thaliana Col 0	WT	30097-001
Arabidopsis thaliana Col 0	WT	30097-002
Arabidopsis thaliana Col 0	WT	30097-003
pER8-P6WT-GFP number 10-121	P6WT-GFP	30097-004
pER8-P6WT-GFP number 10-121	P6WT-GFP	30097-005
pER8-P6WT-GFP number 10-121	P6WT-GFP	30097-006
pER8-P6(ΔTOR)-GFP number 2-11	P6 (TOR-GFP)	30097-007
pER8-P6(ΔTOR)-GFP number 2-11	P6 (TOR-GFP)	30097-008
pER8-P6(ΔTOR)-GFP number 2-11	P6 (TOR-GFP)	30097-009

Table 6.1. Samples used in the RNA-Seq project and their specifications.6.3.2. Trimming and Quality Control

Following sequencing, intensity correction, and base calling (into BCL files), FASTQ files were generated using the appropriate bcl2fastq software (Illumina Inc.), which

includes quality scoring of each individual base in a read. At this stage, the data were separated for Paired-end reads (PE) to determine whether the second read significantly differs from the first in terms of overall quality. Adapter and quality trimming were done by the “Trim Reads” tool from CLC Genomics Workbench. While adapters are often removed directly by the sequencer, part of the adapter region may be included in the sequenced reads. Such adapters artefacts were removed by identifying read-through adapter sequences, whereby the 3’ end of one read includes the reverse complement of the adapter from the other read. Further, reads were trimmed based on quality scores and ambiguous nucleotides, e.g., due to stretches of Ns. A maximum of 2 ambiguous nucleotides was allowed in a read.

6.3.3. Reference genome

Annotation of the obtained sequences was performed using the reference annotation *Arabidopsis_thaliana.* TAIR10. Alignment to the P6WT-GFP sequence was carried out as an internal gene expression control.

6.3.4. Mapping and Yields

Mapping of the sequencing data is a useful quality control step in NGS data analysis, as it can help evaluate the quality of samples. It is possible to align 60-90% of the reads to the reference genome in a typical experiment. However, this number depends on multiple factors, including the quality of the sample and the coverage of the relevant reference genome; if the sample RNA was degraded, fewer reads would be mRNA or lncRNA specific and more material will be degraded rRNA.

6.3.5. Identifying Differential Expression Patterns between lines

6.3.5.1. Principal Component Analysis

Principal Component Analyses (PCA) were performed on the gene expression profile using the “PCA for RNA-seq” tool from CLC Genomic Workbench. PCA is a method used in an unsupervised analysis to reduce the dimension of large data sets and is a

useful tool to explore sample clusters arising naturally based on the gene expression profile. On a PCA plot, the data points representing the samples projected onto the 2D plane such that they spread out in the two directions that explain most of the variance in the data.

6.3.5.2. Statistical testing

The Empirical analysis of gene expression data was implemented in the pipeline as the "Exact Test" for two-group comparisons developed by (Robinson and Smyth, 2008) and incorporated in the EdgeR Bioconductor package (Robinson et al., 2010), The Empirical Analysis of the DGE algorithm in the CLC Genomics Workbench is a re-implementation of the "Exact Test". For each gene, a p-value was assigned to represent the significance of the observed fold change. The statistic fold change determines the likelihood of these genes being similarly expressed, i.e., not differentially expressed. As we test many genes in this experiment, using p-value alone as a measure of significance can be prone to identifying false-positive genes. For example, if we were to test 1000 genes whose expression is unchanged in reality and choose a p-value threshold of 0.05, we would expect 50 genes below the threshold just by chance. To account for this multiple testing problem, *p*-values of all genes were converted to adjusted *p*-values (q-values) based on false discovery rate (FDR) (Benjamini and Hochberg, 1995).

6.3.6. DAVID pathway analysis

The DAVID Functional Classification Tool (Huang et al., 2007) was used to: (A) group the 20 top important genes of each pairwise comparison (i.e., pER8-P6WT-GFP versus Col-0, pER8-P6(ΔTOR)-GFP versus Col-0, pER8-P6WT-GFP versus pER8-P6(ΔTOR)-GFP) based on their functional similarities and their p-value, and (B) identify the corresponding Gene Ontology enrichment of each functional group. All of the gene transcripts were identified, annotated, and their sequences were obtained from reference The Arabidopsis Information Resource, TAIR, Arabidopsis_thaliana. TAIR10.46 (https://www.Arabidopsis.org/servlets/TairObject?type=species_variant&id=90).

Arabidopsis genes were manually collected from the National Center for Biotechnology Information (NCBI), TAIR, and The Universal Protein Resource (UniProt) using approved gene names for *Arabidopsis thaliana* (L.) Heynh wild-type (Col-0).

6.4. Results

6.4.1. Gene expression analysis

A total of 35.8 million raw of RNA-Seq reads per sample were subjected to quality checking and trimming. On average, 97.99% of each sample possessed a Q-score that fell within the 30-40 range (Li and Chou, 2004, Chou and Holmes, 2001). A Q-score of 30 or greater is considered to be high quality. Quality trimmed reads were aligned to the *Arabidopsis thaliana* genome and approximately 97.6% of the trimmed reads were mapped to the genome, and an average of 98.6% was mapped to genes.

6.4.2. Expression of the P6 transgene

Before attempting to analyze the patterns of host gene expression and as a control to determine the abundance of transcripts from the two P6 transgene constructs in the samples, transgene expression was quantified using the known sequence of P6WT-GFP and P6(ΔTOR)-GFP. The results are shown in Table 5.1. Over the three biological replicate samples for each construct, the pER8-P6(ΔTOR)-GFP line had an average of 228018 reads, the pER8-P6WT-GFP line had an average of 3442 reads, and Arabidopsis Col-0 had an average of 2 reads, presumably due to miscalling of the reads as this line does not express P6 (Table 5.1). Thus, the level of expression of the pER8-P6(ΔTOR)-GFP transgene was on average 66-fold higher than pER8-P6WT-GFP. Although there was some variation between the three biological samples of pER8-P6(TOR)-GFP, transgene transcript abundance of pER-P6WT-GFP was consistently very much lower. This result was at variance with the Western Blot and confocal imaging data (chapter IV), which consistently showed protein levels in the two transgenic lines as broadly similar following induction of the transgene by estradiol treatment. Transgene transcripts in the pER8-P6(ΔTOR)-GFP samples comprised up to nearly 1% of total reads – this is consistent with a highly abundant species and the

published data where the pER8 vector provide high transgene expression post estradiol induction (Schlucking et al., 2013, Zuo et al., 2000). However, for all three biological samples, levels of the P6WT transcript comprised less than 0.01% of the total mRNA species. These levels are very much lower than expected and suggest that estradiol induction of transgene expression may have been weak.

Sample Name	Sample No.	Reads mapped to spike-ins (#)	Reads mapped to spike-ins (%)
Arabidopsis Col-0	30097-001	1	3.01E-06
Arabidopsis Col-0	30097-002	1	2.65E-06
Arabidopsis Col-0	30097-003	4	1.2E-05
Average for Arabidopsis Col-0		2	5.89E-06
pER8-P6WT-GFP	30097-004	4453	0.010819
pER8-P6WT-GFP	30097-005	3113	0.009221
pER8-P6WT-GFP	30097-006	2760	0.00766
Average for pER8-P6WT-GFP		3442	9.23E-03
pER8-P6(TOR)-GFP	30097-007	290790	0.877417
pER8-P6(TOR)-GFP	30097-008	356805	0.965265
pER8-P6(TOR)-GFP	30097-009	36460	0.098863
Average for pER8-P6(TOR)-GFP		228018	6.47E-01

Table 6.2. Alignment rates of the tested lines to the transgene sequence.

6.4.3. Differential Gene Expression Analysis

6.4.3.1. Principal Component Analysis (PCA)

The PCA test was conducted using the three comparison genes lists with the highest variance among all samples; the results showed pER8-P6WT-GFP, pER8-P6(ΔTOR)-GFP, and Col-0 generally clustered together based on the homolog gene expression profile within the groups. Except for the third biological replicate of each line was an outlier where they showed differences in gene expression profile compared to the other two samples in Table 6.1 and Table 6.2.

6.4.3.1.1. Comparison of pER8-P6WT-GFP versus Col-0

The impact of P6WT expression on the Arabidopsis gene expression profile was determined by comparing the results from pER8-P6WT-GFP plants with Col-0. Following the inferential statistics, differentially expressed genes were grouped using Principal Component Analysis (PCA). The PCA1 and PCA2 explain 62% of the variance in Plant responses (Figure 6.1). The numbers of expressed genes, informative genes, and the resulting differentially expressed genes (DEGs) identified in the comparison between lines are presented in the supplementary data. In total, 25,776 genes were identified and measured for expression; these explain almost all variation in responses between the two lines. Figure 6.1 shows the two PCA clusters of pER8-P6WT-GFP and Col-0. The clustering implies that gene expression data explains the differences in expression between the two lines. In the comparison between pER8-P6WT-GFP and Col-0, 20 genes showed a significant difference in expression (ESeq2, $q \leq 0.05$, FDR = 0.05); these were considered DEGs. Among these DEGs, 20 DEGs were 5 up-regulated, and 15 were down-regulated in the pER8-P6WT-GFP line shown in Table 6.3 and Table 6.4.

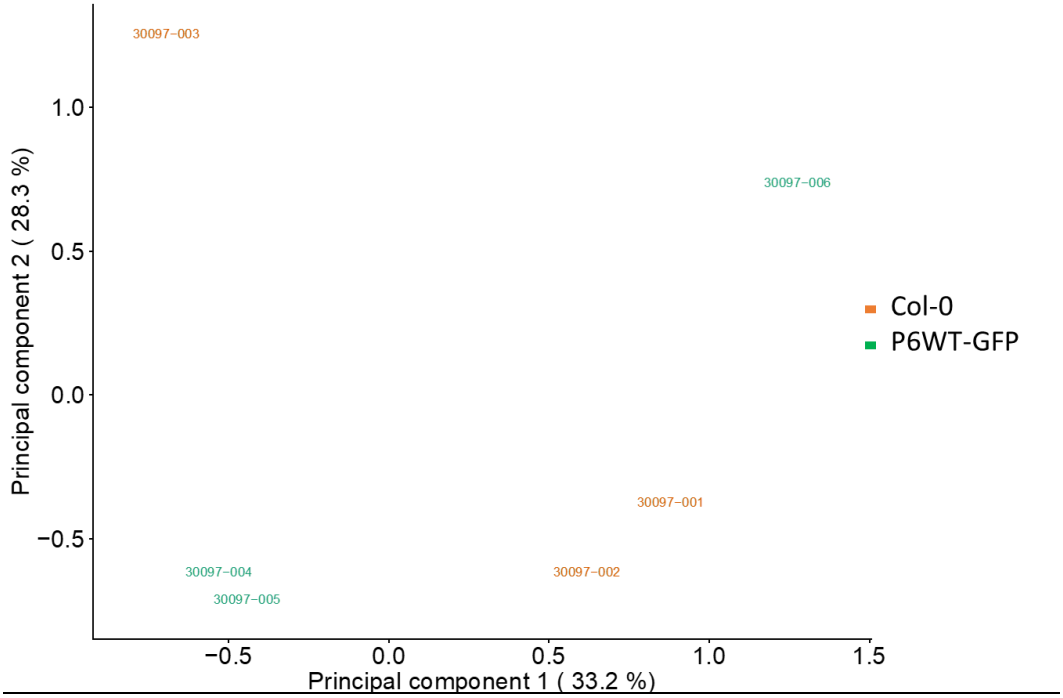

Figure 6.1. Principal Component Analysis using all highest variance genes in the pER8-P6WT-GFP versus Col-0 comparison. The data were clustered together based on gene expression. Green color points show pER8-P6WT-GFP defined as P6WT-GFP, and orange color points show Col-0, defined as WT. PC1 and PC2 are the parameters that comprise all identified genes. parameters that comprise all identified genes.

No.	Gene Name	Gene Code	Adjusted p-value (FDR)
1	MD-2-related lipid-recognition protein ROSY1	*ROSY1*	0.000
2	lipid transfer protein 4	*LTP4*	0.000
3	Non-specific lipid-transfer protein 3	*LTP3*	0.000
4	Cyclic nucleotide-gated channel 19	*CNGC19*	0.002
5	thalianol synthase 1	*THAS1*	0.004
6	Probable apyrase 5	*APY5*	0.033
7	**High affinity nitrate transporter 2.6**	***NRT2.6***	0.065
8	**LOB domain-containing protein 26**	***LBD26***	0.114
9	Expressed in response to phosphate starvation protein	*AT4_1*	0.122
10	Cytochrome P450 708A2	*CYP708A2*	0.170
11	**Germin-like protein subfamily 1 member 18**	***GLP2A***	0.184
12	Isochorismate synthase 2, chloroplastic	*ICS2*	0.193
13	4-aminobutyrate aminotransferase	*PYD4*	0.413
14	**peroxidase 69**	***PER69***	0.464
15	Endothelial cell-specific molecule 1	*ESM1*	0.514
16	**Glycerophosphoinositol inositolphosphodiesterase GDPD2**	***GDPD2***	0.543
17	Protein PLANT CADMIUM RESISTANCE 1	*PCR1*	0.558
18	Glucan 1,3-beta-glucosidase	*BGL2*	0.670

19	Proto-oncogene tyrosine-protein kinase ROS	*ROS1*	0.690
20	Cysteine-rich receptor-like protein kinase 37	*CRK37*	0.695

Table 6.3. Details of the 20 most statistically significant differentially expressed genes in the pER8-P6WT-GFP line compared to Col-0. The genes were ranked based on their significant adjusted *p*-value level (q ≤ 0.05, FDR = 0.05). The bolded genes in the table represent the up-regulated genes between the two lines.

pER8-P6WT-GFP versus Col-0				
No	**Gene Code**	**(- Log2 fold ratio)**	**Elevation Level**	**Biological function**
1	*ROSY1*	-1.875119411	Down Regulated	Regulation of gravitropic response and basipetal auxin transport in roots
2	*LTP4*	-4.246517369	Down Regulated	PR-14 pathogenesis-related protein family and response to abscisic acid
3	*LTP3*	-2.044836693	Down Regulated	PR-14 pathogenesis-related protein family and response to abscisic acid
4	*CNGC19*	-4.420954799	Down Regulated	Response to herbivore
5	*THAS1*	-1.007772117	Down Regulated	Response to gravity response to light stimulus, root development, and thalianol biosynthesis process
6	*APY5*	-1.999186323	Down Regulated	Dephosphorylation
7	***NRT2.6***	3.122616139	**Up Regulated**	Cellular response to nitrate
8	***LBD26***	1.465958976	**Up Regulated**	Transcription factors

9	*AT4_1*	-1.179211163	Down Regulated	Cellular response to phosphate cellular response to phosphate
10	*CYP708A2*	-0.835432109	Down Regulated	Thalianol pathway, brassinosteroid biosynthetic process, and multicellular organism development
11	***GLP2A***	1.631062343	**Up Regulated**	Play a role in plant defense
12	*ICS2*	-1.145906902	Down Regulated	Salicylic acid (SA) biosynthesis and required for both local and systemic acquired resistance (LAR and SAR) plant defense.
13	*PYD4*	-0.973088211	Down Regulated	Cellular response to nitrogen levels
14	***PER69***	1.01521748	**Up Regulated**	Auxin catabolism and response to environmental stresses such as wounding, pathogen attack, and oxidative stress.
15	*ESM1*	-0.969938176	Down Regulated	Defense response to bacterium response to insect and positive regulation of cell population proliferation
16	***GDPD2***	0.908681679	**Up Regulated**	Cellular response to hypoxia
17	*PCR1*	-2.534144762	Down Regulated	Response to abscisic acid, response to bacterium, response to fungus, salicylic acid-mediated signalling pathway
18	*BGL2*	-2.146335142	Down Regulated	SA responsive PR protein
19	*ROS1*	-0.708557158	Down Regulated	Repressor of transcriptional gene silencing, defense response to fungus, and responsiveness of SA-dependent defense genes
20	*CRK37*	-3.798503811	Down Regulated	Protein phosphorylation

Table 6.4. Details of the 20 most significant differentially expressed genes in the pER8-P6WT-GFP line compared to Col-0. The genes were ranked based on their significant adjusted *p*-value level ($q \leq 0.05$, FDR = 0.05). The difference in the elevation

level between the two lines (i.e., P6WT-GFP versus WT) is expressed as the average - Log fold change ratio. The bolded genes in the table represent the up-regulated genes between the two lines.

6.4.3.1.2. Comparison of pER8-P6(ΔTOR)-GFP versus Col-0

To assess the effect of expressing P6 with a TOR binding domain deletion expression, the impact on Arabidopsis gene expression was determined by comparing the results from pER8-P6(ΔTOR)-GFP plants with Col-0. In the pER8-P6(ΔTOR)-GFP and Col-0 comparison, the PCA components comprised of these 25793 genes from each line explain 70% of the lines' variance in Plant responses (Figure 6.2). Similar to the previous comparison, those 25793 genes explain almost all variation in response between the two different lines. PCA analysis shows that two clusters of pER8-P6(ΔTOR)-GFP and Col-0 were formed. The clusters mean that gene expression data explain the differences in expression between the two lines. The comparison between pER8-P6(ΔTOR)-GFP and Col-0 20 genes showed a significant difference in the expression, 12 up-regulated, and 8 were down-regulated in the pER8-P6(ΔTOR)-GFP line shown in Table 6.5 and Table 6.6.

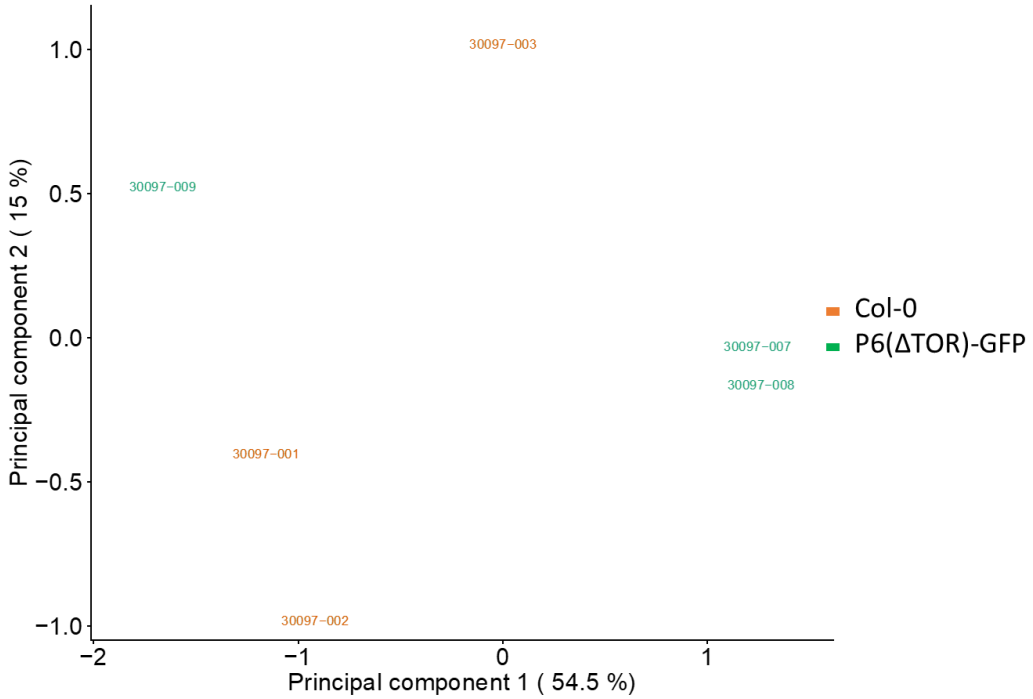

Figure 6.2. Principal Component Analysis using all highest variance genes in the pER8-P6(ΔTOR)-GFP versus Col-0 comparison. The data were clustered together based on gene expression. Green color points show pER8-P6(ΔTOR)-GFP defined as

P6(ΔTOR)-GFP and orange color points show Col-0, defined as WT. PC1 and PC2 are the parameters that comprise all identified genes.

No.	Gene Name	Gene Code	Adjusted p-value (FDR)
1	non-specific phospholipase C3	*NPC3*	0.000
2	Serine/threonine-protein kinase SRK2I	*SRK2I*	0.000
3	**Cytochrome P450 82C3**	***CYP82C3***	0.000
4	**Aquaporin TIP1-3**	***TIP2-3***	0.000
5	Glutathione S-transferase F14	*GSTF14*	0.000
6	Non-specific lipid-transfer protein 3	*LTP3*	0.000
7	**Peroxidase 4**	***PER4***	0.000
8	**Peroxiredoxin-2D**	***PRXIID***	0.000
9	lipid transfer protein 4	*LTP4*	0.000
10	High affinity nitrate transporter 2.6	*NRT2.6*	0.000
11	Protein COLD-REGULATED 15B, chloroplastic	*COR15B*	0.000
12	**Marneral synthase**	***MRN1***	0.000
13	**Cytochrome P450 71B21**	***CYP71B21***	0.000
14	**Protein PLANT CADMIUM RESISTANCE 9**	***PCR9***	0.001
15	PATHOGEN AND CIRCADIAN CONTROLLED 1	*PCC1*	0.001
16	Cytochrome P450 708A2	*CYP708A2*	0.001
17	**Probable inactive L-type lectin-domain containing receptor kinase III.1**	***LECRK31***	0.002
18	**Peroxidase 37**	***PER37***	0.003
19	**Cytochrome P450 72A14**	***CYP72A14***	0.004
20	**Pectinesterase inhibitor 12**	***PMEI12***	0.004

Table 6.5. Details of the 20 most statistically significant differentially expressed genes in the pER8-P6(TOR)-GFP line compared to Col-0. The genes were ranked based on their significant adjusted *p*-value level (q ≤ 0.05, FDR = 0.05). The bolded genes in the table represent the up-regulated genes between the two lines.

pER8-P6(TOR)-GFP versus Col-0				
No	**Gene Code**	**(- Log2 fold ratio)**	**Elevation Level**	**Biological function**
1	*NPC3*	-3.198	Down Regulated	Phosphatase activity and brassinolide-mediated signalling in root development.
2	*SRK2I*	-2.774	Down Regulated	Response to abscisic acid, response to gibberellin, and protein phosphorylation
3	***CYP82C3***	6.103	**Up Regulated**	Defense response to other organisms and oxidoreductase activity
4	***TIP2-3***	1.997	**Up Regulated**	Urea transport and water transport
5	*GSTF14*	-1.602	Down Regulated	Glutathione metabolic process, toxin catabolic process
6	*LTP3*	-2.426	Down Regulated	PR-14 pathogenesis-related protein family and response to abscisic acid
7	***PER4***	3.397	**Up Regulated**	Auxin catabolism, response to environmental stresses such as wounding, pathogen attack, and oxidative stress

8	***PRXIID***	2.620	**Up Regulated**	Cell redox homeostasis and cellular response to oxidative stress
9	*LTP4*	-4.565	Down Regulated	PR-14 pathogenesis-related protein family and response to abscisic acid
10	***NRT2.6***	3.892	**Up Regulated**	Cellular response to nitrate
11	*COR15B*	-1.728	Down Regulated	Response to fungus leaf senescence, response to abscisic acid
12	***MRN1***	2.773	**Up Regulated**	Triterpenoid biosynthetic process
13	***CYP71B21***	7.239	**Up Regulated**	Oxidoreductase activity
14	***PCR9***	3.730	**Up Regulated**	Involved in cadmium resistance
15	*PCC1*	-2.014	Down Regulated	Response to abscisic acid, response to bacterium, response to fungus, SA mediated signalling pathway
16	*CYP708A2*	-1.389	Down Regulated	Thalianol pathway, brassinosteroid biosynthetic process, and multicellular organism development
17	***LECRK31***	5.935	**Up Regulated**	Defense response, defense response to bacterium, defense response to oomycetes, and protein phosphorylation
18	***PER37***	2.477	**Up Regulated**	Negative regulation of growth, response to oxidative stress

19	***CYP72A14***	-0.708557158	**Up Regulated**	Oxidoreductase activity,
20	***PMEI12***	-3.798503811	**Up Regulated**	Response to necrotrophic pathogens, contributes to resistance against the pathogen.

Table 6.6. **Details of the 20 most significant differentially expressed genes in the pER8-P6(∆TOR)-GFP line compared to Col-0.** The genes were ranked based on their significant adjusted *p*-value level (q ≤ 0.05, FDR = 0.05). The difference in the elevation level between the two lines (i.e., P6(∆TOR)-GFP versus WT) is expressed as the average - Log fold change ratio. The bolded genes in the table represent the up-regulated genes between the two lines.

6.4.3.1.3. Comparison of pER8-P6WT-GFP versus pER8-P6(ΔTOR)-GFP

To determine the role of the interaction with TOR on the effect of P6 expression on transcript abundance in Arabidopsis, results from the two P6 transgenic lines, P6WT and P6(ΔTOR) were compared. Because there were great differences in transgene expression levels between the pER8-P6WT-GFP and pER8-P6(ΔTOR)-GFP samples (see Table 6.3), this will have a major on the impact the outcomes of any comparison between the two lines, and any apparent differences in expression might be attributable solely to imbalance in levels of P6 in the two sets of samples. Therefore, differences in gene expression profiles that are dependent on the presence or absence of the TOR-binding domain need to be regarded as potential artefacts. Nevertheless, the results are worthwhile reporting provided these caveats are kept in mind. In the future, confirmation will need to be carried out by repeating the RNA-seq experiments using samples with similar levels of transgene expression and with higher numbers of biological replicates. Highlight the differences between P6WT and P6(ΔTOR) expression impact on Arabidopsis gene expression profile.

The comparison between pER8-P6WT-GFP and pER8-P6(ΔTOR)-GFP had PCA components comprised of 25705 genes from each line and explains 62% of the lines' variance in Plant responses (Figure 6.3). Similar to the previous comparison, those 25705 genes explain almost all variation in response between the two different lines. The clusters mean that gene expression data explain the differences in transcript abundance between the two lines. In the comparison between pER8-P6WT-GFP and Col-0, 20 genes showed a significant difference in the expression, where 3 genes were more abundant in the P6WT line, and 17 genes were less abundant in the pER8-P6WT-GFP line compared to the pER8-P6(ΔTOR)-GFP line, as shown in Table 6.7 and Table 6.8.

For all three comparisons, pER8-P6WT-GFP versus Col-0, pER8-P6(ΔTOR)-GFP versus Col-0, and pER8-P6WT-GFP versus pER8-P6(ΔTOR)-GFP, the PCA analysis demonstrated clear differences in patterns of gene expression between the three lines.

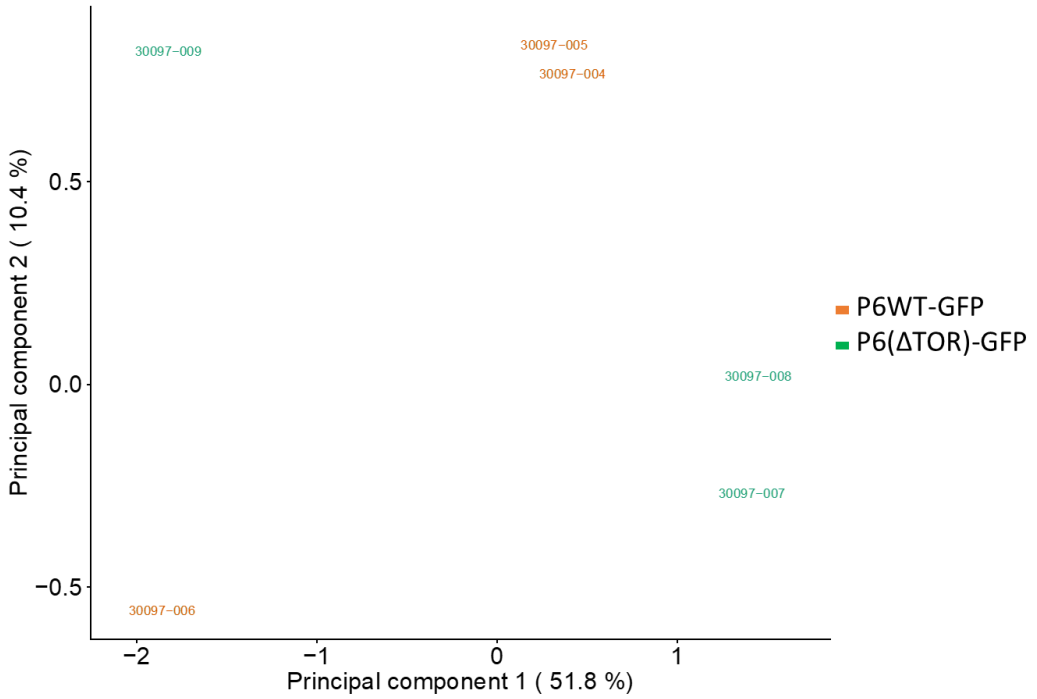

Figure 6.3. Principal Component Analysis using all highest variance genes in the pER8-P6WT-GFP versus pER8-P6(ΔTOR)-GFP comparison. The data were clustered together based on gene expression. Green color points show pER8-P6(ΔTOR)-GFP defined as P6(ΔTOR)-GFP and orange color points show pER8-P6WT-GFP, defined as P6WT-GFP. PC1 and PC2 are the parameters that comprise all identified genes.

No.	Gene Name	Gene Code	Adjusted p-value (FDR)
1	**non-specific phospholipase C3**	***NPC3***	0.000
2	**Serine/threonine-protein kinase SRK2I**	***SRK2I***	0.000
3	**LOB domain-containing protein 26**	***LBD26***	0.000
4	Cytochrome P450 82C3	*CYP82C3*	0.000
5	Disease resistance-responsive (dirigent-like protein) family protein	*DIR5*	0.000
6	Putative plant defensin 1.2b	*PDF1.2B*	0.001
7	Plant defensin 1.2c	*PDF1.2C*	0.001
8	Purple acid phosphatase	*PAP20*	0.001
9	Caffeoyl-CoA 3-O-methyltransferase	*CCOAMT*	0.002
10	VQ motif-containing protein 29	*VQ29*	0.003
11	Cyclic nucleotide-gated channel 19	*CNGC19*	0.004
12	NDR1/HIN1-like protein 10	*NHL10*	0.006
13	PLANT DEFENSIN 1.1	*PDF1.1*	0.008
14	NDR1/HIN1-like 25	*NHL25*	0.009
15	Cytochrome P450 710A1	*CYP710A1*	0.009
16	PLANT DEFENSIN 1.2A	*PDF1.2A*	0.009
17	CYTOCHROME P450, FAMILY 715, SUBFAMILY A, POLYPEPTIDE 1	*CYP715A1*	0.010
18	Phosphatidylinositol 4-kinase gamma 3	*PI4KG3*	0.010
19	Putative wall-associated receptor kinase-like 16	*WAKL16*	0.010

20	Peroxiredoxin-2D	*PRXIID*	0.014

Table 6.7. Details of the 20 most statistically significant differentially expressed genes in the pER8-P6WT-GFP line compared to pER8-P6(ΔTOR)-GFP. The genes were ranked based on their significant adjusted *p*-value level (q ≤ 0.05, FDR = 0.05). The bolded genes in the table represent the genes whose expression was more abundant in the P6WT line.

pER8-P6WT-GFP versus pER8-P6(ΔTOR)-GFP				
No	**Gene Code**	**(- Log2 fold ratio)**	**Elevation Level**	**Biological function**
1	***NPC3***	3.300	**Up Regulated**	Phosphatase activity and brassinolide-mediated signalling in root development.
2	***SRK2I***	2.919	**Up Regulated**	Response to abscisic acid, response to gibberellin, and protein phosphorylation
3	***LBD26***	2.961	**Up Regulated**	Suggested to regulate plant-specific processes
4	*CYP82C3*	-5.610	Down Regulated	Defense response to other organisms and oxidoreductase activity
5	*DIR5*	-2.360	Down Regulated	Guiding stereospecific synthesis activity
6	*PDF1.2B*	-3.097	Down Regulated	Defense responses: ethylene and JA response, response to fungus
7	*PDF1.2C*	-3.799	Down Regulated	Defense responses: ethylene and JA response, response to fungus
8	*PAP20*	-4.229	Down Regulated	Acid phosphatase activity
9	*CCOAMT*	-2.033	Down Regulated	Methylation

10	*VQ29*	-5.247	Down Regulated	Flower devolvement
11	*CNGC19*	-4.241	Down Regulated	Response to herbivore and JA response
12	*NHL10*	-2.235	Down Regulated	Defense response to virus
13	*PDF1.1*	-3.886	Down Regulated	Confers broad-spectrum resistance to pathogens (antifungal activity)
14	*NHL25*	-3.958	Down Regulated	Salicylic acid-mediated signalling pathway
15	*CYP710A1*	-1.407	Down Regulated	Sterol biosynthesis
16	*PDF1.2A*	-2.784	Down Regulated	Defense response, JA response, and ethylene-dependent systemic resistance and response to insect
17	*CYP715A1*	-5.029	Down Regulated	Iron ion binding and oxidation activity
18	*PI4KG3*	-2.213	Down Regulated	Response to abscisic acid Source and protein phosphorylation
19	*WAKL16*	-5.190	Down Regulated	Protein phosphorylation
20	*PRXIID*	-2.034	Down Regulated	Plays a role in cell protection against oxidative stress

Table 6.8. **Details of the 20 most significant differentially expressed genes in the pER8-P6WT-GFP line compared to pER8-P6(∆TOR)-GFP.** The genes were ranked based on their significant adjusted *p*-value level (q ≤ 0.05, FDR = 0.05). The difference in the elevation level between the two lines (i.e., P6WT-GFP versus P6(∆TOR)-GFP) is expressed as the average - Log fold change ratio. The bolded genes in the table represent the transcripts that were more abundant in the P6WT line.

6.4.3.2. DAVID pathway analysis

The DAVID Functional Classification Tool was used to identify potential functions of the top 20 most significant changes in abundance for gene transcripts from each of the three pairwise comparisons, pER8-P6WT-GFP versus Col-0 (Table 6.4), pER8-P6(ΔTOR)-GFP versus Col-0 (Table 6.6), pER8-P6WT-GFP versus pER8-P6(ΔTOR)-GFP (Table 6.8). These are, classified via their significant adjusted p-value level ($q \leq 0.05$, FDR = 0.05). The results are shown below:

6.4.3.2.1. pER8-P6WT-GFP versus Col-0

The PCA analysis of pER8-P6WT-GFP versus Col-0 had two annotation clusters that represented two distinct functional groups (Table 6.9). Cluster I contains 4 genes with an enrichment score of 1.03 and p-values with a range of 0.03 – 0.41. Cluster II contains 5 genes with an enrichment score of 0.37 and p-values with a range of 0.28 – 0.60. The clusters, genes, and functional GO (Gene Ontology) classes are shown in Table 6.9. GO enrichment analysis identified several important genes involved in hormonal signalling associated with the plasma membrane, metabolism, biotic responses, abiotic responses, cell proliferation, and differentiation.

Annotation	GO Class	Gene Members	*p*-value	Enrichment Score
Cluster 1	Apoplast Signal peptide Signal Extracellular region	*LTP4*, *LTP3*, *CRK37*, *BGL2*	(0.03 – 0.41)	1.03
Cluster 2	Transmembrane helix Transmembrane Membrane integral component of membrane plasma membrane transmembrane region	***NRT2.6****, CYP708A2, PCR1, CNGC19, CRK37*	(0.28 – 0.60)	0.37

Table 6.9. DAVID Functional Annotation Clustering report based on the top 20 most statistically significant expressed gene transcripts in the pER8-P6WT-GFP line compared to Col-0. The genes were ranked based on their significant adjusted p-value level ($q \leq 0.05$, FDR = 0.05). Each Annotation cluster has gene members with related biological functions. Gene Ontology (GO) class provides the shard biological properties for all the Gene Members in the corresponding cluster. The Enrichment Score and the p-value of each cluster are provided. The bolded genes in the table represent the up-regulated genes between the two lines.

6.4.3.2.2. pER8-P6(ΔTOR)-GFP versus Col-0

The-P6(ΔOR)-GFP versus Col-0 comparison revealed three annotation clusters that represented distinct functional groups (Table 6.10). Cluster I comprised of 4 genes with an enrichment score of 2.57 and a p-value with a range of 0.001 – 0.007. Cluster II comprised of 7 genes with an enrichment score of 2.34 and a p-value with a range of 0.0001 – 0.24. Cluster III contains 7 genes with an enrichment score of 1.25 and a p-value with a range of 0.016 – 0.31. The clusters, genes, and functional GO classes are shown in Table 6.10. GO enrichment analysis identified several important genes involved in hormonal signalling associated with the plasma membrane, metabolism, biotic, abiotic responses, cell proliferation, and differentiation.

Annotation	GO Class	Gene Members	*p*-value	Enrichment Score
Cluster 1	Lipid-binding response to abscisic acid lipid binding	*PCC1, COR15B, LTP4, LTP3*	(0.001 – 0.007)	2.57
Cluster 2	Heme heme binding Cytochrome P450 Monooxygenase oxygen binding Iron iron ion binding Oxidoreductase oxidoreductase activity, acting on paired donors, with incorporation or reduction of molecular oxygen monooxygenase activity	***CYP72A14***, ***NRT2.6***, *PCC1, CYP708A2,* ***CYP71B21***, ***CYP82C3***, ***PER4***	(0.0001 – 0.24)	2.34

	Cytochrome P450, conserved site Cytochrome P450, E-class, group I metal ion-binding site: Iron (heme axial ligand) Secondary metabolites biosynthesis, transport, and catabolism oxidation-reduction process Metal-binding Transmembrane helix Transmembrane integral component of membrane Membrane			
Cluster 3	disulfide bond Disulfide bond extracellular region	*LTP4, LTP3, PDF1.2C,* ***PER4****,* ***CYP71B21***	(0.016 – 0.31)	1.25

	signal peptide
	Signal

Table 6.10. DAVID Functional Annotation Clustering report based on the top 20 most statistically significant differentially expressed gene transcripts in the pER8-P6(ΔTOR)-GFP line compared to Col-0. The genes were ranked based on their significant adjusted p-value level ($q \leq 0.05$, FDR = 0.05). Each Annotation cluster has gene members with related biological functions. Gene Ontology (GO) class provides the shard biological properties for all the Gene Members in the corresponding cluster. The Enrichment Score and the p-value of each cluster are provided. The bolded genes in the table represent the up-regulated genes between the two lines.

6.4.3.2.3. pER8-P6WT-GFP versus pER8-P6(ΔTOR)-GFP

The pER8-P6WT-GFP versus pER8-P6(ΔTOR)-GFP comparison had two annotation clusters that represented distinct functional groups (Table 6.11). Cluster I comprise 7 genes with an enrichment score of 1.75 and a p-value with a range of 0.001 – 0.44. Cluster II comprises 6 genes with an enrichment score of 1.33 and a p-value with a range of 0.013 – 0.20. The clusters, genes, and functional GO classes are shown in Table 6.11. GO enrichment analysis identified several important genes involved in hormonal signalling associated with the plasma membrane, metabolism, biotic responses, abiotic responses, cell proliferation, and differentiation

Annotation	GO Class	Gene Members	*p*-value	Enrichment Score
Cluster 1	oxidoreductase activity, acting on paired donors, with incorporation or reduction of molecular oxygen monooxygenase activity Iron oxygen binding Cytochrome P450, conserved site Cytochrome P450, E-class, group I Monooxygenase Cytochrome P450 iron ion binding heme binding Heme Metal-binding	*CCOAMT, PAP20, CYP82C3, CYP710A1, CYP715A1, NHL25, CNGC19*	(0.001 – 0.44)	1.75

	Secondary metabolites biosynthesis, transport, and catabolism Oxidoreductase oxidation-reduction process Transmembrane helix Transmembrane Membrane integral component of membrane			
Cluster 2	Secreted extracellular region defense response Signal Disulfide bond signal peptide	*PDF1.2C, PDF1.2B, DIR5, CCOAMT, PAP20, CYP715A1*	(0.013 – 0.20)	1.33

Table 6.11. DAVID Functional Annotation Clustering report based on the top 20 most statistically significant differentially expressed gene transcripts in the pER8-P6WT-GFP line compared to pER8-P6(ΔTOR)-GFP. The genes were ranked based on their significant adjusted p-value level (q ≤ 0.05, FDR = 0.05). Each Annotation cluster has gene members with related biological

functions. Gene Ontology (GO) class provides the shard biological properties for all the Gene Members in the corresponding cluster. The Enrichment Score and the p-value of each cluster are provided. The bolded genes in the table represent the transcripts that were more abundant in the P6WT line.

6.5. Discussion

Genes identified as important in this transcriptomic aspect of the study were used to reveal biological functions and processes that are differentially regulated in P6 and P6(ΔTOR) expressing plants. This analysis used the gene lists presented in Table 6.3, Table 6.5, and Table 6.7 and is detailed in gene expression data provided by Qiagen (not shown). The PCA plots using the data genes lists in the three comparisons, pER8-P6WT-GFP versus Col-0, pER8-P6(ΔTOR)-GFP versus Col-0, and pER8-P6WT-GFP versus pER8-P6(ΔTOR)-GFP, showed a tendency to form clusters. These clusters are indicative of distinct gene expression profiles input between lines (Figure 6.1, 6.2, and 6.3). The PCA analysis showed that samples from the pER8-P6WT-GFP, pER8-P6(ΔTOR)-GFP, and Col-0 lines generally had similar gene expression profiles within the groups, although one biological replicate from each line had a gene expression profile that formed an outlier. The outlier might be attributable to; variation in growth conditions (light intensity, temperature, and humidity) or differences in the expression of the transgene between replicates. One sample (Table 6.3) of each line also exhibited poorer RNA quality, possibly attributable to degradation during transit to Qiagen. The most important cause of difficulties in interpreting the results was the unexpected differences in levels of expression (approximately 66-fold) of the transgene in the pER8-P6(ΔTOR)-GFP compared to the pER8-P6WT-GFP lines (~66-fold). Since these transgenic lines consistently showed similar protein expression levels following estradiol treatment as evidenced by western blots and confocal imaging, the most plausible explanation is that for unknown reasons, the estradiol treatment of the pER-P6WT-GFP plants was ineffective in inducing expression of the transgene in these samples. However, the data seemed to be consistent with earlier findings. This hypothesis is supported by the very low number of P6 reads (expressed as a proportion of total reads) in these plants. In contrast, the numbers of P6(ΔTOR) reads for the estradiol-induced P6(ΔTOR) plants was at approx. 0.9% of total reads, around the level expected for the efficient promoter in the pER8 vector (Zuo et al., 2000, Schlucking et al., 2013).A second RNA-seq experiment will be needed with additional samples to confirm and reproduce the outcomes of the gene expression analyses, particularly the comparison between pER8-P6(ΔTOR)-GFP and pER8-P6WT-GFP lines.

6.5.1. P6WT-GFP impact on Arabidopsis gene expression

Overall, the PCA of the comparison between pER8-P6WT-GFP and Col-0 was able to account for 62% of the variance in gene expression (Figure 6.1). Comparing pER8-P6WT-GFP and Col-0, 20 genes showed significant differences in the expression, of which 5 genes were up-regulated, and 15 genes were down-regulated (Table 6.4). These genes are associated with several critical biological functions related to cellular development and response, i.e., growth, cell shape regulation, defense response, signalling, metabolism, and cell proliferation activation.

No	Gene Code	SA	JA/ET	ABA	Aux	Biological function
1	*ROSY1*				Role in basipetal auxin transport in plant roots	has been shown to play a role in gravitropic response and
2	*LTP4*			increased endogenous ABA levels		PR-14 pathogenesis-related protein (PRP) family
3	*LTP3*	a negative SA regulator and		increased endogenous ABA levels		PR-14 pathogenesis-related protein (PRP) family
4	*CNGC19*	Mediates SA signalling pathways	Mediates JA/ET signalling pathways			responses to herbivores by modifying both JA/ET and SA signalling pathways
5	*THAS1*					responses to light stimulus and gravity, root development
6	*APY5*					dephosphorylation and suggested to participate in regulating Arabidopsis growth (Thomas et al., 1999, Wu et al., 2007)
7	***NRT2.6***					cellular response to nitrate
8	***LBD26***					unknown suggested response to pathogens and nitrogen metabolisms
9	*AT4_1*					cellular response to phosphate
10	*CYP708A2*					brassinosteroid biosynthetic process

11	***GLP2A***			play a role in plant defense
12	*ICS2*	SA biosynthesis		both local and systemic acquired resistance (LAR and SAR)
13	*PYD4*			cellular response to nitrogen levels
14	***PER69***		auxin catabolism	wounding, pathogen attack, and oxidative stress
15	*ESM1*			contributes to the defense response against bacteria and insects, herbivores
16	***GDPD2***			cellular response to hypoxia and lipid metabolic process
17	*PCR1*			Cd resistance
18	*BGL2*	SA-dependent host responses		SA-dependent host responses enacted via the NPR1-dependent pathway, in particular, SAR
19	*ROS1*	Repressor of responsive SA-dependent defense genes		a repressor of transcriptional gene silencing
20	*CRK37*			involved in protein phosphorylation, associated with plant defense response

Table 6.12. The biological function of the top 20 most statistically significant differentially expressed gene transcripts in the pER8-P6WT-GFP line compared to Col-0. Salicylic acid pathway (SA), jasmonic acid ethylene pathway (JA/ET), abscisic acid pathway (ABA), and auxin pathway (AUX). The bolded genes in the table represent the up-regulated genes between the two lines.

The five genes with the highest ranking based on FDR and p-value that were identified as up-regulated in the P6WT-GFP expressing line were *NRT2.6, LBD26, GLP2A, PER69, and GDPD2* (Table 6.4). These genes were further categorized according to their biological function (Table 6.3). Three genes, *PER69*, *LBD26*, and *GLP2A* have been identified in annotations as contributing to plant responses against biotic and abiotic stress. The gene *peroxidase* 69 (*PER69*) plays a role in response to

environmental stresses such as wounding, pathogen attack, oxidative stress, and is associated with auxin catabolism (Cosio and Dunand, 2009). Potentially, it might be involved in the increased resistance to the auxin transport inhibitor TIBA identified in the results presented in Chapter 4. The LOB domain-containing protein 26 (*LBD26*) is a transcription factor. Its exact role is unknown, although LBD proteins have been identified as a family of plant-specific transcription factors that regulate the development of plant organs, regeneration of plants, response to pathogens, and nitrogen metabolisms (Grimplet et al., 2017). Likewise, Germin-like protein subfamily 1 member 18 (*GLP2A*) is believed to play a role in plant defense, although this is yet to be confirmed. Two genes that participate in the cellular responses and metabolic processes, *GDPD2* and *NRT2.6* were identified as being up-regulated. *Glycerophosphoinositol inositolphosphodiesterase GDPD2* (*GDPD2*) participates in the cellular response to hypoxia and lipid metabolic process (Cheng et al., 2011). The high-affinity nitrate transporter 2.6 (*NRT2.6*) contributes to the cellular response to nitrate (Dechorgnat et al., 2012).

ROSY1, LTP4, LTP3, CNGC19, THAS1, APY5, AT4_1, CYP708A2, ICS2, PYD4, ESM1, PCR1, BGL2, ROS1, CRK37 were the fifteen most significant genes identified as being down-regulated in the P6WT-GFP expressing line compared to Col-0. Of these, 11 out of the 15 have been cited as contributing to plant responses against biotic and abiotic stress, particularly those associated with defense involving the SA-dependent and ethylene-dependent pathways or protein phosphorylation associated with signalling. Two genes encoding the lipid transfer proteins (LTP4) and non-specific lipid transfer protein 3 (LTP3) were identified as being down-regulated. These belong to the PR-14 pathogenesis-related protein (PRP) family. They are believed to participate in lipid transport and abscisic acid responses. There is evidence that LTP3 is modulating both SA and ABA biosynthesis. It was identified as a negative SA regulator and increased endogenous ABA levels. LTP3 was characterized as a negative plant immunity regulator, in which overexpression of *LTP3* enhanced susceptibility to the virulent bacteria *Pseudomonas syringae* pv. tomato (*Pst*) DC3000 strain and compromised the resistance to avirulent bacteria *Pseudomonas syringae* pv. tomato (*Pst*) *avrRpm1*. An Arabidopsis double mutant *ltp3,ltp4* demonstrated a

reduction in both susceptibility to DC3000 and ABA biosynthesis (Gao et al., 2016). *LTP3* and *LTP4* expression were induced by infection and ABA, while suppressed by brassinolide. So far, there is no evidence showing a direct relationship between *LTP4* and *LTP3* expression and the other phytohormones; auxin, ethylene, gibberellin, and jasmonate (Julke and Ludwig-Muller, 2015, Hruz et al., 2008). PRP synthesis is known to be induced by PAMPs, DAMPs, pathogens effector proteins, and phytohormones, including auxins, abscisic acid, salicylic acids, jasmonic acid, and ethylene (Carvalho Ade and Gomes, 2007, Hruz et al., 2008, Julke and Ludwig-Muller, 2015, Gao et al., 2016).

LTP proteins have been assessed to have multiple roles in plant responses to biotic and abiotic stress and play a role in plant defense (Jung et al., 2003), usually supporting disease resistance and overcoming stress. Several proteins were annotated as LTPs and putative LTPs, and their complete biological functions are yet to be characterized. Several studies report that expression of *LTP* genes is elevated in response to pathogen infection such as the oomycete *Phytophthora nicotianae*, the bacterial pathogens, *Pseudomonas syringae* pv. *tabaci*. and *Xanthomonas campestris* pv. *vescatoria*, and the viral pathogen, pepper mosaic mottle virus. This overexpression of *LTP* genes appears to be associated with increased resistance against pathogens and reduced severity of symptoms. However, which of the many LTP homologs are involved in defense responses against pathogens is unknown (Patkar and Chattoo, 2006, Jung et al., 2003, Julke and Ludwig-Muller, 2015, Sarowar et al., 2009). Importantly, (Sohal et al., 1999) reported that CaMV infection induced the increased expression of an *LTP* gene in Arabidopsis. Perhaps P6 functions during infection to counter this response by downregulating the expression of *LTP* genes, such as *LTP4* and *LTP3*. Moreover, it is consistent with the previous finding (Love et al., 2012, Love et al., 2007b) that transgenic Arabidopsis expressing P6 show increased susceptibility to infection by *Pseudomonas syringae*.

ICS2 encodes the enzyme isochorismate synthase, a key component of the chloroplastic (*ICS2*) pathway, the most important contributor to SA biosynthesis. As such it is required for both local and systemic acquired resistance (LAR and SAR) and

multiple aspects of plant defense (Garcion et al., 2008, Pokotylo et al., 2019). The downregulation of *ICS2* expression might be associated with the suppression of defense against a range of biotrophic pathogens and viruses due to its impact on SA biosynthesis, thereby suppressing SA-dependent responses. Previously, Arabidopsis overexpressing LTP3 displayed downregulation of SA-related genes, particularly the *ICS1* gene, which encodes enzyme isochorismate synthase and contributes to the SA biosynthesis (Gao et al., 2016, Garcion et al., 2008). The *ICS1* was not identified in the RNA-seq data here; however, it is possible that the downregulation of *ICS1* has not been detected because of the low level of P6WT transgene expression. A future study needs to be carried out to determine if the LTP3 also modulates the ICS2 expression. The downregulation of *ICS2* expression in the P6(WT) transgenic plants is therefore entirely consistent with the hypothesis that P6 plays a key role in suppressing defense against biotrophic pathogens, presumably by modifying SA and JA/ET signalling pathways (Leisner and Schoelz, 2018, Laird et al., 2013, Love et al., 2012). This also supports the previous findings that P6 increased host susceptibility to bacterial infection and enhanced the resistance against necrotrophic pathogens and insects (Leisner and Schoelz, 2018, Love et al., 2012).

Cyclic nucleotide-gated channel 19 (*CNGC19*) has been shown to mediate responses to herbivores by modifying both JA/ET and SA signalling pathways (Moeder et al., 2011). This is consistent with several reports that P6 increases host resistance to necrotrophic pathogens (by enhancing JA-dependent defense responses) and increases the host susceptibility to biotrophic pathogens by suppressing SA-responsive defense signalling (Leisner and Schoelz, 2018, Laird et al., 2013, Love et al., 2012).

BGL2 (also known as *PR2)* encodes 1,3-beta-glucosidase and has been used extensively as a marker for SA-dependent host responses enacted via the NPR1-dependent pathway, in particular SAR (Thibaud et al., 2004, Kong et al., 2020, Pokotylo et al., 2019). The SA response was found to depend on NPR1, a key transcriptional regulator of SA and JA responses. NPR1 has been shown to bind directly to SA (Wu et al., 2012), and SA was found to facilitate monomerization of NPR1 by inducing redox changes. The monomeric form of NPR1 modulates PR gene expression, i.e.,

modulates the plant defense responses (Jin et al., 2018, Zhang et al., 2021, Jayakannan et al., 2015). During CaMV infection, expression of reactive oxygen species genes, SA, and ET responsive genes will be modulated in Arabidopsis. Several SA-responsive genes, *PR-1* and *BGL2* have been found to be up-regulated during CaMV infection (Love et al., 2007b, Pokotylo et al., 2019). Love et al (2012) previously demonstrated that the increased expression of *PR2* in response to SA treatment is suppressed in P6 transgenic Arabidopsis; the RNA-seq identification of *BGL2* as an important down-regulated gene is consistent with this. Love et al (2012) also provided evidence that the P6-dependent suppression of SA-mediated defense appeared to involve modification of the central regulator NPR1 (Thibaud et al., 2004, Zhang et al., 2021). Both *npr1* mutant Arabidopsis and P6WT transgenic Arabidopsis displayed similar phenotypes, in which susceptibility to both virulent and avirulent *P. syringae* strains were enhanced, and *PR-1* and *BGL2* expression levels were down-regulated (Zhang et al., 2021, Love et al., 2012, Thibaud et al., 2004, Pieterse and Van Loon, 2004). Nevertheless, some of the SA responses are independent of NPR1, suggesting that NPR1 is not the only SA-binding protein (Pokotylo et al., 2019), and the plant has more than one way to regulate SA biosynthesis and responses. This fits with the RNA-seq data identifying *ICS2* and *LTP3* as down-regulated, and there is evidence for SA biosynthesis being itself regulated by a feedback loop involving NPR1 (Garcion et al., 2008, Love et al., 2012, Jayakannan et al., 2015, Nagashima et al., 2014, Kong et al., 2020, Gao et al., 2016, Zhang et al., 2021, Thibaud et al., 2004, Pieterse and Van Loon, 2004) The suppression of *PR2* may promote LR development, i.e., auxin-activated signalling and also, associated with the abscisic acid response, systemic acquired resistance, and defense against fungi (Oide et al., 2013, Kong et al., 2020, Zhang et al., 2020, Love et al., 2012). It is interesting that all these genes were found to contribute to the biosynthesis of SA and modulate SA responses. Many of these genes also modulate other hormonal pathways such as ABA and JA/ET, which means they interfere with the JA response. Downregulation of these genes may lead to suppression of SAR. These findings support the previous proposal (Leisner and Schoelz, 2018, Laird et al., 2013, Love et al., 2012, Love et al., 2007a) that P6 manipulates the plants' defenses, making them more susceptible to be infected by SA sensitive pathogens, such as biotrophic pathogens, and enhancing the resistance to JA sensitive pathogens,

such as necrotrophic pathogens, by modifying the SA and JA/ET signalling pathways, i.e., suppressing the SA responses and enhancing the JA/ET response. Salicylic acid is a crucial phytohormone for plant virus defense response. It was found form the DEGs results that P6 was able to suppress genes involved in the SA pathway, which will facilitate the infection by the virus or biotrophic pathogens like P. syringae (Love et al., 2012) and alter the JA/ET pathway genes; with the SA and JA/ET mediated defense pathways are commonly antagonistic (Derksen et al., 2013, Oka et al., 2013). Further confirmation needs to be carried out by challenging the new transgenic lines with different bacteria, fungi, and insects, etc.

Proto-oncogene tyrosine-protein kinase ROS (*ROS1*) is considered to be responsible for DNA demethylation, a repressor of transcriptional gene silencing, and responsiveness of SA-dependent defense genes. Mutant plants with *ros1* gene knockdown were more susceptible to infection by obligate biotrophic oomycete *Hyaloperonospora arabidopsidis* (Hpa) than wildtype and constrained *PR-1* gene expression, i.e., they showed repressed SA-dependent defenses. Also, ROS1 enhanced resistance to the necrotrophic pathogens *Plectosphaerella cucumerina* in an independent manner of JA-responsive gene expression (López Sánchez et al., 2016, Liping et al., 2021). ROS1 will increase the ABA-responsive genes expression level (Kim et al., 2019). In addition, *ROS1* is associated with the activation of several downstream signalling pathways connected to cell differentiation, proliferation, growth, and metabolism. One of the critical pathways is the PI3 kinase-mTOR signalling pathway, which plays a vital role in regulating signal transduction and biological processes (Charest et al., 2006, Zeng et al., 2000, Le et al., 2014, Bharti et al., 2015, Liping et al., 2021). This outcome supports the model in which P6 modulates plant defense responses against pathogens via phytohormones signalling, including the SA and ABA responses.

Endothelial cell-specific molecule 1 (*ESM1*) contributes to the defense response against bacteria, and insects. It is also considered a positive regulator of cell proliferation (Burow et al., 2008, Sato et al., 2019). Cysteine-rich receptor-like protein kinase 37 (*CRK37*) is involved in protein phosphorylation, associated with plant defense

responses (Yeh et al., 2015). These genes were directly or indirectly linked to modulating plant signalling pathways and defense responses. Moreover, the indirectly regulation might participate in a decrease in plant ethylene sensitivity. Subsequently, the expression of several genes associated with the ABA signalling pathway is modulated by P6 expression. The ABA pathway is documented to crosstalk with the JA and SA pathways and is also known to participate in plant defense responses against pathogens sensitive to JA defense response, fungi. Further investigations need to be carried out to determine the impact of P6 on the ABA signalling pathway and how that relates to the plant responses and developed phenotypes. Plant phosphorylation cellular states, responses to abiotic factors, and plant development will be affected by the modulation of phytohormonal signalling pathways, ABA, SA, and JA/ET signalling pathways. They might participate in the developed phenotypes found earlier, increasing the plant resistance to auxin transport inhibitor, and decreasing plant ethylene precursor's sensitivity.

Several additional genes that were down-regulated in plants expressing P6WT have been identified as encoding proteins associated with other cellular responses and metabolic processes. The MD-2-related lipid-recognition protein (ROSY1) has been shown to play a role in gravitropic response and basipetal auxin transport in plant roots (Dalal et al., 2016). This might aid support to the plant to resist the auxin transport inhibitor. Thalianol synthase 1 (*THAS1*) is recognized to play a role in responses to light stimulus and gravity, root development, and the thalianol biosynthesis process (Nutzmann and Osbourn, 2015, Field et al., 2011). Probable apyrase 5 (*APY5*) primary role is dephosphorylation and suggested to participate in Arabidopsis growth regulation (Thomas et al., 1999, Wu et al., 2007). The *AT4_1* plays a role in the cellular response to phosphate and expressed in response to phosphate starvation protein (Shin et al., 2006). These two genes might indicate that the P6 modulates the cellular phosphate state. This also means P6 modifies the cellular signalling pathways that certainly may require phosphorylation. Cytochrome P450 708A2 (*CYP708A2*) is involved in the thalianol pathway, brassinosteroid biosynthetic process, and multicellular organism development. Also, a potential role in the crosstalk between abiotic and biotic stress responses has been suggested. Still, more pieces of evidence are needed to confirm

this role (Pandian et al., 2020, Field and Osbourn, 2008). Modulating the expression of CYP708A2 might also support the P6 impact on plant growth and plant responses to pathogens, including viruses. 4-aminobutyrate aminotransferase (*PYD4*) has been shown to involve in the cellular response to nitrogen levels (Parthasarathy et al., 2019, Liepman and Olsen, 2003). Protein PLANT CADMIUM RESISTANCE 1 (*PCR1*) plays a vital role in the resistance to the toxic effects of Cd. It is also linked to responses to abscisic acid, bacteria, fungi, and SA signalling pathway regulation (Song et al., 2004, Zeng et al., 2017, Ascencio-Ibáñez et al., 2008, Du et al., 2009).

Overall, these observations of the impact of P6 on modulating different phytohormonal signalling pathways, ABA, SA, and JA/ET signalling pathway, support that P6 expression will modify the host to be more susceptible to SA sensitive pathogens such as bacteria, biotrophs, and increases the resistance against JA sensitive pathogens such as insects and fungi, necrotrophs. The findings here suggest that P6 protein, even at low levels of expression, substantially impacts the expression of genes involved in a variety of plant responses, in particular genes related to the signalling pathways and defense against pathogens. P6 suppressed genes were also involved in other signalling pathways and stress responses, which might negatively affect plant performance against pathogen and stress. Consequently, P6 might indirectly alter the plant's behavior and might support the increase in CaMV and biotrophic pathogens' susceptibility (Love et al., 2012, Wu and Ye, 2020). This is supported by modifying the gene expression profile of genes with biological functions related to plant performance, including phosphorylation, phytohormonal signalling, defense response, biological processes, cell proliferation, and cell differentiation.

6.5.2. The impact of P6(ΔTOR)-GFP on Arabidopsis gene expression

Like the previous PCA comparison, the comparison between pER8-P6(ΔTOR)-GFP and Col-0 was able to differentiate 70% of the variance in plant responses, i.e., phytohormonal signalling responses (Figure 6.2), and the 20 genes showing the most statistically significant difference in the expression (Table 6.5) have been identified. These genes are also found to have biological functions related to growth, cell shape

regulation, defense response, signalling, metabolism, and cell proliferation activation. There were 12 genes up-regulated, and 8 genes were down-regulated (Table 6.6). Out of the 20 genes with the most statistically significant changes in expression level, four genes (*LTP4*, *LTP3*, *NRT2.6*, and *CYP708A2*) were also identified in the top 20 most statistically significant candidates from the previous comparison (P6WT vs. Col-0). Like the P6WT-GFP, P6(ΔTOR)-GFP expression led to up-regulation of the *NRT2.6* expression and downregulation of the *LTP4*, *LTP3*, and *CYP708A2* expression. This is evidence that for these, the TOR binding domain deletion has no apparent effect on their expression, and these responses must be regulated by a different P6 domain.

No	Gene Code	SA	JA/ET	ABA	Aux	GB	Biological function
1	*NPC3*				Associated with auxin signalling responses		mediates brassinolide signalling
2	*SRK2I*			modulates ABA		modulates GB	plays a role in directing protein phosphorylation.
3	***CYP82C3***						role in defense responses against pathogens sensitive to JA, cell redox homeostasis, and cellular response to oxidative stress
4	***TIP2-3***						transport of water and small urea
5	*GSTF14*						plant detoxification
6	*LTP3*	a negative SA regulator and		increased endogenous ABA levels			PR-14 pathogenesis-related protein (PRP) family
7	***PER4***				auxin catabolism		Wounding, pathogen attack, and oxidative stress. cell redox homeostasis and cellular response to oxidative stress
8	***PRXIID***						cell redox homeostasis and cellular response to oxidative stress
9	*LTP4*				increased endogenous ABA levels		PR-14 pathogenesis-related protein (PRP) family
10	***NRT2.6***						cellular response to nitrate
11	*COR15B*				abscisic acid signalling		play a role in weaken plant defense and leaf senescence

12	***MRN1***			triterpenoid biosynthetic process
13	***CYP71B21***			cell redox homeostasis and cellular response to oxidative stress
14	***PCR9***			a role in resistance to the toxic effect of Cd
15	*PCC1*	Regulating SA	Regulating ABA	modulating Plant responses against bacteria and fungi
16	*CYP708A2*			brassinosteroid biosynthetic process
17	***LECRK31***			promotes plant defense responses against bacteria and oomycetes
18	***PER37***			cell redox homeostasis and cellular response to oxidative stress
19	***CYP72A14***			cell redox homeostasis and cellular response to oxidative stress
20	***PMEI12***			contributes to resistance against pathogens, particularly necrotrophic pathogens

Table 6.13. The biological function of the top 20 most statistically significant differentially expressed gene transcripts in the pER8-P6(∆TOR)-GFP line compared to Col-0. Salicylic acid pathway (SA), jasmonic acid ethylene pathway (JA/ET), abscisic acid pathway (ABA), auxin pathway (AUX), and gibberellin pathway (GB). The bolded genes in the table represent the up-regulated genes between the two lines.

In the P6(∆TOR)-GFP expressing line, 12 of the top 20 genes *CYP82C3*, *TIP2-3*, *PER4*, *PRXIID*, *NRT2.6*, *MRN1*, *CYP71B21*, *PCR9*, *LECRK31*, *PER37*, *CYP72A14*, and *PMEI12* were up-regulated. Out of these genes, *PMEI12*, *LECRK31*, *PCR9*, *PER4*, and *CYP82C3* were identified in contributing to plant responses against biotic and abiotic stress. Pectinesterase inhibitor 12 (*PMEI12*) contributes to resistance against pathogens, particularly necrotrophic pathogens (Marzin et al., 2016, Lionetti et al., 2007). Probable inactive L-type lectin-domain containing receptor kinase III.1 (*LECRK31*) promotes plant defense responses against bacteria and oomycetes. Additionally, it modulates protein phosphorylation (Wang and Bouwmeester, 2017,

Eggermont et al., 2017). Similarly, TOR will promote the plant responses against biotic and abiotic stress; it would be interesting to test if deletion of the TOR binding domain will affect the elevated resistance against necrotrophic pathogens observed in plants expressing the native form of P6, i.e., P6-TOR interaction might responsible for this phenomena (Leisner and Schoelz, 2018, Laird et al., 2013, Love et al., 2012). The protein PLANT CADMIUM RESISTANCE 9 (*PCR9*) has been identified as having an important role in resistance to the toxic effect of Cd (Song et al., 2004). Peroxidase 4 (*PER4*) has been identified as having a similar role to *PER69*. They are both involved in responses to stresses such as wounding, oxidative stress, pathogen attack, and auxin catabolism (Fernández-Pérez et al., 2015, Yang et al., 2011a). These findings provide an explanation for the increase in resistance to the auxin transport inhibitor TIBA, demonstrated in chapter 4. Cytochrome P450 82C3 (*CYP82C3*), which was up-regulated in the transgenic plants, has previously been identified as playing a role in defense responses against pathogens sensitive to JA defense responses (Liu et al., 2010) and has shown oxidoreductase activity. Significantly, it has been identified as a reporter gene induced by the flagellin peptide flg22, which is a classic elicitor of basal defense responses and PAMP-triggered immunity (Czarnecka et al., 2012, Zipfel et al., 2004). Several of the genes that were identified participate in cellular responses and metabolic processes. In particular, Peroxidase 37 (*PER37*), Cytochrome P450 72A14 (*CYP72A14*), Cytochrome P450 71B21 (*CYP71B21*), Peroxiredoxin-2D (*PRXIID*), Cytochrome P450 82C3 (*CYP82C3*), and Peroxidase 4 (*PER4*) genes play a role in cell redox homeostasis and cellular response to oxidative stress. Besides *CYP82C3* and *PER4* role in responses to oxidative stress, they also participate in defense responses against pathogens (Fernández-Pérez et al., 2015, Yang et al., 2011a, Czarnecka et al., 2012, Zipfel et al., 2004, Ramírez et al., 2011, Pandian et al., 2020). As mentioned earlier, the High-affinity nitrate transporter 2.6 (*NRT2.6*) contributes to nitrate's cellular response (Dechorgnat et al., 2012). Aquaporin TIP1-3 (*TIP2-3*) facilitates the transport of water and small urea across cell membranes in Arabidopsis (Soto et al., 2008). Marneral synthase (*MRN1*) plays a crucial role in Arabidopsis growth and development via its association with the triterpenoid biosynthetic process (Go et al., 2012, Field et al., 2011).

Eight down-regulated genes were *NPC3, SRK2I, GSTF14, COR15B*, *PCC1*, *LTP4*, *LTP3*, and *CYP708A2* were associated with the P6(ΔTOR)-GFP expressing line. The non-specific phospholipase C3 (*NPC3*) has phosphatase activity and mediates brassinolide signalling (Wimalasekera et al., 2010). It is known that the cross-talk between auxin (Aux) and brassinosteroid (BR) pathways regulate diverse plant developmental and physiological processes (Durbak et al., 2012, Depuydt and Hardtke, 2011). The modulation of the brassinosteroid signalling pathway by NPC3 might result in modification of auxin signalling responses. Another protein, serine/threonine-protein kinase SRK2I (*SRK2I*) plays a role in directing protein phosphorylation and modulating the abscisic acid and gibberellin signalling pathway (Shinozawa et al., 2019). Glutathione S-transferase F14 (*GSTF14*) is involved in the metabolic process of glutathione and plant detoxification. Additionally, it is considered to be a gene responsive to stress conditions such as drought, salinity, cold, and heat (Islam et al., 2019a, Pégeot et al., 2014). Protein COLD-REGULATED 15B, chloroplastic (*COR15B*) contributes to the modulation of abscisic acid signalling and leaf senescence (Yang et al., 2011b). In general, the *COR* genes expression increases during compatible infection and abiotic stress such as nutrient loss and drought. *COR15B* expression was induced during fungal infection and suggested to be associated with lowering plant defenses (Huibers et al., 2009, Yang et al., 2011b). More studied needs to be carried out to determine the exact role of *COR15B* during infections and disease susceptibility. Furthermore, it was found to increase the freezing tolerance of Arabidopsis (Thalhammer and Hincha, 2014). PATHOGEN AND CIRCADIAN CONTROLLED 1 (*PCC1*) plays a role in regulating the SA signalling pathway, circadian signalling pathway, and abscisic acid signalling pathway. Additionally, it is involved in modulating Plant responses against bacteria and fungi, increasing the resistance against virulent oomycetes (Sauerbrunn and Schlaich, 2004). Consistent with the P6WT-GFP expressing line, the *LTP4*, *LTP3*, and *CYP708A2* expression were down-regulated. As mentioned earlier, both *LTP4* and *LTP3* contribute to lipid transportation and abscisic acid responses (Julke and Ludwig-Muller, 2015), where *CYP708A2* is involved in plant development, brassinosteroid synthesis, and thalianol pathway (Pandian et al., 2020, Field and Osbourn, 2008). Zvereva (2016) identified the suppression of PTI as a phenotype associated with P6-transgenic plants and showed that this was dependent

TOR binding. The RNA-seq data of the P6(ΔTOR)-GFP expressing line indicated that several genes associated with defense responses were up-regulated, suggesting that the deletion of the TOR domain might not only results in weakening the suppression ability of P6, but it might also convert P6 into a protein that induces rather than suppresses defense responses.

Interestingly, lines expressing either native or mutant forms of P6 had an effect in modulating genes that regulate abscisic acid (ABA) responses. ABA responses are known be associated with defense responses against some pathogens. Also, found to significantly increase the resistance against pathogens sensitive to JA defense response. This also supports the idea that P6 might indirectly modulate the SA and JA/ET signalling pathways via modulating the ABA signalling, i.e., phytohormonal crosstalk. Indeed, the ABA signalling pathway is known to synchronize with SA and JA/ET signalling pathways, in which mainly ABA and JA/ET act synergistically to modulates plant responses against biotic and abiotic tress while antagonist with SA (Derksen et al., 2013, Robert-Seilaniantz et al., 2011, Durbak et al., 2012, Depuydt and Hardtke, 2011, Kong et al., 2020, Islam et al., 2019b, Collum and Culver, 2016, Liu and Timko, 2021)

The 20 most statistically significant genes differentially expressed in the P6(ΔTOR)-GFP lines comprised fewer down-regulated genes than the lines expressing P6WT-GFP. These results may possibly suggest that deletion of the P6 TOR binding domain profoundly alters the ability of P6 to regulate host gene expression. In particular, the deletion mutant loses the ability to suppress the expression of many important genes involved in plant defense responses and phytohormone signalling. This evidence emphasizes the critical role of TOR binding during CaMV infection. Nevertheless, the deletion of the TOR binding domain did not fully abolish the ability to regulate plant gene expression. Some host genes must be regulated independently of the TOR-dependent pathways and involve a different P6 domain.

6.5.3. Differences between the impact of P6WT-GFP and P6(ΔTOR)-GFP on Arabidopsis gene expression

Like the previous PCA comparison, the comparison between pER8- P6WT-GFP and pER8-P6(ΔTOR)-GFP was able to differentiate 62% of the variance in plant responses, i.e., phytohormonal signalling responses (Figure 6.3). The 20 most significantly differentially expressed genes (Table 6.7). These genes were also found to have biological functions related to cellular development and response, i.e., growth, cell shape regulation, defense response, signalling, metabolism, and cell proliferation activation. This comparison provided us with more insight into the P6 TOR binding domain's important role in regulating plant gene expression. However, when carrying out this comparison, it must be kept into consideration that pER8-P6WT-GFP had a much lower transgene expression than pER8-P6(ΔTOR)-GFP, making interpretation of differences very difficult. Further RNA-seq analysis will need to be carried to repeat the experiments.

Based on the results from the experiments above, a number of genes had lower apparent levels of expression in the P6WT expressing line than the P6(ΔTOR)-GFP expressing line. There were 3 genes that were more abundant, and 17 genes were less abundant in the P6WT than in the P6(ΔTOR) line (Table 6.8). The deletion of the P6 TOR binding domain might constrain the ability of P6 to regulate the expression of some genes, especially genes involved in phytohormonal signalling and defense responses (Table 6.7). When compared to non-transgenic controls, the patterns of gene expression in plants expressing P6WT and P6(ΔTOR) were very different (Table 6.4 and 6.5), highlighting the TOR binding domain role in regulating plant gene expression and possible involvement in facilitating CaMV infection and manipulating plant responses. The differences observed in the comparison between the two transgenic lines would tend to support this observation.

However, the difference in gene expression profiles between the two transgenic lines might equally be attributable to differences in the transgene expression level between the P6WT and P6(ΔTOR) lines. These uncertainties will only be resolved following a repeat RNA-seq experiment in which transgene expression levels between lines are equivalent. Nevertheless, the outcomes here provide a valuable indication of the genes

that might be worth for further examination and identify marker genes that can be used in the future for CaMV and P6 related studies.

No	Gene Code	SA	JA/ET	ABA	Aux	GB	Biological function
1	***NPC3***				Associated with auxin signalling responses		mediates brassinolide signalling
2	***SRK2I***			modulates ABA signalling pathways		modulates GB signalling pathways	plays a role in directing protein phosphorylation.
3	***LBD26***						unknown Suggested response to pathogens and nitrogen metabolisms
4	*CYP82C3*						regulation role in the cellular response to oxidative stress and associated with defense responses
5	*DIR5*						synthesis of (-) pinoresinol
6	*PDF1.2B*		modulates JA/ET signalling pathways				dependent systemic resistance, defense response to insect, fungus, and bacteria
7	*PDF1.2C*		modulates JA/ET signalling pathways				ethylene-dependent systemic resistance, defense response to insect, fungus, and bacteria
8	*PAP20*						phosphatase activity
9	*CCOAMT*						Mediates lignin biosynthetic pathway
10	*VQ29*						negative regulator of basal defenses
11	*CNGC19*	Mediates SA signalling pathways	Mediates JA/ET signalling pathways				responses to herbivores by modifying both JA/ET and SA signalling pathways
12	*NHL10*						response to viruses
13	*PDF1.1*		modulates JA/ET				ethylene-dependent systemic resistance, defense response to insect, fungus, and bacteria

14	*NHL25*			Defense responses against bacteria, oomycetes, and viruses
15	*CYP710A1*			sterol biosynthesis and oxidoreductase activity
16	*PDF1.2A*	modulates JA/ET, a marker gene for JA/ET		ethylene-dependent systemic resistance, defense response to insect, fungus, and bacteria
17	*CYP715A1*			oxidoreductase activity
18	*PI4KG3*		Associated with ABA signalling pathways	plant tolerance upon abiotic stress,
19	*WAKL16*			Suggested to play a role in plant growth and development
20	*PRXIID*			cell redox homeostasis and cellular response to oxidative stress

Table 6.14. The biological function of the top 20 most statistically significant differentially expressed gene transcripts in the pER8-P6WT-GFP line compared to pER8-P6(∆TOR)-GFP. Salicylic acid pathway (SA), jasmonic acid ethylene pathway (JA/ET), abscisic acid pathway (ABA), auxin pathway (AUX), and gibberellin pathway (GB). The bolded genes in the table represent the up-regulated genes between the two lines.

Out of the 20 genes with the most significant differences in expression, three gene transcripts (*NPC3*, *SRK2I*, and *LBD26*) were more abundant in the P6WT than in the P6(∆TOR) lines. As mentioned earlier, *SRK2I* regulates protein phosphorylation, the abscisic acid signalling pathway, and the gibberellin signalling pathway, whereas *LBD26* is a transcription factor suspected of participating in plant development and response to pathogens (Shinozawa et al., 2019, Grimplet et al., 2017). The *NPC3* was shown to have phosphatase activity and to mediate brassinolide signalling (Wimalasekera et al., 2010). These genes support the suggestion that P6 directly or indirectly modulates phytohormonal signalling pathways, in which modulation might be accomplished through synergistic or antagonistic crosstalk with the other phytohormonal signalling pathways; auxin, SA, and JA/ET.

Remarkably, nine genes out of seventeen genes that were apparently expressed at lower abundance in the P6WT compared to the P6(ΔTOR) lines have all been identified as contributing to plant responses against biotic stress. Of course, because of the differences in the levels of transgene expression between these lines, it is not possible to say whether these apparent differences reflect a role for the TOR binding domain or whether they are regulated independently of TOR binding and differences are attributable to the much higher levels of transgene expression in the P6(ΔTOR). In either case, these results would suggest that the expression of these genes is regulated by P6 in some way.

Four genes belonging to the plant defensins family were amongst the genes whose expression was apparently differentially expressed. Plant defensins contribute significantly to defense against pathogens and participate in mediating signalling pathways and plant growth. The plant defensin 1.1 (*PDF1.1*), plant defensin 1.2a (*PDF1.2A*), plant defensin 1.2c (*PDF1.2C*), and Putative plant defensin 1.2b (*PDF1.2B*) confer broad-spectrum resistance to pathogens, predominantly involved in antifungal defenses. Additionally, they modulate JA/ET signalling, ethylene-dependent systemic resistance, and responses to insects and bacteria (Stotz et al., 2009, Parisi et al., 2019, Sathoff and Samac, 2018, Lacerda et al., 2014, Sher Khan et al., 2019, De Coninck et al., 2010). The *PDF1.2A* gene is not limited to defense responses; it is considered a marker gene for the JA/ET signalling pathway (De Coninck et al., 2010). Roberts et al (2007) identified the plant defensin gene *PDF1.2* as being down-regulated in CaMV-infected leaves of Arabidopsis providing direct evidence of a possible role for plant defensins in responses to CaMV infection.

The VQ motif-containing protein 29 (*VQ29*) acts as a negative regulator of flowering transition, seedling light-mediated development, photomorphogenesis, and basal defenses. Interestingly, it is induced in early Arabidopsis roots infection and constrains pathogen development independently of plant defenses relating to SA and JA/ET-dependent signalling pathways (Le Berre et al., 2017, Li et al., 2014b, Jing and Lin, 2015). In contrast, the overexpression of *VQ29* will promote negative regulation of Arabidopsis defense response against *Botrytis cinerea*; hence, it increases Arabidopsis

susceptibility to *B. cinerea* (Wang et al., 2015). Next, as stated prior *CNGC19* mediates both JA/ET and SA signalling pathways and response to herbivores. The NDR1/HIN1-like protein 10 (*NHL10*) promotes defense response to viruses, in particular, hypersensitive response (HR) triggered by the exposure to an avirulent *Cucumber mosaic virus* (CMV). Remarkably *NHL10* expression during CMV exposure is independent of the SA pathway (Zheng et al., 2004). NDR1/HIN1-like 25 (*NHL25*) has one or more potential roles in plant resistance, in which *NHL25* expression is induced by avirulent pathogens (incompatible interaction) such as bacteria, oomycetes, and viruses. Unlike NHL10, the SA signalling pathway mediates the expression of *NHL25* (Varet et al., 2002). From previous findings (Love et al., 2012, Love et al., 2007a) that P6 suppressed the SA responses and enhanced the JA/ET responses and along with the ethylene triple response assay results in chapter 3 and 4, it can be suggested that these responses are modulated through mediating the expression of these defense genes.

Eight out of seventeen apparently differentially expressed genes were participants in cellular responses and metabolic processes. Both *PRXIID* and *CYP82C3* genes demonstrated a regulation role in the cellular response to oxidative stress. Also, *CYP82C3* is associated with responses to pathogens (Pandian et al., 2020, Yang et al., 2011a). Both CYTOCHROME P450, FAMILY 715, SUBFAMILY A, POLYPEPTIDE1 (*CYP715A1*), and Cytochrome P450 710A1 (*CYP710A1*) established a role in the oxidation-reduction process and has oxidoreductase activity. The *CYP710A1* alone has proven to participate in sterol biosynthesis (Arnqvist et al., 2008, Pandian et al., 2020). The Disease resistance-responsive (dirigent-like protein) family protein (DIR5) is involved in the synthesis of (-) pinoresinol and is suspected to be associated with defense responses against oomycetes but not confirmed yet (Kim et al., 2012, Chen et al., 2018). In general, dirigent proteins are known to participate in plant responses against biotic and abiotic stress(Kim et al., 2012, Chen et al., 2018). Also demonstrated a stereospecific synthesis activity, in which they control the biosynthesis of natural plant products via regioselectivity and stereoselectivity (Kim et al., 2012).The Purple acid phosphatase (*PAP20*) is implied to play a dynamic role in plant adaptation to phosphorus (P) deficiency and have phosphatase activity, i.e.,

protein phosphorylation (Ashykhmina et al., 2019, Feder et al., 2020, Wang et al., 2014). Phosphatidylinositol 4-kinase gamma 3 (*PI4KG3*) elevates the plant tolerance upon abiotic stress, i.e., salt stress tolerance. Furthermore, it participates in the regulation of floral transition and response to abscisic acid. Also, it possesses a protein phosphorylation activity (Akhter et al., 2016). The function of Putative wall-associated receptor kinase-like 16 (*WAKL16*) is yet to be documented. It was implied that it has phosphorylation activity and plays a role in plant growth and development (Kanneganti and Gupta, 2008). The Caffeoyl-CoA 3-O-methyltransferase (*CCOAMT*) has methyltransferase activity, in which it mediates methylation reaction in the lignin biosynthetic pathway (Guo et al., 2001, Zhong et al., 2000).

These findings suggest that P6 may be important in regulating the expression of these genes, although it is not possible to say whether this involves the TOR binding domain. However, the identification of genes regulating the JA/ET signalling pathways is consistent with the ethylene triple response assay results reported in chapter 4, in which Arabidopsis plants expressing P6WT became less sensitive to ethylene precursor.

Furthermore, the P6 impact on the regulation of gene expression expanded our understanding of the role of P6 in manipulating plant responses, including the documented increase in the host resistance against pathogens sensitive to JA defense response while increases the host susceptibility to pathogens sensitive to SA defense response. P6WT was found to modulates the expression of genes involved directly and indirectly regulating SA and JA/ET signalling pathways. P6 with intact TOR binding domain showed a higher expression suppression ability upon genes involved in the plant defense responses, phytohormones signalling pathways, and stress responses. Thus, the deletion of the TOR binding domain did not abolish the ability to regulate different gene expression, including the expression of some genes involved in the phytohormones signalling pathways and stress responses, which indicate they are not regulated in TOR binding domain manner. Taking all these together shows that P6 acts pathogenicity effector and plant gene expression regulator.

6.6. Conclusion for the three comparisons

Overall, the 20 most statistically significant differentially expressed gene transcripts were found for pER8-P6WT-GFP comparisons, which confirmed their importance to plant responses, signalling pathways, and growth. These genes all could serve as biomarkers of P6WT and P6(ΔTOR) expression in Arabidopsis and perhaps as well other plant hosts. The findings represented convincing evidence of P6 modulation of phosphorylation cellular status, phytohormonal signalling pathways, defense responses, and plant growth relative to wild-type plants. Such findings reveal a potential mechanism by which phytohormonal signalling is affected, suggesting that those affected may be less healthy, weaken the defense responses against pathogens, and under abiotic stress leading to the modification of host responses observed here. Running the DAVID Functional Classification Tool on the top 20 most statistically significant differentially expressed gene transcripts classified DEGs lists of each comparison, i.e., pER8-P6WT-GFP versus Col-0, pER8-P6(ΔTOR)-GFP versus Col-0, and pER8-P6WT-GFP versus pER8-P6(ΔTOR)-GFP revealed functional groups (Table 6.9, 6.10, and 6.11). The gene members in these groups share a commonality in biological function related to plant performance, including regulatory functions such as phosphorylation, phytohormonal signalling, defense response, biological processes associated with the plasma membrane, cell proliferation, and cell differentiation. These major pathways are highlighted above as an overview of the key biomarkers' functions shared between the ranked gene lists. The gene expression data support the hormonal modulation response results, in which several genes differ in their expression, down/up-regulation, between the lines due to the expression of P6 and the presence of functional P6 TOR binding domain. Expectedly, genes involved with phytohormonal signalling pathways, phosphorylation, defense responses, and biosynthesis were identified. Phytohormonal signalling is capable of controlling plant development (proliferation and differentiation of plant cells), metabolism and defense responses. Also, it was demonstrated that there is extensive interaction between the different phytohormone pathways that take place to regulate responses to abiotic and biotic factors (Depuydt and Hardtke, 2011, Song et al., 2014, Derksen et al., 2013). Therefore, phytohormonal signalling pathways also may be important for promoting the phenotypes observed

earlier. The transcriptome sequencing data indicated that P6 should be recognized as an important phytohormonal regulator rather than simply only considered a pathogenicity effector that suppresses innate immunity. Here, we uncovered that P6 regulated many genes, and several of these genes were associated with SA, JA/ET, ABA GB, and BR pathways. Moreover, modulation of expression of genes that directly regulates plant metabolism, biotic and abiotic stress responses was identified. Furthermore, lines expressing P6, and mutant P6 in TOR binding domain had significantly different gene expression profiles. The P6 expressing line suppressed more genes than the P6 mutant expressing line, mainly genes contributing to the phytohormonal signalling, defense response, and stress response. Remarkably, the P6 TOR binding domain was found to be associated with regulating the expression of several plant genes, including genes involved in phytohormonal signalling, defense response, and stress response. Interestingly, both lines shared similarities in some genes' expression levels, which means their regulation is independent of the presence of functional TOR binding domain, i.e., regulated by different P6 domain. The similarity between the lines was also seen earlier when both lines displayed the same resistance to the auxin transport inhibitor treatment meaning this resistance is provided in a non-TOR binding domain manner. Proteomics and further physiological analyses will expand our understanding of how P6 impacts the plant responses and modulate the phytohormones Signalling pathways. These findings will set the stage for future P6 research aimed to improve plant performance, breed for resistance, and control specific signalling pathways. A further, more detailed analysis of these gene pathways and their shared functions with metabolite pathways must be carried out.

Chapter VII: General Discussion

7.1. General Discussion

Pathogens are known to modulate the host responses to ensure their survival and spread their infection (Islam et al., 2019b, Toruno et al., 2016, Mudgett, 2005). Host modification is well known to be carried by plant pathogens to establish infection, especially by plant viruses. It was found that the viruses hijacked the plant machinery and modulated the plant responses against biotic or abiotic stress. The modification of plant responses is achieved by modulating phytohormone signalling pathways (Islam et al., 2019b, Collum and Culver, 2016, Wu and Ye, 2020, Carr et al., 2020, Ingwell et al., 2012). Plant viruses are well-known pathogens that modulate the host responses using viral proteins (Collum and Culver, 2016, Tungadi et al., 2017, Zhou et al., 2014, Zvereva et al., 2016, Laird et al., 2013, Love et al., 2012, Leisner and Schoelz, 2018). Viral proteins might be involved in modulating one or more of the phytohormonal signalling pathways. The modulation might be carried directly or indirectly due to the phytohormones crosstalk occurrence all the time (Collum and Culver, 2016, Toruno et al., 2016, Leisner and Schoelz, 2018). CaMV encodes P6, a multifunctional protein known to play a significant role during CaMV infection, where it manipulates plant defense responses (Leisner and Schoelz, 2018, Laird et al., 2013, Love et al., 2012, Geri et al., 2004). Previously, it was shown that the transgenic Arabidopsis expressing CaMV P6 was more susceptible to biotrophic pathogens and more resistant to necrotrophic pathogens in which P6 suppressed the SA response and enhanced the JA/ET response (Laird et al., 2013, Love et al., 2012, Love et al., 2007a, Love et al., 2007b, Love et al., 2005, Geri et al., 2004). In this study, the expression impact of both P6WT-GFP and P6(ΔTOR)-GFP was analyzed in Arabidopsis plants against different hormonal treatments and their ability to modulate plant gene expression. Transgenic Arabidopsis expressing P6WT-GFP or P6(ΔTOR)-GFP exhibits the same elevated resistance phenotype upon auxin transport inhibitor treatments. This suggests that the ability of P6 to interact with Auxin signalling does not require the TOR binding domain and is therefore independent of P6-TOR interaction. P6 is a multifunctional protein, and at least 4 different functional domains have been identified with different roles and

interactions with host proteins (Haas et al., 2008, Haas et al., 2005, Schoelz and Leisner, 2017, Hohn and Rothnie, 2013, Schepetilnikov et al., 2011, Schepetilnikov et al., 2013, Angel et al., 2013, Podevin and du Jardin, 2012, Thiebeauld et al., 2009, Laird et al., 2013, Love et al., 2012, Love et al., 2007a, Love et al., 2007b, Roberts et al., 2007). Presumably, the interactions that modulate Auxin signalling in the host may not involve Domain II. In contrast, the ethylene triple response assay shows that although plants expressing P6WT-GFP are significantly less sensitive to ethylene than non-transgenic controls, those expressing P6(ΔTOR)-GFP were closer to Wild Type in their responses., i.e., showed different modulation impacts on the JA/ET signalling pathway and that this modulation is not completely independent of P6-TOR interaction TOR. Therefore, the ability of P6 to interact with the JA/ET-dependent responses may be partially but not completely independent of the interaction with TOR. The data suggest that during CaMV infection in nature, P6 expression modulates both auxin and ethylene signalling pathways and implies TOR-binding of P6 plays a role in modulating some but not all of these plant responses.

The RNA-Seq data shows that P6WT-GFP exhibits a gene expression profile distinct from P6(ΔTOR)-GFP, a protein with a deleted TOR binding domain. These outcomes indicate that P6WT-GFP and P6(ΔTOR)-GFP differ regarding their impact on Arabidopsis genes expression profile and phenotypes. It underlines the P6 TOR binding domain's critical role in regulating plant responses during CaMV infection, and its deletion will alter the plant gene expression profile. However, it also demonstrates that even in the absence of the TOR binding domain, expression of P6 from a transgene has an extensive and wide-range impact on patterns of host transcript abundance. This is consistent with the finding that the impact of P6 expression on responses to TIBA is at least partially independent of the presence of the TOR binding domain. The P6(ΔTOR)-GFP and Col-0 comparison identified a number of genes identified as involved in the SA pathway, ET pathway, and other phytohormonal pathways such as ABA and GB. This indicated that these genes are regulated independently of the TOR binding domain and involve a different P6 domain. In contrast, the major class of genes identified in the P6WT-GFP and Col-0 comparison were those involved in SA-mediated or similar defense responses and were down-regulated, consistent with the known role

of the P6-TOR interaction identified previously (Leisner and Schoelz, 2018, Schepetilnikov et al., 2011, Lukhovitskaya and Ryabova, 2019)

Transcriptional analyses of plants expressing P6 expression suggest that P6 modulates plant responses against both biotic and abiotic stresses, including responses to environmental stress and defense responses against pathogens. P6 particularly altered the expression of genes involved in phytohormonal signalling pathways, phosphorylation, and defense responses (Figure 7.1). These effects could involve direct modification to the expression of genes directly involved in specific pathways or related genes or indirectly by regulating other genes that affect downstream the pathways (Leisner and Schoelz, 2018, Kong et al., 2020, Collum and Culver, 2016, Derksen et al., 2013), i.e., P6 can directly or indirectly modulate plant responses. Changes in gene expression in P6-transgenic plants involved up-regulation as well as down-regulation, including some genes that are involved in plant defense responses. This might be because P6 was unable to suppress them, or P6 elevates their expression.

These findings agree well with the proposal that P6 acts as a pathogenicity effector and regulates phytohormonal signalling pathways, including those involving SA and JA/ET (Leisner and Schoelz, 2018, Zvereva et al., 2016, Laird et al., 2013, Love et al., 2012, Haas et al., 2008, Love et al., 2007a, Geri et al., 2004, Love et al., 2007b, Love et al., 2005). Moreover, P6 is also found to increase the resistance to a polar auxin transport inhibitor, demonstrating that P6 interacts with components of the auxin signalling pathway. This is consistent with the findings of the auxin inhibiter treatment experiments and the transcriptional profile of the P6 expressing plants.

Remarkably the RNA-Seq results suggest that P6 also modulates the expression of genes involved in other phytohormonal signalling pathways such as those involving ABA, GA, and BR (Figure 7.1). A role for P6 in interacting with these pathways has not been previously reported. The modulations of other phytohormonal signalling pathways might also lead to indirect regulation of the SA and JA/ET singling pathways as it is recognized that broad crosstalk between phytohormone pathways occurs. The

identification of several genes related to ABA responses whose expression was modulated by P6 expression is of interest because ABA is known to participate in Arabidopsis defense against fungi such as *Leptosphaeria maculans* (Oide et al., 2013, Robert-Seilaniantz et al., 2011, Islam et al., 2019b, Derksen et al., 2013). This indicates that ABA participates in increasing the resistance against JA-sensitive pathogens and crosstalk to SA and JA/ET pathways. The increase in the resistance against JA-sensitive pathogens/pests such as insects and fungi might be due to modification in the crosstalk between ABA and JA/ET singling pathways (Collum and Culver, 2016, Derksen et al., 2013, Robert-Seilaniantz et al., 2011, Islam et al., 2019b, Zvereva et al., 2016, Song et al., 2014, Durbak et al., 2012, Depuydt and Hardtke, 2011). This supports the previous finding that P6 expression will modify the plant resistance to pathogens, becoming more resistant to necrotrophic pathogens and insects, and more susceptible to biotrophic pathogens, i.e., enhancing the JA/ET and suppresses the SA (Love et al., 2012, Laird et al., 2013, Love et al., 2007a, Love et al., 2007b, Love et al., 2005, Geri et al., 2004, Zvereva et al., 2016, Leisner and Schoelz, 2018). The gene expression data propose that P6 is elevating genes involved in responses to abiotic stress. It was previously noticed in different virus infections where they are false the plant by promoting its responses to absent abiotic stress continuously making them more vulnerable to the virus infection, i.e., P6 is mimic abiotic stress, which might facilities CaMV infection and making the plant more favorable to their insect vector. Moreover, some of these genes are found to interfere with signalling pathways (Wu and Ye, 2020, Carr et al., 2020, van Munster, 2020).

Taking all these results together, P6WT-GFP expression modulates the expression of genes involved in plant defense and phytohormonal signalling, i.e., JA/ET and SA, and plant physiology might result in symptoms development. This modulation of gene expression support that P6 increases modulate the ethylene sensitivity and auxin inhibitor resistance.

Next, the P6 TOR binding domain provides a significant role in regulating the expression of plant genes, mainly genes involved in defense responses and phosphorylation, i.e., regulation of specific genes occurs in the TOR binding domain manner (Figure 7.1). Our results from the gene expression profile comparisons between the lines demonstrated that P6WT was able to suppress gene expression of several genes associated with SA, JA/ET, ABA, BR, GB, and Aux pathway while P6(ΔTOR)-GFP were unable to suppress them. This might explain the differences in plant performance and responses, such as the sensitivity to ethylene precursor. This is also supported by the ethylene triple response assay results, in which the transgenic line expressing P6 with TOR binding domain deletion was more sensitive to the ethylene precursor than the transgenic line expressing intact P6. In contrast, the results of the auxin inhibitor treatment experiments demonstrated a phenotype in which the transgenic lines expressing P6 and mutant P6 had a similar resistance degree to the inhibitor, i.e., in a non-TOR binding domain manner. In other words, the increases in the resistance to auxin transport initiator are supported by one of the other P6 domains. Besides the role in the modulation of SA and JA/ET genes, which are known to play a role in the defense against a broad range of pathogens, specific genes documented to play a role in the basal plant defense, defense against viruses, and methylation were suppressed by intact P6, i.e., P6 will make the plant more favorable for CaMV infection and facilitate the virus replication and gene expression. In contrast, those genes were up-regulated in P6(ΔTOR) lines.

In future, the expression of important genes from the RNA-seq data needs to be confirmed by quantitative real-time PCR, Practically *ICS2, BGL2, NPR1, ERF6, ERF2, EIN2, EIN3 LTP2, LTP3, LTP4, ROS1, CRK37, NPC3, SRK2I, LBD26*, *DIR5, PDF1.2B, PDF1.2C, CNGC19, PDF1.1,* and *PDF1.2A*. These genes know to contribute to the plant defense responses and ethylene signalling pathway. Some of them were found to be down-regulated as a result of P6WT expression.

Previously (Love et al., 2012) showed that transgenic Arabidopsis expressing P6 enhanced the susceptibility to virulent and avirulent strains of the biotrophic bacterial pathogen, *Pseudomonas syringae* pv. Tomato (Pst), but in contrast, P6 reduced the

susceptibility to the necrotrophic fungus, *Botrytis cinerea*. Additionally, transgenic Arabidopsis expressing P6 was found to have weakened basal defense responses (Zvereva et al., 2016). Test the transgenic lines against other pathogens, including fungi, oomycetes, bacteria, nematodes, and viruses, to determine if resistance enhancement against pathogens occurs and if a P6 or P6(ΔTOR) can be applied as a defense stimulator. The outcome of this experiment will be that P6 potentially can be used as a candidate for engineering crop species or a tool to increase the tolerance to biotic and abiotic stresses.

Pathogens have been shown to modify board range hosts phenotypes, including hosts color, chemistry, morphology, physiology, immunity, and behavior. Accordingly, the vector behavior and performance will be modified due to modification in hosts phenotypes. This impact might provide and support pathogens' survival, reproduction, transportation, and spreading (Westwood et al., 2013, Chesnais et al., 2019, Ingwell et al., 2012, Belliure et al., 2005). The Vector Manipulation Hypothesis (VMH) was proposed to clarify the plant virus strategies to increase infection spread, i.e., transmission to a new host by the direct and indirect impact on vectors (Ingwell et al., 2012). Viruses induce changes in the host plant, including plant phenotypes, emissions, and defense responses, influencing vector-plant interactions in a way that supports viruses infection and spreading. Moreover, viruses will alter the insect vector behavior, including colonization, reproduction, performance, and feeding behavior, which elevate transmission and spread infection due to modifying the host physiology and responses. Viral pathogen regulates host plant metabolism to establish indirect mutualism with its insect vector, which was found in begomovirus-infected plants where the whiteflies' performance (*Bemisia tabaci*) was enhanced. This enhancement occurs due to the suppression of plant terpene biosynthesis by the bC1 protein of begomovirus (Li et al., 2014a).

Aphid, *Myzus persicae* demonstrated different feeding behavior and performance among several hosts such as tobacco (*Nicotiana tabacum*), *Arabidopsis thaliana*, and cucurbits. Interestingly, aphid behavior and performance were modified when these hosts were infected by *Cucumber mosaic virus* (CMV). CMV infection in Arabidopsis

and cucurbits direct the emitting of aphid-attracting volatiles, which may favor virus acquisition and enhance virus transmission rates, whereas infected tobacco (cv. Xanthi) promotes enhancement to aphid survival and reproduction (Tungadi et al., 2017). Previously, CMV was shown to modify Arabidopsis plant physiology, supporting their dispersal after virus acquisition. The aphids were deterred by the smell and taste of the infected plants and moved for a healthy plant (Westwood et al., 2013). Like CMV, the subject of these experiments aphids is the insect vector of CaMV (Haas et al., 2002). Changing aphid feeding behavior, the vector of both viruses, enhanced the CaMV and *Turnip yellows virus* (TuYV) acquisition and transmission (Chesnais et al., 2019, Martiniere et al., 2009). Based on the previous findings (Love et al., 2012, Love et al., 2007a, Love et al., 2007b, Geri et al., 2004), P6 enhanced the JA/ET responses, which will enhance the defense responses against herbivores such as aphids, and our findings that P6 will modulate the gene expression profiles including genes contribute in responses against biotic and abiotic stress is consistent with this. It would be interesting to carry out experiments to determine the impact of P6 expression on aphid behavior, performance, and host preferences, and volatile compounds emission. Here, we can inspect the relationship between CaMV and the changes in host behavior. In the future, expand our understanding of how viruses impact aphid performance and behavior with plants will help to develop approaches designed at constraining virus transmission in crop fields.

P6 expression impacts plant phenotype by induce symptoms such as stunting, in which P6-TOR interaction appears to increase the stunting severity, judged by the phenotypes of the transgenic lines. P6 was found to modulate the transcription of genes involved in hormonal signalling pathways such as ABA, BR, GB, SA, JA/ET, and phosphorylation proteins, which are known hormones to participate in plant development and prefiltration that might correlate why P6 expression leads to stunting. Additionally, P6 manipulates the host responses and directs host energy to tolerate the false abiotic stresses; this might also support why P6 is directing plant stunting.

Further phenotypic studies need to be conducted coupled with proteomics and metabolomics analysis to determine the P6 interactors, P6 mode of action, impact on

the vector performance, interaction specificity to other phytohormones, the exact role of TOR binding domain in plant defense responses against biotrophic and necrotrophic pathogens determine. Also, the localization study determines if there are differences between P6 and P6(ΔTOR), i.e., if TOR plays a role in P6 movement and localization. Taken together, these findings suggest that the P6, via its TOR-binding domain, can modulate phytohormonal responses by interacting with plant TOR kinase.

Metabolomics is a technology that provides a comprehensive characterisation and quantification of all metabolites in a biological sample. Notably, the combined responses of metabolites in the plant after pathogen infection or expressing specific protein can expand our understanding of plant responses. For example, the significance of specific amino acids as building blocks of protein and other metabolites, such as lipids and carbohydrates of the plant, can be assessed in a single sample using metabolomics approaches (Szpunar, 2005). Therefore, Metabolomics and proteomics investigations need to be conducted to have an overall picture of P6 impact on plant performance, coupled with RNA-seq data (transcriptomics). These two approaches will identify and measure the abundance of compounds, in which metabolomics will determine the small molecules (metabolites) from various biochemical classes and pathways. Simultaneously, proteomics will resolve peptides derived from proteins providing information about the protein-to-protein interaction, i.e., determine the P6 interactors. Additionally, the three lines' protein expression profile comparisons will identify plant proteins involved in the different Plant responses capabilities. The outcome of this study will identify several important metabolites, indicate the different expression patterns of proteins and metabolites associated with plant responses and signalling pathways, and obtain a more detailed characterisation of P6 and mutant P6 impact on plant protein expression profile (Wu et al., 2018). This study will initiate the basis for future research, which aims to develop molecular and genetic methods and protocols for defining viral protein impact on plant responses.

Moreover, metabolomics and transcriptomics data can be analyzed using the novel machine learning-based model analysis using Support Vector Machines (SVMAttributeEval). Machine learning is a powerful method that will provide more data

resolution, identifying patterns, and an informative list of the most important metabolites and transcripts and their possible integrated pathways associated with plant performance. It will eliminate the limitation of using the conventional p-value approach where we could not distinguish between gene expression after a certain value. The P-value of all genes will be the same (false negative). Secondly, Ingenuity Pathway Analysis (IPA) (as provided by Qiagen company) is extensively used on the transcripts and metabolites of humans and animals to classify them according to their cellular localization and biological function, which will be more detailed than GO. Unfortunately, it is not as yet developed for plant applications. Little is known about the impact of P6 on the plant's overall metabolite profile, and this study will be one of the first to characterisations it. Therefore, the hypothesis that small molecules identified in plant metabolomics study of transgenic lines expressing P6 and mutant P6 correspond to phytohormonal signalling might be used as principal indicators of plant infection and plant responses, i.e., potential biomarkers.

Hormone signaling is associated with the modulation of abiotic stress responses and biotic responses (defense responses). Phytohormones regulate plant defense responses, including systemic acquired resistance (SAR) and induced systemic resistance (ISR). The SAR works against biotrophic and depends mainly on the SA signalling pathway and levels. High levels of SA activate the expression of pathogenesis-related (PR) genes, where the produced PR proteins work against the biotrophic bacteria and fungi, and in several cases, constrained viruses (Collum and Culver, 2016, Gao et al., 2015, Yang et al., 2020, Islam et al., 2019b, Toruno et al., 2016), while ISR generally work against the necrotrophic pathogens and insects and depend on the JA/ET signaling. However, in some cases, ET triggers SAR responses and expression of PR genes during the hypersensitive response, previously found in responses against TMV, i.e., phytohormones cross-talk and their involvement and impact on plant responses depend on the infection time and phase (Liu and Timko, 2021, Yang et al., 2020, Parisi et al., 2019, Islam et al., 2019b, Oka et al., 2013). ABA is a stress phytohormone that is responsible for stomatal closure and regulates plant growth and root development. One way to detect the P6 modulation of ABA and TOR involvement is by determining the plant's ability to limit water loss by transpiration

(Robert-Seilaniantz et al., 2011, Cutler et al., 2010). Generally, ABA has an antagonistic relationship with ET and GA; however, this might change in a particular phase, circumstances, and tissue (Liu and Timko, 2021).

Moreover, ABA plays a role in the defense responses against pathogens and cross-talk with ET to modulate these responses, i.e., P6 directly modulates the ET/JA-dependent defense responses by or might indirectly be by regulating the ABA signalling pathway (antagonistic cross talk) (Islam et al., 2019b, Collum and Culver, 2016, Derksen et al., 2013, Liu and Timko, 2021). Furthermore, ABA was found to interfere with the SAR-SA signalling and result in the suppression of SAR responses, that is another way P6 might modulate the phytohormonal signalling and defense responses by interacting to plant components, including signalling components such as TOR (Oide et al., 2013, Islam et al., 2019b, Derksen et al., 2013, Cutler et al., 2010). However, more knowledge is needed on phytohormones-pathogen interactions because of the complexity of phytohormonal cross-talk and their involvement in ISR or SAR responses.

Interestingly, P6 modulates the expression of various genes involved in the different phytohormonal signalling pathways; many genes identified by RNA-Seq were related to ABA pathway based on their annotations. An experiment needs to be carried out looking at the P6 regulatory specificity, the role of the TOR binding domain effect on the regulation specificity, and the P6 impact on the crosstalk between ABA, SA, and JA/ET pathways. ABA is known to be essential for Arabidopsis defense against fungi such as *Leptosphaeria maculans* (Oide et al., 2013). However, its role in responses to viral infection is unknown. Potentially, we can assess the role of P6 in regulating ABA by studying the expression of PR genes such as PR2, callose deposition, susceptibility to biotrophic and necrotrophic pathogens with ABA treatment. This study will expand understating about the mechanism of P6 interferences with ABA and P6 impact on the crosstalk between phytohormones. Furthermore, the P6 impact needs to be assessed on the agricultural corps.

Because TOR kinase regulates mRNA translation (Schepetilnikov et al., 2013), P6-TOR interaction might modify the host gene expression profile, as shown in the chapter.

The P6-TOR interaction impact might also occur in the modification of defense responses, in which modulation in some of the responsive genes involved in SA, JA/ET, ABA, ROS, and autophagy was downregulated. Moreover, TOR-P6 interfered with the plant development where plants expressing P6WT were relatively longer than plants expressing P6(ΔTOR). Further experiments needed to be carried out to highlight the genes that would be regulated as soon as P6 or P6(ΔTOR) expressed in the plant using the inducible lines. An additional experiment is assessing the susceptibility of a TOR silenced Arabidopsis by RNA interference (RNAi) lines, which will have a reduced TOR expression level, with CaMV or the infectious clones of P6 and P6(ΔTOR). The expected results are that the severity of the infection and developed symptoms will be less than wild-type Arabidopsis, i.e., TOR is a crucial component for CaMV infection, in which low TOR expresser plants might recover easily or escape infection. This will suggest that CaMV requires an active TOR pathway for the initial and systemic infection. Thus, a confirmative experiment of host susceptibility needs to be conducted to confirm this CaMV-TOR requirement and If CaMV controls TOR-dependent antiviral defense mechanisms or if CaMV-TOR interaction supports the initial infection or the systemic spread. However, some pathways are not regulated by the P6-TOR interaction, such as the Auxin, which is regulated by other P6 domains or might be regulated indirectly by the modulation of other phytohormonal pathways ABA JA/ET, SA, and GA as they found to cross-talk (Liu and Timko, 2021, Song et al., 2014, Durbak et al., 2012, Depuydt and Hardtke, 2011). P6 is known to be a multifunctional effector by interacting with a broad range of host proteins that will trigger innate immunity reactions in a non-host and modulate defenses in the host plant (Leisner and Schoelz, 2018, Schoelz and Leisner, 2017, Laird et al., 2013) and acts as a silencing suppressor with being dependent on the NLS. Mutations in the NLS lead to loss of the silencing suppression ability (Feng et al., 2018, Laird et al., 2013, Love et al., 2007a)

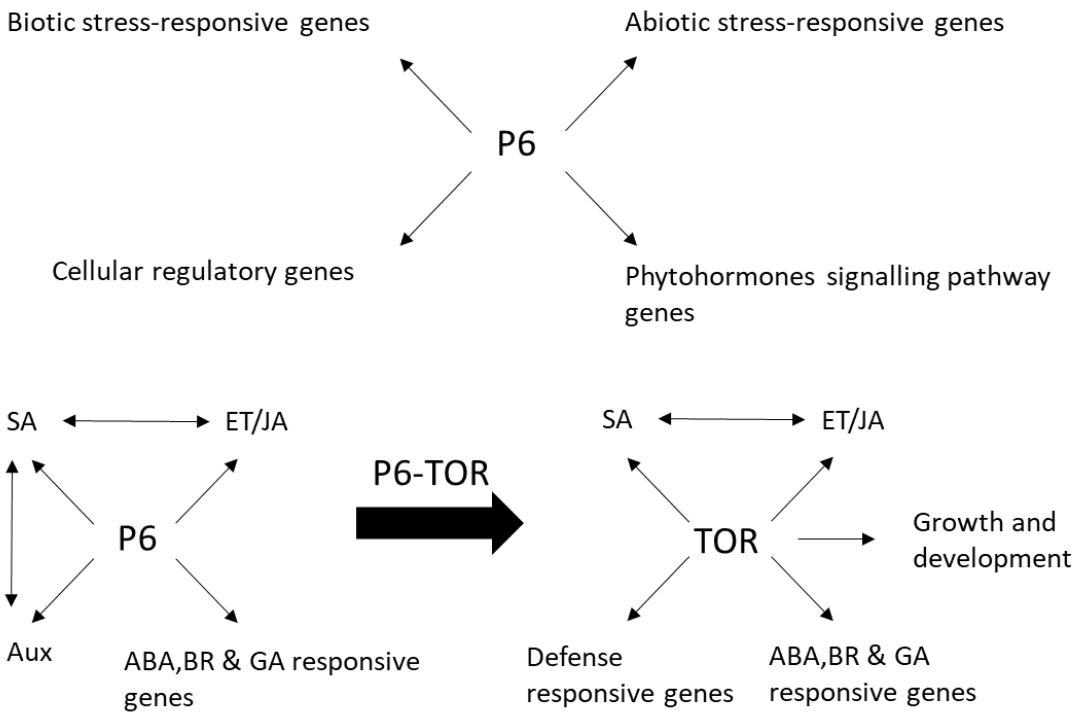

Figure 7.1. Modification of Arabidopsis gene expression profile associated with CaMV P6 expression. P6 expression altered the expression of biotic stress-responsive genes and abiotic stress-responsive genes. The expression of these genes is modulated by phytohormones signalling pathways and other stress response pathways. P6 also modulates the regulatory genes, metabolic genes, and phytohormones signalling genes resulting in interference with the plant development, growth, and plant responses.

7.2. Conclusions

This study's results take advantage of the induction of P6 expression in the plant to distinguish transcriptional responses. P6 expression elicited a reduction in plant gene expression in multiple pathways associated with phytohormonal signalling pathways, plant defense response, and stress response. Deletion of the P6 TOR binding domain constrained the P6 ability to regulate the expression of some of these genes. However, even when the TOR binding domain was deleted, P6 and P6 mutant shared some pathway regulation, suggesting that other P6 domains are responsible for regulating these genes. Therefore, the results confine the effect TOR binding domain at the whole

transcriptional level. P6 and P6 with the TOR binding domain deleted working at different regulatory levels. Future use of transgenic lines will help us confirm and extend our findings, suggesting a deep connection between TOR binding domain and biotic and abiotic responses in Arabidopsis. In the long term, these results on the P6 interaction will be important for elevating the plant performance to support the agriculture industry.

Our findings provide a valuable resource for further exploration and expand our understanding of the molecular regulatory mechanisms of P6 in plants and provide insight into P6 interaction with signalling pathways and phytohormonal cross-talk in plant defense regulation responses, metabolism, phytohormonal signalling, and growth.

Chapter VIII: Appendices

Sample name	0 - 10	10 - 20	20 - 30	30 - 40	40 - 50	50 - 60	> 60
30097-001	0	0.00078	2.076377	97.92284	0	0	0
30097-002	0	0.000676	1.974658	98.02467	0	0	0
30097-003	0	0.000717	1.97404	98.02524	0	0	0
30097-004	0	0.000666	1.987216	98.01212	0	0	0
30097-005	0	0.000527	1.902395	98.09708	0	0	0
30097-006	0	0.000744	2.071029	97.92823	0	0	0
30097-007	0	0.000546	2.030054	97.9694	0	0	0
30097-008	0	0.000441	1.857743	98.14182	0	0	0
30097-009	0	0.000873	2.145257	97.85387	0	0	0
Minimum	0	0.000441	1.857743	97.85387	0	0	0
Median	0	0.000676	1.987216	98.01212	0	0	0
Mean	0	0.000663	2.002085	97.99725	0	0	0
Standard deviation	0	0.000136	0.089502	0.089621	0	0	0
Maximum	0	0.000873	2.145257	98.14182	0	0	0

Table 8.1. Summarizes the distribution of average sequence quality scores. The quality of a sequence is calculated as the arithmetic mean of its base qualities. On average, 97.99% of each sample possessed a Q-score that fell within the 30-40 range. A Q-score of 30 or greater is considered to be high quality.

Sample name	1 - 10	11 - 20	21 - 30	31 - 40	41 - 50	51 - 60	61 - 70	71 - 80
30097-001	34	36	36	36	36	36	36	36
30097-002	34	36	36	36	36	36	36	36
30097-003	34	36	36	36	36	36	36	36
30097-004	34	36	36	36	36	36	36	36
30097-005	34	36	36	36	36	36	36	36
30097-006	34	36	36	36	36	36	36	36
30097-007	34	36	36	36	36	36	36	36
30097-008	34	36	36	36	36	36	36	36
30097-009	34	36	36	36	36	36	36	36
Minimum	34	36	36	36	36	36	36	36
Median	34	36	36	36	36	36	36	36
Mean	34	36	36	36	36	36	36	36
Standard deviation	0	0	0	0	0	0	0	0

Maximum	34	36	36	36	36	36	36	36

Table 8.2. Summarizes the base-quality distribution along the base positions. As with the quality distribution per sequence, a Q-Score of 30 or greater is considered to be high quality.

Sample name	**0 - 10**	**10 - 20**	**20 - 30**	**30 - 40**	**40 - 50**	**50 - 60**	**60 - 70**	**70 - 80**	**80 - 90**	**> 90**
30097-001	70.985	9.849	4.501	2.716	1.829	1.336	1.014	0.813	0.644	0.552
30097-002	69.580	10.408	4.814	2.920	1.925	1.359	1.063	0.815	0.714	0.587
30097-003	71.966	10.180	4.560	2.632	1.750	1.286	0.932	0.745	0.611	0.506
30097-004	68.052	10.643	4.954	2.986	2.029	1.454	1.129	0.913	0.739	0.615
30097-005	70.930	10.326	4.599	2.788	1.833	1.362	1.007	0.819	0.645	0.538
30097-006	69.889	10.349	4.711	2.832	1.894	1.382	1.047	0.826	0.686	0.584
30097-007	71.688	9.951	4.468	2.707	1.789	1.304	0.964	0.764	0.640	0.520
30097-008	70.316	10.252	4.740	2.818	1.857	1.409	1.008	0.824	0.691	0.522
30097-009	68.307	10.484	4.842	2.949	1.984	1.399	1.096	0.895	0.726	0.638
Minimum	68.052	9.849	4.468	2.632	1.750	1.286	0.932	0.745	0.611	0.506
Median	70.316	10.326	4.711	2.818	1.857	1.362	1.014	0.819	0.686	0.552
Mean	70.190	10.271	4.688	2.816	1.877	1.366	1.029	0.824	0.677	0.562
Standard deviation	1.377	0.250	0.166	0.119	0.091	0.053	0.062	0.054	0.044	0.046
Maximum	71.966	10.643	4.954	2.986	2.029	1.454	1.129	0.913	0.739	0.638

Table 8.3. Summarizes the duplication level distribution. Duplication levels are simply the count of how often a particular sequence has been found.

Sample Name	Read Count	Single, mapped (%)	Single, not mapped (%)	Mapped to genes (%)	Mapped to intergenic (%)
30097-001	33200527	98.43256	1.567442	98.91133	1.088668
30097-002	37718377	98.15843	1.841572	99.25066	0.749343
30097-003	33336306	97.93537	2.064629	99.07336	0.926644
30097-004	41160490	97.9807	2.019303	99.24257	0.757434
30097-005	33761233	98.64823	1.351772	98.9321	1.067904
30097-006	36031706	98.20983	1.790168	98.49945	1.500548
30097-007	33141579	95.04751	4.952489	98.82649	1.173511
30097-008	36964470	94.59945	5.400551	98.0905	1.909501
30097-009	36879313	99.0188	0.9812	96.35185	3.648146
Minimum	33141579	94.59945	0.9812	96.35185	0.749343
Median	36031706	98.15843	1.841572	98.91133	1.088668
Maximum	41160490	99.0188	5.400551	99.25066	3.648146
Mean	35799333	97.55899	2.441014	98.57537	1.424633
Standard deviation	2716626	1.590968	1.590968	0.910853	0.910853

Table 8.4. The overall mapping rates to the reference genome.

Sample name	Detected spike-ins	R^2	Reads mapped to spike-ins (#)	Reads mapped to spike-ins (%)	Lower limit of detection (attomoles/µL)
30097-001	1/1	0	1	3.01E-06	0
30097-002	1/1	0	1	2.65E-06	0
30097-003	1/1	0	4	1.2E-05	100
30097-004	1/1	0	4453	0.010819	100
30097-005	1/1	0	3113	0.009221	100
30097-006	1/1	0	2760	0.00766	100
30097-007	1/1	0	290790	0.877417	100
30097-008	1/1	0	356805	0.965265	100
30097-009	1/1	0	36460	0.098863	100
Minimum		0	1	2.65E-06	0
Median		0	3113	0.009221	100
Maximum		0	356805	0.965265	100
Mean		0	77154.11	0.218807	77.77778
Standard deviation		0	141271.1	0.400116	44.09586

Table 8.5. The alignment rates to the transgenic sequence provided.

Sample name	protein_coding	rRNA	unknown	lncRNA	ncRNA
30097-001	98.84336	0.852593	3.11E-06	0.144424	0.097617
30097-002	99.37922	0.305395	2.74E-06	0.147848	0.100164
30097-003	99.15699	0.466121	1.25E-05	0.168224	0.137351
30097-004	99.41896	0.277025	0.011199	0.139943	0.088702
30097-005	98.94665	0.751138	0.009503	0.132628	0.094761
30097-006	98.38164	1.251822	0.007971	0.170692	0.122746
30097-007	98.24284	0.494859	0.940069	0.140171	0.11577
30097-008	97.83179	0.802131	1.04699	0.135681	0.11571
30097-009	94.4619	5.065218	0.104328	0.167359	0.138198
Minimum	94.4619	0.277025	2.74E-06	0.132628	0.088702
Median	98.84336	0.751138	0.009503	0.144424	0.11571
Maximum	99.41896	5.065218	1.04699	0.170692	0.138198
Mean	98.29593	1.1407	0.235564	0.149664	0.112336
Standard deviation	1.533977	1.503306	0.431808	0.015004	0.018229
Sample name	**nontranslating_CDS**	**snoRNA**	**miRNA**	**snRNA**	**tRNA**
30097-001	0.058139	0.001775	0.001407	0.000651	2.8E-05
30097-002	0.063397	0.001811	0.001512	0.000619	2.74E-05
30097-003	0.067601	0.001751	0.001409	0.000524	1.25E-05
30097-004	0.060807	0.00162	0.001147	0.000576	2.01E-05
30097-005	0.061924	0.001499	0.001239	0.000623	3.66E-05
30097-006	0.061458	0.001759	0.001184	0.000702	2.31E-05
30097-007	0.062581	0.001626	0.001306	0.000769	6.47E-06
30097-008	0.064066	0.001681	0.001221	0.000704	2.35E-05
30097-009	0.057835	0.002475	0.001279	0.001322	8.87E-05
Minimum	0.057835	0.001499	0.001147	0.000524	6.47E-06
Median	0.061924	0.001751	0.001279	0.000651	2.35E-05
Maximum	0.067601	0.002475	0.001512	0.001322	8.87E-05
Mean	0.061979	0.001777	0.0013	0.000721	2.96E-05
Standard deviation	0.002998	0.000279	0.00012	0.000237	2.38E-05

Table 8.6. The distribution of biotypes.

Name	Max group means	Fold change	Log fold change	P-value	FDR p-value	Bonferroni
gene:AT2G40955	2.008889	10.60203	3.406269	2.22E-16	5.72E-12	5.72E-12
gene:AT1G62580	3.040662	6.694122	2.742895	1.98E-12	2.55E-08	5.1E-08
gene:AT4G04223	5.659297	-7.73207	-2.95085	3.97E-09	3.41E-05	0.000102
ROSY1	13.84223	-3.66832	-1.87512	6.3E-09	4.06E-05	0.000162
LTP4	2.469952	-18.9814	-4.24652	2.58E-08	0.000133	0.000665
LTP3	5.330757	-4.12627	-2.04484	6.34E-08	0.000272	0.001633
CNGC19	0.309442	-21.421	-4.42095	5.5E-07	0.002026	0.01418
THAS1	21.92183	-2.0108	-1.00777	1.2E-06	0.003869	0.03095
gene:AT3G01345	1.503178	7.30911	2.869696	1.85E-06	0.005289	0.047599
gene:AT4G14548	3.82329	3.732185	1.90002	5.81E-06	0.014978	0.149785
APY5	25.98915	-3.99774	-1.99919	1.41E-05	0.033115	0.364268
gene:AT3G23060	0.537249	8.497065	3.086965	1.94E-05	0.041659	0.499902
NRT2.6	1.621655	8.709658	3.122616	3.27E-05	0.064828	0.842769
gene:AT5G35480	3.85497	-2.96296	-1.56704	6.53E-05	0.113749	1
LBD26	4.016657	2.76247	1.465959	6.62E-05	0.113749	1
AT4_1	18.93886	-2.26453	-1.17921	7.55E-05	0.121582	1
gene:AT1G26240	9.218981	8.056731	3.010195	9.59E-05	0.14535	1
gene:AT5G52390	0.689021	-5.36006	-2.42225	0.000113	0.162325	1
CYP708A2	19.52152	-1.78439	-0.83543	0.000125	0.169526	1
GLP2A	3.792314	3.09741	1.631062	0.000143	0.184463	1
ICS2	8.643154	-2.21285	-1.14591	0.000157	0.193216	1
gene:AT2G01310	0.721964	12.16139	3.604237	0.000242	0.283135	1
gene:AT2G05635	0.51719	10.93039	3.450273	0.000335	0.375438	1
PYD4	8.005681	-1.96304	-0.97309	0.000384	0.412924	1
gene:AT3G49340	0.465652	-8.60337	-3.1049	0.00043	0.44371	1

Table 8.7. The differential expression results for the top 25 genes (the 25 genes with the lowest FDR p-value) for the comparison between P6WT-GFP vs. WT. For each gene, a p-value was assigned to represent the significance of the observed fold change. This statistic determines how likely the fold change result was observed if the gene was not differentially-expressed. As we are testing many genes in this experiment, using p-value alone as a measure of significance can be prone to identifying false positive genes. For example, if we were to test 1000 genes whose expression is unchanged in reality and were to choose a p-value threshold of 0.05, we would expect 50 genes below the threshold just by chance. To account for this multiple testing problem, “FDR p-values” were calculated using the Benjamini-Hochberg method.

Name	Max group means	Fold change	Log fold change	P-value	FDR p-value	Bonferroni
MET2_1	0.001984	-3.51104	-1.8119	0.496674	0.997994	1
gene:AT1G63210	0.002505	-3.51104	-1.8119	0.496674	0.997994	1
AHA6	0.002735	3.829175	1.937034	0.465108	0.997994	1
ACA7_2	0.002759	1.049801	0.070116	0.967879	0.997994	1
ABCB22	0.002767	-3.51117	-1.81195	0.496659	0.997994	1
ABCA12	0.002816	3.82931	1.937085	0.465094	0.997994	1
ABI3	0.002936	1.049801	0.070116	0.967879	0.997994	1
MYOB4	0.002937	-3.51104	-1.8119	0.496674	0.997994	1
PPC4	0.003031	-3.51117	-1.81195	0.496659	0.997994	1
gene:AT3G54800	0.003289	3.829175	1.937034	0.465108	0.997994	1
NET2C	0.003322	3.829289	1.937077	0.465096	0.997994	1
HDG3	0.00333	3.829175	1.937034	0.465108	0.997994	1
gene:AT2G19210	0.003403	-3.51104	-1.8119	0.496674	0.997994	1
GDPDL7	0.003434	-3.51104	-1.8119	0.496674	0.997994	1
gene:AT2G42835	0.003507	3.829175	1.937034	0.465108	0.997994	1
PME21	0.003521	-3.51104	-1.8119	0.496674	0.997994	1
CHX13	0.003561	-3.51125	-1.81199	0.49665	0.997994	1
gene:AT5G22470	0.003599	-3.51117	-1.81195	0.496659	0.997994	1
gene:AT3G60950	0.00372	-3.51104	-1.8119	0.496674	0.997994	1
gene:AT3G28780	0.003765	-3.51104	-1.8119	0.496674	0.997994	1
CHX25	0.003768	-3.51125	-1.81199	0.49665	0.997994	1
HDG9	0.003807	3.829289	1.937077	0.465096	0.997994	1
ATTPS3	0.00383	-3.51104	-1.8119	0.496674	0.997994	1
gene:AT4G20700	0.003834	3.829175	1.937034	0.465108	0.997994	1
gene:AT4G20080	0.003872	-3.51104	-1.8119	0.496674	0.997994	1

Table 8.8. The differential expression results for the top 25 genes (the 25 genes with the lowest FDR p-value) for the comparison between P6 (TOR-GFP) vs. WT. For each gene, a p-value was assigned to represent the significance of the observed fold change. This statistic determines how likely the fold change result was observed if the gene was not differentially-expressed. As we are testing many genes in this experiment, using p-value alone as a measure of significance can be prone to identifying false positive genes. For example, if we were to test 1000 genes whose expression is unchanged in reality and were to choose a p-value threshold of 0.05, we would expect 50 genes below the threshold just by chance. To account for this multiple testing problem, “FDR p-values” were calculated using the Benjamini-Hochberg method.

Name	Max group means	Fold change	Log fold change	P-value	FDR p-value	Bonferroni
gene:AT3G23270	0.002339	-3.51646	-1.81412	0.50114	0.999966	1
gene:AT5G45230	0.002549	-3.51661	-1.81418	0.501124	0.999966	1
gene:AT1G65780	0.002585	-3.51646	-1.81412	0.50114	0.999966	1
gene:AT5G42490	0.002687	-3.51658	-1.81417	0.501126	0.999966	1
AHA6	0.002735	3.828271	1.936693	0.460318	0.999966	1
ABCA12	0.002816	3.828405	1.936743	0.460304	0.999966	1
AFH3	0.002865	-3.51646	-1.81412	0.50114	0.999966	1
gene:AT1G20400	0.002926	3.828405	1.936743	0.460304	0.999966	1
ABI3	0.002936	3.828354	1.936724	0.460309	0.999966	1
gene:AT1G20750	0.003067	3.828405	1.936743	0.460304	0.999966	1
MORC5	0.003085	-3.51646	-1.81412	0.50114	0.999966	1
gene:AT2G29040	0.003112	-3.51646	-1.81412	0.50114	0.999966	1
FIS2	0.003152	-3.51646	-1.81412	0.50114	0.999966	1
gene:AT2G34210	0.00321	3.828271	1.936693	0.460318	0.999966	1
gene:AT2G19230	0.003247	-3.51658	-1.81417	0.501126	0.999966	1
MYOB4	0.003265	-3.51658	-1.81417	0.501126	0.999966	1
gene:AT3G54800	0.003289	3.828271	1.936693	0.460318	0.999966	1
NET2C	0.003322	1.072754	0.10132	0.953601	0.999966	1
HDG3	0.00333	3.828271	1.936693	0.460318	0.999966	1
CNGC7	0.003357	-3.51646	-1.81412	0.50114	0.999966	1
NPF2.12	0.003528	-3.51661	-1.81418	0.501124	0.999966	1
BGAL15	0.003532	-3.51646	-1.81412	0.50114	0.999966	1
CHX5	0.003634	-3.51658	-1.81417	0.501126	0.999966	1
gene:AT5G45640	0.003649	-3.51646	-1.81412	0.50114	0.999966	1
gene:AT2G42835	0.003682	1.072692	0.101236	0.953639	0.999966	1

Table 8.9. The differential expression results for the top 25 genes (the 25 genes with the lowest FDR p-value) for the comparison between P6 (TOR-GFP) vs. P6WT-GFP. For each gene, a p-value was assigned to represent the significance of the observed fold change. This statistic determines how likely the fold change result was observed if the gene was not differentially-expressed. As we are testing many genes in this experiment, using p-value alone as a measure of significance can be prone to identifying false positive genes. For example, if we were to test 1000 genes whose expression is unchanged in reality and were to choose a p-value threshold of 0.05, we would expect 50 genes below the threshold just by chance. To account for this multiple testing problem, “FDR p-values” were calculated using the Benjamini-Hochberg method.

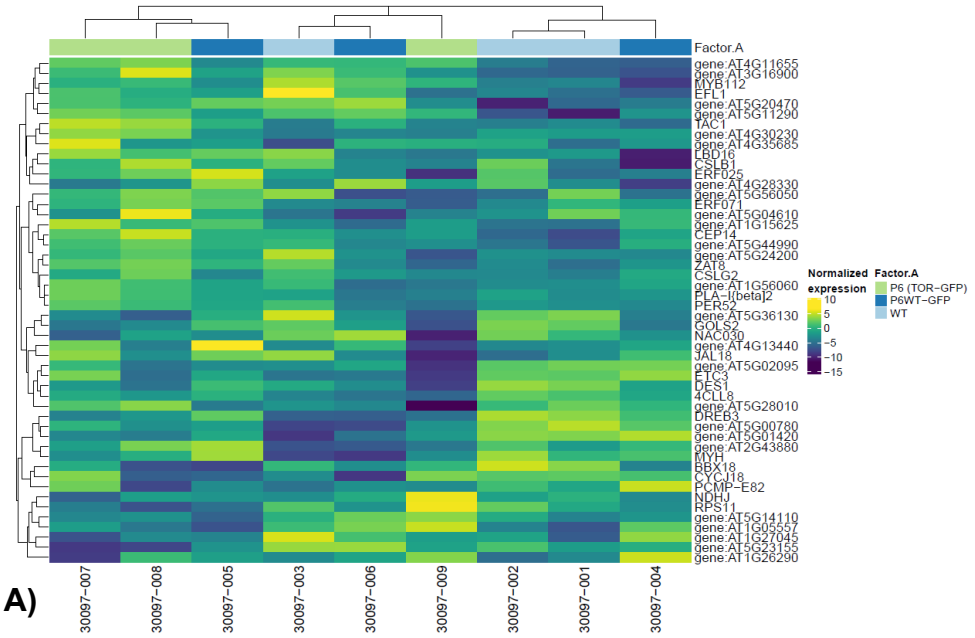
Factor.A
gene:AT4G11655
gene:AT3G16900
MYB112
EFL1
gene:AT5G20470
gene:AT5G11290
TAC1
gene:AT4G30230
gene:AT4G35685
LBD16
CSLB1
ERF025
gene:AT4G28330
gene:AT5G56050
ERF071
gene:AT5G04610
gene:AT1G15625
CEP14
gene:AT5G44990
gene:AT5G24200
ZAT8
CSLG2
gene:AT1G56060
PLA-I[beta]2
PER52
gene:AT5G36130
GOLS2
NAC030
gene:AT4G13440
JAL18
gene:AT5G02095
ETC3
DES1
4CLL8
gene:AT5G28010
DREB3
gene:AT5G00780
gene:AT5G01420
gene:AT2G43880
MYH
BBX18
CYC-I18
PCMP-E82
NDHJ
RPS11
gene:AT5G14110
gene:AT1G05557
gene:AT1G27045
gene:AT5G23155
gene:AT1G26290
Normalized expression
10
5
0
−5
−10
−15
Factor.A
P6 (TOR−GFP)
P6WT−GFP
WT
30097−007
30097−008
30097−005
30097−003
30097−006
30097−009
30097−002
30097−001
30097−004

A)

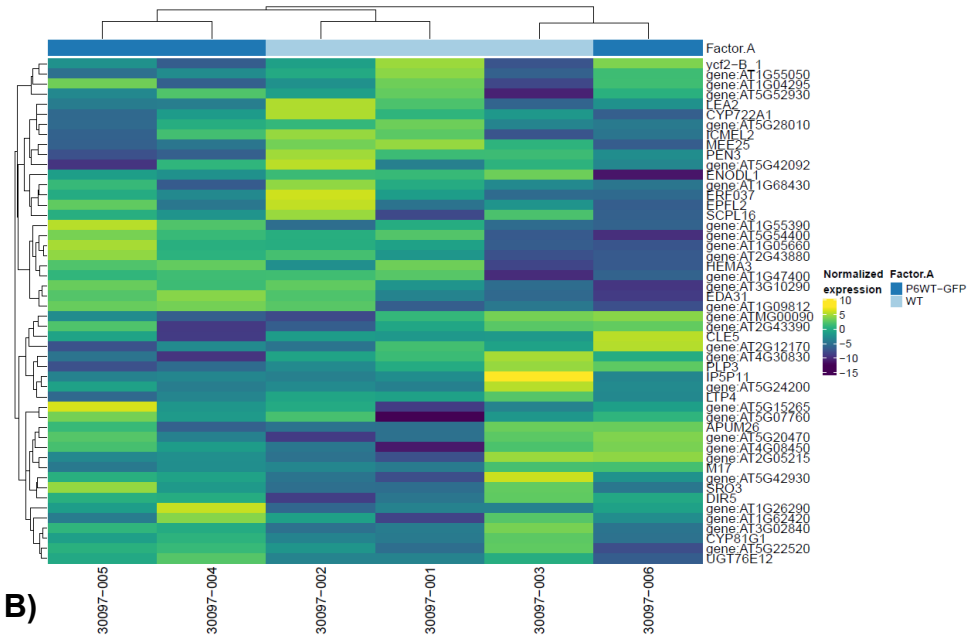
Factor.A
ycf2−B_1
gene:AT1G55050
gene:AT1G04295
gene:AT5G52930
LEA2
CYP722A1
gene:AT5G28010
TCMEL2
MEE25
PEN3
gene:AT5G42092
ENODL1
gene:AT1G68430
ERF037
EPEL2
SCPL16
gene:AT1G55390
gene:AT5G54400
gene:AT1G05660
gene:AT2G43880
HEMA3
gene:AT1G47400
gene:AT3G10290
EDA31
gene:AT1G09812
gene:ATMG00090
gene:AT2G43390
CLE5
gene:AT2G12170
gene:AT4G30830
PLP3
IPSP11
gene:AT5G24200
LTP4
gene:AT5G15265
gene:AT5G07760
APUM26
gene:AT5G20470
gene:AT4G08450
gene:AT2G05215
M17
gene:AT5G42930
SRO3
DIR5
gene:AT1G26290
gene:AT1G62420
gene:AT3G02840
CYP81G1
gene:AT5G22520
UGT76E12
Normalized expression
10
5
0
−5
−10
−15
Factor.A
P6WT−GFP
WT
30097−005
30097−004
30097−002
30097−001
30097−003
30097−006

B)

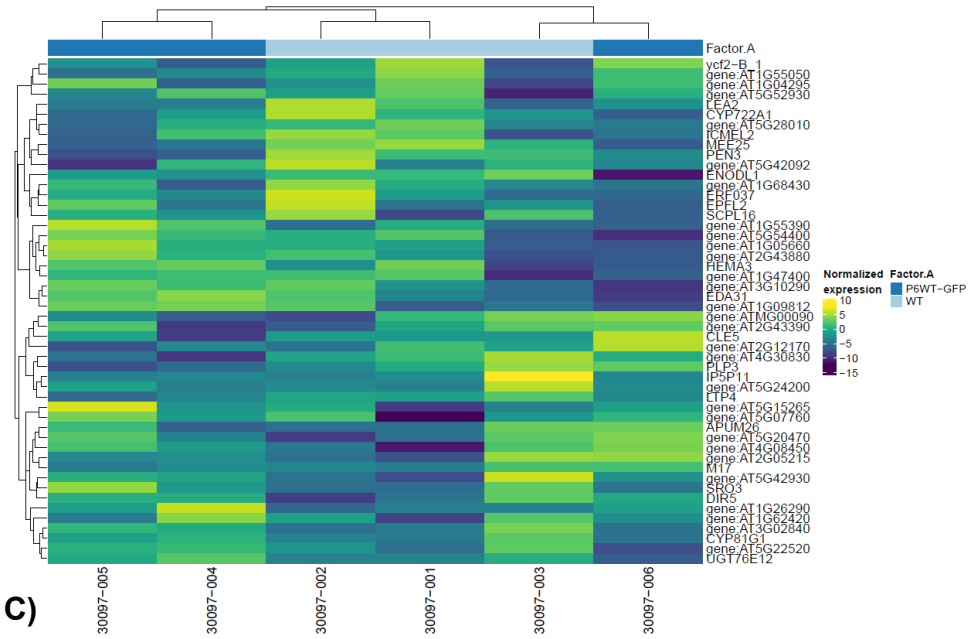

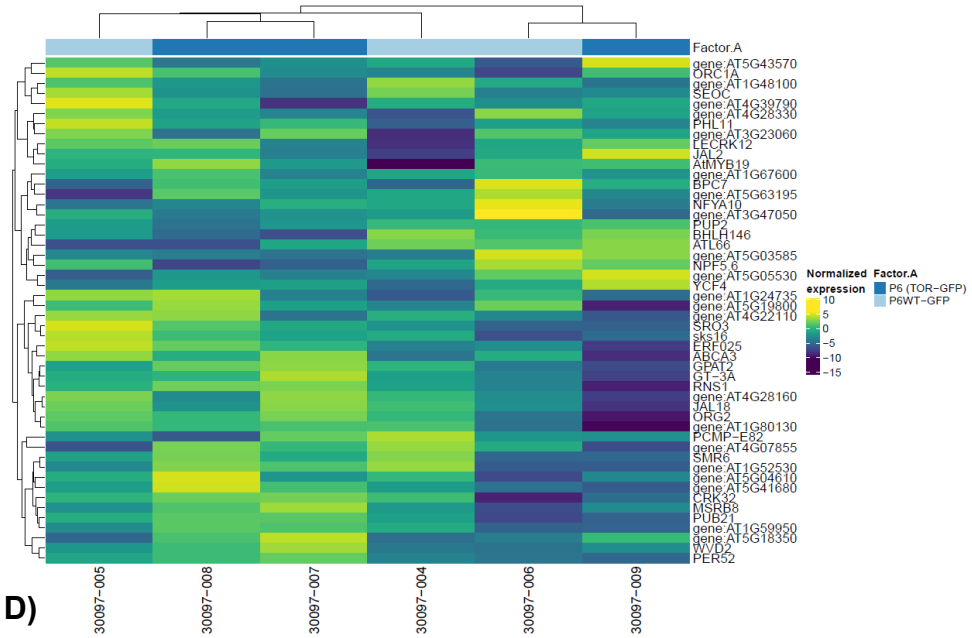

Supplement Figure 8.4. Unsupervised Clustering and Heat Maps. The following figure displays the unsupervised heatmap and clustering distribution for all 9 samples. A) P6WT-GFP vs. P6 (TOR-GFP) vs. WT, B) P6WT-GFP vs. WT, C) P6 (TOR-GFP) vs. WT and D) P6 (TOR-GFP) vs. P6WT-GFP. Heatmaps that simultaneously cluster similarly-expressed genes and samples were generated by the “Create Heat Map for RNA-seq” tool from CLC Genomic Workbench. 50 genes

with the highest variance across samples were selected for unsupervised clustering. Each row represents one gene, and each column represents one sample. The colour represents the difference of the count value to the row mean. The more similar the expression of the selected genes are between samples, the closer the samples will be related in the dendrogram.

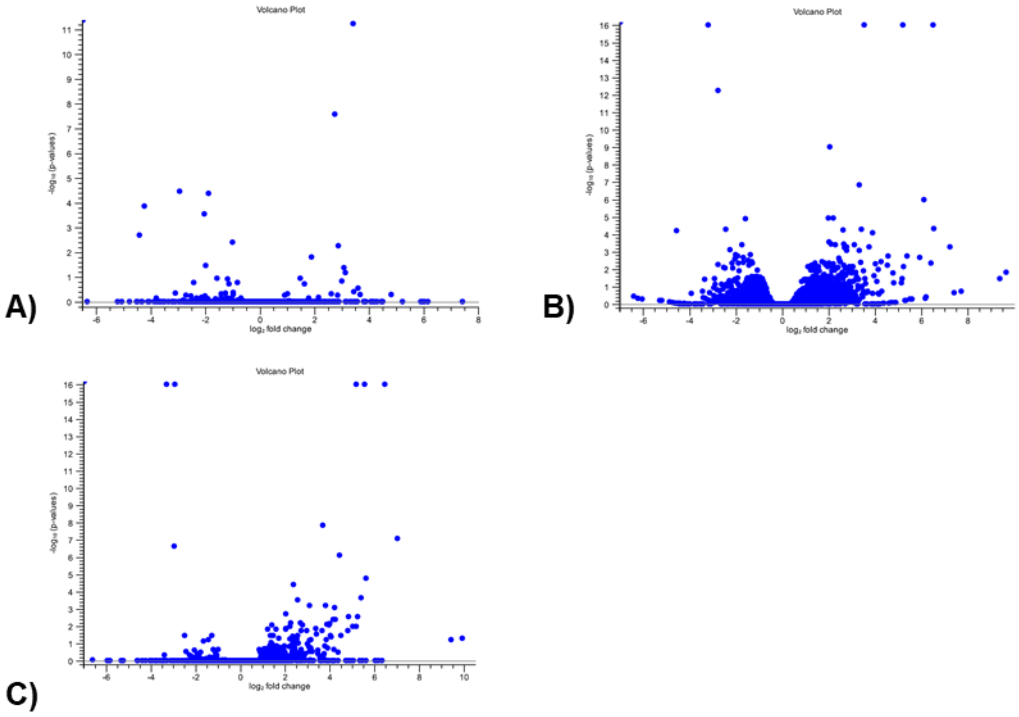

Supplement Figure 8.5. The volcano plot shows the relationship between the p-values of a statistical test and the magnitude of the difference in expression values of the samples in the groups. A) P6WT-GFP vs. WT, B) P6 (TOR-GFP) vs. WT and C) P6 (TOR-GFP) vs. P6WT-GFP. The plot is constructed by plotting the FDR corrected negative log10(p-value) on the y-axis, and the expression fold change between the two experimental groups on the x-axis. The larger the difference in expression of a feature, the more extreme it's point will lie on the X-axis. The more significant the difference, the smaller the p-value and thus the higher the -log10(p) value. Thus, points for features with highly significant differences will lie high in the plot. Features of interest are typically those which change significantly

and by a certain magnitude. These are the points in the upper left and upper right-hand parts of the volcano plot.

List of References

AGUDELO-ROMERO, P., CARBONELL, P., DE LA IGLESIA, F., CARRERA, J., RODRIGO, G., JARAMILLO, A., PÉREZ-AMADOR, M. A. & ELENA, S. F. 2008. Changes in the gene expression profile of Arabidopsis thaliana after infection with Tobacco etch virus. *Virology Journal,* 5**,** 92.

AKHTER, S., UDDIN, M. N., JEONG, I. S., KIM, D. W., LIU, X. M. & BAHK, J. D. 2016. Role of Arabidopsis AtPI4Kγ3, a type II phosphoinositide 4-kinase, in abiotic stress responses and floral transition. *Plant Biotechnol J,* 14**,** 215-30.

ANGEL, C. A., LUTZ, L., YANG, X., RODRIGUEZ, A., ADAIR, A., ZHANG, Y., LEISNER, S. M., NELSON, R. S. & SCHOELZ, J. E. 2013. The P6 protein of Cauliflower mosaic virus interacts with CHUP1, a plant protein which moves chloroplasts on actin microfilaments. *Virology,* 443**,** 363-74.

ARAMBURU, J., ORTELLS, M. C., TEJEDOR, S., BUXADE, M. & LOPEZ-RODRIGUEZ, C. 2014. Transcriptional regulation of the stress response by mTOR. *Sci Signal,* 7**,** re2.

ARENA, G. D., RAMOS-GONZÁLEZ, P. L., FALK, B. W., CASTEEL, C. L., FREITAS-ASTÚA, J. & MACHADO, M. A. 2020. Plant Immune System Activation Upon Citrus Leprosis Virus C Infection Is Mimicked by the Ectopic Expression of the P61 Viral Protein. *Frontiers in Plant Science,* 11.

ARNQVIST, L., PERSSON, M., JONSSON, L., DUTTA, P. C. & SITBON, F. 2008. Overexpression of CYP710A1 and CYP710A4 in transgenic Arabidopsis plants increases the level of stigmasterol at the expense of sitosterol. *Planta,* 227**,** 309-17.

ASCENCIO-IBÁÑEZ, J. T., SOZZANI, R., LEE, T. J., CHU, T. M., WOLFINGER, R. D., CELLA, R. & HANLEY-BOWDOIN, L. 2008. Global analysis of Arabidopsis gene

expression uncovers a complex array of changes impacting pathogen response and cell cycle during geminivirus infection. *Plant Physiol,* 148**,** 436-54.

ASHYKHMINA, N., LORENZ, M., FRERIGMANN, H., KOPRIVOVA, A., HOFSETZ, E., STÜHRWOHLDT, N., FLÜGGE, U.-I., HAFERKAMP, I., KOPRIVA, S. & GIGOLASHVILI, T. 2019. PAPST2 Plays Critical Roles in Removing the Stress Signaling Molecule 3′-Phosphoadenosine 5′-Phosphate from the Cytosol and Its Subsequent Degradation in Plastids and Mitochondria. *The Plant Cell,* 31**,** 231-249.

BAK, A. & EMERSON, J. B. 2020. Cauliflower mosaic virus (CaMV) Biology, Management, and Relevance to GM Plant Detection for Sustainable Organic Agriculture. *Frontiers in Sustainable Food Systems,* 4.

BAK, A., GARGANI, D., MACIA, J. L., MALOUVET, E., VERNEREY, M. S., BLANC, S. & DRUCKER, M. 2013. Virus factories of cauliflower mosaic virus are virion reservoirs that engage actively in vector transmission. *J Virol,* 87**,** 12207-15.

BALAKIREVA, A. V. & ZAMYATNIN, A. A. 2018. Indispensable Role of Proteases in Plant Innate Immunity. *International Journal of Molecular Sciences,* 19**,** 629.

BARBEZ, E., KUBES, M., ROLCIK, J., BEZIAT, C., PENCIK, A., WANG, B., ROSQUETE, M. R., ZHU, J., DOBREV, P. I., LEE, Y., ZAZIMALOVA, E., PETRASEK, J., GEISLER, M., FRIML, J. & KLEINE-VEHN, J. 2012. A novel putative auxin carrier family regulates intracellular auxin homeostasis in plants. *Nature,* 485**,** 119-22.

BARRADA, A., MONTANE, M. H., ROBAGLIA, C. & MENAND, B. 2015. Spatial Regulation of Root Growth: Placing the Plant TOR Pathway in a Developmental Perspective. *Int J Mol Sci,* 16**,** 19671-97.

BELLIURE, B., JANSSEN, A., MARIS, P. C., PETERS, D. & SABELIS, M. W. 2005. Herbivore arthropods benefit from vectoring plant viruses. *Ecology Letters,* 8**,** 70-79.

BENJAMINI, Y. & HOCHBERG, Y. 1995. Controlling the False Discovery Rate: A Practical and Powerful Approach to Multiple Testing. *Journal of the Royal Statistical Society. Series B (Methodological),* 57**,** 289-300.

BENJAMINS, R., MALENICA, N. & LUSCHNIG, C. 2005. Regulating the regulator: the control of auxin transport. *Bioessays,* 27**,** 1246-55.

BENJAMINS, R. & SCHERES, B. 2008. Auxin: the looping star in plant development. *Annu Rev Plant Biol,* 59**,** 443-65.

BERGÈS, S. E., VASSEUR, F., BEDIÉE, A., ROLLAND, G., MASCLEF, D., DAUZAT, M., VAN MUNSTER, M. & VILE, D. 2020. Natural variation of Arabidopsis thaliana responses to Cauliflower mosaic virus infection upon water deficit. *PLoS Pathog,* 16**,** e1008557.

BHARTI, P., MAHAJAN, M., VISHWAKARMA, A. K., BHARDWAJ, J. & YADAV, S. K. 2015. AtROS1 overexpression provides evidence for epigenetic regulation of genes encoding enzymes of flavonoid biosynthesis and antioxidant pathways during salt stress in transgenic tobacco. *J Exp Bot,* 66**,** 5959-69.

BHAT, A. I., HOHN, T. & SELVARAJAN, R. 2016. Badnaviruses: The Current Global Scenario. *Viruses,* 8.

BLEECKER, A. B. & KENDE, H. 2000. Ethylene: A gaseous signal molecule in plants. *Annual Review of Cell and Developmental Biology,* 16**,** 1-+.

BOGRE, L., HENRIQUES, R. & MAGYAR, Z. 2013. TOR tour to auxin. *EMBO J,* 32**,** 1069-71.

BONNER, J. & BANDURSKI, R. S. 1952. Studies of the Physiology, Pharmacology, and Biochemistry of the Auxins. *Annual Review of Plant Physiology and Plant Molecular Biology,* 3**,** 59-86.

BOUSALEM, M., DOUZERY, E. J. & SEAL, S. E. 2008. Taxonomy, molecular phylogeny and evolution of plant reverse transcribing viruses (family Caulimoviridae) inferred from full-length genome and reverse transcriptase sequences. *Arch Virol,* 153**,** 1085-102.

BOUTROT, F., SEGONZAC, C., CHANG, K. N., QIAO, H., ECKER, J. R., ZIPFEL, C. & RATHJEN, J. P. 2010. Direct transcriptional control of the Arabidopsis immune receptor FLS2 by the ethylene-dependent transcription factors EIN3 and EIL1. *Proc Natl Acad Sci U S A,* 107**,** 14502-7.

BUROW, M., ZHANG, Z.-Y., OBER, J. A., LAMBRIX, V. M., WITTSTOCK, U., GERSHENZON, J. & KLIEBENSTEIN, D. J. 2008. ESP and ESM1 mediate indol-3-acetonitrile production from indol-3-ylmethyl glucosinolate in Arabidopsis. *Phytochemistry,* 69**,** 663-671.

CAMPOS, L., GRANELL, P., TARRAGA, S., LOPEZ-GRESA, P., CONEJERO, V., BELLES, J. M., RODRIGO, I. & LISON, P. 2014a. Salicylic acid and gentisic acid induce RNA silencing-related genes and plant resistance to RNA pathogens. *Plant Physiol Biochem,* 77**,** 35-43.

CAMPOS, L., GRANELL, P., TÁRRAGA, S., LÓPEZ-GRESA, P., CONEJERO, V., BELLÉS, J. M., RODRIGO, I. & LISÓN, P. 2014b. Salicylic acid and gentisic acid induce RNA silencing-related genes and plant resistance to RNA pathogens. *Plant Physiology and Biochemistry,* 77**,** 35-43.

CARR, J. P., TUNGADI, T., DONNELLY, R., BRAVO-CAZAR, A., RHEE, S. J., WATT, L. G., MUTUKU, J. M., WAMONJE, F. O., MURPHY, A. M., ARINAITWE, W., PATE, A. E., CUNNIFFE, N. J. & GILLIGAN, C. A. 2020. Modelling and

manipulation of aphid-mediated spread of non-persistently transmitted viruses. *Virus Res,* 277**,** 197845.

CARVALHO ADE, O. & GOMES, V. M. 2007. Role of plant lipid transfer proteins in plant cell physiology-a concise review. *Peptides,* 28**,** 1144-53.

CECCHINI, E., AL-KAFF, N. S., BANNISTER, A., GIANNAKOU, M. E., MCCALLUM, D. G., MAULE, A. J., MILNER, J. J. & COVEY, S. N. 1998. Pathogenic interactions between variants of cauliflower mosaic virus and Arabidopsis thaliana. *Journal of Experimental Botany,* 49**,** 731-737.

CECCHINI, E., GONG, Z., GERI, C., COVEY, S. N. & MILNER, J. J. 1997. Transgenic Arabidopsis lines expressing gene VI from cauliflower mosaic virus variants exhibit a range of symptom-like phenotypes and accumulate inclusion bodies. *Mol Plant Microbe Interact,* 10**,** 1094-101.

CHAPMAN, E. J. & ESTELLE, M. 2009. Mechanism of auxin-regulated gene expression in plants. *Annu Rev Genet,* 43**,** 265-85.

CHAPMAN, S., FAULKNER, C., KAISERLI, E., GARCIA-MATA, C., SAVENKOV, E. I., ROBERTS, A. G., OPARKA, K. J. & CHRISTIE, J. M. 2008. The photoreversible fluorescent protein iLOV outperforms GFP as a reporter of plant virus infection. *Proceedings of the National Academy of Sciences,* 105**,** 20038-20043.

CHAREST, A., WILKER, E. W., MCLAUGHLIN, M. E., LANE, K., GOWDA, R., COVEN, S., MCMAHON, K., KOVACH, S., FENG, Y., YAFFE, M. B., JACKS, T. & HOUSMAN, D. 2006. ROS fusion tyrosine kinase activates a SH2 domain-containing phosphatase-2/phosphatidylinositol 3-kinase/mammalian target of rapamycin signaling axis to form glioblastoma in mice. *Cancer Res,* 66**,** 7473-81.

CHEN, L. F., ROJAS, M., KON, T., GAMBY, K., XOCONOSTLE-CAZARES, B. & GILBERTSON, R. L. 2009. A severe symptom phenotype in tomato in Mali is

caused by a reassortant between a novel recombinant begomovirus (Tomato yellow leaf curl Mali virus) and a betasatellite. *Mol Plant Pathol,* 10**,** 415-30.

CHEN, Q.-S., YU, G.-L., ZOU, J.-N., WANG, J., QIU, H.-M., ZHU, R.-S., CHANG, H.-L., JIANG, H.-W., HU, Z.-B., LI, C.-Y., ZHANG, Y.-J., WANG, J.-H., WANG, X.-D., GAO, S., LIU, C.-Y., QI, Z.-M., FU, Y.-F. & XIN, D.-W. 2018. GmDRR1, a dirigent protein resistant to Phytophthora sojae in Glycine max (L.) Merr. *Journal of Integrative Agriculture,* 17**,** 1289-1298.

CHEN, Z., WANG, J., YE, M.-X., LI, H., JI, L.-X., LI, Y., CUI, D.-Q., LIU, J.-M. & AN, X.-M. 2013. A Novel Moderate Constitutive Promoter Derived from Poplar (Populus tomentosa Carrière). *International journal of molecular sciences,* 14**,** 6187-6204.

CHENG, R. H., OLSON, N. H. & BAKER, T. S. 1992. Cauliflower mosaic virus: a 420 subunit (T = 7), multilayer structure. *Virology,* 186**,** 655-68.

CHENG, Y., ZHOU, W., EL SHEERY, N. I., PETERS, C., LI, M., WANG, X. & HUANG, J. 2011. Characterization of the Arabidopsis glycerophosphodiester phosphodiesterase (GDPD) family reveals a role of the plastid-localized AtGDPD1 in maintaining cellular phosphate homeostasis under phosphate starvation. *Plant J,* 66**,** 781-95.

CHESNAIS, Q., COUTY, A., UZEST, M., BRAULT, V. & AMELINE, A. 2019. Plant infection by two different viruses induce contrasting changes of vectors fitness and behavior. *Insect Science,* 26**,** 86-96.

CHIANG, Y.-H. & COAKER, G. 2015. Effector Triggered Immunity: NLR Immune Perception and Downstream Defense Responses. *The Arabidopsis Book,* 2015.

CHOU, H. H. & HOLMES, M. H. 2001. DNA sequence quality trimming and vector removal. *Bioinformatics,* 17**,** 1093-104.

CHOW, B. & MCCOURT, P. 2006. Plant hormone receptors: perception is everything. *Genes Dev,* 20**,** 1998-2008.

CHRISTIE, J. M., HITOMI, K., ARVAI, A. S., HARTFIELD, K. A., METTLEN, M., PRATT, A. J., TAINER, J. A. & GETZOFF, E. D. 2012. Structural tuning of the fluorescent protein iLOV for improved photostability. *J Biol Chem,* 287**,** 22295-304.

CHRISTIE, J. M., SWARTZ, T. E., BOGOMOLNI, R. A. & BRIGGS, W. R. 2002. Phototropin LOV domains exhibit distinct roles in regulating photoreceptor function. *Plant Journal,* 32**,** 205-219.

CLOUGH, S. J. & BENT, A. F. 1998. Floral dip: a simplified method for Agrobacterium-mediated transformation of Arabidopsis thaliana. *Plant Journal,* 16**,** 735-743.

COLLUM, T. D. & CULVER, J. N. 2016. The impact of phytohormones on virus infection and disease. *Current Opinion in Virology,* 17**,** 25-31.

COSIO, C. & DUNAND, C. 2009. Specific functions of individual class III peroxidase genes. *J Exp Bot,* 60**,** 391-408.

COUTO, D. & ZIPFEL, C. 2016. Regulation of pattern recognition receptor signalling in plants. *Nature Reviews Immunology,* 16**,** 537-552.

CUTLER, S. R., RODRIGUEZ, P. L., FINKELSTEIN, R. R. & ABRAMS, S. R. 2010. Abscisic Acid: Emergence of a Core Signaling Network. *Annual Review of Plant Biology,* 61**,** 651-679.

CZARNECKA, E., VERNER, F. L. & GURLEY, W. B. 2012. A strategy for building an amplified transcriptional switch to detect bacterial contamination of plants. *Plant Mol Biol,* 78**,** 59-75.

DALAL, J., LEWIS, D. R., TIETZ, O., BROWN, E. M., BROWN, C. S., PALME, K., MUDAY, G. K. & SEDEROFF, H. W. 2016. ROSY1, a novel regulator of gravitropic response is a stigmasterol binding protein. *J Plant Physiol,* 196-197**,** 28-40.

DAVIS, A. M., HALL, A., MILLAR, A. J., DARRAH, C. & DAVIS, S. J. 2009. Protocol: Streamlined sub-protocols for floral-dip transformation and selection of transformants in Arabidopsis thaliana. *Plant Methods,* 5**,** 3.

DE CONINCK, B. M. A., SELS, J., VENMANS, E., THYS, W., GODERIS, I. J. W. M., CARR, XF, N, D., DELAUR, XE, L., S., CAMMUE, B. P. A., DE BOLLE, M. F. C. & MATHYS, J. 2010. Arabidopsis thaliana plant defensin AtPDF1. 1 is involved in the plant response to biotic stress. *The New Phytologist,* 187**,** 1075-1088.

DE TAPIA, M., HIMMELBACH, A. & HOHN, T. 1993. Molecular dissection of the cauliflower mosaic virus translation transactivator. *EMBO J,* 12**,** 3305-14.

DECHORGNAT, J., PATRIT, O., KRAPP, A., FAGARD, M. & DANIEL-VEDELE, F. 2012. Characterization of the Nrt2.6 gene in Arabidopsis thaliana: a link with plant response to biotic and abiotic stress. *PLoS One,* 7**,** e42491.

DELLAPORTA SL, W. J., HICKS JB 1983. A plant DNA mini- preparation: version II. *Plant Mol Biol Rep,* 1**,** 19–21.

DEPLEDGE, D. P., MOHR, I. & WILSON, A. C. 2019. Going the Distance: Optimizing RNA-Seq Strategies for Transcriptomic Analysis of Complex Viral Genomes. *Journal of Virology,* 93**,** e01342-18.

DEPUYDT, S. & HARDTKE, C. S. 2011. Hormone Signalling Crosstalk in Plant Growth Regulation. *Current Biology,* 21**,** R365-R373.

DERKSEN, H., RAMPITSCH, C. & DAAYF, F. 2013. Signaling cross-talk in plant disease resistance. *Plant Science,* 207**,** 79-87.

DHONDT, S., GEOFFROY, P., STELMACH, B. A., LEGRAND, M. & HEITZ, T. 2000. Soluble phospholipase A2 activity is induced before oxylipin accumulation in tobacco mosaic virus-infected tobacco leaves and is contributed by patatin-like enzymes. *The Plant Journal,* 23**,** 431-440.

DHONUKSHE, P., GRIGORIEV, I., FISCHER, R., TOMINAGA, M., ROBINSON, D. G., HASEK, J., PACIOREK, T., PETRASEK, J., SEIFERTOVA, D., TEJOS, R., MEISEL, L. A., ZAZIMALOVA, E., GADELLA, T. W., JR., STIERHOF, Y. D., UEDA, T., OIWA, K., AKHMANOVA, A., BROCK, R., SPANG, A. & FRIML, J. 2008. Auxin transport inhibitors impair vesicle motility and actin cytoskeleton dynamics in diverse eukaryotes. *Proc Natl Acad Sci U S A,* 105**,** 4489-94.

DIOP, S. I., GEERING, A. D. W., ALFAMA-DEPAUW, F., LOAEC, M., TEYCHENEY, P. Y. & MAUMUS, F. 2018. Tracheophyte genomes keep track of the deep evolution of the Caulimoviridae. *Sci Rep,* 8**,** 572.

DOBRENEL, T., CALDANA, C., HANSON, J., ROBAGLIA, C., VINCENTZ, M., VEIT, B. & MEYER, C. 2016. TOR Signaling and Nutrient Sensing. *Annu Rev Plant Biol,* 67**,** 261-85.

DONG, P., XIONG, F., QUE, Y., WANG, K., YU, L., LI, Z. & REN, M. 2015. Expression profiling and functional analysis reveals that TOR is a key player in regulating photosynthesis and phytohormone signaling pathways in Arabidopsis. *Front Plant Sci,* 6**,** 677.

DU, L., ALI, G. S., SIMONS, K. A., HOU, J., YANG, T., REDDY, A. S. N. & POOVAIAH, B. W. 2009. Ca2+/calmodulin regulates salicylic-acid-mediated plant immunity. *Nature,* 457**,** 1154-1158.

DURBAK, A., YAO, H. & MCSTEEN, P. 2012. Hormone signaling in plant development. *Current Opinion in Plant Biology,* 15**,** 92-96.

EARLEY, K., SMITH, M., WEBER, R., GREGORY, B. & POETHIG, R. 2010. An endogenous F-box protein regulates ARGONAUTE1 in Arabidopsis thaliana. *Silence,* 1**,** 15.

EGGERMONT, L., VERSTRAETEN, B. & VAN DAMME, E. J. M. 2017. Genome-Wide Screening for Lectin Motifs in Arabidopsis thaliana. *Plant Genome,* 10.

FEDER, D., MCGEARY, R. P., MITIC, N., LONHIENNE, T., FURTADO, A., SCHULZ, B. L., HENRY, R. J., SCHMIDT, S., GUDDAT, L. W. & SCHENK, G. 2020. Structural elements that modulate the substrate specificity of plant purple acid phosphatases: Avenues for improved phosphorus acquisition in crops. *Plant Sci,* 294**,** 110445.

FENG, M., ZUO, D., JIANG, X., LI, S., CHEN, J., JIANG, L., ZHOU, X. & JIANG, T. 2018. Identification of Strawberry vein banding virus encoded P6 as an RNA silencing suppressor. *Virology,* 520**,** 103-110.

FERNÁNDEZ-PÉREZ, F., VIVAR, T., POMAR, F., PEDREÑO, M. A. & NOVO-UZAL, E. 2015. Peroxidase 4 is involved in syringyl lignin formation in Arabidopsis thaliana. *J Plant Physiol,* 175**,** 86-94.

FIELD, B., FISTON-LAVIER, A.-S., KEMEN, A., GEISLER, K., QUESNEVILLE, H. & OSBOURN, A. E. 2011. Formation of plant metabolic gene clusters within dynamic chromosomal regions. *Proceedings of the National Academy of Sciences,* 108**,** 16116-16121.

FIELD, B. & OSBOURN, A. E. 2008. Metabolic diversification--independent assembly of operon-like gene clusters in different plants. *Science,* 320**,** 543-7.

FINK, G. R. 1998. Anatomy of a revolution. *Genetics,* 149**,** 473-7.

FONDONG, V. N. 2013. Geminivirus protein structure and function. *Mol Plant Pathol,* 14**,** 635-49.

FRIML, J., YANG, X., MICHNIEWICZ, M., WEIJERS, D., QUINT, A., TIETZ, O., BENJAMINS, R., OUWERKERK, P. B., LJUNG, K., SANDBERG, G., HOOYKAAS, P. J., PALME, K. & OFFRINGA, R. 2004. A PINOID-dependent binary switch in apical-basal PIN polar targeting directs auxin efflux. *Science,* 306**,** 862-5.

FUKAKI, H., TAMEDA, S., MASUDA, H. & TASAKA, M. 2002. Lateral root formation is blocked by a gain-of-function mutation in the SOLITARY-ROOT/IAA14 gene of Arabidopsis. *Plant J,* 29**,** 153-68.

GAO, Q.-M., ZHU, S., KACHROO, P. & KACHROO, A. 2015. Signal regulators of systemic acquired resistance. *Frontiers in Plant Science,* 6.

GAO, S., GUO, W., FENG, W., LIU, L., SONG, X., CHEN, J., HOU, W., ZHU, H., TANG, S. & HU, J. 2016. LTP3 contributes to disease susceptibility in Arabidopsis by enhancing abscisic acid (ABA) biosynthesis. *Molecular Plant Pathology,* 17**,** 412-426.

GARCION, C., LOHMANN, A., LAMODIÈRE, E., CATINOT, J., BUCHALA, A., DOERMANN, P. & MÉTRAUX, J. P. 2008. Characterization and biological function of the ISOCHORISMATE SYNTHASE2 gene of Arabidopsis. *Plant Physiol,* 147**,** 1279-87.

GAWTHORNE, J. A., REDDICK, L. E., AKPUNARLIEVA, S. N., BECKHAM, K. S. H., CHRISTIE, J. M., ALTO, N. M., GABRIELSEN, M. & ROE, A. J. 2012. Express Your LOV: An Engineered Flavoprotein as a Reporter for Protein Expression and Purification. *PLOS ONE,* 7**,** e52962.

GEERING, A. D. W. 2014. Caulimoviridae(Plant Pararetroviruses).

GEERING ADW, H. R. 2012. Family Caulimoviridae. *In: King AMQ, Adams MJ, Carestens EB, Lefkowitz EJ (eds) Virus taxonomy classification and*

nomenclature of viruses ninth report of the international committee on taxonomy of viruses, San Diego, Elsevier pp 424–443.

GEERING, A. D. W. & RANDLES, J. W. 2012. Virus Diseases of Tropical Crops.

GELDNER, N., ANDERS, N., WOLTERS, H., KEICHER, J., KORNBERGER, W., MULLER, P., DELBARRE, A., UEDA, T., NAKANO, A. & JURGENS, G. 2003. The Arabidopsis GNOM ARF-GEF mediates endosomal recycling, auxin transport, and auxin-dependent plant growth. *Cell,* 112**,** 219-30.

GERI, C., CECCHINI, E., GIANNAKOU, M. E., COVEY, S. N. & MILNER, J. J. 1999. Altered patterns of gene expression in Arabidopsis elicited by cauliflower mosaic virus (CaMV) infection and by a CaMV gene VI transgene. *Molecular Plant-Microbe Interactions,* 12**,** 377-384.

GERI, C., LOVE, A. J., CECCHINI, E., BARRETT, S. J., LAIRD, J., COVEY, S. N. & MILNER, J. J. 2004. Arabidopsis mutants that suppress the phenotype induced by transgene-mediated expression of cauliflower mosaic virus (CaMV) gene VI are less susceptible to CaMV-infection and show reduced ethylene sensitivity. *Plant Mol Biol,* 56**,** 111-24.

GIBSON, D. G., SMITH, H. O., HUTCHISON, C. A., 3RD, VENTER, J. C. & MERRYMAN, C. 2010. Chemical synthesis of the mouse mitochondrial genome. *Nat Methods,* 7**,** 901-3.

GIBSON, D. G., YOUNG, L., CHUANG, R. Y., VENTER, J. C., HUTCHISON, C. A., 3RD & SMITH, H. O. 2009. Enzymatic assembly of DNA molecules up to several hundred kilobases. *Nat Methods,* 6**,** 343-5.

GIMENEZ-IBANEZ, S. & SOLANO, R. 2013. Nuclear jasmonate and salicylate signaling and crosstalk in defense against pathogens. *Frontiers in Plant Science,* 4.

GIOLAI, M., VERWEIJ, W., LISTER, A., HEAVENS, D., MACAULAY, I. & CLARK, M. D. 2019. Spatially resolved transcriptomics reveals plant host responses to pathogens. *Plant Methods,* 15**,** 114.

GO, Y. S., LEE, S. B., KIM, H. J., KIM, J., PARK, H. Y., KIM, J. K., SHIBATA, K., YOKOTA, T., OHYAMA, K., MURANAKA, T., ARSENIYADIS, S. & SUH, M. C. 2012. Identification of marneral synthase, which is critical for growth and development in Arabidopsis. *Plant J,* 72**,** 791-804.

GRIMPLET, J., PIMENTEL, D., AGUDELO-ROMERO, P., MARTINEZ-ZAPATER, J. M. & FORTES, A. M. 2017. The LATERAL ORGAN BOUNDARIES Domain gene family in grapevine: genome-wide characterization and expression analyses during developmental processes and stress responses. *Sci Rep,* 7**,** 15968.

GUO, D., CHEN, F., INOUE, K., BLOUNT, J. W. & DIXON, R. A. 2001. Downregulation of caffeic acid 3-O-methyltransferase and caffeoyl CoA 3-O-methyltransferase in transgenic alfalfa. impacts on lignin structure and implications for the biosynthesis of G and S lignin. *The Plant cell,* 13**,** 73-88.

GUO, H. W. & ECKER, J. R. 2004. The ethylene signaling pathway: new insights. *Current Opinion in Plant Biology,* 7**,** 40-49.

HAAS, G., AZEVEDO, J., MOISSIARD, G., GELDREICH, A., HIMBER, C., BUREAU, M., FUKUHARA, T., KELLER, M. & VOINNET, O. 2008. Nuclear import of CaMV P6 is required for infection and suppression of the RNA silencing factor DRB4. *EMBO J,* 27**,** 2102-12.

HAAS, M., BUREAU, M., GELDREICH, A., YOT, P. & KELLER, M. 2002. Cauliflower mosaic virus: still in the news. *Mol Plant Pathol,* 3**,** 419-29.

HAAS, M., GELDREICH, A., BUREAU, M., DUPUIS, L., LEH, V., VETTER, G., KOBAYASHI, K., HOHN, T., RYABOVA, L., YOT, P. & KELLER, M. 2005. The

open reading frame VI product of Cauliflower mosaic virus is a nucleocytoplasmic protein: its N terminus mediates its nuclear export and formation of electron-dense viroplasms. *Plant Cell,* 17**,** 927-43.

HARRIES, P. A., PALANICHELVAM, K., YU, W. C., SCHOELZ, J. E. & NELSON, R. S. 2009. The Cauliflower Mosaic Virus Protein P6 Forms Motile Inclusions That Traffic along Actin Microfilaments and Stabilize Microtubules. *Plant Physiology,* 149**,** 1005-1016.

HARRISON, S. J., MOTT, E. K., PARSLEY, K., ASPINALL, S., GRAY, J. C. & COTTAGE, A. 2006. A rapid and robust method of identifying transformed Arabidopsis thaliana seedlings following floral dip transformation. *Plant Methods,* 2**,** 19.

HERRANZ, R., VANDENBRINK, J. P., VILLACAMPA, A., MANZANO, A., POEHLMAN, W. L., FELTUS, F. A., KISS, J. Z. & MEDINA, F. J. 2019. RNAseq Analysis of the Response of Arabidopsis thaliana to Fractional Gravity Under Blue-Light Stimulation During Spaceflight. *Frontiers in Plant Science,* 10.

HOH, F., UZEST, M., DRUCKER, M., PLISSON-CHASTANG, C., BRON, P., BLANC, S. & DUMAS, C. 2010. Structural insights into the molecular mechanisms of cauliflower mosaic virus transmission by its insect vector. *J Virol,* 84**,** 4706-13.

HOHN, T., CORSTEN, S., DOMINGUEZ, D., FUTTERER, J., KIRK, D., HEMMINGS-MIESZCZAK, M., POOGGIN, M., SCHARER-HERNANDEZ, N. & RYABOVA, L. 2001. Shunting is a translation strategy used by plant pararetroviruses (Caulimoviridae). *Micron,* 32**,** 51-7.

HOHN, T. & ROTHNIE, H. 2013. Plant pararetroviruses: replication and expression. *Curr Opin Virol,* 3**,** 621-8.

HRUZ, T., LAULE, O., SZABO, G., WESSENDORP, F., BLEULER, S., OERTLE, L., WIDMAYER, P., GRUISSEM, W. & ZIMMERMANN, P. 2008. Genevestigator

v3: a reference expression database for the meta-analysis of transcriptomes. *Adv Bioinformatics,* 2008**,** 420747.

HUIBERS, R. P., DE JONG, M., DEKTER, R. W. & VAN DEN ACKERVEKEN, G. 2009. Disease-specific expression of host genes during downy mildew infection of Arabidopsis. *Mol Plant Microbe Interact,* 22**,** 1104-15.

HUNTER, L. J., WESTWOOD, J. H., HEATH, G., MACAULAY, K., SMITH, A. G., MACFARLANE, S. A., PALUKAITIS, P. & CARR, J. P. 2013. Regulation of RNA-dependent RNA polymerase 1 and isochorismate synthase gene expression in Arabidopsis. *PLoS One,* 8**,** e66530.

INABA, J.-I. & NAGY, P. D. 2018. Tombusvirus RNA replication depends on the TOR pathway in yeast and plants. *Virology,* 519**,** 207-222.

INGWELL, L. L., EIGENBRODE, S. D. & BOSQUE-PEREZ, N. A. 2012. Plant viruses alter insect behavior to enhance their spread. *Scientific Reports,* 2.

ISLAM, S., SAJIB, S. D., JUI, Z. S., ARABIA, S., ISLAM, T. & GHOSH, A. 2019a. Genome-wide identification of glutathione S-transferase gene family in pepper, its classification, and expression profiling under different anatomical and environmental conditions. *Scientific Reports,* 9**,** 9101.

ISLAM, W., NAVEED, H., ZAYNAB, M., HUANG, Z. & CHEN, H. Y. H. 2019b. Plant defense against virus diseases; growth hormones in highlights. *Plant signaling & behavior,* 14**,** 1596719-1596719.

JAYAKANNAN, M., BOSE, J., BABOURINA, O., SHABALA, S., MASSART, A., POSCHENRIEDER, C. & RENGEL, Z. 2015. The NPR1-dependent salicylic acid signalling pathway is pivotal for enhanced salt and oxidative stress tolerance in Arabidopsis. *Journal of experimental botany,* 66**,** 1865-1875.

JIANG, Z., LI, J. & QU, L.-J. 2017. 2 - Auxins. *In:* LI, J., LI, C. & SMITH, S. M. (eds.) *Hormone Metabolism and Signaling in Plants.* Academic Press.

JIN, H., CHOI, S.-M., KANG, M.-J., YUN, S.-H., KWON, D.-J., NOH, Y.-S. & NOH, B. 2018. Salicylic acid-induced transcriptional reprogramming by the HAC–NPR1–TGA histone acetyltransferase complex in Arabidopsis. *Nucleic Acids Research,* 46**,** 11712-11725.

JING, Y. & LIN, R. 2015. The VQ Motif-Containing Protein Family of Plant-Specific Transcriptional Regulators. *Plant physiology,* 169**,** 371-378.

JOHNSON, P. R. & ECKER, J. R. 1998. The ethylene gas signal transduction pathway: A molecular perspective. *Annual Review of Genetics,* 32**,** 227-254.

JONES, J. D. & DANGL, J. L. 2006. The plant immune system. *Nature,* 444**,** 323-9.

JONES, R. A. 2009. Plant virus emergence and evolution: origins, new encounter scenarios, factors driving emergence, effects of changing world conditions, and prospects for control. *Virus Res,* 141**,** 113-30.

JULKE, S. & LUDWIG-MULLER, J. 2015. Response of Arabidopsis thaliana Roots with Altered Lipid Transfer Protein (LTP) Gene Expression to the Clubroot Disease and Salt Stress. *Plants (Basel),* 5.

JUNG, H. W., KIM, W. & HWANG, B. K. 2003. Three pathogen-inducible genes encoding lipid transfer protein from pepper are differentially activated by pathogens, abiotic, and environmental stresses. *Plant Cell Environ,* 26**,** 915-928.

KANNEGANTI, V. & GUPTA, A. K. 2008. Wall associated kinases from plants - an overview. *Physiology and molecular biology of plants : an international journal of functional plant biology,* 14**,** 109-118.

KASSCHAU, K. D., XIE, Z., ALLEN, E., LLAVE, C., CHAPMAN, E. J., KRIZAN, K. A. & CARRINGTON, J. C. 2003. P1/HC-Pro, a viral suppressor of RNA silencing, interferes with Arabidopsis development and miRNA unction. *Dev Cell,* 4**,** 205-17.

KAZAN, K. & MANNERS, J. M. 2009. Linking development to defense: auxin in plant-pathogen interactions. *Trends Plant Sci,* 14**,** 373-82.

KHELIFA, M., JOURNOU, S., KRISHNAN, K., GARGANI, D., ESPERANDIEU, P., BLANC, S. & DRUCKER, M. 2007. Electron-lucent inclusion bodies are structures specialized for aphid transmission of cauliflower mosaic virus. *J Gen Virol,* 88**,** 2872-80.

KIM, J.-S., LIM, J. Y., SHIN, H., KIM, B.-G., YOO, S.-D., KIM, W. T. & HUH, J. H. 2019. ROS1-Dependent DNA Demethylation Is Required for ABA-Inducible NIC3 Expression. *Plant Physiology,* 179**,** 1810-1821.

KIM, K. W., MOINUDDIN, S. G., ATWELL, K. M., COSTA, M. A., DAVIN, L. B. & LEWIS, N. G. 2012. Opposite stereoselectivities of dirigent proteins in Arabidopsis and schizandra species. *J Biol Chem,* 287**,** 33957-72.

KOBAYASHI, K. & HOHN, T. 2003. Dissection of cauliflower mosaic virus transactivator/viroplasmin reveals distinct essential functions in basic virus replication. *J Virol,* 77**,** 8577-83.

KOBAYASHI, K. & HOHN, T. 2004. The avirulence domain of Cauliflower mosaic virus transactivator/viroplasmin is a determinant of viral virulence in susceptible hosts. *Mol Plant Microbe Interact,* 17**,** 475-83.

KON, T. & GILBERTSON, R. L. 2012. Two genetically related begomoviruses causing tomato leaf curl disease in Togo and Nigeria differ in virulence and host range but do not require a betasatellite for induction of disease symptoms. *Arch Virol,* 157**,** 107-20.

KONG, X., ZHANG, C., ZHENG, H., SUN, M., ZHANG, F., ZHANG, M., CUI, F., LV, D., LIU, L., GUO, S., ZHANG, Y., YUAN, X., ZHAO, S., TIAN, H. & DING, Z. 2020. Antagonistic Interaction between Auxin and SA Signaling Pathways Regulates Bacterial Infection through Lateral Root in Arabidopsis. *Cell Rep,* 32**,** 108060.

KOORNNEEF, M. & MEINKE, D. 2010. The development of Arabidopsis as a model plant. *Plant J,* 61**,** 909-21.

KOVAČ, M., MÜLLER, A., JARH, D. M., MILAVEC, M., DÜCHTING, P. & RAVNIKAR, M. 2009. Multiple hormone analysis indicates involvement of jasmonate signalling in the early defence of potato to potato virus Y NTN. *Biologia plantarum,* 53**,** 195-199.

KRASAVINA, M. S., MALYSHENKO, S. I., RALDUGINA, G. N., BURMISTROVA, N. A. & NOSOV, A. V. 2002. Can Salicylic Acid Affect the Intercellular Transport of the Tobacco Mosaic Virus by Changing Plasmodesmal Permeability? *Russian Journal of Plant Physiology,* 49**,** 61-67.

KRAVCHENKO, A., CITERNE, S., JEHANNO, I., BERSIMBAEV, R. I., VEIT, B., MEYER, C. & LEPRINCE, A. S. 2015. Mutations in the Arabidopsis Lst8 and Raptor genes encoding partners of the TOR complex, or inhibition of TOR activity decrease abscisic acid (ABA) synthesis. *Biochem Biophys Res Commun,* 467**,** 992-7.

LACERDA, A., VASCONCELOS, É., PELEGRINI, P. & GROSSI-DE-SA, M. F. 2014. Antifungal defensins and their role in plant defense. *Frontiers in Microbiology,* 5.

LAIRD, J., MCINALLY, C., CARR, C., DODDIAH, S., YATES, G., CHRYSANTHOU, E., KHATTAB, A., LOVE, A. J., GERI, C., SADANANDOM, A., SMITH, B. O., KOBAYASHI, K. & MILNER, J. J. 2013. Identification of the domains of cauliflower mosaic virus protein P6 responsible for suppression of RNA silencing and salicylic acid signalling. *J Gen Virol,* 94**,** 2777-89.

LE BERRE, J. Y., GOURGUES, M., SAMANS, B., KELLER, H., PANABIÈRES, F. & ATTARD, A. 2017. Transcriptome dynamic of Arabidopsis roots infected with Phytophthora parasitica identifies VQ29, a gene induced during the penetration and involved in the restriction of infection. *PLoS One,* 12**,** e0190341.

LE, T. N., SCHUMANN, U., SMITH, N. A., TIWARI, S., AU, P. C., ZHU, Q. H., TAYLOR, J. M., KAZAN, K., LLEWELLYN, D. J., ZHANG, R., DENNIS, E. S. & WANG, M. B. 2014. DNA demethylases target promoter transposable elements to positively regulate stress responsive genes in Arabidopsis. *Genome Biol,* 15**,** 458.

LEE, W.-S., FU, S.-F., LI, Z., MURPHY, A. M., DOBSON, E. A., GARLAND, L., CHALUVADI, S. R., LEWSEY, M. G., NELSON, R. S. & CARR, J. P. 2016. Salicylic acid treatment and expression of an RNA-dependent RNA polymerase 1 transgene inhibit lethal symptoms and meristem invasion during tobacco mosaic virus infection in Nicotiana benthamiana. *BMC Plant Biology,* 16**,** 15.

LEISNER, S. M. & SCHOELZ, J. E. 2018. Joining the Crowd: Integrating Plant Virus Proteins into the Larger World of Pathogen Effectors. *Annu Rev Phytopathol,* 56**,** 89-110.

LEUZINGER, K., DENT, M., HURTADO, J., STAHNKE, J., LAI, H., ZHOU, X. & CHEN, Q. 2013. Efficient agroinfiltration of plants for high-level transient expression of recombinant proteins. *J Vis Exp*.

LI, R., WELDEGERGIS, B. T., LI, J., JUNG, C., QU, J., SUN, Y. W., QIAN, H. M., TEE, C., VAN LOON, J. J. A., DICKE, M., CHUA, N. H., LIU, S. S. & YE, J. 2014a. Virulence Factors of Geminivirus Interact with MYC2 to Subvert Plant Resistance and Promote Vector Performance. *Plant Cell,* 26**,** 4991-5008.

LI, S. & CHOU, H. H. 2004. LUCY2: an interactive DNA sequence quality trimming and vector removal tool. *Bioinformatics,* 20**,** 2865-6.

LI, T., HUANG, Y., XU, Z.-S., WANG, F. & XIONG, A.-S. 2019. Salicylic acid-induced differential resistance to the Tomato yellow leaf curl virus among resistant and susceptible tomato cultivars. *BMC Plant Biology,* 19**,** 173.

LI, Y., JING, Y., LI, J., XU, G. & LIN, R. 2014b. Arabidopsis VQ MOTIF-CONTAINING PROTEIN29 represses seedling deetiolation by interacting with PHYTOCHROME-INTERACTING FACTOR1. *Plant Physiol,* 164**,** 2068-80.

LI, Y. & LEISNER, S. M. 2002. Multiple domains within the Cauliflower mosaic virus gene VI product interact with the full-length protein. *Mol Plant Microbe Interact,* 15**,** 1050-7.

LIANG, C., OH, B. H. & JUNG, J. U. 2015. Novel functions of viral anti-apoptotic factors. *Nat Rev Microbiol,* 13**,** 7-12.

LIEBERTHAL, W. & LEVINE, J. S. 2012. Mammalian target of rapamycin and the kidney. I. The signaling pathway. *Am J Physiol Renal Physiol,* 303**,** F1-10.

LIEPMAN, A. H. & OLSEN, L. J. 2003. Alanine aminotransferase homologs catalyze the glutamate:glyoxylate aminotransferase reaction in peroxisomes of Arabidopsis. *Plant Physiol,* 131**,** 215-27.

LIONETTI, V., RAIOLA, A., CAMARDELLA, L., GIOVANE, A., OBEL, N., PAULY, M., FAVARON, F., CERVONE, F. & BELLINCAMPI, D. 2007. Overexpression of pectin methylesterase inhibitors in Arabidopsis restricts fungal infection by Botrytis cinerea. *Plant Physiol,* 143**,** 1871-80.

LIPING, Y., TAICHENG, J., YANJU, W., CHENJING, L., DAWEI, M., YUE, W. & XIAOFU, Z. 2021. *Research Square*.

LIU, F., JIANG, H., YE, S., CHEN, W.-P., LIANG, W., XU, Y., SUN, B., SUN, J., WANG, Q., COHEN, J. D. & LI, C. 2010. The Arabidopsis P450 protein CYP82C2

modulates jasmonate-induced root growth inhibition, defense gene expression and indole glucosinolate biosynthesis. *Cell Research,* 20**,** 539-552.

LIU, H. & TIMKO, M. P. 2021. Jasmonic Acid Signaling and Molecular Crosstalk with Other Phytohormones. *Int J Mol Sci,* 22.

LOEWITH, R. & HALL, M. N. 2011. Target of rapamycin (TOR) in nutrient signaling and growth control. *Genetics,* 189**,** 1177-201.

LOLLE, S., STEVENS, D. & COAKER, G. 2020. Plant NLR-triggered immunity: from receptor activation to downstream signaling. *Current Opinion in Immunology,* 62**,** 99-105.

LÓPEZ SÁNCHEZ, A., STASSEN, J. H., FURCI, L., SMITH, L. M. & TON, J. 2016. The role of DNA (de)methylation in immune responsiveness of Arabidopsis. *Plant J,* 88**,** 361-374.

LOVE, A. J., GERI, C., LAIRD, J., CARR, C., YUN, B. W., LOAKE, G. J., TADA, Y., SADANANDOM, A. & MILNER, J. J. 2012. Cauliflower mosaic virus protein P6 inhibits signaling responses to salicylic acid and regulates innate immunity. *PLoS One,* 7**,** e47535.

LOVE, A. J., LAIRD, J., HOLT, J., HAMILTON, A. J., SADANANDOM, A. & MILNER, J. J. 2007a. Cauliflower mosaic virus protein P6 is a suppressor of RNA silencing. *J Gen Virol,* 88**,** 3439-44.

LOVE, A. J., LAVAL, V., GERI, C., LAIRD, J., TOMOS, A. D., HOOKS, M. A. & MILNER, J. J. 2007b. Components of Arabidopsis defense- and ethylene-signaling pathways regulate susceptibility to Cauliflower mosaic virus by restricting long-distance movement. *Mol Plant Microbe Interact,* 20**,** 659-70.

LOVE, A. J., YUN, B. W., LAVAL, V., LOAKE, G. J. & MILNER, J. J. 2005. Cauliflower mosaic virus, a compatible pathogen of Arabidopsis, engages three distinct

defense-signaling pathways and activates rapid systemic generation of reactive oxygen species. *Plant Physiol,* 139**,** 935-48.

LOZANO-DURAN, R., ROSAS-DIAZ, T., GUSMAROLI, G., LUNA, A. P., TACONNAT, L., DENG, X. W. & BEJARANO, E. R. 2011. Geminiviruses subvert ubiquitination by altering CSN-mediated derubylation of SCF E3 ligase complexes and inhibit jasmonate signaling in Arabidopsis thaliana. *Plant Cell,* 23**,** 1014-32.

LUCAS, W. J. 2006. Plant viral movement proteins: agents for cell-to-cell trafficking of viral genomes. *Virology,* 344**,** 169-84.

LUKHOVITSKAYA, N. & RYABOVA, L. A. 2019. Cauliflower mosaic virus transactivator protein (TAV) can suppress nonsense-mediated decay by targeting VARICOSE, a scaffold protein of the decapping complex. *Sci Rep,* 9**,** 7042.

LUTZ, L., OKENKA, G., SCHOELZ, J. & LEISNER, S. 2015. Mutations within A 35 amino acid region of P6 influence self-association, inclusion body formation, and Caulimovirus infectivity. *Virology,* 476**,** 26-36.

LUTZ, L., RAIKHY, G. & LEISNER, S. M. 2012. Cauliflower mosaic virus major inclusion body protein interacts with the aphid transmission factor, the virion-associated protein, and gene VII product. *Virus Res,* 170**,** 150-3.

MARTINIERE, A., ZANCARINI, A. & DRUCKER, M. 2009. Aphid transmission of cauliflower mosaic virus: the role of the host plant. *Plant Signal Behav,* 4**,** 548-50.

MARZIN, S., HANEMANN, A., SHARMA, S., HENSEL, G., KUMLEHN, J., SCHWEIZER, G. & RÖDER, M. S. 2016. Are PECTIN ESTERASE INHIBITOR Genes Involved in Mediating Resistance to Rhynchosporium commune in Barley? *PloS one,* 11**,** e0150485-e0150485.

MAULE, A. J. 2007. Virus and Host Plant Interactions.

MCFADDEN, G. & SIMON, A. E. 2011. Building bridges between plant and animal viruses. *Curr Opin Virol,* 1**,** 319-21.

MENAND, B., MEYER, C. & ROBAGLIA, C. 2004. Plant growth and the TOR pathway. *Curr Top Microbiol Immunol,* 279**,** 97-113.

MERCHANTE, C. & STEPANOVA, A. N. 2017. The Triple Response Assay and Its Use to Characterize Ethylene Mutants in Arabidopsis. *Methods Mol Biol,* 1573**,** 163-209.

MICHNIEWICZ, M., ZAGO, M. K., ABAS, L., WEIJERS, D., SCHWEIGHOFER, A., MESKIENE, I., HEISLER, M. G., OHNO, C., ZHANG, J., HUANG, F., SCHWAB, R., WEIGEL, D., MEYEROWITZ, E. M., LUSCHNIG, C., OFFRINGA, R. & FRIML, J. 2007. Antagonistic regulation of PIN phosphorylation by PP2A and PINOID directs auxin flux. *Cell,* 130**,** 1044-56.

MILLS-LUJAN, K. & DEOM, C. M. 2010. Geminivirus C4 protein alters Arabidopsis development. *Protoplasma,* 239**,** 95-110.

MOEDER, W., URQUHART, W., UNG, H. & YOSHIOKA, K. 2011. The Role of Cyclic Nucleotide-Gated Ion Channels in Plant Immunity. *Molecular Plant,* 4**,** 442-452.

MOISSIARD, G. & VOINNET, O. 2004. Viral suppression of RNA silencing in plants. *Mol Plant Pathol,* 5**,** 71-82.

MUDGETT, M. B. 2005. New insights to the function of phytopathogenic bacterial type III effectors in plants. *Annu Rev Plant Biol,* 56**,** 509-31.

MURPHY, A. M., ZHOU, T. & CARR, J. P. 2020. An update on salicylic acid biosynthesis, its induction and potential exploitation by plant viruses. *Current Opinion in Virology,* 42**,** 8-17.

MYHRE, M. R., FENTON, K. A., EGGERT, J., NIELSEN, K. M. & TRAAVIK, T. 2005. The 35S CaMV plant virus promoter is active in human enterocyte-like cells. *European Food Research and Technology,* 222**,** 185-193.

NAGASHIMA, Y., IWATA, Y., ASHIDA, M., MISHIBA, K. & KOIZUMI, N. 2014. Exogenous salicylic acid activates two signaling arms of the unfolded protein response in Arabidopsis. *Plant Cell Physiol,* 55**,** 1772-8.

NICAISE, V. 2014. Crop immunity against viruses: outcomes and future challenges. *Front Plant Sci,* 5**,** 660.

NUTZMANN, H. W. & OSBOURN, A. 2015. Regulation of metabolic gene clusters in Arabidopsis thaliana. *New Phytol,* 205**,** 503-10.

OIDE, S., BEJAI, S., STAAL, J., GUAN, N., KALIFF, M. & DIXELIUS, C. 2013. A novel role of PR2 in abscisic acid (ABA) mediated, pathogen-induced callose deposition in Arabidopsis thaliana. *New Phytol,* 200**,** 1187-99.

OKA, K., KOBAYASHI, M., MITSUHARA, I. & SEO, S. 2013. Jasmonic acid negatively regulates resistance to Tobacco mosaic virus in tobacco. *Plant Cell Physiol,* 54**,** 1999-2010.

OUIBRAHIM, L., RUBIO, A. G., MORETTI, A., MONTANÉ, M.-H., MENAND, B., MEYER, C., ROBAGLIA, C. & CARANTA, C. 2015. Potyviruses differ in their requirement for TOR signalling. *Journal of General Virology,* 96**,** 2898-2903.

PADMANABHAN, M. S., GOREGAOKER, S. P., GOLEM, S., SHIFERAW, H. & CULVER, J. N. 2005. Interaction of the tobacco mosaic virus replicase protein with the Aux/IAA protein PAP1/IAA26 is associated with disease development. *J Virol,* 79**,** 2549-58.

PAGÁN, I., FRAILE, A., FERNANDEZ-FUEYO, E., MONTES, N., ALONSO-BLANCO, C. & GARCÍA-ARENAL, F. 2010. Arabidopsis thaliana as a model for the study

of plant-virus co-evolution. *Philosophical transactions of the Royal Society of London. Series B, Biological sciences,* 365**,** 1983-1995.

PALUKAITIS, P., YOON, J. Y., CHOI, S. K. & CARR, J. P. 2017. Manipulation of induced resistance to viruses. *Curr Opin Virol,* 26**,** 141-148.

PANDIAN, B. A., SATHISHRAJ, R., DJANAGUIRAMAN, M., PRASAD, P. V. V. & JUGULAM, M. 2020. Role of Cytochrome P450 Enzymes in Plant Stress Response. *Antioxidants (Basel, Switzerland),* 9**,** 454.

PARISI, K., SHAFEE, T. M. A., QUIMBAR, P., VAN DER WEERDEN, N. L., BLEACKLEY, M. R. & ANDERSON, M. A. 2019. The evolution, function and mechanisms of action for plant defensins. *Seminars in Cell & Developmental Biology,* 88**,** 107-118.

PARK, H. S., HIMMELBACH, A., BROWNING, K. S., HOHN, T. & RYABOVA, L. A. 2001. A plant viral "reinitiation" factor interacts with the host translational machinery. *Cell,* 106**,** 723-33.

PARTHASARATHY, A., ADAMS, L. E., SAVKA, F. C. & HUDSON, A. O. 2019. The Arabidopsis thaliana gene annotated by the locus tag At3g08860 encodes alanine aminotransferase. *Plant Direct,* 3**,** e00171.

PATKAR, R. N. & CHATTOO, B. B. 2006. Transgenic indica Rice Expressing ns-LTP-Like Protein Shows Enhanced Resistance to Both Fungal and Bacterial Pathogens. *Molecular Breeding,* 17**,** 159-171.

PÉGEOT, H., KOH, C. S., PETRE, B., MATHIOT, S., DUPLESSIS, S., HECKER, A., DIDIERJEAN, C. & ROUHIER, N. 2014. The poplar Phi class glutathione transferase: expression, activity and structure of GSTF1. *Frontiers in Plant Science,* 5.

PESTI, R., KONTRA, L., PAUL, K., VASS, I., CSORBA, T., HAVELDA, Z. & VARALLYAY, E. 2019. Differential gene expression and physiological changes during acute or persistent plant virus interactions may contribute to viral symptom differences. *PLoS One,* 14**,** e0216618.

PFEIFFER, P. & HOHN, T. 1983. Involvement of reverse transcription in the replication of cauliflower mosaic virus: a detailed model and test of some aspects. *Cell,* 33**,** 781-9.

PIETERSE, C. M. & VAN LOON, L. C. 2004. NPR1: the spider in the web of induced resistance signaling pathways. *Curr Opin Plant Biol,* 7**,** 456-64.

PIROUX, N., SAUNDERS, K., PAGE, A. & STANLEY, J. 2007. Geminivirus pathogenicity protein C4 interacts with Arabidopsis thaliana shaggy-related protein kinase AtSKeta, a component of the brassinosteroid signalling pathway. *Virology,* 362**,** 428-40.

PLISSON, C., UZEST, M., DRUCKER, M., FROISSART, R., DUMAS, C., CONWAY, J., THOMAS, D., BLANC, S. & BRON, P. 2005. Structure of the mature P3-virus particle complex of cauliflower mosaic virus revealed by cryo-electron microscopy. *J Mol Biol,* 346**,** 267-77.

PODEVIN, N. & DU JARDIN, P. 2012. Possible consequences of the overlap between the CaMV 35S promoter regions in plant transformation vectors used and the viral gene VI in transgenic plants. *GM Crops Food,* 3**,** 296-300.

POKOTYLO, I., KRAVETS, V. & RUELLAND, E. 2019. Salicylic Acid Binding Proteins (SABPs): The Hidden Forefront of Salicylic Acid Signalling. *Int J Mol Sci,* 20.

RAMÍREZ, V., AGORIO, A., COEGO, A., GARCÍA-ANDRADE, J., HERNÁNDEZ, M. J., BALAGUER, B., OUWERKERK, P. B. F., ZARRA, I. & VERA, P. 2011. MYB46 Modulates Disease Susceptibility to Botrytis cinerea in Arabidopsis. *Plant Physiology,* 155**,** 1920-1935.

RICH-GRIFFIN, C., STECHEMESSER, A., FINCH, J., LUCAS, E., OTT, S. & SCHAFER, P. 2020. Single-Cell Transcriptomics: A High-Resolution Avenue for Plant Functional Genomics. *Trends Plant Sci,* 25**,** 186-197.

ROBAGLIA, C., THOMAS, M. & MEYER, C. 2012. Sensing nutrient and energy status by SnRK1 and TOR kinases. *Curr Opin Plant Biol,* 15**,** 301-7.

ROBERT-SEILANIANTZ, A., GRANT, M. & JONES, J. D. G. 2011. Hormone Crosstalk in Plant Disease and Defense: More Than Just JASMONATE-SALICYLATE Antagonism. *Annual Review of Phytopathology, Vol 49,* 49**,** 317-343.

ROBERTS, K., LOVE, A. J., LAVAL, V., LAIRD, J., TOMOS, A. D., HOOKS, M. A. & MILNER, J. J. 2007. Long-distance movement of Cauliflower mosaic virus and host defence responses in Arabidopsis follow a predictable pattern that is determined by the leaf orthostichy. *New Phytol,* 175**,** 707-17.

ROBINSON, M. D., MCCARTHY, D. J. & SMYTH, G. K. 2010. edgeR: a Bioconductor package for differential expression analysis of digital gene expression data. *Bioinformatics,* 26**,** 139-40.

ROBINSON, M. D. & SMYTH, G. K. 2008. Small-sample estimation of negative binomial dispersion, with applications to SAGE data. *Biostatistics,* 9**,** 321-32.

RODRIGUEZ, A., ANGEL, C. A., LUTZ, L., LEISNER, S. M., NELSON, R. S. & SCHOELZ, J. E. 2014. Association of the P6 protein of Cauliflower mosaic virus with plasmodesmata and plasmodesmal proteins. *Plant Physiol,* 166**,** 1345-58.

ROTHNIE, H. M., CHAPDELAINE, Y. & HOHN, T. 1994. Pararetroviruses and retroviruses: a comparative review of viral structure and gene expression strategies. *Adv Virus Res,* 44**,** 1-67.

RYABOVA, L., PARK, H. S. & HOHN, T. 2004. Control of translation reinitiation on the cauliflower mosaic virus (CaMV) polycistronic RNA. *Biochem Soc Trans,* 32**,** 592-6.

RYBICKI, E. 2015. *A Short History of the Discovery of Viruses*.

SANTNER, A. & ESTELLE, M. 2009. Recent advances and emerging trends in plant hormone signalling. *Nature,* 459**,** 1071-1078.

SAROWAR, S., KIM, Y. J., KIM, K. D., HWANG, B. K., OK, S. H. & SHIN, J. S. 2009. Overexpression of lipid transfer protein (LTP) genes enhances resistance to plant pathogens and LTP functions in long-distance systemic signaling in tobacco. *Plant Cell Reports,* 28**,** 419-427.

SASAYA, T., NAKAZONO-NAGAOKA, E., SAIKA, H., AOKI, H., HIRAGURI, A., NETSU, O., UEHARA-ICHIKI, T., ONUKI, M., TOKI, S., SAITO, K. & YATOU, O. 2014. Transgenic strategies to confer resistance against viruses in rice plants. *Front Microbiol,* 4**,** 409.

SATHOFF, A. E. & SAMAC, D. A. 2018. Antibacterial Activity of Plant Defensins. *Molecular Plant-Microbe Interactions®,* 32**,** 507-514.

SATO, Y., TEZUKA, A., KASHIMA, M., DEGUCHI, A., SHIMIZU-INATSUGI, R., YAMAZAKI, M., SHIMIZU, K. K. & NAGANO, A. J. 2019. Transcriptional Variation in Glucosinolate Biosynthetic Genes and Inducible Responses to Aphid Herbivory on Field-Grown Arabidopsis thaliana. *Front Genet,* 10**,** 787.

SAUERBRUNN, N. & SCHLAICH, N. L. 2004. PCC1: a merging point for pathogen defence and circadian signalling in Arabidopsis. *Planta,* 218**,** 552-61.

SAUNDERS, K., LUCY, A. P. & COVEY, S. N. 1990. Susceptibility of Brassica species to cauliflower mosaic virus infection is related to a specific stage in the virus multiplication cycle. *J Gen Virol,* 71 (Pt 8)**,** 1641-7.

SCHEPETILNIKOV, M., DIMITROVA, M., MANCERA-MARTINEZ, E., GELDREICH, A., KELLER, M. & RYABOVA, L. A. 2013. TOR and S6K1 promote translation reinitiation of uORF-containing mRNAs via phosphorylation of eIF3h. *EMBO J,* 32**,** 1087-102.

SCHEPETILNIKOV, M., KOBAYASHI, K., GELDREICH, A., CARANTA, C., ROBAGLIA, C., KELLER, M. & RYABOVA, L. A. 2011. Viral factor TAV recruits TOR/S6K1 signalling to activate reinitiation after long ORF translation. *EMBO J,* 30**,** 1343-56.

SCHLUCKING, K., EDEL, K. H., KOSTER, P., DRERUP, M. M., ECKERT, C., STEINHORST, L., WAADT, R., BATISTIC, O. & KUDLA, J. 2013. A new beta-estradiol-inducible vector set that facilitates easy construction and efficient expression of transgenes reveals CBL3-dependent cytoplasm to tonoplast translocation of CIPK5. *Mol Plant,* 6**,** 1814-29.

SCHMELZLE, T., BECK, T., MARTIN, D. E. & HALL, M. N. 2004. Activation of the RAS/cyclic AMP pathway suppresses a TOR deficiency in yeast. *Mol Cell Biol,* 24**,** 338-51.

SCHOELZ, J. E., ANGEL, C. A., NELSON, R. S. & LEISNER, S. M. 2016. A model for intracellular movement of Cauliflower mosaic virus: the concept of the mobile virion factory. *J Exp Bot,* 67**,** 2039-48.

SCHOELZ, J. E. & LEISNER, S. 2017. Setting Up Shop: The Formation and Function of the Viral Factories of Cauliflower mosaic virus. *Frontiers in Plant Science,* 8.

SEVIK, H. & GUNEY, K. 2013. Effects of IAA, IBA, NAA, and GA3 on Rooting and Morphological Features of Melissa officinalis L. Stem Cuttings. *The Scientific World Journal,* 2013**,** 909507.

SHEPHERD, R. J., WAKEMAN, R. J. & ROMANKO, R. R. 1968. DNA in cauliflower mosaic virus. *Virology,* 36**,** 150-2.

SHER KHAN, R., IQBAL, A., MALAK, R., SHEHRYAR, K., ATTIA, S., AHMED, T., ALI KHAN, M., ARIF, M. & MII, M. 2019. Plant defensins: types, mechanism of action and prospects of genetic engineering for enhanced disease resistance in plants. *3 Biotech,* 9**,** 192.

SHIMOBAYASHI, M. & HALL, M. N. 2014. Making new contacts: the mTOR network in metabolism and signalling crosstalk. *Nat Rev Mol Cell Biol,* 15**,** 155-62.

SHIN, H., SHIN, H. S., CHEN, R. & HARRISON, M. J. 2006. Loss of At4 function impacts phosphate distribution between the roots and the shoots during phosphate starvation. *Plant J,* 45**,** 712-26.

SHINOZAWA, A., OTAKE, R., TAKEZAWA, D., UMEZAWA, T., KOMATSU, K., TANAKA, K., AMAGAI, A., ISHIKAWA, S., HARA, Y., KAMISUGI, Y., CUMING, A. C., HORI, K., OHTA, H., TAKAHASHI, F., SHINOZAKI, K., HAYASHI, T., TAJI, T. & SAKATA, Y. 2019. SnRK2 protein kinases represent an ancient system in plants for adaptation to a terrestrial environment. *Communications Biology,* 2**,** 30.

SHIVAPRASAD, P. V., RAJESWARAN, R., BLEVINS, T., SCHOELZ, J., MEINS, F., JR., HOHN, T. & POOGGIN, M. M. 2008. The CaMV transactivator/viroplasmin interferes with RDR6-dependent trans-acting and secondary siRNA pathways in Arabidopsis. *Nucleic Acids Res,* 36**,** 5896-909.

SMITH, L. A. 2007. Interactions between cauliflower mosaic virus and auxin signalling. *PhD Thesis, University of Glasgow, UK*.

SOHAL, A. K., LOVE, CECCHINI, E., COVEY, S. N., JENKINS, G. I. & MILNER, J. J. 1999. Cauliflower mosaic virus infection stimulates lipid transfer protein gene expression in Arabidopsis. *Journal of Experimental Botany,* 50**,** 1727-1733.

SONG, S. S., QI, T. C., WASTERNACK, C. & XIE, D. X. 2014. Jasmonate signaling and crosstalk with gibberellin and ethylene. *Current Opinion in Plant Biology,* 21**,** 112-119.

SONG, W. Y., MARTINOIA, E., LEE, J., KIM, D., KIM, D. Y., VOGT, E., SHIM, D., CHOI, K. S., HWANG, I. & LEE, Y. 2004. A novel family of cys-rich membrane proteins mediates cadmium resistance in Arabidopsis. *Plant Physiol,* 135**,** 1027-39.

SOTO, G., ALLEVA, K., MAZZELLA, M. A., AMODEO, G. & MUSCHIETTI, J. P. 2008. AtTIP1;3 and AtTIP5;1, the only highly expressed Arabidopsis pollen-specific aquaporins, transport water and urea. *FEBS Lett,* 582**,** 4077-82.

SPALDING, E. P. 2013. Diverting the downhill flow of auxin to steer growth during tropisms. *Am J Bot,* 100**,** 203-14.

SRIVASTAVA, A., GEORGE, J. & KARUTURI, R. K. M. 2019. Transcriptome Analysis. *In:* RANGANATHAN, S., GRIBSKOV, M., NAKAI, K. & SCHÖNBACH, C. (eds.) *Encyclopedia of Bioinformatics and Computational Biology.* Oxford: Academic Press.

STONE, S. L., BRAYBROOK, S. A., PAULA, S. L., KWONG, L. W., MEUSER, J., PELLETIER, J., HSIEH, T. F., FISCHER, R. L., GOLDBERG, R. B. & HARADA, J. J. 2008. Arabidopsis LEAFY COTYLEDON2 induces maturation traits and auxin activity: Implications for somatic embryogenesis. *Proc Natl Acad Sci U S A,* 105**,** 3151-6.

STOTZ, H. U., THOMSON, J. G. & WANG, Y. 2009. Plant defensins: defense, development and application. *Plant signaling & behavior,* 4**,** 1010-1012.

SUKAL, A. C., KIDANEMARIAM, D. B., DALE, J. L., HARDING, R. M. & JAMES, A. P. 2018. Characterization of a novel member of the family Caulimoviridae infecting

Dioscorea nummularia in the Pacific, which may represent a new genus of dsDNA plant viruses. *PLoS One,* 13**,** e0203038.

SWARTZ, T. E., CORCHNOY, S. B., CHRISTIE, J. M., LEWIS, J. W., SZUNDI, I., BRIGGS, W. R. & BOGOMOLNI, R. A. 2001. The photocycle of a flavin-binding domain of the blue light photoreceptor phototropin. *J Biol Chem,* 276**,** 36493-500.

SZPUNAR, J. 2005. Advances in analytical methodology for bioinorganic speciation analysis: metallomics, metalloproteomics and heteroatom-tagged proteomics and metabolomics. *Analyst,* 130**,** 442-65.

TAKAHASHI, H., KANAYAMA, Y., ZHENG, M. S., KUSANO, T., HASE, S., IKEGAMI, M. & SHAH, J. 2004. Antagonistic interactions between the SA and JA signaling pathways in Arabidopsis modulate expression of defense genes and gene-for-gene resistance to cucumber mosaic virus. *Plant Cell Physiol,* 45**,** 803-9.

TEPFER, M., GAUBERT, S., LEROUX-COYAU, M., PRINCE, S. & HOUDEBINE, L. M. 2004. Transient expression in mammalian cells of transgenes transcribed from the Cauliflower mosaic virus 35S promoter. *Environ Biosafety Res,* 3**,** 91-7.

THALHAMMER, A. & HINCHA, D. K. 2014. A mechanistic model of COR15 protein function in plant freezing tolerance: integration of structural and functional characteristics. *Plant signaling & behavior,* 9**,** e977722-e977722.

THIBAUD, M. C., GINESTE, S., NUSSAUME, L. & ROBAGLIA, C. 2004. Sucrose increases pathogenesis-related PR-2 gene expression in Arabidopsis thaliana through an SA-dependent but NPR1-independent signaling pathway. *Plant Physiol Biochem,* 42**,** 81-8.

THIEBEAULD, O., SCHEPETILNIKOV, M., PARK, H. S., GELDREICH, A., KOBAYASHI, K., KELLER, M., HOHN, T. & RYABOVA, L. A. 2009. A new plant

protein interacts with eIF3 and 60S to enhance virus-activated translation re-initiation. *EMBO J,* 28**,** 3171-84.

THOMAS, C., SUN, Y., NAUS, K., LLOYD, A. & ROUX, S. 1999. Apyrase functions in plant phosphate nutrition and mobilizes phosphate from extracellular ATP. *Plant physiology,* 119**,** 543-552.

TORUNO, T. Y., STERGIOPOULOS, I. & COAKER, G. 2016. Plant-Pathogen Effectors: Cellular Probes Interfering with Plant Defenses in Spatial and Temporal Manners. *Annu Rev Phytopathol,* 54**,** 419-41.

TRINKS, D., RAJESWARAN, R., SHIVAPRASAD, P. V., AKBERGENOV, R., OAKELEY, E. J., VELUTHAMBI, K., HOHN, T. & POOGGIN, M. M. 2005. Suppression of RNA silencing by a geminivirus nuclear protein, AC2, correlates with transactivation of host genes. *J Virol,* 79**,** 2517-27.

TSUGE, S., KOBAYASHI, K., NAKAYASHIKI, H., MISE, K. & FURUSAWA, I. 1999. Cauliflower mosaic virus ORF III product forms a tetramer in planta: its implication in viral DNA folding during encapsidation. *Microbiol Immunol,* 43**,** 773-80.

TUNGADI, T., GROEN, S. C., MURPHY, A. M., PATE, A. E., IQBAL, J., BRUCE, T. J. A., CUNNIFFE, N. J. & CARR, J. P. 2017. Cucumber mosaic virus and its 2b protein alter emission of host volatile organic compounds but not aphid vector settling in tobacco. *Virology Journal,* 14.

UZEST, M., GARGANI, D., DRUCKER, M., HEBRARD, E., GARZO, E., CANDRESSE, T., FERERES, A. & BLANC, S. 2007. A protein key to plant virus transmission at the tip of the insect vector stylet. *Proc Natl Acad Sci U S A,* 104**,** 17959-64.

VAN MUNSTER, M. 2020. Impact of Abiotic Stresses on Plant Virus Transmission by Aphids. *Viruses,* 12**,** 216.

VANNESTE, S. & FRIML, J. 2009. Auxin: a trigger for change in plant development. *Cell,* 136**,** 1005-16.

VARET, A., PARKER, J., TORNERO, P., NASS, N., NÜRNBERGER, T., DANGL, J. L., SCHEEL, D. & LEE, J. 2002. NHL25 and NHL3, two NDR1/HIN1-1ike genes in Arabidopsis thaliana with potential role(s) in plant defense. *Mol Plant Microbe Interact,* 15**,** 608-16.

WANG, H., HU, Y., PAN, J. & YU, D. 2015. Arabidopsis VQ motif-containing proteins VQ12 and VQ29 negatively modulate basal defense against Botrytis cinerea. *Sci Rep,* 5**,** 14185.

WANG, L., LU, S., ZHANG, Y., LI, Z., DU, X. & LIU, D. 2014. Comparative genetic analysis of Arabidopsis purple acid phosphatases AtPAP10, AtPAP12, and AtPAP26 provides new insights into their roles in plant adaptation to phosphate deprivation. *J Integr Plant Biol,* 56**,** 299-314.

WANG, X., GOREGAOKER, S. P. & CULVER, J. N. 2009. Interaction of the Tobacco mosaic virus replicase protein with a NAC domain transcription factor is associated with the suppression of systemic host defenses. *J Virol,* 83**,** 9720-30.

WANG, Y. & BOUWMEESTER, K. 2017. L-type lectin receptor kinases: New forces in plant immunity. *PLoS Pathog,* 13**,** e1006433.

WESTWOOD, J. H., GROEN, S. C., DU, Z. Y., MURPHY, A. M., ANGGORO, D. T., TUNGADI, T., LUANG-IN, V., LEWSEY, M. G., ROSSITER, J. T., POWELL, G., SMITH, A. G. & CARR, J. P. 2013. A Trio of Viral Proteins Tunes Aphid-Plant Interactions inArabidopsis thaliana. *Plos One,* 8.

WILLEMSEN, V., FRIML, J., GREBE, M., VAN DEN TOORN, A., PALME, K. & SCHERES, B. 2003. Cell polarity and PIN protein positioning in Arabidopsis require STEROL METHYLTRANSFERASE1 function. *Plant Cell,* 15**,** 612-25.

WIMALASEKERA, R., PEJCHAR, P., HOLK, A., MARTINEC, J. & SCHERER, G. F. 2010. Plant phosphatidylcholine-hydrolyzing phospholipases C NPC3 and NPC4 with roles in root development and brassinolide signaling in Arabidopsis thaliana. *Mol Plant,* 3**,** 610-25.

WOODWARD, A. W. & BARTEL, B. 2005. Auxin: regulation, action, and interaction. *Ann Bot,* 95**,** 707-35.

WU, J., STEINEBRUNNER, I., SUN, Y., BUTTERFIELD, T., TORRES, J., ARNOLD, D., GONZALEZ, A., JACOB, F., REICHLER, S. & ROUX, S. J. 2007. Apyrases (nucleoside triphosphate-diphosphohydrolases) play a key role in growth control in Arabidopsis. *Plant physiology,* 144**,** 961-975.

WU, S., TOHGE, T., CUADROS-INOSTROZA, Á., TONG, H., TENENBOIM, H., KOOKE, R., MÉRET, M., KEURENTJES, J. B., NIKOLOSKI, Z., FERNIE, A. R., WILLMITZER, L. & BROTMAN, Y. 2018. Mapping the Arabidopsis Metabolic Landscape by Untargeted Metabolomics at Different Environmental Conditions. *Molecular Plant,* 11**,** 118-134.

WU, X. & YE, J. 2020. Manipulation of Jasmonate Signaling by Plant Viruses and Their Insect Vectors. *Viruses,* 12.

WU, Y., ZHANG, D., CHU, J. Y., BOYLE, P., WANG, Y., BRINDLE, I. D., DE LUCA, V. & DESPRÉS, C. 2012. The Arabidopsis NPR1 protein is a receptor for the plant defense hormone salicylic acid. *Cell Rep,* 1**,** 639-47.

WULLSCHLEGER, S., LOEWITH, R. & HALL, M. N. 2006. TOR signaling in growth and metabolism. *Cell,* 124**,** 471-84.

XIONG, F., ZHANG, R., MENG, Z., DENG, K., QUE, Y., ZHUO, F., FENG, L., GUO, S., DATLA, R. & REN, M. 2017. Brassinosteriod Insensitive 2 (BIN2) acts as a downstream effector of the Target of Rapamycin (TOR) signaling pathway to

regulate photoautotrophic growth in Arabidopsis. *New Phytologist,* 213**,** 233-249.

XIONG, Y. & SHEEN, J. 2014. The role of target of rapamycin signaling networks in plant growth and metabolism. *Plant Physiol,* 164**,** 499-512.

YANG, C., GUO, R., JIE, F., NETTLETON, D., PENG, J., CARR, T., YEAKLEY, J. M., FAN, J. B. & WHITHAM, S. A. 2007. Spatial analysis of arabidopsis thaliana gene expression in response to Turnip mosaic virus infection. *Mol Plant Microbe Interact,* 20**,** 358-70.

YANG, C. Y., HSU, F. C., LI, J. P., WANG, N. N. & SHIH, M. C. 2011a. The AP2/ERF transcription factor AtERF73/HRE1 modulates ethylene responses during hypoxia in Arabidopsis. *Plant Physiol,* 156**,** 202-12.

YANG, M., ISMAYIL, A. & LIU, Y. 2020. Autophagy in Plant-Virus Interactions. *Annual Review of Virology,* 7**,** 403-419.

YANG, S. D., SEO, P. J., YOON, H. K. & PARK, C. M. 2011b. The Arabidopsis NAC transcription factor VNI2 integrates abscisic acid signals into leaf senescence via the COR/RD genes. *Plant Cell,* 23**,** 2155-68.

YEH, Y.-H., CHANG, Y.-H., HUANG, P.-Y., HUANG, J.-B. & ZIMMERLI, L. 2015. Enhanced Arabidopsis pattern-triggered immunity by overexpression of cysteine-rich receptor-like kinases. *Frontiers in Plant Science,* 6.

YU, W., MURFETT, J. & SCHOELZ, J. E. 2003. Differential induction of symptoms in Arabidopsis by P6 of Cauliflower mosaic virus. *Mol Plant Microbe Interact,* 16**,** 35-42.

YUAN, J., ZHANG, W., SUN, K., TANG, M. J., CHEN, P. X., LI, X. & DAI, C. C. 2019. Comparative Transcriptomics and Proteomics of Atractylodes lancea in

Response to Endophytic Fungus Gilmaniella sp. AL12 Reveals Regulation in Plant Metabolism. *Front Microbiol,* 10**,** 1208.

ZENG, L., SACHDEV, P., YAN, L., CHAN, J. L., TRENKLE, T., MCCLELLAND, M., WELSH, J. & WANG, L. H. 2000. Vav3 mediates receptor protein tyrosine kinase signaling, regulates GTPase activity, modulates cell morphology, and induces cell transformation. *Mol Cell Biol,* 20**,** 9212-24.

ZENG, L., ZHU, T., GAO, Y., WANG, Y., NING, C., BJÖRN, L. O., CHEN, D. & LI, S. 2017. Effects of Ca addition on the uptake, translocation, and distribution of Cd in Arabidopsis thaliana. *Ecotoxicol Environ Saf,* 139**,** 228-237.

ZHAN, B., ZHAO, W., LI, S., YANG, X. & ZHOU, X. 2018. Functional Scanning of Apple Geminivirus Proteins as Symptom Determinants and Suppressors of Posttranscriptional Gene Silencing. *Viruses,* 10.

ZHANG, D., ZHU, Z., GAO, J., ZHOU, X., ZHU, S., WANG, X., WANG, X., REN, G. & KUAI, B. 2021. The NPR1-WRKY46-WRKY6 signaling cascade mediates probenazole/salicylic acid-elicited leaf senescence in Arabidopsis thaliana. *J Integr Plant Biol,* 63**,** 924-936.

ZHANG, X., MÉNARD, R., LI, Y., CORUZZI, G. M., HEITZ, T., SHEN, W. H. & BERR, A. 2020. Arabidopsis SDG8 Potentiates the Sustainable Transcriptional Induction of the Pathogenesis-Related Genes PR1 and PR2 During Plant Defense Response. *Front Plant Sci,* 11**,** 277.

ZHANG, Z., ZHU, J.-Y., ROH, J., MARCHIVE, C., KIM, S.-K., MEYER, C., SUN, Y., WANG, W. & WANG, Z.-Y. 2016. TOR Signaling Promotes Accumulation of BZR1 to Balance Growth with Carbon Availability in Arabidopsis. *Current Biology,* 26**,** 1854-1860.

ZHAO, Y. 2008. The role of local biosynthesis of auxin and cytokinin in plant development. *Curr Opin Plant Biol,* 11**,** 16-22.

ZHAO, Y. 2010. Auxin biosynthesis and its role in plant development. Annu Rev Plant Biol, 61, 49-64.

ZHENG, M. S., TAKAHASHI, H., MIYAZAKI, A., HAMAMOTO, H., SHAH, J., YAMAGUCHI, I. & KUSANO, T. 2004. Up-regulation of Arabidopsis thaliana NHL10 in the hypersensitive response to Cucumber mosaic virus infection and in senescing leaves is controlled by signalling pathways that differ in salicylate involvement. Planta, 218, 740-50.

ZHONG, R., MORRISON, W. H., HIMMELSBACH, D. S., POOLE, F. L. & YE, Z.-H. 2000. Essential Role of Caffeoyl Coenzyme A O-Methyltransferase in Lignin Biosynthesis in Woody Poplar Plants. Plant Physiology, 124, 563-578.

ZHOU, T., MURPHY, A. M., LEWSEY, M. G., WESTWOOD, J. H., ZHANG, H.-M., GONZÁLEZ, I., CANTO, T. & CARR, J. P. 2014. Domains of the cucumber mosaic virus 2b silencing suppressor protein affecting inhibition of salicylic acid-induced resistance and priming of salicylic acid accumulation during infection. The Journal of general virology, 95, 1408-1413.

ZHU, S., GAO, F., CAO, X., CHEN, M., YE, G., WEI, C. & LI, Y. 2005. The rice dwarf virus P2 protein interacts with ent-kaurene oxidases in vivo, leading to reduced biosynthesis of gibberellins and rice dwarf symptoms. Plant Physiol, 139, 1935-45.

ZIJLSTRA, C. & HOHN, T. 1992. Cauliflower Mosaic Virus Gene VI Controls Translation from Dicistronic Expression Units in Transgenic Arabidopsis Plants. Plant Cell, 4, 1471-1484.

ZIPFEL, C., ROBATZEK, S., NAVARRO, L., OAKELEY, E. J., JONES, J. D., FELIX, G. & BOLLER, T. 2004. Bacterial disease resistance in Arabidopsis through flagellin perception. Nature, 428, 764-7.

ZUO, J., NIU, Q. W. & CHUA, N. H. 2000. Technical advance: An estrogen receptor-based transactivator XVE mediates highly inducible gene expression in transgenic plants. Plant J, 24, 265-73.

ZVEREVA, A. S., GOLYAEV, V., TURCO, S., GUBAEVA, E. G., RAJESWARAN, R., SCHEPETILNIKOV, M. V., SROUR, O., RYABOVA, L. A., BOLLER, T. & POOGGIN, M. M. 2016. Viral protein suppresses oxidative burst and salicylic acid-dependent autophagy and facilitates bacterial growth on virus-infected plants. New Phytol, 211, 1020-34.